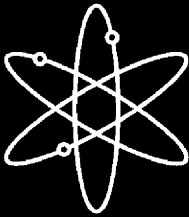


# **Containment Integrity Research at Sandia National Laboratories**

## **An Overview**



**Sandia National Laboratories**



**U.S. Nuclear Regulatory Commission  
Office of Nuclear Regulatory Research  
Washington, DC 20555-0001**



---

---

# Containment Integrity Research at Sandia National Laboratories

---

---

## An Overview

---

---

Manuscript Completed: March 2006  
Date Published: July 2006

Prepared by  
M. F. Hessheimer<sup>1</sup>  
R. A. Dameron<sup>2</sup>

<sup>1</sup> Sandia National Laboratories  
P.O. Box 5800  
Albuquerque, NM 87185

<sup>2</sup> David Evans and Associates, Inc.  
9635 Granite Ridge Drive  
Suite 300  
San Diego, CA 92123

A. Sheikh, Program Manager

**Prepared for**  
**Division of Fuel, Engineering & Radiological Research**  
**Office of Nuclear Regulatory Research**  
**U.S. Nuclear Regulatory Commission**  
**Washington, DC 20555-0001**  
**Job Code Y6757**



**This page intentionally blank**

## **ABSTRACT**

For nearly thirty years, significant research has been performed at Sandia National Laboratories to improve the understanding of the response of nuclear power plant steel and concrete containment structures and their capacity to withstand accidents beyond their design basis and other extreme loads. This work has consisted of experimental programs and analytical studies to investigate the response and capacity of containment structures and components for a wide variety of loading conditions with a primary emphasis on internal overpressurization. This report summarizes the work that has been performed and the results of these efforts, and identifies common themes that have emerged. The most detailed information provided is of the research conducted at Sandia National Laboratories, sponsored by the Nuclear Regulatory Commission. But effort is made to also highlight work conducted by other research organizations throughout the world to put the Sandia/NRC research into context and to attempt to summarize the current practice for evaluating containments subjected to accident loads.

**This page intentionally blank**

## FOREWORD

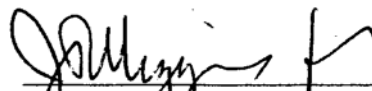
The U.S. Nuclear Regulatory Commission (NRC) regulates the operation of the civilian nuclear power plants by establishing and enforcing regulatory requirements for their design, construction, and operation. In particular, to protect the health and safety of the public and environment, the NRC requires all nuclear power plants to have a containment structure, which is essentially a leak-tight barrier between the reactor's primary system and the environment. Nonetheless, in the wake of the 1979 accident at Three Mile Island Unit 2, beginning in the early 1980s, the NRC sponsored a comprehensive research study of containment structure integrity. Under that study, the researchers tested (to failure) several large-scale models of containment buildings and full-scale containment components, and performed extensive analytical simulations to assess the risk associated with accidents beyond those considered in designing the existing population of containment structures. Most of these tests and analytical simulations were performed at Sandia National Laboratories (SNL) in Albuquerque, New Mexico, although some tests of containment components were also performed at Idaho and Argonne National Laboratories.

Building on that research foundation, this report summarizes the current understanding regarding the integrity of nuclear power plant containment structures and components under severe accident pressure and temperature loads. The scope of the current project is to document and summarize the results obtained from all of the earlier research activities conducted at SNL, along with some relevant research conducted by other organizations over the past 25 years, as they relate to the performance of containment structures and components. The scope also includes documenting the lessons learned during the containment model testing and analytical simulations, which are directly applicable to regulating and licensing the operation of the current fleet of nuclear power plants, as well as the design of new plants.

The results of the experiments and analyses summarized in this report clearly demonstrate that margins between the design capacity and ultimate capacity of containment structures are on the order of a factor of 2–5. The specific margin for a given plant is highly dependent on the details of construction, for which this report recommends specific improvements; however, it is clear that the current design and construction methods ensure a margin of safety or capacity beyond the design condition. This report also discusses the adequacy of current analytical methods by comparing a variety of simulation strategies, and concludes with an appendix that provides recommendations and guidance for developing containment capacity estimates.

Although this report presents some details of recent work, the primary focus of this report is to comment on and tie the results of earlier experiments and analyses into current research. This report does not explicitly address uncertainty in the results. However, the individual experiments and analyses provide valuable insights into the uncertainties inherent in containment model testing, as well as the simplifications and assumptions required for analytical and numerical simulations. In addition, the report notes where information is currently incomplete or lacking.

The research summarized in this report clearly supports the NRC's goals of moving toward risk-informed regulation, while maintaining a "defense-in-depth" strategy. Risk-informed decision-making requires confidence in the quality of probabilistic risk assessments (PRAs), which, in turn, depend on the quality of the simulations of containment performance. Current estimates of containment performance, typically based on the individual plant examinations, use a variety of criteria and methods for determining containment failure. The results of the research summarized in this report should contribute to establishing a standard for containment performance estimates and, thereby, improve the quality of new plant PRAs. In addition, the response of different types of containments to beyond design basis internal pressure and temperature, documented in this report, can be used as a starting point for the proposed state-of-the-art reactor consequence analysis.



Carl J. Paperfello, Director  
Office of Nuclear Regulatory Research  
U.S. Nuclear Regulatory Commission

**This page intentionally blank**

## CONTENTS

ABSTRACT .....	iii
FOREWORD.....	v
EXECUTIVE SUMMARY .....	xv
ACKNOWLEDGEMENTS .....	xix
ACRONYMS .....	xxi
1 INTRODUCTION.....	1
1.1 Objectives.....	1
1.2 Scope .....	1
1.3 Report Organization .....	2
2 BACKGROUND.....	3
2.1 Historical Background on U.S. Containment Design and Performance Criteria.....	3
2.2 Containment Design Practice .....	6
2.2.1 Containment Types.....	6
2.2.2 Containment Design.....	22
2.2.3 Containment Response to Severe Accidents .....	25
2.3 Background of Containment Testing at Sandia.....	35
3 CONTAINMENT MODEL TESTS.....	37
3.1 Containment Model Testing for ‘Beyond-Design Basis’ Loading.....	37
3.2 Modeling Considerations.....	40
3.2.1 Scaling .....	41
3.2.2 Failure.....	42
3.3 Steel Containment Model Tests.....	44
3.3.1 NRC 1:32-scale steel models.....	44
3.3.2 NRC 1:8-scale steel containment model.....	47
3.3.3 NUPEC/NRC 1:10/1:4-scale steel containment vessel model .....	52
3.3.4 Other Steel Model Tests .....	59
3.3.5 Conclusions of Steel Model Tests .....	59
3.4 Reinforced Concrete Containment Model Tests.....	61
3.4.1 NRC 1:6-scale reinforced concrete model.....	62
3.4.2 Separate Effects Tests for Reinforced Concrete Model .....	66
3.4.3 CTL/EPRI Tests .....	68
3.5 Prestressed Concrete Containment Models .....	74



3.5.1	NUPEC/NRC Prestressed Concrete Containment Vessel (PCCV) Model Test .....	74
3.5.1.1	Pressure Tests .....	78
3.5.1.2	Analysis .....	88
3.5.2	1:10-scale prestressed concrete model (Sizewell-B) .....	99
3.5.3	Other Prestressed Concrete Containment Model Tests .....	103
3.5.3.1	1:12-scale prestressed concrete model (India) [59] .....	103
3.5.3.2	1:10-scale prestressed concrete model (Poland) [60] .....	103
3.5.3.3	1:14-scale prestressed concrete CANDU model (Canada) [61, 62, 63, 64] .....	103
3.5.3.4	Large-scale prestressed concrete model (EPR, France/Germany, Civaux) .....	104
3.6	Component (Penetration) Tests .....	104
3.6.1	Compression Seals & Gaskets [83, 84] .....	104
3.6.2	Electrical Penetration Assemblies [85] .....	104
3.6.3	Personnel Airlocks [86, 87] .....	105
3.6.4	Inflatable Seals [88] .....	106
3.6.5	Equipment Hatch, Drywell Head [89, 90] .....	106
3.6.6	Bellows [93, 94] .....	106
3.7	Related Containment Research Activities .....	108
3.7.1	Containment Performance Goals .....	108
3.7.2	Degraded Containment Capacity Analyses .....	109
3.7.3	Risk-Informed Assessment of Degraded Containment Capacity .....	110
3.7.4	Seismic Capacity Tests and Analyses .....	112
3.7.5	Impact Tests and Analyses .....	112
3.7.5.1	Turbine Missile Tests .....	113
3.7.5.2	Full-Scale Aircraft Impact Test at SNL .....	113
3.7.5.3	Full Scale Engine Tests .....	114
3.7.5.4	‘Water-Slug’ Tests .....	114
3.7.6	Leakage Tests .....	114
4	ASSESSMENT OF CONTAINMENT PRESSURE CAPACITY .....	117
4.1	Insights from Containment Testing .....	117
4.2	Insights from Containment Analysis .....	119
4.3	Analysis Goals .....	120
4.3.1	Global Response Prediction .....	120
4.3.2	Local Response Prediction .....	121
4.3.3	Failure Prediction .....	122

4.4	Analytical Research Findings.....	123
4.4.1	Steel Containment Analysis.....	123
4.4.1.1	Material Modeling .....	123
4.4.1.2	Geometric Nonlinearities.....	124
4.4.1.3	Element Formulation .....	124
4.4.2	Concrete Containment Analysis .....	124
4.4.2.1	Material Modeling .....	124
4.4.2.2	Geometric Nonlinearities and Other Issues .....	125
4.4.3	Comparison of Analyses Methods Used for Predicting Model Behavior with US Containment Design Practice .....	125
4.4.4	Temperature Effects .....	126
4.5	Recommendations for Prototype Containment Capacity Estimates .....	133
4.5.1	Current Practice .....	133
4.5.2	Recommendations for Design and Performance .....	136
4.5.3	Recommendations for Containment Capacity Analysis .....	137
4.5.3.1	Steel Containments.....	137
4.5.3.2	Concrete Containments.....	137
4.6	Conclusions from Containment Model Tests .....	140
4.7	Issues for Future Consideration.....	141
4.7.1	Leakage.....	141
4.7.2	Other Considerations .....	142
5	REFERENCES .....	145
	APPENDIX - Containment Capacity Analysis Guidelines.....	A-1

## FIGURES

Figure 1	Typical PWR Large Dry Containment with Prestressed Containment (e.g. Palisades).....	11
Figure 2	Large Dry Steel Containment with Reinforced Concrete Shield Building (e.g. Davis-Besse).....	12
Figure 3	Typical PWR Subatmospheric Reinforced Concrete Containment (e.g. Diablo Canyon) .....	13
Figure 4	Typical PWR Ice Condenser Steel Containment with Concrete Shield Building (e.g. Sequoyah).....	14
Figure 5	Typical BWR Mark I Concrete Containment with Steel Torus.....	15
Figure 6	Typical BWR Mark II Containment [1] .....	16
Figure 7	BWR Mark II Concrete Containment (LaSalle Units 1 & 2) .....	17
Figure 8	BWR Mark II Steel Containment with Concrete Shield Building (Columbia, previously WNP-2).....	18
Figure 9	BWR Mark II Reinforced Concrete Containment (Limerick 1 & 2).....	19
Figure 10	Typical BWR Mark III Containment.....	20
Figure 11	Typical BWR Mark III Containment.....	21
Figure 12	Typical Containment Volume and Design Pressure for US plants [1] .....	24
Figure 13	Containment Failure Pressures for NUREG-1150 Plants [7] .....	28
Figure 14	IPE Fragility Curves for Large Dry Prestressed Concrete Containments .....	30
Figure 15	IPE Fragility Curves for Large Dry Reinforced Concrete Containments.....	31
Figure 16	IPE Fragility Curves for Large Dry Steel Containments.....	31
Figure 17	IPE Fragility Curves for Ice Condenser Containments .....	32
Figure 18	IPE Fragility Curves for Sub-Atmospheric Reinforced Concrete Containments.....	32
Figure 19	IPE Fragility Curves for BWR Mark I .....	33
Figure 20	IPE Fragility Curves for BWR Mark II .....	33
Figure 21	IPE Fragility Curves for BWR Mark III.....	34
Figure 22	Timeline for Containment Integrity Research at SNL.....	38
Figure 23	1:32-Scale Steel Containment Vessel Models.....	46
Figure 24	SC-1 and SC-3 Tests .....	46
Figure 25	1:8-Scale Steel Containment Model Layout.....	47
Figure 26	1:8-Scale Steel Containment Model .....	48
Figure 27	Results of 1:8-Scale Steel Containment Vessel Model Test.....	49 & 50
Figure 28	Comparison of Predicted and Measured Hoop Strains in the 1:8-Scale Steel Containment Vessel Model. [25].....	51

Figure 29	Pretest Analysis vs. As-built Configuration of Stiffeners at 1:8-Scale Steel Model Equipment Hatch.....	51
Figure 30	1:10-Scale Steel Containment Model Summary.....	54
Figure 31	Posttest View of Tears at E/H, 1:10-Scale Steel Containment Model.....	55
Figure 32	Posttest Interior View of the 1:10-Scale Steel Model .....	55
Figure 33	Tear at Horizontal Stiffener ‘Rat-Hole’, 1:10-Scale Steel Containment Model.....	56
Figure 34	Displacement contours (x10) @ 4.5 MPa.....	57
Figure 35	Cross-section through large tear at equipment hatch.....	57
Figure 36	Comparison of Pretest Predictions of Hoop Strain with Test Results .....	59
Figure 37	Cross-section of the 1:6-Scale Reinforced Concrete Containment Vessel Model.....	62
Figure 38	1:6-Scale Reinforced Concrete Containment Model Construction .....	63
Figure 39	Major Liner Tear in 1:6-Scale Reinforced Concrete Model.....	64
Figure 40	Developed Elevation of the 1:6 Scale RC Model Cylinder showing Liner Tear Locations .....	64
Figure 41	Posttest Analysis of 1:6-Scale RC Model Liner at 1.0 MPa (145 psig) .....	66
Figure 42	Separate Effects Test Liner Specimens .....	67
Figure 43	Containment Wall Panel Specimen Test Strategy for EPRI/CTL Tests [51] .....	69
Figure 44	Typical R/C, P/C Containment Geometries used in EPRI Global Analyses [51] .....	70
Figure 45	Liner Vertical Strains Measured (and Analyzed) in EPRI/CTL Specimen 2.5, Wall-Skirt Junction of a Typical P/C Containment.....	70
Figure 46	Liner Plate Details for EPRI/CTL Specimen 2.4.....	71
Figure 47	Liner Plate Details for EPRI/CTL Specimen 2.2, Which Studied Leak Rates Through an Advancing Liner Crack Tip .....	72
Figure 48	Idealization of Flow of Pressurized Gas Through a Liner Tear [56].....	73
Figure 49	Ohi Nuclear Power Station, Ohi-cho, Fukui, Japan.....	75
Figure 50	PCCV Model Elevation and Cross-Section.....	76
Figure 51	PCCV Model Construction.....	77
Figure 52	Completed PCCV Model.....	77
Figure 53	PCCV Pressurization Plan Sequence (not to scale).....	78
Figure 54	Limit State Test Pressure and Average Temperature .....	79
Figure 55	Internal Acoustic Sensor Signals @ the Equipment Hatch .....	80
Figure 56	LST - Estimated Leak Rates (2.5-3.1 P <sub>d</sub> ) .....	80
Figure 57	LST Estimated Terminal Leak Rates.....	81
Figure 58	LST - Deformation @ Az. 135° and 324° (Z and L).....	82

Figure 59	Post-LST Liner Tears .....	82
Figure 60	Tear #7 at Equipment Hatch.....	83
Figure 61	Tear #12 at Equipment Hatch.....	83
Figure 62	SFMT: Rupture of the PCCV Model.....	85
Figure 63	PCCV Model after the Structural Failure Mode Test.....	85
Figure 64	SFMT – Radial Displacement at Az. 135°, El. 6200 .....	86
Figure 65	SFMT Wire Break Events vs. Pressure vs. Displacement.....	87
Figure 66	SFMT - Deformation @ Az. 135° (Z) .....	87
Figure 67	SFMT - Deformation @ Az. 324° (L) .....	88
Figure 68	Axisymmetric Model of 1:4-scale PCCV.....	89
Figure 69	Local Model of Equipment Hatch .....	89
Figure 70	Three-Dimensional Cylinder Mid-Height Model (#DCM) .....	90
Figure 71	Radial Displacement at Cylinder Wall Mid-height (SOL 6).....	92
Figure 72	Posttest Analysis of SFMT at Rupture (~1.38MPa).....	94
Figure 73	Case 1 Saturated Steam Pseudo-Time History .....	98
Figure 74	Case 2 Station Black-Out Time History .....	98
Figure 75	Schematic of 1:10 Scale Sizewell Model .....	101
Figure 76	Section View of Posttest Condition of the 1:10-Scale Model .....	101
Figure 77	Hoop Tendon Gage Data Near Cylinder Mid-height .....	102
Figure 78	Comparison of Pretest Analyses vs. Experiment Results for 1:10 Scale P/C Model.....	102
Figure 79	Typical applications of inflatable seals in personnel airlock doors [82] .....	105
Figure 80	Inflatable Seal Schematic and Typical Designs [82].....	106
Figure 81	Typical application of process piping bellows [82].....	107
Figure 82	Bellow Test.....	107
Figure 83	Acceptance Guidelines for Large Early Release Frequency .....	111
Figure 84	Leak Fragility for Surry Containment with Liner Corrosion.....	111
Figure 85	Turbine Missile Test Sequence.....	113
Figure 86	Full-Scale Aircraft Impact Test Sequence.....	113
Figure 87	‘Water Slug’ Test Sequence .....	114
Figure 88	ISP 48 Phase 3, Case 1 Loading and Temperature .....	128
Figure 89	ISP 48 Phase 3, Case 2 Loading and Temperature .....	128
Figure 90	Axisymmetric Model Thermal Boundary Conditions .....	129
Figure 91	Concrete Compression Strength Ratio vs. Temperature.....	132
Figure 92	Steel Yield Strength and Modulus Ratio vs. Temperature .....	132

Figure 93	Combined Probability of Liner Tear by PLPM Software for the Reinforced Concrete Containment Example .....	135
Figure 94	Probability of either Leakage, Rupture, or Catastrophic Rupture Occurring given that failure has occurred for Reinforced Concrete Containment .....	135
Figure 95	Idealization of Reinforced Concrete Containment Behavior.....	139
Figure 96	Idealization of Prestressed Concrete Containment Behavior .....	139
Figure A-1	Examples of Steel Containment Models [97].....	A-8
Figure A-2	Typical Axisymmetric Model and Temperature Boundary Conditions .....	A-22

## TABLES

Table 1	Number of U.S. Containments by Type .....	7
Table 2	PWR Containment Construction Types .....	8
Table 3	BWR Containment Construction Types .....	9
Table 4	Containment Strength Under Static Pressure[7].....	29
Table 5	Replica Modeling Law to Satisfy Pi Terms.....	42
Table 6	Summary of Results of Experiments for Steel Containment Models.....	45
Table 7	Pretest Failure Predictions for 1:10-Scale Steel Containment Model .....	58
Table 8	Summary of Results of Experiments for Reinforced Concrete Containment Models and Liner Tearing and Leakage .....	61
Table 9	Summary of Results of Experiments for Prestressed Concrete Containment Models .....	74
Table 10	Summary of PCCV RR Pretest Results .....	93
Table 11	Summary of ISP 48 Results.....	99
Table 12	Release Paths in LWR Containments .....	122
Table A-1	Summary of Analytical Model Types Used for Containment Studies .....	A-6

## EXECUTIVE SUMMARY

Research into the integrity of containment structures or vessels for nuclear power plants has been conducted around the world in those countries where nuclear energy is produced and provides, or is expected to provide, a significant portion of the domestic energy supply. While the contributions of each of these efforts to the understanding of the role of containment in ensuring the safe operation on nuclear power plants is important, the most comprehensive experimental effort has been conducted at Sandia National Laboratories, primarily under the sponsorship of the US Nuclear Regulatory Commission (NRC). This report describes the background and context for the more than 25 years of NRC-sponsored Containment Integrity Research at Sandia National Laboratories and summarizes the major results of the experimental efforts and the observations and insights gained from the analytical efforts.

Beginning in the 1950's, the US Atomic Energy Commission and its successor, the NRC, established the safety requirements for US nuclear power reactors. The safety strategy that emerged became known as 'defense in depth'. The elements of 'defense in depth' included accident prevention, redundancy of safety systems, **containment**, accident management and remote siting/emergency planning (sheltering and evacuation). Along with defining the rules which governed design, construction and operation and licensing and regulating the plants, the NRC engaged in an extensive research program to investigate safety issues associated with highly unlikely events, such as the complete rupture of the pressure vessel, which were not considered in the design of the plants. While research into the performance of the containment to resist these 'beyond-design-basis' loads had already been initiated, the accident in 1979 at Unit 2 of the Three Mile Island nuclear power plant in Pennsylvania, gave new impetus to this research.

All of the 103 operating nuclear power plants in the United States are light-water reactors, either pressurized water reactors (69) or boiling water reactors (34). Each of these plants includes either a steel or steel-lined, reinforced concrete containment as the final barrier against the release of radio-nuclides to the environment. The reinforced concrete containments use either conventional or prestressed/posttensioned reinforcing. The containments are designed to accommodate the pressures associated with a loss of coolant accident by either having large volumes, as in the large dry and subatmospheric containments, or by utilizing a pressure suppression system to reduce the volume, as in the ice-condenser or the Mark-I, -II, or -III boiling water reactors which include a suppression pool filled with water.

A 1980 study conducted for the NRC by Sandia concluded that the scant empirical data on the ultimate capacity of containment structures were not adequate to ensure that predictions based on analysis were accurate or reliable. Based on this conclusion, an ambitious program to conduct tests of models of containment structures to failure and determine the suitability of existing analytical methods to predict failure was undertaken.

A series of increasingly large and complex tests of scale models of containment structures and components were conducted at Sandia National Laboratories between 1983 and 2001. In conjunction with these experiments, an exhaustive analytical effort was conducted to predict the behavior of the models during the tests and to understand and simulate the actual behavior after the tests. The Sandia models, which were all subjected to static overpressurization at ambient temperature, consisted of

- Four 1:32-scale models of steel containment structures typical of a large dry or ice-condenser PWR containment
  - Two simple cylindrical shells with a hemispherical dome



- One of similar geometry with hoop stiffeners
- One of similar geometry with simulated penetrations
- A 1:8-scale model of a free-standing steel containment typical of ice-condenser PWR containments
- A mixed scale model of the steel containment of an improved BWR Mark II
  - The overall geometric scale was 1:10, the shell thickness scale was 1:4 to facilitate fabrication and to allow the use of prototypical materials
  - This model was constructed by the Nuclear Power Engineering Corporation (NUPEC) of Japan and tested by Sandia National Laboratories as part of a Cooperative Containment Research Program between NUPEC and the NRC.
- A nominal 1:6-scale model of a reinforced concrete PWR containment
- A 1:4-scale model of a large, dry PWR prestressed concrete containment
  - This model was also constructed by NUPEC and tested by Sandia National Laboratories as part of the Cooperative Containment Research Program.

For most of these tests, various international nuclear research agencies, including regulatory bodies, designers, operators, universities and consultants, were invited to participate in test planning, pretest prediction and posttest analysis. Over 25 different agencies agreed to participate in the various tests. Their efforts complimented the analyses performed by Sandia and its subcontractors and supported the objectives of the program to demonstrate and improve the ability to predict containment performance up to and including failure.

In addition to these tests of models of the containment structure, Sandia also tested full-scale and scale models of electrical penetration assemblies, personnel air locks, equipment hatches, drywell heads, penetration bellows and penetration seals and gaskets.

Some general conclusions on predicting containment behavior can be made from this series of containment vessel model tests:

- Although establishing a generic margin of safety was not the purpose of the SNL program, the steel models have pressure capacities of 4-6 times, of the design pressure and the reinforced concrete models have pressure capacities of 2.5 to 3.5 times the design pressure.
- Global, free-field strains on the order of 2-3% for steel, 1.5 to 2% for reinforced concrete and 0.5 to 1.0% for prestressed concrete can be achieved before failure or rupture.
- Model (and presumably prototype) capacities are limited by high strains arising at local discontinuities which are present in both the model and the prototype.
- In the absence of a 'backup' structure, steel containment structure model capacities tend to be limited by gross structural failure or 'rupture'. Due to the inherent structural redundancy of the liner and concrete system, steel lined concrete containments appear to be limited by functional failure (leakage). While the behavior that leads to tearing of the steel vessel or the steel liner is similar, i.e. local exceedence of the ductility limits of the

steel at geometric discontinuities, the subsequent response of the vessels differs due to the presence of the surrounding structure.

- It seems reasonable to assume that with the added complexity of the actual containments, there is a higher probability that these local strain risers are present in, and possibly more severe than in any of the models tested. As a result, the capacities of the model, can, at best, be interpreted as an upper bound on capacity of prototypical containments.
- Analytical methods currently used are adequate to predict global response into the inelastic regime. One caveat on this statement is the discrepancy between predictions and observations of global yielding. Further investigation is required to understand the nature of this discrepancy (e.g. residual stresses, etc.) and its significance for calculation of prototypical containment capacities.
- Predictions of local failure mechanisms are highly dependent on the experience of the analyst, on the availability of accurate as-built information (geometry and material properties) at discontinuities, and on fabrication processes. Even if this information is available (not typical for actual containments) the prediction, a priori, of local failures is at best an uncertain proposition. The large scale model tests have, however, educated and sensitized the community to the types of details which may be critical in limiting containment capacities, and, hopefully, have improved the reliability of the predictions.
- These conclusions are predicated on failure of the containment structure. Any evaluation of the capacity of an actual containment must be based on the entire system, including mechanical and electrical penetrations and other potential leak paths.

**This page intentionally blank**

## ACKNOWLEDGEMENTS

It is impossible to identify all of the individuals who participated in the work described in this report and contributed to the current understanding of containment integrity, however we would like to acknowledge their efforts and dedication, albeit anonymously.

Some individuals, however, deserve special mention. Dr. James F. Costello, US NRC (retired) and Dr. Walter A. von Rieseemann, Sandia National Laboratories (retired) provided the inspiration and were the guiding force behind the majority of the efforts described in this report. Similarly, Dr. Yusef R. Rashid, ANATECH, was instrumental in the development and application of many of the analytical tools and methods described in this report.

It should also be noted that at the inception of this program, a Peer Review Panel, consisting of representatives from industry, academia, other research laboratories and private consultants, was organized. This panel, the specific make-up of which varied over the course of the program, actively participated in reviewing the research plans and results and provided guidance to the NRC and Sandia on the direction of the program. The author's are especially indebted to Mr. Thomas J. Ahl, CBI (retired), private consultant; Mr. Bryan A. Erler, Sargent and Lundy, Engr's (retired), private consultant; Mr. Lyle Gerdes, ABB Combustion (retired); Mr. Theodore E. Johnson, Bechtel (retired), private consultant; Dr. Richard S. Orr, Westinghouse Electric Corporation; Mr. Bert Pfeiffer, Bechtel (retired); Professor Mete A. Sozen, Purdue University; Dr. John D. Stevenson, Stevenson & Associates; Dr. H. T. Tang, Electric Power Research Institute; Mr. Harold Townsend, General Electric (retired); Dr. Joseph Ucciferro, Day & Zimmerman; and Professor Richard N. White, Cornell University (emeritus).

The authors are, to a large extent, gratefully standing on their shoulders.

*Sandia is a multiprogram laboratory operated by Sandia Corporation, a Lockheed Martin Company, for the United States Department of Energy's National Nuclear Security Administration under Contract DE-AC04-94AL85000.*

**This page intentionally blank**

## ACRONYMS

3DCM	Three-dimensional Cylinder Mid-height model
A/L	(Personnel) Air Lock
ACI	American Concrete Institute
ACRS	Advisory Committee on Reactor Safeguards
AEC	Atomic Energy Commission
AECL	Atomic Energy of Canada Limited
ALWR	Advanced Light Water Reactor
ANL	Argonne National Laboratory, US
ANPA	Agenzie Nazionale per la Protezione dell' Ambiente, Italy
ASCE	American Society of Civil Engineers
ASME	American Society of Mechanical Engineers
ASTM	American Society for Testing and Materials
B&PV	Boiler and Pressure Vessel (Code)
BARC	Bhabha Atomic Research Center, India
BE	British Energy
BWR	boiling water reactor
CANDU	Canadian Heavy Water Reactor
CBI	Chicago Bridge and Iron
CCFP	conditional containment failure probability
CEA	Commissariat a l'Énergie Atomique, France
CEGB	Central Electric Generating Board, UK
CFF	containment failure frequency
CFR	Code of Federal Regulations
CS	contact structure
CSNI	Committee on Safety of Nuclear Installations (OECD/NEA)
CTL	Construction Technologies Laboratory
DAS	data acquisition system
DBA	design-basis accident
DEA	David Evans and Associates
DOD	Department of Defense
E/H	Equipment Hatch
EDF	Électricité de France
EGP	Energoprojekt Praha, UJV Rez. Div.

EPDM	ethylene propylene
EPR	European (or Evolutionary) Pressurized Reactor
EPRI	Electric Power Research Institute, US
ESF	engineered safety features
FORTUM	Fortum Nuclear Services, Ltd.
FSAR	Final Safety Analysis Report
GD/EB	General Dynamics/Electric Boat Division, US
GRS	Gesellschaft für Anlagen und Reaktorsicherheit mbH
HAZ	heat affected zone
HSE	Health and Safety Executive, U.K.
HTGR	High Temperature Gas Reactor
IBRAE	Nuclear Safety Institute, Russia
ICONE	International Conference on Nuclear Engineering
ILRT	Integrated Leak Rate Test
INEL	Idaho National Engineering Laboratory
INER	Institute of Nuclear Energy Research, Republic of China
IPE	Individual Plant Examinations
IPSN	Institut de Protection et de Sûreté Nucléaire, France
IRSN	Institut de Radioprotection et de Sûreté Nucléaire
ISP	International Standard Problem
JAERI	Japan Atomic Energy Research Institute
JAPC	Japan Atomic Power Company, Japan
JPRG	Japan PCCV Research Group
KINS	Korea Institute of Nuclear Safety, Korea
KOPEC	Korea Power Engineering Company, Korea
LERF	Large Early Release Frequency
LST	limit state test
LOCA	loss-of-coolant accident
LVDT	linearly variable displacement transducer
LWR	light water reactor
METI	Ministry of Economics, Trade and Industry, Japan
MIT	Massachusetts Institute of Technology
MPA	Materialprüfungsanstalt Universität Stuttgart, Universität Stuttgart, Germany
NASA	National Aeronautics and Space Administration
NEA	Nuclear Energy Agency (OECD)

NII/HSE	Nuclear Installations Inspectorate/Health & Safety Executive
NPP	nuclear power plant
NRC	Nuclear Regulatory Commission
NSSS	nuclear steam supply system
NUPEC	Nuclear Power Engineering Corporations, Japan
OBE	operating basis earthquake
OECD	Organization for Economic Cooperation and Development
P/C	prestressed concrete
PCCV	prestressed concrete containment vessel
$P_d$	design pressure
PLPM	Probabilistic Leakage Prediction Methodology
PORV	pressure operated relief valve
PRA	probabilistic risk assessment
PRIN	Principia Ingenieros Consultores, S.A., Spain
PWR	pressurized water reactor
R/C	reinforced concrete
RCCV	reinforced concrete containment vessel
RINSC	Russia International Nuclear Safety Center, Russia
RPV	reactor pressure vessel
SAR	Safety Analysis Report
SCANSCOT	Scanscot Technology, Sweden
SCV	steel containment vessel
SFMT	structural failure mode test
SIT	structural integrity test
SMiRT	Structural Mechanics in Reactor Technology (Conference)
SNL	Sandia National Laboratories
SOL	standard output location
SRP	Standard Review Plan
SSE	safe shutdown earthquake
TMI-2	Three Mile Island, Unit 2
UKAEA	United Kingdom Atomic Energy Agency



**This page intentionally blank**

# 1 INTRODUCTION

## 1.1 Objectives

The objectives of this report are

- to describe the background and context for the more than 25 years of NRC-sponsored Containment Integrity Research at Sandia National Laboratories. The support, partnership and participation of a large variety of domestic and international organizations, notably the Nuclear Power Engineering Program of Japan will also be described;
- to provide a knowledge base and reference list, documenting SNL's containment integrity research,
- to summarize of the major results of the experimental efforts performed at Sandia National Laboratories and the observations and insights gained from the analytical efforts, both internal and the international Round Robin exercises;
- to document 'lessons learned' from the containment model testing and analyses, provide insights on the current level of understanding of containment overpressure behavior and the 'state of the practice' for containment beyond design basis loads evaluation;
- to provide recommendations for containment design to improve reliability and performance to beyond-design basis loads;
- to recommend principles and procedures for analysis of containment structures to beyond-design basis loads and criteria for interpreting analytical results with regard to functional or structural behavior;
- to provide more realistic, physics-based approach to modeling containment behavior in PRA models and in risk-informed decision making,
- to provide an assessment of the level of success of the analytical methods in predicting/simulating containment model response and failure modes,
- to discuss criteria for functional and structural failure,
- to recommend methods for prediction of containment capacity, including insights on model error and model uncertainty for PRAs and risk-informed regulations,
- and to identify future work that may support the safety and licensing review of the next generation of U.S. containments.

## 1.2 Scope

Research into the integrity of containment structures or vessels for nuclear power plants has been conducted around the world in those countries where nuclear energy is produced and provides, or is expected to provide, a significant portion of the domestic energy supply. While the contributions of each of these efforts to the understanding of the role of containment in ensuring the safe operation on nuclear power plants is important, the most comprehensive experimental effort has been conducted at Sandia National Laboratories, primarily under the sponsorship of the

US NRC. The scope of this report focuses primarily on the work conducted at SNL. While it would be a very useful exercise, it is beyond the scope of this report to provide a complete and comprehensive summary of work conducted elsewhere, although some relevant summaries and references have been included.

Also, while the experiments and analyses summarized in this report have broad relevance to safety-related issues for nuclear power plants throughout the world, the insights and lessons learned are focused primarily on the current fleet of US light water reactors and advanced light water reactors which might be constructed in the future. Some of these insights and lessons learned may also have applicability to future generations of LWR and non-LWR plants. However, the designs of these plants may have significantly different demands, and significantly different approaches to meeting those demands, for containment systems.

### **1.3 Report Organization**

This report summarizes the major accomplishments and insights obtained over 25 years of primarily NRC-sponsored research on the integrity of nuclear power plant containment structures and their capacity to resist loads beyond those for which they were designed. Chapter 2 describes the evolution of containment design in the context of the US commercial nuclear power industry. Chapter 2 also describes the typical design of the six major containment types used in the US, the statutory design requirements and the role of containment in severe accident, probabilistic risk assessment and risk-informed regulation.

Chapter 3 summarizes the major experimental and analytical programs conducted at Sandia National Laboratories along with the results and conclusion from each program. Relevant programs conducted elsewhere are also briefly summarized.

Chapter 4 synthesizes the experimental and analytical results, and attempts to summarize the major insights and lessons learned from all the experiments, identify issues which are unresolved or which were not addressed and suggest future work needed to resolve these items, and document the implications for on-going regulation of existing plants and licensing of future plants.

In addition to providing detailed references for the information summarized in this report, Chapter 5 provides a fairly extensive bibliography of the relevant literature on containment integrity issues.

## 2 BACKGROUND

### 2.1 Historical Background on U.S. Containment Design and Performance Criteria<sup>1</sup>

Following World War II, peaceful uses of nuclear energy included plans to construct commercial reactors for electric power generation. The Atomic Energy Act of 1946 established the Atomic Energy Commission (AEC) and provided the statutory basis for the development of commercial nuclear power plants in the US. In the first few years after the war, several low power (<50MWt) test reactors were constructed. These reactors followed the practice established during the Manhattan Project of siting them on remote government reservations. WASH-3 [2] defined this siting practice. The rule of thumb for the residence exclusion distance, R, was given as

$$R \text{ (miles)} = 0.01 [P \text{ (kWt)}]^{1/2}$$

For a 3000 MWt plant (P=3,000.000 kWt), this would result in an exclusion distance of 17.3 m (27.8 km).

An early exception to this siting approach and the first use of containment in the US was the Submarine Intermediate Reactor Mark A at the Knolls Atomic Power Laboratory which was only 19 miles from Schenectady, NY. The entire reactor was enclosed in a gas-tight steel sphere, or **containment** (although this term was not applied to this structure), designed to withstand “a disruptive core explosion” and to contain radionuclides that might be released in a reactor accident.

Early commercial nuclear power plants in the US were based on naval nuclear power submarines. Since submarine bases were major ports with generally large population centers, remote siting criteria could not be applied to submarines. The Navy therefore relied on rigorous accident prevention strategies along with the containment capability provided by the hull (although this did not protect the crew). Prevention and safety-system strategies developed for submarine reactors evolved in the 1950s and 1960s for application to commercial nuclear reactors.

The safety strategy that emerged became known as ‘defense in depth’. The elements of ‘defense in depth’ included accident prevention, redundancy of safety systems, **containment**, accident management and remote siting/emergency planning (sheltering and evacuation). While this describes the layers of the defense-in-depth strategy, it does not specify, with regard to containment for example, how strong the containment should be or what containment leakage rate should be limited to.

The first civilian nuclear power plant, the Shippingport Atomic Power Station was a pressurized water reactor owned by the Duquesne Light Company and designed and operated by Westinghouse. The Shippingport plant was located about 20 miles from Pittsburgh, PA and did not meet the siting criteria, hence a containment building was provided. In 1955 and 1956 the AEC received applications for three large commercial power reactors: Dresden 1, about 35 miles from Chicago, IL; Indian Point 1, 24 miles north of New York City; and the Enrico Fermi plant, 25 miles south of Detroit, MI. Containments were proposed for all three reactors.

---

<sup>1</sup> Background information extracted from Reference [1]

The advent of containment was a decisive step in moving large power reactors closer to populated electrical load centers. Containment provided a barrier to the release of radionuclides that was desirable for public safety and public acceptance of nuclear power. All commercial nuclear power plants approved for construction in the US have containments.

The earliest rules for containment were given in the Reactor Site Criteria, 10 CFR 100 published in 1962. 10 CFR 100 introduced the concepts of a maximum credible accident, subsequently referred to as the design-basis accident (DBA) or design basis loss-of-coolant accident (LOCA), and the expected leak rate from the containment. Containments were designed to withstand the peak pressure associated with the reactor coolant system blowdown and remain intact, limiting the release of radionuclides to the environment at a specified design leak rate. They were not designed to withstand the loads associated with gross rupture of the vessel.

The industry response to the 10 CFR 100 criteria was to take credit for engineered safety features (ESFs) such as suppression pools, containment sprays, containment heat removal systems and air-cleaning systems. San Onofre, Connecticut Yankee, Oyster Creek, Nine Mile Point and Dresden 2 were approved for construction based on the use of ESFs. In 1962, an application was submitted for the two-unit Ravenswood plant, which included double containments for the Westinghouse nuclear steam supply system (NSSS), to be located, essentially in the heart of New York City. Calculations by the AEC staff indicated that, even while taking credit for the ESFs, the containment leak rate would have to be limited to  $10^{-4}$  cfm in order to meet the siting guidelines. Consolidated Edison subsequently withdrew its application in 1963.

In 1966, two issues called into question the assumption of containment as an independent barrier: reactor pressure vessel integrity and the 'China syndrome'. Containments were not designed to withstand a gross rupture of the reactor pressure vessel since this was not considered to be a credible event. Further research and actual failures which occurred during pressure testing of steam generators led the Advisory Committee on Reactor Safeguards (ACRS) to express concerns regarding this assumption and require improved design and inspection methods for reactor pressure vessels. In 1974 the ACRS concluded that the possibility of a RPV failure was less than  $10^{-6}$  per vessel year. Studies also suggested that a loss of coolant could lead to the molten core breaching the lower head of the Reactor Pressure Vessel (RPV), penetrating the concrete containment basemat and coming into contact with the earth. This scenario was euphemistically referred to as the 'China Syndrome'. As a result, emphasis shifted from containment to prevention and, until the TMI-2 accident in 1979, the focus was on demonstrating emergency core cooling, not on what to do if core cooling failed.

The Reactor Safety Study was initiated in response to a congressional request for a comprehensive assessment of reactor safety. WASH-1250, "The Reactor Safety Study of Nuclear Power Reactors (Light Water-Cooled) and Related Facilities"[3] discussed the conservatism applied on the design of nuclear power plants, but did not address the likelihood or potential consequences of beyond-design-basis accidents. Beyond-design-basis accidents include those initiated by reactor pressure vessel rupture, by seismic events greater than the Safe Shutdown earthquake (SSE) and those involving multiple system failures. A subset of beyond-design-basis accidents that could lead to substantial core damage are called severe (or Class 9) accidents.

In response to the questions raised by WASH-1250, a major probabilistic study was initiated in 1972. Also known as the Rasmussen report after the study director, Professor Norman Rasmussen of MIT, this study used a methodology pioneered by the DOD and NASA, called probabilistic risk assessment (PRA) to predict the effects of component failures on large, complex systems. One of the tasks "...was to determine the thresholds and modes of failure of reactor buildings (containments)...when subjected to internal pressures and temperatures greater than the

design values” for two prototypical plants. Some computer analyses plus hand calculation solutions were used, but no experimental work was carried out. The results were issued as WASH-1400 (NUREG-75/014) [4]. The study concluded that, while the risks of a core melt accident were small, they were more likely than previously thought, approximately  $5 \times 10^{-5}$  per reactor year. The study also suggested that different containment types may differ in their capability to withstand core melt accidents.

At 4:00 AM on March 28, 1979, the most severe accident in US nuclear history began when a resin blockage in the condensate system caused the condensate and condensate booster pumps to trip. The sequence of events and actions which eventually led to damage and partial melting of the core of the Three Mile Island-2 plant, an 880 MWe PWR, detailed in various documents and reports, are summarized in Reference 1. During the course of the accident, the containment building was subjected to a peak pressure spike (recorded by one sensor as 28 psig) when hydrogen, released when a pressure operated relief valve (PORV) was opened, ignited and burned with oxygen in the reactor building atmosphere. The accident at Three Mile Island 2 put to rest the notion that severe nuclear power accidents were not credible. It also led to significant changes in the NRC and the industry and increased emphasis on the importance of containment survival during severe accidents.

Following the TMI-2 investigations and after several years of deliberation, the NRC established both qualitative and quantitative safety goals in August 1986.<sup>2</sup> The quantitative safety goals established are:

*“Individual members of the public should be provided a level of protection from the consequences of nuclear power operations such that individuals bear no significant additional risk to life and health.”*

*“Societal risks to life and health from nuclear power plant operation should be comparable or less than the risks of generating electricity by viable competing technologies and should not be a significant addition to other societal risk.”*

The corresponding quantitative safety goals are:

*“The risk to an average individual in the vicinity of a nuclear power plant of prompt fatalities that might result from reactor accidents should not exceed one-tenth of one percent of the sum of prompt fatality risks resulting from other accidents to which members of the U.S. population are generally exposed.”*

*“The risk to the population near a nuclear power plant of cancer fatalities that might result from nuclear power plant operation should not exceed one tenth of one percent of the sum of cancer fatality risks resulting from all other causes.”*

Also following TMI-2, NRC research was redirected to focus on severe accidents. The NRC issued a policy statement on severe accidents in 1985<sup>3</sup>. Recognizing the plant specific nature of severe accident vulnerabilities, the NRC issued a generic letter in 1988 [5] requiring each nuclear power plant operating or under construction to perform a systematic Individual Plant Examination (IPE) [6]. The results of the research efforts were integrated into a major PRA for five reference

---

<sup>2</sup> Federal Register, Vol. 51, No. 149, 1986

<sup>3</sup> Federal Register, Vol. 50, 32,138, August 8, 1985

plants in 1990, known as NUREG-1150 [7], which essentially replaced the earlier Reactor Safety Study. Both of these efforts attempted to show that containments have the capacity to withstand many of the beyond-design basis challenges including severe accidents.

Prior to the TMI-2 accident, the NRC had initiated work at Sandia National Laboratories and elsewhere to study containment systems. This effort gained new impetus following the accident. The first Sandia study [8], described in more detail in Section 2.3 concluded that the few experiments on containment integrity had been either of too small a scale or lacked sufficient details of actual plants to be of reliable use for understanding containment response to beyond-design-basis accidents. Based on this study, the program, which is the subject of this report, was formulated to investigate containment systems subjected to beyond-design-basis loads. This program's objective has been the validation of methods used to predict the performance of light water reactor (LWR) containment systems when subjected to loads beyond those specified in the design codes and **not** to determine the pressure carrying capacity of actual containments by testing scale models.

## 2.2 Containment Design Practice

### 2.2.1 Containment Types

Before discussing the Containment Integrity Research program, it is worth a brief review of containment designs for the current fleet of US nuclear power reactors. As of 2006, there were 103 US commercial light-water nuclear reactors (LWR) with operating licenses at 64 sites in 31 states, 69 pressurized water reactors (PWR) and 34 boiling water reactors (BWR). There are six basic containment types in the fleet. Four of these designs primarily use the passive pressure suppression concept, and two rely primarily on large, strong volumes. All of these containments are constructed of either steel or concrete with a steel liner for leak tightness. BWR designs, which have evolved from the Mark I to the Mark III design, all use a pressure suppression pool. A few Westinghouse PWRs have ice-condenser (pressure suppression) containments, but most PWRs have large dry containments or a subatmospheric variation of the large dry containment. Table 1 summarizes the number of containments for each of the six basic types. Tables 2 and 3 further characterize these containments by construction type. Even within these subcategories, further differences exist in terms of liner and liner anchorage details, reinforcing and, prestressing details, etc. It is safe to say that no two containments, even so-called twin units, are identical.

Around the world, a larger variety of primary systems are used for nuclear power generation. In addition to light-water systems, a number of plants use gas, heavy water or, in a few, liquid metal, as the primary coolant. **Most** of these plants use some type of containment or confinement structure in a variety of configurations. Most are made of steel or reinforced concrete in a variety of shapes ranging from steel spheres to double wall reinforced or prestressed concrete, unlined or with steel or epoxy liners. It is beyond the scope of this report to investigate the full range of containment types in the world-wide fleet, however, a more thorough review of these designs may prove useful for any new plant construction in the US.

**Table 1**                      **Number of U.S. Containments by Type**

<b>Containment Type</b>	<b>Number</b>
PWR Large Dry	53
PWR Subatmospheric	7
PWR Ice Condenser	9
Total PWRs	69
BWR Mark I	22
BWR Mark II	8
BWR Mark III	4
Total BWRs	34
<b>US Total</b>	<b>103</b>

A database of US containments prepared by Sandia provides more extensive information about each containment in the fleet [9]. A brief description of each of the six basic US containment types follows.

*Large Dry PWR*

A large dry containment (Figures 1 and 2) is designed to contain the blow-down mass and energy from a large break LOCA, assuming any single active failure in the containment heat removal systems. These systems may include containment sprays and/or fan coolers, depending on the particular design. Large dry containments can be of either concrete or steel construction. All US concrete containments have steel liners to assure leak tightness. (Some non-US concrete containments are unlined or include non-metallic liners.) Large dry (and all other) containments have a large, thick basemat that provides seismic capability, supports the structures, and, while not designed for this, may serve to contain molten material during a severe accident.

*Subatmospheric PWR*

Subatmospheric containments (Figure 3) are very similar to large dry containments. The major difference is that the containment is maintained at a negative pressure (~ 5 psi or 35 kPa) with respect to the outside atmosphere. This negative pressure means that leakage during normal operation is into the containment rather than to the atmosphere. Further, this negative pressure provides some additional margin for response to design basis accidents, and therefore the design pressure and/or volume can be reduced accordingly. Keeping the containment at a subatmospheric pressure also means that any significant containment leaks will be readily detected, when maintaining the negative pressure becomes more difficult.

*Ice Condenser PWR*

Ice condenser containments (Figure 4) are constructed of either concrete or steel. Ice condenser containments are the only PWR containments that rely primarily on passive pressure suppression. The containment consists of an upper and a lower compartment connected through an ice bed. In the event of a design basis LOCA, steam flows from the break, into the lower compartment, and up into the ice beds where most of the steam is condensed. Return air fans maintain a forced circulation from the upper to lower compartments, enhancing flow through the ice beds. One-



way doors are present at the entrance and exit of the ice bed region. These doors open upon slight pressure from the lower compartment, but close if air flow occurs in the reverse direction.

**Table 2 PWR Containment Construction Types**

Large Dry Primary Containment	Steel Cylinder	Steel Cylinder with Reinforced Concrete Shield Building	Kewaunee Prarie Island 1 Prarie Island 2 Davis-Besse St. Lucie 1 St. Lucie 2 Waterford 3	Arkansas 1 Arkansas 2 Oconee 1 Oconee 2 Oconee 3 Crystal River 3 Three Mile Island 1 Calvert Cliffs 1 Calvert Cliffs 2 Palisades Palo Verde 1 Palo Verde 2 Palo Verde 3 San Onofre 2 San Onofre 3 Braidwood 1 Braidwood 2 Byron 1 Byron 2 Callaway Farley 1 Farley 2 Point Beach 1 Point Beach 2 South Texas 1 South Texas 2 Summer Turkey Point 3 Turkey Point 4 Vogtle 1 Vogtle 2 Wolf Creek
	Reinforced Concrete Cylinder with Steel Liner	Reinforced Concrete Cylinder with Steel Liner	Comanche Peak 1 Comanche Peak 2 Diablo Canyon 1 Diablo Canyon 2 Indian Point 2 Indian Point 3 Salem 1 Salem 2 Shearon Harris 1	
		Reinforced Concrete Cylinder with Steel Liner and Secondary Containment	Seabrook 1	
	Posttensioned Concrete Cylinder with Steel Liner	1-D Vertical Posttensioned Concrete Cylinder with Steel Liner	GINNA HB Robinson	
		Diagonal Posttensioned Concrete Cylinder with Steel Liner	Fort Calhoun	
		3-D Posttensioned Concrete Cylinder with Steel Liner		
		3-D Posttensioned Concrete Cylinder with Steel Liner and Secondary Containment	Millstone 2	
	Subatmospheric Primary Containment	Reinforced Concrete Cylinder with Steel Liner	Beaver Valley 1 Beaver Valley 2 North Anna 1 North Anna 2 Surry 1 Surry 2	
		Reinforced Concrete Cylinder with Steel Liner	Millstone 3	
	Ice Condenser Primary Containment	Steel Cylinder with Reinforced Concrete Shield Building	Sequoyah 1 Sequoyah 2 Watts Bar 1 Catawba 1 Catawba 2 McGuire 1 McGuire 2	
Reinforced Concrete Cylinder with Steel Liner		DC Cook 1 DC Cook 2		

**Table 3 BWR Containment Construction Types**

<b>Free Standing Steel Primary Containment</b>	<b>Mark I Steel Drywell &amp; Wetwell</b>	<b>Nine Mile Point 1 Oyster Creek Dresden 2 Dresden 3 Monticello Pilgrim 1 Quad Cities 1 Quad Cities 2 Browns Ferry 1 Browns Ferry 2 Browns Ferry 3 Cooper Duane Arnold Fermi 2 Fitzpatrick Hatch 1 Hatch 2 Hope Creek 1 Peach Bottom 2 Peach Bottom 3</b>
	<b>Mark II Steel Drywell &amp; Wetwell</b>	<b>Columbia</b>
	<b>Mark III Reinforced Concrete Drywell Steel Wetwell</b>	<b>Perry 1 Riverbend 1</b>
<b>Reinforced Concrete Primary Containment with Steel Liner</b>	<b>Mark I Reinforced Concrete Drywell &amp; Wetwell</b>	<b>Brunswick 1 Brunswick 2</b>
	<b>Mark II Reinforced Concrete Drywell &amp; Wetwell</b>	<b>Limerick 1 Limerick 2 Susquehanna 1 Susquehanna 2 Nine Mile Point 2</b>
	<b>Mark III Reinforced Concrete Drywell &amp; Wetwell</b>	<b>Clinton 1 Grand Gulf 1</b>
<b>Post-tensioned Concrete Primary Containment with Steel Liner</b>	<b>Mark II Reinforced Concrete Drywell Posttensioned Wetwell</b>	<b>LaSalle 1 LaSalle 2</b>

The ice beds are more than adequate to limit the peak pressure from a design-basis LOCA. However, in a long-term accident, the ice will eventually melt and containment heat removal will be required. Thus, containment sprays are provided in the upper compartment of the containment. Water from the sprays drains through sump drain lines, down into the lower compartment sump, where it can be recirculated for long term heat removal.

#### *BWR Mark I*

The Mark I is a pressure suppression containment (Figure 5), which allows the containment to be smaller in volume. The containment is divided into the drywell containing the reactor vessel and the wetwell (torus) containing the suppression pool. The containments are constructed of either concrete or steel. The water in the suppression pool acts as an energy absorbing medium in the event of an accident. If a LOCA occurs, steam flows from the drywell through a set of vent lines and downcomers into the suppression pool, where the steam is condensed. Steam can also be released from the reactor vessel through the safety relief valves and associated piping directly into the suppression pool. In the event that the pressure in the wetwell exceeds the pressure in the drywell, vacuum breakers are provided that equalize the pressure. Mark I containments are equipped with lines connected to the wetwell that can be used to vent the containment if the pressure becomes too high.

#### *BWR Mark II*

Mark II containments (Figures 6 through 9) are similar in concept to Mark I containments. The suppression pool design is simplified, and the entire containment structure is more unified. Instead of the complicated torus design included in the Mark I containment, the suppression pool simply sits in the wetwell region below the drywell. Containment heat removal systems (sprays and suppression pool cooling) are the same as for the Mark I containments. Containment venting can also be performed in a similar fashion to the Mark I containments.

#### *BWR Mark III*

The Mark III design (Figures 10 and 11) is an intermediate-sized containment, much like the ice condenser containment. Mark III containments can be freestanding steel or steel-lined concrete. These containments have a drywell that functions much as the older designs, but have a larger surrounding containment that includes the wetwell. In the Mark III design, the suppression pool is located in an annular region outside the drywell. If the pressure in the outer containment exceeds the pressure in the drywell, then vacuum breakers open to equalize the pressure. Long-term containment heat removal can be accomplished with suppression pool cooling or by containment sprays (with appropriate circulation of the water through heat exchangers) in the outer containment. An important asset of the Mark III design is construction of the outer containment around the drywell, effectively providing a double layer of protection. If containment failure were to occur, in many cases the outer containment would fail first, leaving the drywell and suppression pool intact. Any subsequent fission product releases would still be scrubbed as they passed through the suppression pool, greatly reducing the source term. Thus, the only accidents (other than bypass sequences) likely to produce large source terms must involve failure of the outer containment plus either loss of the suppression pool or failure of the drywell.

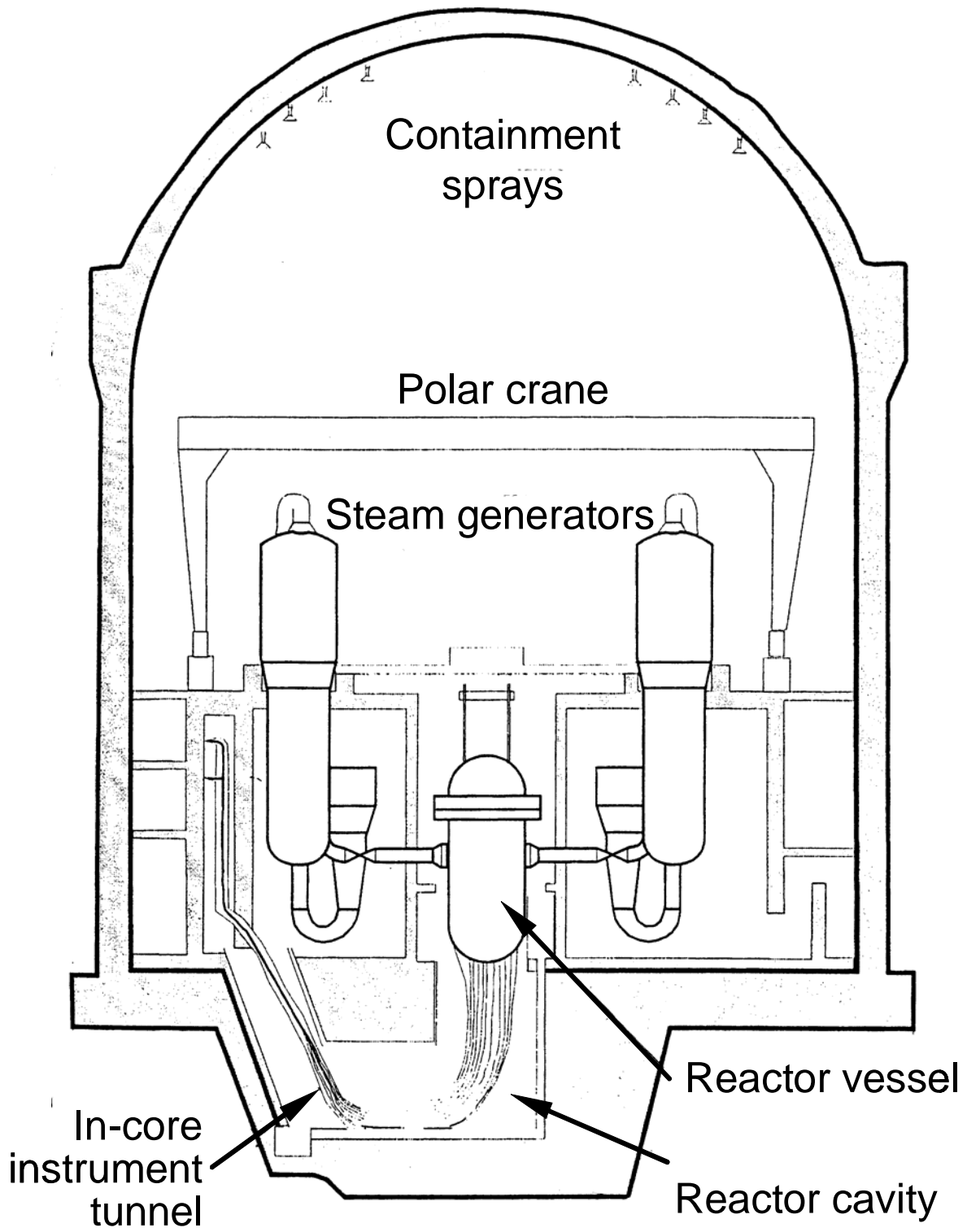


**Figure 1** Typical PWR Large Dry Containment with Prestressed Containment (e.g. Palisades)

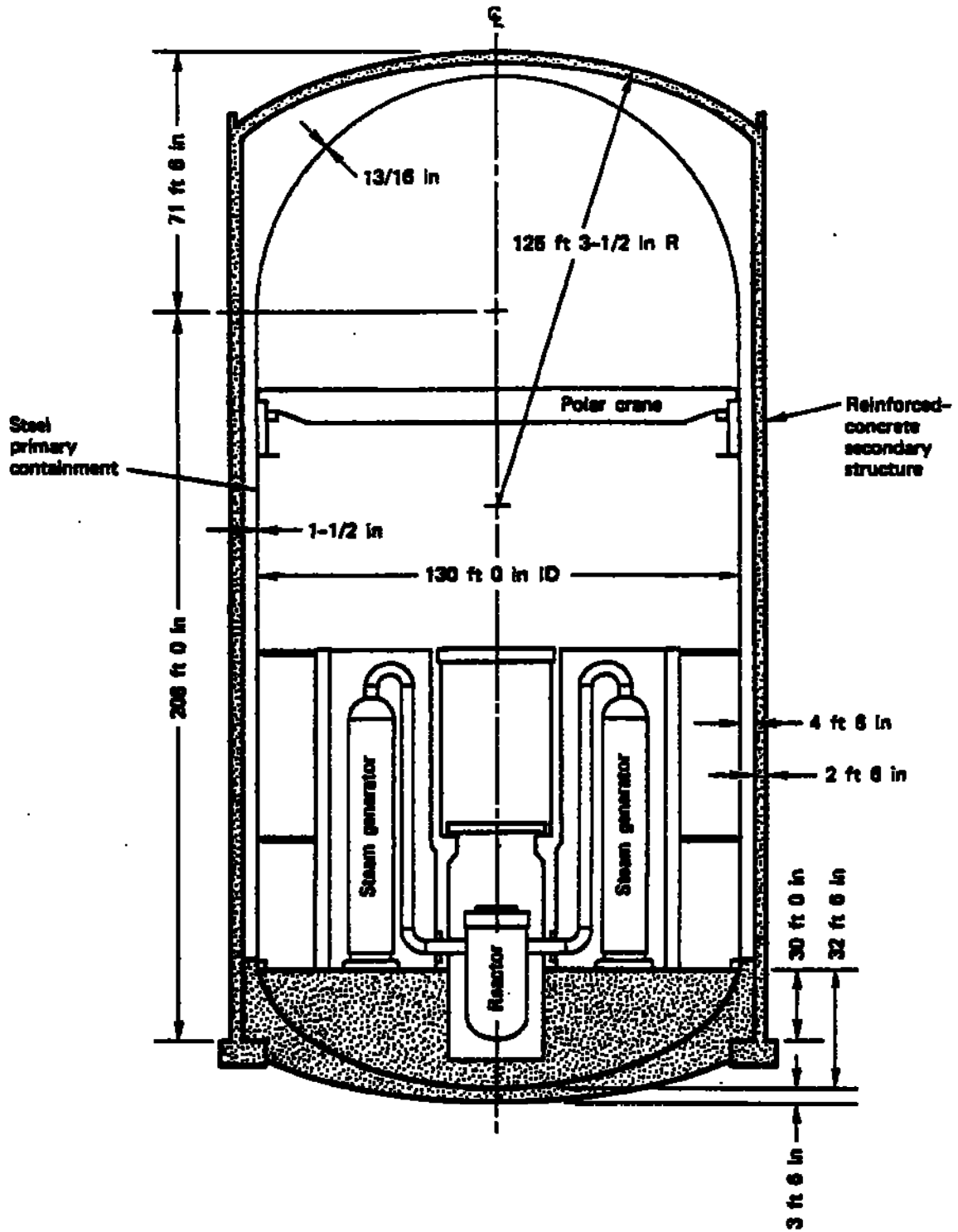


Figure 2 Large Dry Steel Containment with Reinforced Concrete Shield Building (e.g. Davis-Besse)

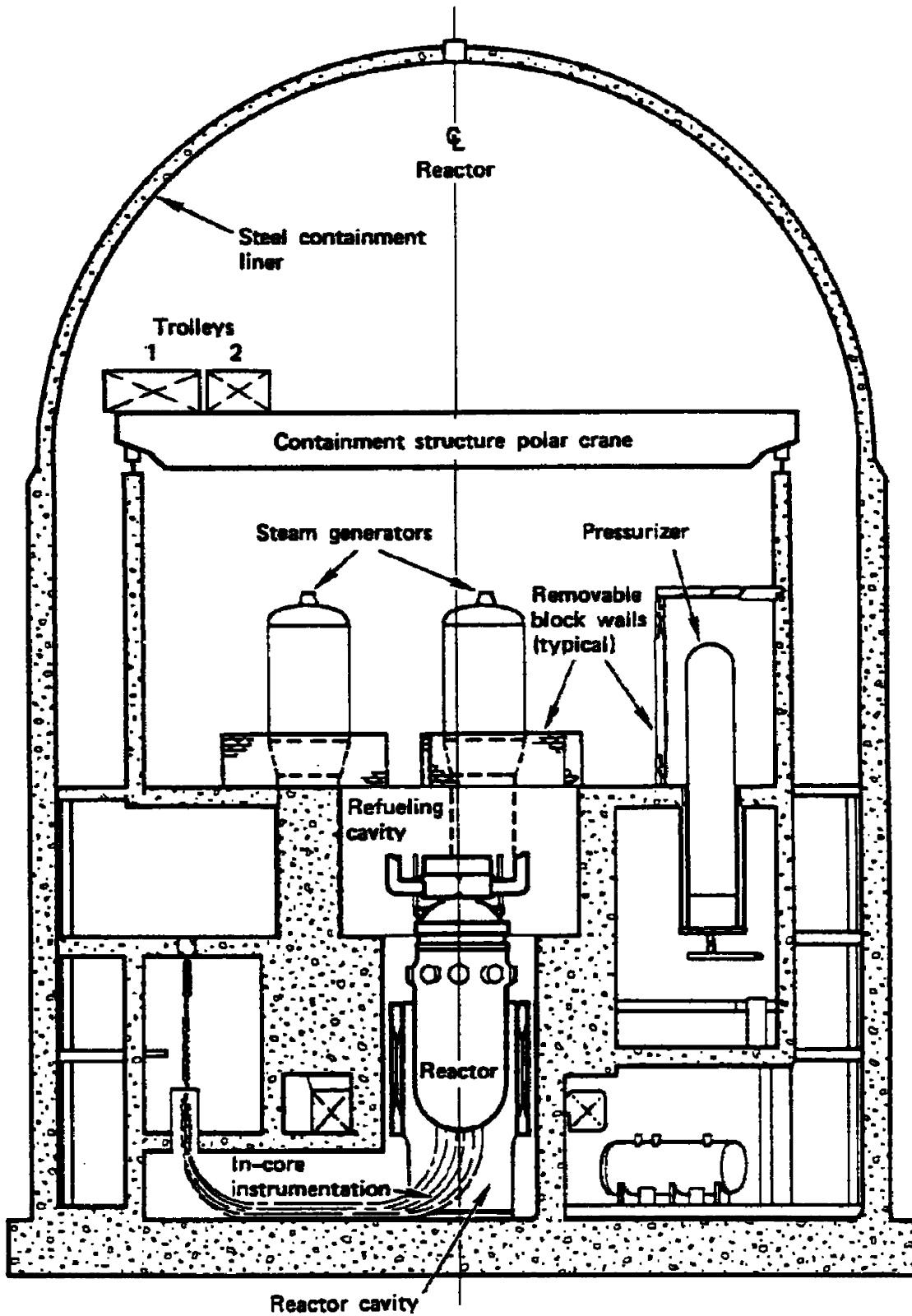


Figure 3 Typical PWR Subatmospheric Reinforced Concrete Containment (e.g. Diablo Canyon)

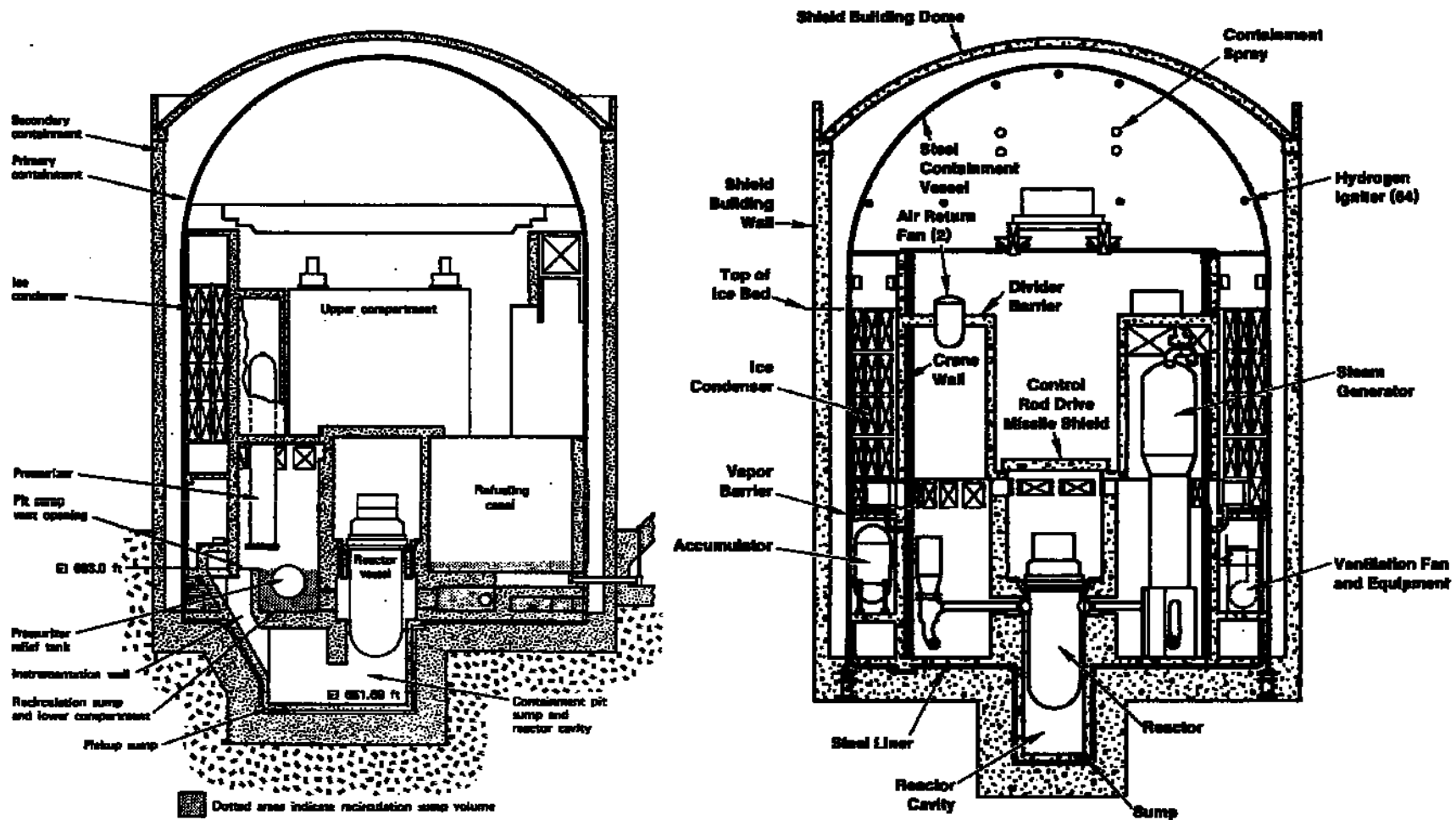


Figure 4 Typical PWR Ice Condenser Steel Containment with Concrete Shield Building (e.g. Sequoyah)

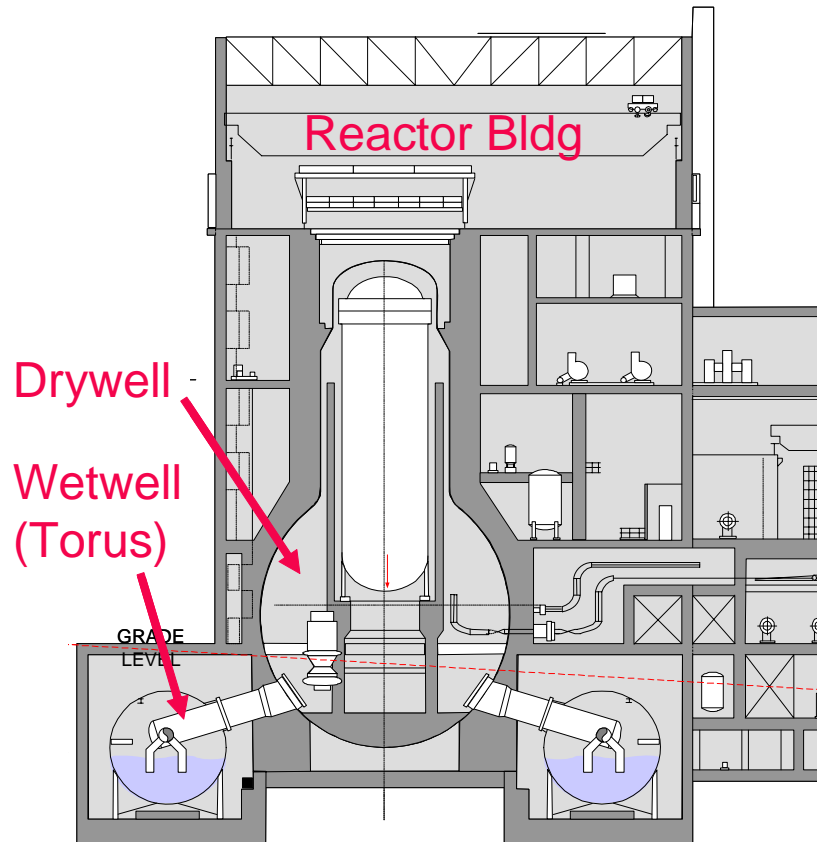
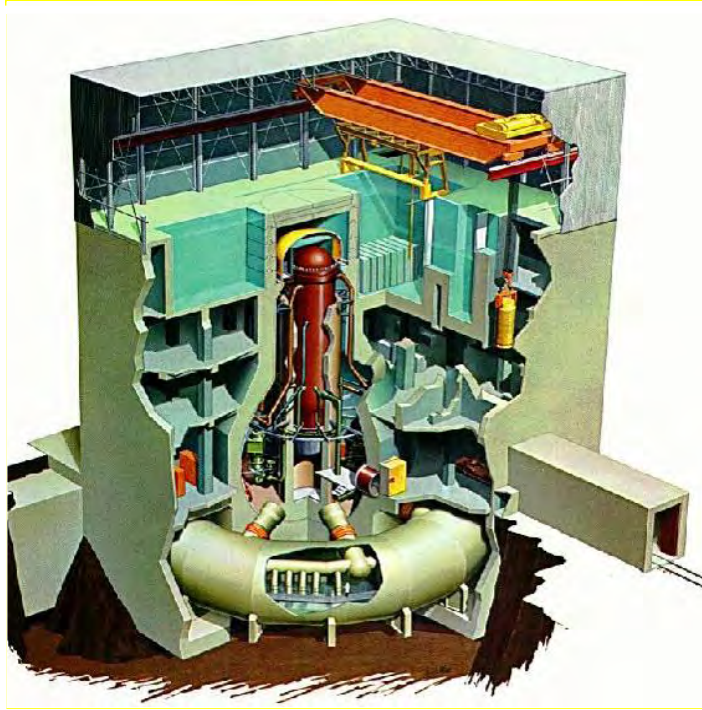
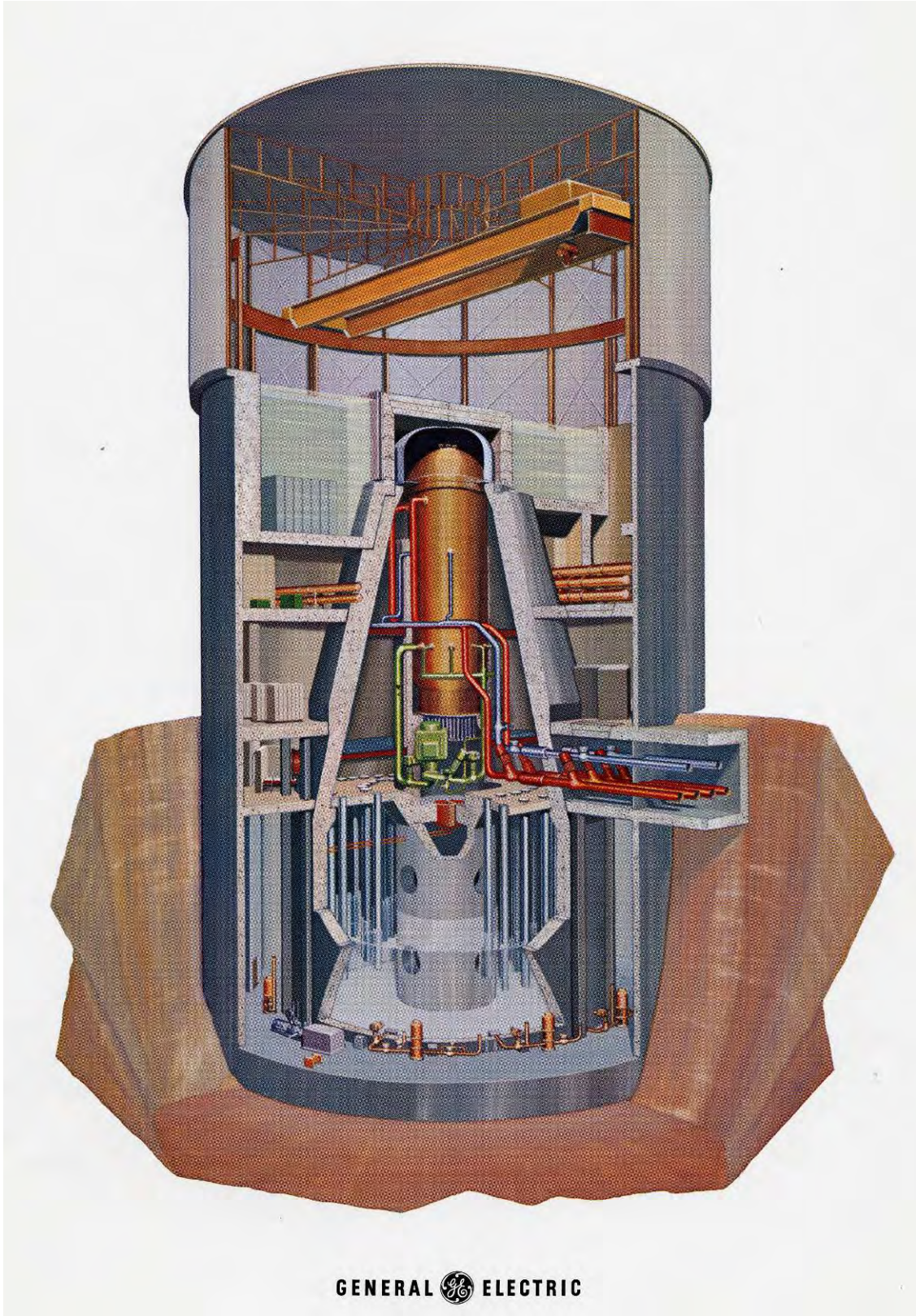
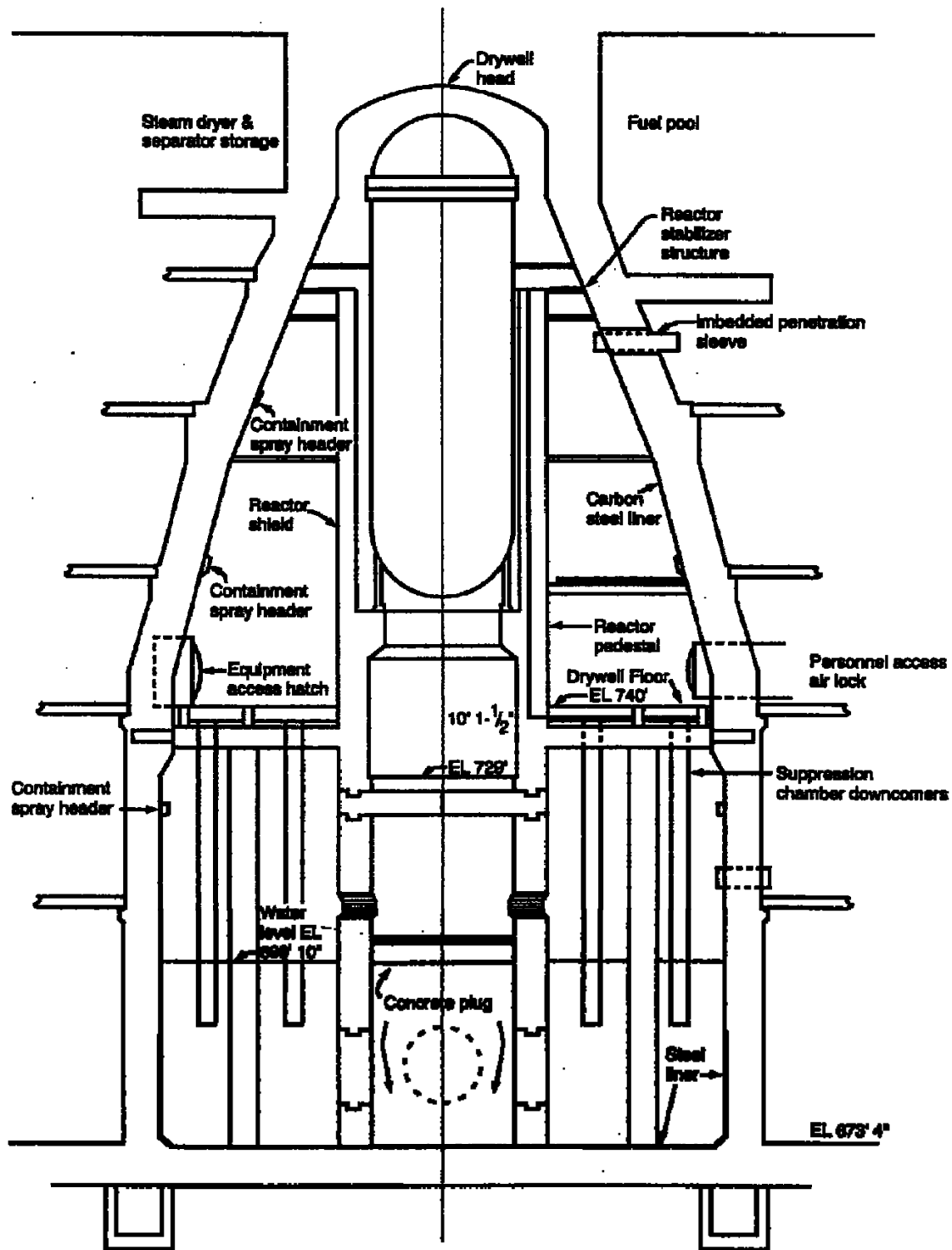


Figure 5 Typical BWR Mark I Concrete Containment with Steel Torus





**Figure 6** Typical BWR Mark II Containment [1]



P801

Figure 7 BWR Mark II Concrete Containment (LaSalle Units 1 & 2)

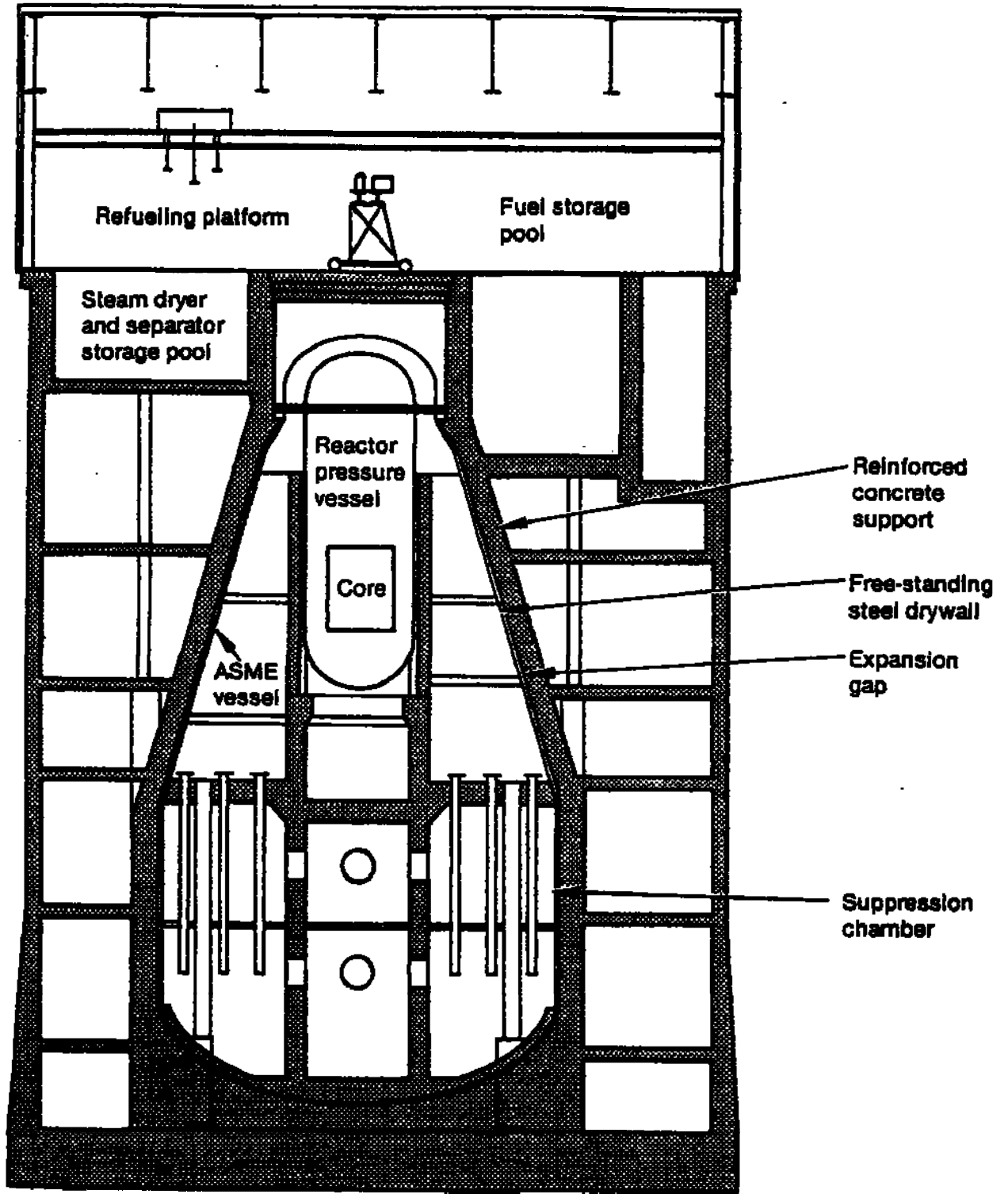


Figure 8 BWR Mark II Steel Containment with Concrete Shield Building (Columbia, previously WNP-2)

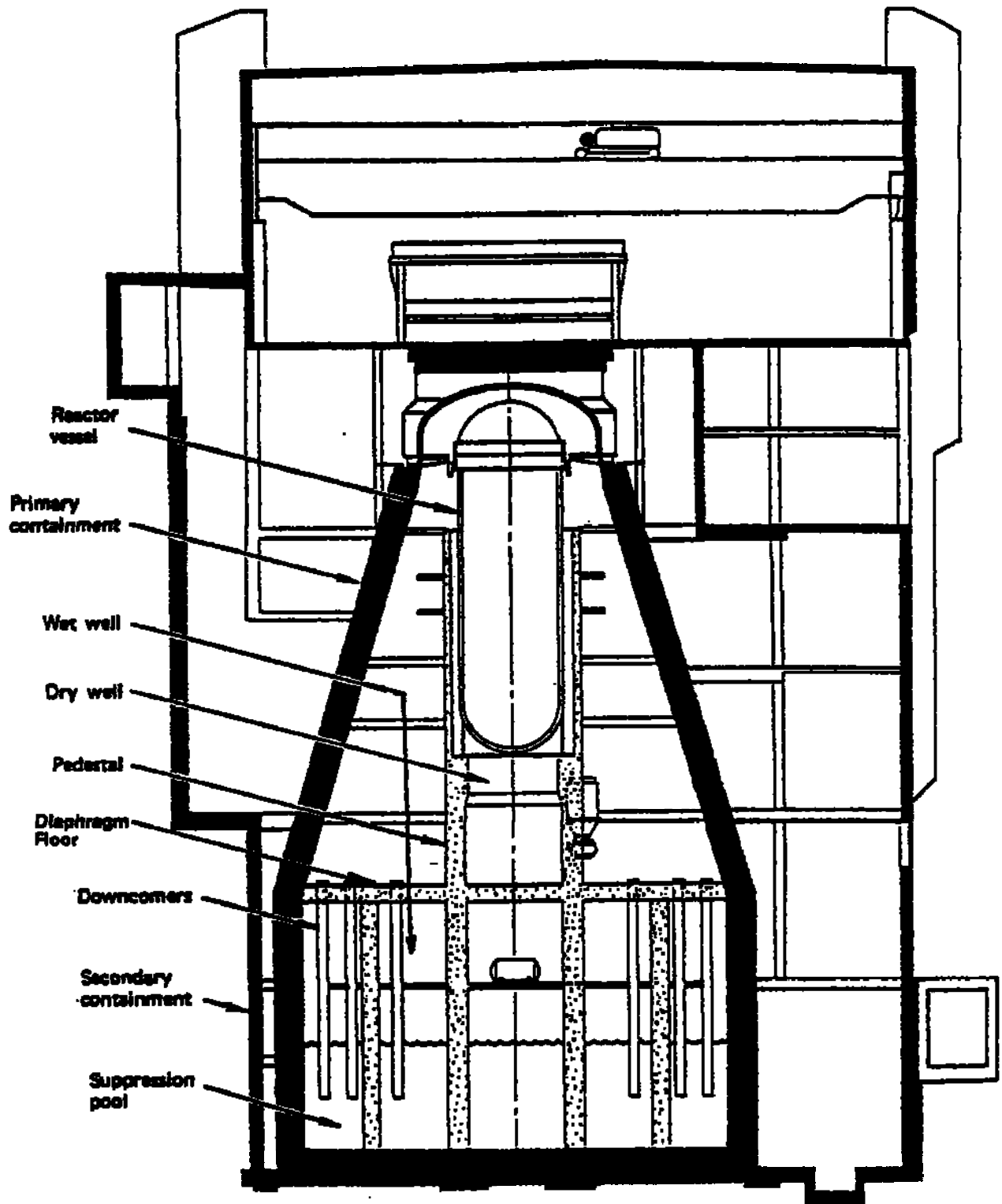
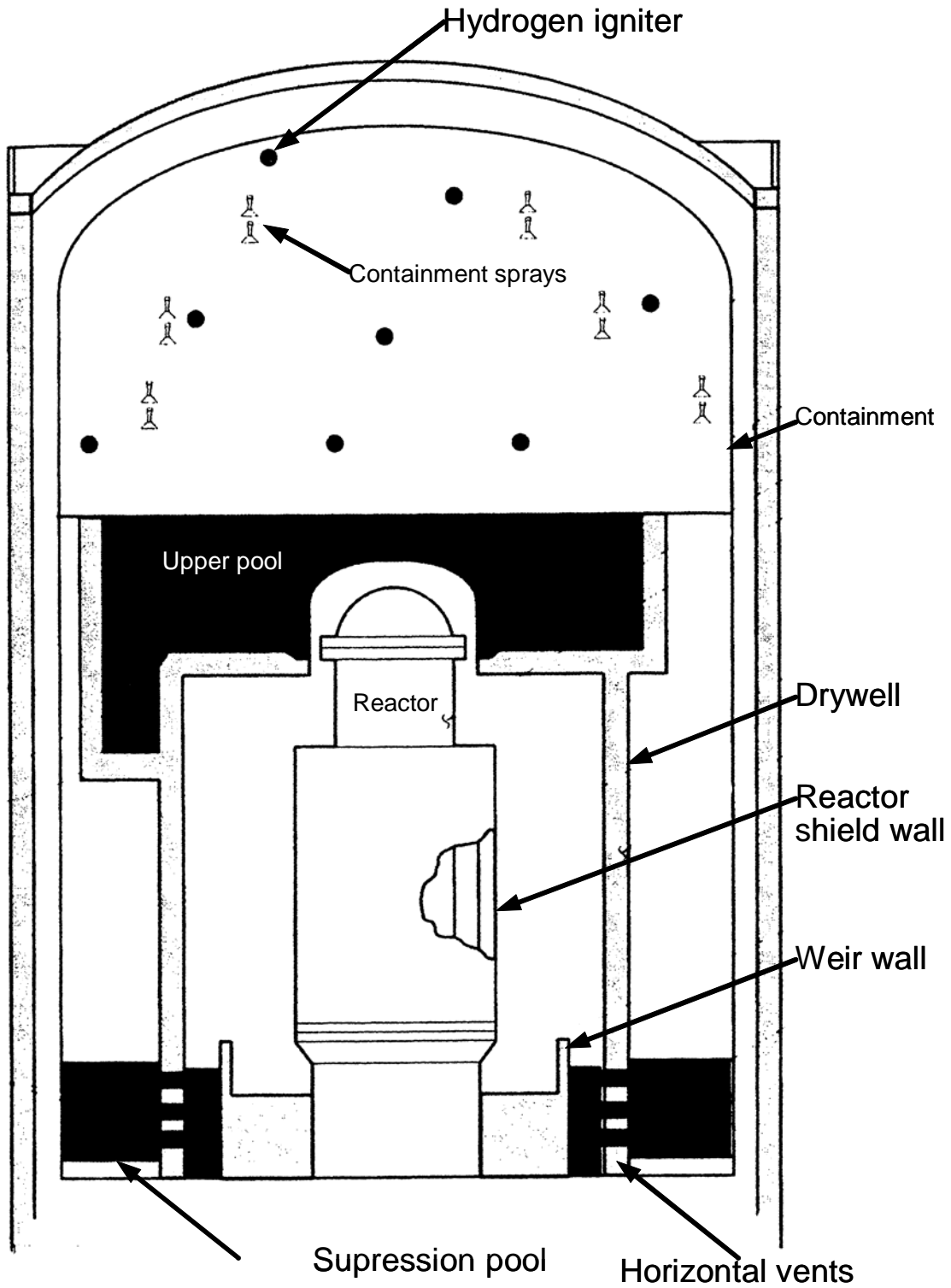


Figure 9 BWR Mark II Reinforced Concrete Containment (Limerick 1 & 2)



**Figure 10** Typical BWR Mark III Containment  
 Freestanding Steel with Concrete Shield Building  
 (Perry, Riverbend)

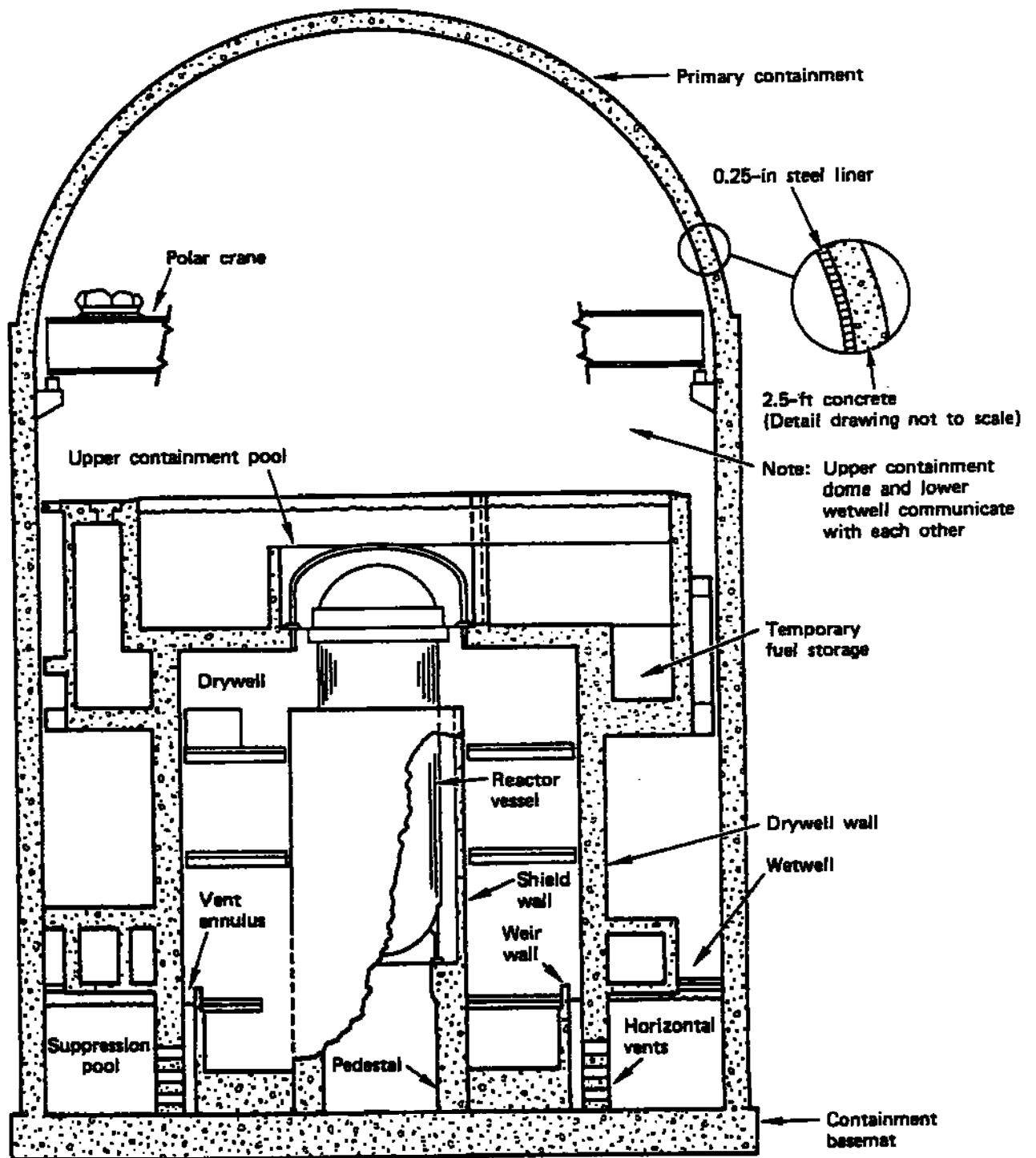


Figure 11 Typical BWR Mark III Containment Reinforced Concrete with Steel Liner (Clinton, Grand Gulf)

### 2.2.2 Containment Design

The containment is often thought to consist of only the structural concrete and/or steel shell surrounding the nuclear steam supply system. In reality the containment not only includes the structural shell and basemat, but also all of the penetrations (fixed and operable) and any other component which completes the pressure boundary. Any evaluation of containment integrity must also include an evaluation of these penetrations. The containment system is primarily designed to:

1. Contain any radioactive material that may be released from the primary system in case of an accident.
2. Protect the nuclear system from weather and other external threats such as missiles produced by earthquakes, tornadoes, wind, and in some cases aircraft impact.
3. Act as a supporting structure for operational equipment, e.g. cranes.

Until 1965, there were no written criteria for design and review of all commercial power reactor licenses was on a case-by-case basis. In 1965, the AEC issued the first draft of the General Design Criteria, Appendix A of 10 CFR 50. (10 CFR Part 50 specifies the regulations promulgated by the Nuclear Regulatory Commission pursuant to the Atomic Energy Act of 1954 to provide for the licensing of production and utilization facilities.) The final version of Appendix A, published in 1971, did not require the containment to be designed to withstand a full core meltdown (as the original draft had). The first five criteria define overall requirements for quality assurance and protection against natural phenomena, fire, environmental and dynamic effects (including loss of coolant accidents), and sharing of systems, structures and components. Criterion 1, *Quality standards and records*, requires, in part, that

*“Structures, systems, and components important to safety shall be designed, fabricated, erected, and tested to quality standards commensurate with the importance of the safety functions to be performed. Where **generally recognized codes and standards are used**, they shall be identified and evaluated to determine their applicability, adequacy, and sufficiency and shall be supplemented or modified as necessary to assure a quality product in keeping with the required safety function.”*

Criterion 16, *Containment Design* states:

*“Reactor containment and associated systems shall be provided to establish an **essentially leak-tight barrier** against the uncontrolled release of radioactivity to the environment and to assure that the containment design conditions important to safety are not exceeded for as long as postulated accident conditions require.”*

Criteria 50 through 57 give specific requirements for reactor containment. These criteria address the containment design basis, testing and inspection requirements and containment isolation requirements.

10 CFR 50.55a, *Codes and Standards*, specifies that structures, systems and components of boiling and pressurized, water-cooled nuclear power reactors must be designed, fabricated, erected, constructed, tested, and inspected according to the requirements of the ASME Boiler and Pressure Vessel (B&PV) Code [10] as amended by NRC Regulatory Guide 1.84, *Design and Fabrication and Materials Code Case Acceptability, ASME Section III*. The ASME publishes a new edition of the B&PV Code, which includes Section III for nuclear power, every 3 years, and

new addenda every year. The latest editions and addenda of Section III that have been approved for use by the NRC are referenced in 10 CFR 50.55a(b). The ASME also publishes Code Cases quarterly. Code Cases provide alternatives developed and approved by ASME or explain the intent of existing Code requirements. Reg. Guide 1.84 identifies the Code Cases that have been determined by the NRC to be acceptable alternatives to applicable parts of Section III.

Division 1, Subsection NE of Section III “establishes rules for material, design, fabrication, examination, inspection, testing and preparation or reports for metal containment vessels” or Class MC Components. Regulatory Guide 1.57 specifies the ‘Design Limits and Loading Combinations for Metal Primary Reactor Containment System Components’.

Division 2 (comprised of Subsection CC) of Section III “establishes rules for material, design, fabrication, construction, examination, testing, marking, stamping, and preparation or reports for prestressed and reinforced containments”. The containments covered by Subsection CC include the “structural concrete pressure resisting shells and shell components, shell metallic liners and the penetrations liners extending the containment liner through the surrounding shell concrete”. Subsection CC applies for containments having a design pressure greater than 5 psi (35 kPa). For “parts and appurtenances of concrete containments not backed by structural concrete for load carrying purposes, the rules of Division 1 apply”.

Section III, Division 2 was prepared and is maintained by the Joint ACI-ASME Technical Committee on Concrete Components for Nuclear Service under the sponsorship of the American Concrete Institute and the American Society of Mechanical Engineers. Basis documents prepared independently by ACI and ASME committees were merged in 1972 and published as a proposed standard for Concrete Reactor Vessels and Containments which became Section III, Division 2 in 1973. This standard is also designated as ACI 359, *Concrete Components for Nuclear Reactors*. Provisions for concrete reactor vessels, which comprised Subsection CB of Division 2, were removed from the B&PV Code in 1990.

ASCE Manual No. 58 [11] and Klamers, et. al., [12] provide comprehensive summaries and comparison of the design practices for both steel and reinforced concrete containments. Without repeating these summaries, a few significant observations are worth noting. Historically, design practices for steel containments (Division 1) were developed solely by ASME which treats them as pressure vessels and specifies allowable stresses for the prescribed loads. Design practices for concrete containments (Division 2), which were developed primarily by ACI and ASME, treats them as a structure. This approach combines the ACI practice of applying Load Factors (ranging from 1.0 to 1.5 per Table CC-3230-1) to the design loads in consideration of their importance to safety, while retaining the concept of allowable stresses used by ASME. This difference in approach, leads to some inherent differences in design margin between steel and concrete containments, depending on the mode of failure.

Application reviews for commercial power reactor construction and operating licenses are based on the preliminary and final safety analysis reports prepared by the licensees. Regulatory Guide 1.70, “Standard Format and Content of Safety Analysis Reports for Nuclear Power Plants” specifies the requirements for these safety analysis reports (SARs). NUREG-0800, “Standard Review Plan (SRP) for the Review of Safety Analysis Reports for Nuclear Power Plants” describes the criteria used by the NRC to review the SARs. Chapter 3.8.1 of the SRP specifies the extent of compliance with Subsection CC-3000 of Section III, Division 2 for concrete containments. Chapter 3.8.2 specifies the extent of compliance with Subsection NE of Section III, Division 1 and with Regulatory Guide 1.57 for steel containments. The applicants are also required to identify the potential accident initiating events in Chapter 15 of the SAR. The design-basis accident (DBA) is the postulated set of failure events that the plant is designed and built to



withstand without exceeding the offsite exposure criteria (10 CFR 100). The containment is designed to have a very low leakage rate when subjected to the maximum internal pressure predicted for the DBA. Typical containment volumes and design pressures for the six types of US containments are shown in Figure 12.

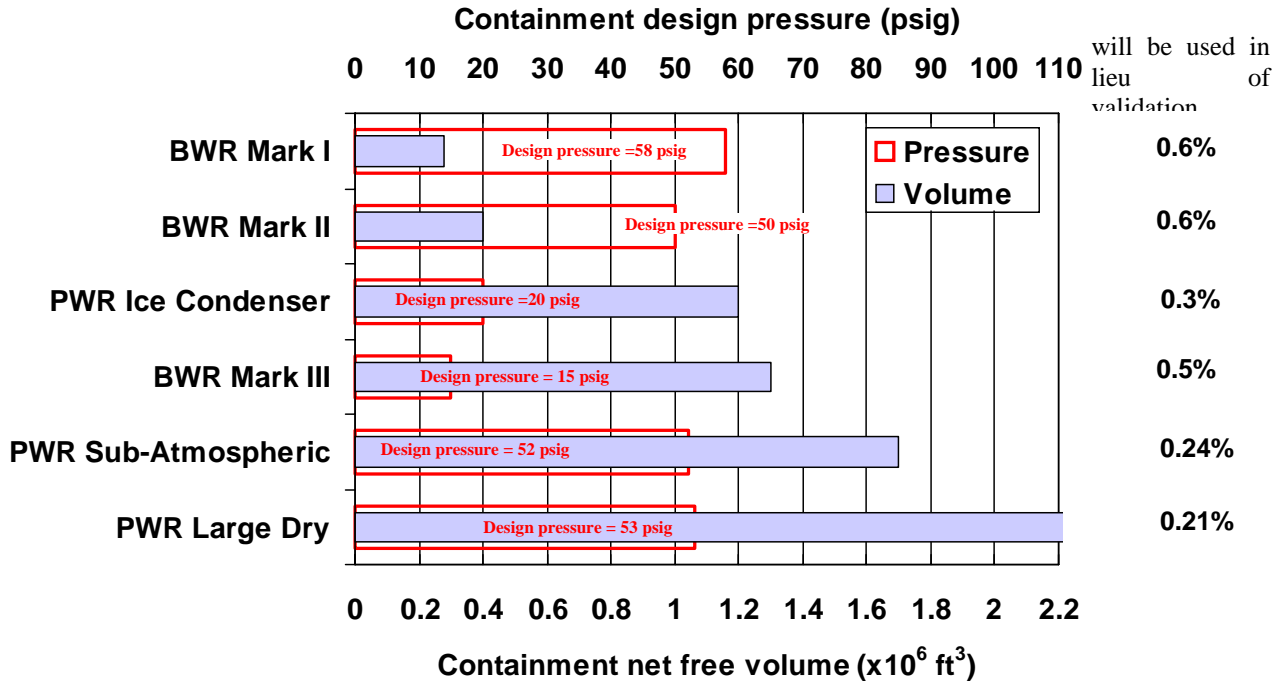


**Figure 12 Typical Containment Volume and Design Pressure for US plants [1]**

Containment leakage rates are determined in the SAR and Technical Specifications. Figure 12 also shows the typical maximum leakage rates for each type of containment. Leakage rates are typically described in terms of a percentage of the total containment atmosphere mass or weight leaked over a 24 hour day. Criteria for testing containment leakage are set forth in 10 CFR 50, Appendix J. This appendix became effective in 1973. Its purpose is to implement, in part, 10 CFR 50, Appendix A, General Design Criteria 16 which mandates “an essentially leak-tight barrier against the uncontrolled release of radioactivity to the environment ...” for postulated accidents.

The design loads and their combinations as well as the response limits are specified in NRC Reg. Guide 1.57 (for steel containments), the ASME B&PV Code Section III, Div. 2 and the SRP. There are other types of loads that must be considered in the design. These loads include:

1. temperature transients and gradients
2. safe shutdown earthquake loads
3. internal and external missiles
4. mechanical loads from pipe rupture

5. external pressures
6. winds and tornadoes.

Severe accidents are not part of the design bases, due to their perceived low probability of occurrence, and pressure relief valves on the containment are not required (although Mark I and Mark II BWR containments include vents, as noted).

### **2.2.3 Containment Response to Severe Accidents**

As noted in Section 1.1.1, the most exhaustive study of the risks of severe accidents to date is the benchmark study, NUREG-1150 [7]. NUREG-1150, hereafter referred to as the Risk Study, was a detailed assessment of the risks of severe accidents at five plants:

- Zion, a large dry PWR
- Surry, a subatmospheric PWR
- Sequoyah, and ice condenser PWR
- Peach Bottom, a Mark I BWR and
- Grand Gulf, a Mark III BWR

An analysis of LaSalle, a Mark II BWR was performed in a separate study [13].

These plants were selected as representative examples of the US fleet. A variety of internal (equipment failure, operator error) and external (earthquakes) initiating events were investigated to estimate the frequency of severe accidents. Plant performance models, which took into account containment response and other mitigating features, were coupled with probabilistic risk assessment (PRA) to determine accident consequences in terms of health effects and property damage.

Since the containment building constitutes the ultimate barrier between the in-plant environment and the outside atmosphere, its performance during a severe accident has a substantial impact on the severe accident risk characteristics of the plant. Uncertainty regarding the capability of a containment is, therefore, an important contributor to the uncertainty in risk. In risk models, determining containment performance involves assessing the probability that the containment would 'fail' under a range of severe accident conditions.

Containment failure probability is largely dependent on the individual containment design and the particular phenomena or load that challenges the integrity of the containment. Particular severe accident challenges to the containment include:

1. overpressure
2. dynamic pressure (shock waves)
3. internal missiles
4. external missiles

5. melt-through
6. bypass

While the last four challenges were recognized, the Risk Study focused on the response of the containment to overpressurization and the corresponding thermal loads. Some of the severe accident pressure loads can be quite rapid from a thermo-physical perspective (e.g. deflagrations, detonations, etc.) however, the rate of loading for most scenarios is essentially static from a structural perspective. (In addition to these severe accident challenges, other external threats from acts of terrorism or war can both challenge containment integrity as well as initiating core damage sequences.)

No precise definition of containment failure was given, however, it generally implied a loss of containment function (i.e. excess leakage) and not necessarily gross structural failure. For risk purposes, the containment was considered to have failed to perform its function when the leak rate of radionuclides to the environment is substantial (~10% mass/day). Thus, failure could occur as the result of a structural failure of the containment, tearing of the containment liner, or a high rate of a leakage through a penetration. Containment bypass was not considered containment failure in the risk study and the approach to characterizing failure sizes was subjective and based on a consideration of public health consequences.

In addition to the likelihood of failure, other critical factors in the characterization of containment performance in NUREG-1150 included:

- *Failure size:* The larger the hole in the containment, the more rapid the escape of radioactive material in the containment atmosphere to the outside environment. This reduces the time available for radioactive material to deposit within the containment building and also reduces the opportunity for effective offsite emergency response.

Three possible failure sizes were distinguished in the risk study: leak, rupture, and catastrophic rupture. Working quantitative definitions of each failure size were based on thermal-hydraulic evaluations of containment depressurization times.

- A leak was defined as a containment breach that would arrest a gradual pressure buildup but would not result in containment depressurization in less than 2 hours. (The 2 hour 'threshold' was likely based on consideration of minimum evacuation times.) The typical leak size was evaluated for all plants to be on the order of 0.1 ft<sup>2</sup>. (This estimate of leak size was subsequently revised to 0.3 ft<sup>2</sup> to 0.5 ft<sup>2</sup>)
  - A rupture was defined as a containment breach that would arrest a gradual pressure buildup and would depressurize the containment within 2 hours. For all plants, a rupture was evaluated to correspond to a hole size in excess of approximately 1.0 ft<sup>2</sup>.
  - A catastrophic rupture was defined as the loss of a substantial portion of the containment boundary.
- *Location of failure:* The retention of radioactive material by a breached containment building may be highly dependent upon the location of failure relative to containment systems designed to mitigate accident conditions. For example, in an ice condenser containment, failure of the containment in the lower compartment permits radioactive material to bypass the ice compartments while escaping to the outside environment. In contrast, containment failure in the upper compartment, provided the ice condenser is not degraded, requires that

radioactive material pass through the ice compartments before escaping to the outside. In the latter case, retention of material by the ice would substantially reduce the radioactive release.

- *Rate of loading:* The rate of loading may be important in determining the failure mode and the ultimate severity of the failure.
- *Time of failure:* If the containment function does fail, the timing of failure can be very important. The longer the containment remains intact relative to the time of core melting and radionuclide release from the reactor coolant system, the more time is available to remove radioactive material from the containment atmosphere by engineered safety features or natural deposition processes.

In evaluating the performance of a containment in NUREG-1150, it was convenient to consider no failure, late failure, bypass, and early failure of containment as separate categories characterizing different degrees of severity. For those plants in which intentional venting was an option, this was also represented as a separate category.

With this somewhat subjective definition of failure, a panel of experts from universities, industry and the national laboratories was assembled to provide estimates of containment structural performance subjected to predicted severe accident loads. The experts provided distributions that defined the probability of failure as a function of pressure and of the mode and location of failure. Previous structural evaluations of varying degree of sophistication for each plant (or a similar plant), supplemented by calculations performed by individual experts, were used in the elicitation process which provided the basis for quantification of containment failure probabilities for each plant.

The results of the expert estimates of the range of containment failure pressure are summarized in Appendix C.8 of NUREG-1150. Figure 13 shows the range of failure pressures. Table 4 adds a description of the dominant failure location. The detailed results of the expert elicitation are documented in a separate report [14]. The basis for the expert panel's estimates of the range of failure pressures for each plant is summarized below:

- |               |  |
|---------------|--|
| Zion:         | Prestressed concrete w/ steel liner, 1-2% strain in hoop tendons, shear at the wall base junction, both resulting in leakage although the possibility of rupture or catastrophic rupture were possible at the upper range of pressures   |
| Surry:        | Yielding of hoop rebar and tearing of steel liner resulting in leakage near the springline; possible leakage at penetrations; little consensus; catastrophic rupture at upper pressure, unlikely.  |
| Sequoyah:     | Free-standing steel; membrane failure in upper compartment at 2-10% strain resulting in rupture or catastrophic rupture; ovalization of equipment hatch resulting in leakage.  |
| Peach Bottom: | Steel Mark I; material failure in the drywell or wetwell, no specific criteria defined but strains in the range of 1% to 5% were proposed in the detailed report, resulting in leak and possibly catastrophic rupture; effects of high temperatures on material properties considered. |
| Grand Gulf:   | Reinforced Concrete with steel liner; Drywell design pressure 30 psi, Wetwell 15 psi; range of failure pressures was from approximately twice the design pressure to pressure resulting in ultimate hoop strength of the wetwell   |

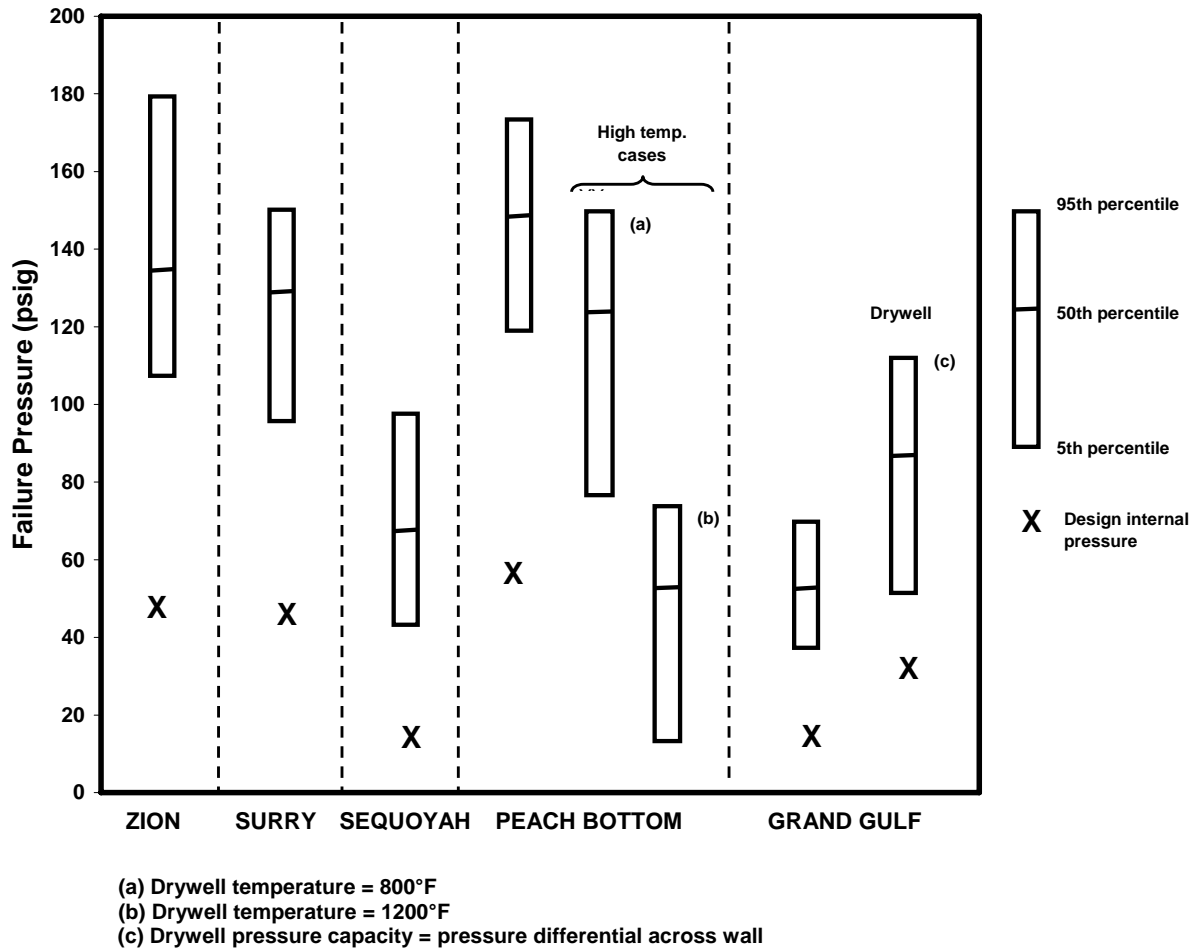


**Figure 13 Containment Failure Pressures for NUREG-1150 Plants [7]**

One of the documented review comments on the estimates of containment failure pressures stated:

*“Experimental data on the ultimate potential strength of containment buildings and their failure modes are lacking. This lack of data renders questionable the methods used in draft NUREG-1150 for assigning probabilities and locations of failure.”*

The author’s response included the following acknowledgement:

*“The present data on the potential strength of containment structures under severe accident loadings and the potential modes of failure are limited..”*

It should be noted that the Risk Study was conducted at the same time NRC-sponsored and other research into containment integrity and other severe accident processes were in progress. Some of the estimates of containment capacity were informed by some of the early results of this research, however, the bulk of the results of this research was not available and no comprehensive effort to integrate this research into the risk models have subsequently been made. The broad range of failure pressures shown in Figure 8 and Table 4 are not surprising given that it resulted from elicitation of panelists who had no agreed upon methodology for containment overpressure response assessment and no real consensus on the definition of failure. It should also be noted

that there has been criticism, by the utility side of the industry, of the failure sizes and consequence definitions. Some have argued that the very existence of a rupture or catastrophic rupture definition presupposes that such rupture sizes are possible, and counter that they are not possible for concrete containments due to the hypothesis of leak-before-break. These topics are discussed in more detail in later chapters, but are mentioned here for historical perspective.

**Table 4 Containment Strength Under Static Pressure[7]**

<b>Plant</b>	<b>Containment Free Volume (Millions of Cubic Feet)</b>	<b>Design Internal Pressure (psig)</b>	<b>Failure Pressure Range (a) (psig)</b>	<i>Sizes/Locations Dominant Failure</i>
Zion	2.6	47	108-180	Leak/rupture in cylinder wall or basemat/wall intersection
Surry	1.8	45	95-150	Leak/rupture near dome/wall intersection
Sequoyah	1.2	11	40-95	Gross rupture of the containment or rupture in the lower compartment
Peach Bottom	0.16 (drywell) 0.12 (wetwell)	56	120-174	Leak at drywell head or leak/rupture of wetwell
			high temp case: 75-150	(b) Leak at drywell head or in wetwell above suppression pool
			high temp case: 6-67	(c) Leak at drywell head or rupture of the drywell wall
Grand Gulf	0.27 (drywell) 1.4 (wetwell)	15	38-72	Leak/rupture near dome/wall intersection
		Drywell: 30	50-120	(d)

(a) 5<sup>th</sup>-95<sup>th</sup> percentile range

(b) Drywell temperature at 800°F

(c) Drywell temperature at 1200°F

(d) Drywell/wetwell pressure differential in psi

As noted previously, alongside NUREG-1150, the licensees were required to perform ‘Individual Plant Evaluations’ or IPEs [6]. The results of these IPEs included estimates of containment fragility, i.e. the cumulative containment failure probability for a given pressure. The fragilities reported by the licensees for each operating (and several closed) plants are summarized in the previously referenced Containment Data Base [9]. A cursory review of the containment overpressure fragility curves suggests considerable variation in: the definitions of failure used by the licensees; the failure modes and corresponding criteria considered; the methods used to calculate the response; and the methods used to incorporate uncertainty. The fragility curves summarized in the Containment Data Base represent the cumulative probability of containment failure as a function of overpressure, where failure is primarily characterized as either leak or rupture, although the application of these terms is not as rigorous as the definition in NUREG-1150.

It is beyond the scope of this report to perform a comprehensive review and comparison of the plant IPEs (and by extension the plant PRAs), however, the current (2005) emphasis on risk-informed regulation suggests that such a review could be an invaluable asset in ensuring a level of quality and consistency which is currently lacking. Furthermore, lessons learned from the experimental efforts described in Chapter 2, could be incorporated into improved estimates of containment fragility resulting in higher quality PRAs and risk-informed decision making.

With these caveats in mind, it is nevertheless worthwhile summarizing the containment fragility estimates for the current fleet of plants. Figures 14 through 21 show the normalized overpressure

fragility curves (where available) for the current fleet of US plants, grouped by reactor and containment type. These figures illustrate the large variation in overpressure fragility, even among similar containment types. This variation reflects further differences in containment design, even within each category, but also reflects the different approaches to estimating containment overpressure capacities and fragility.

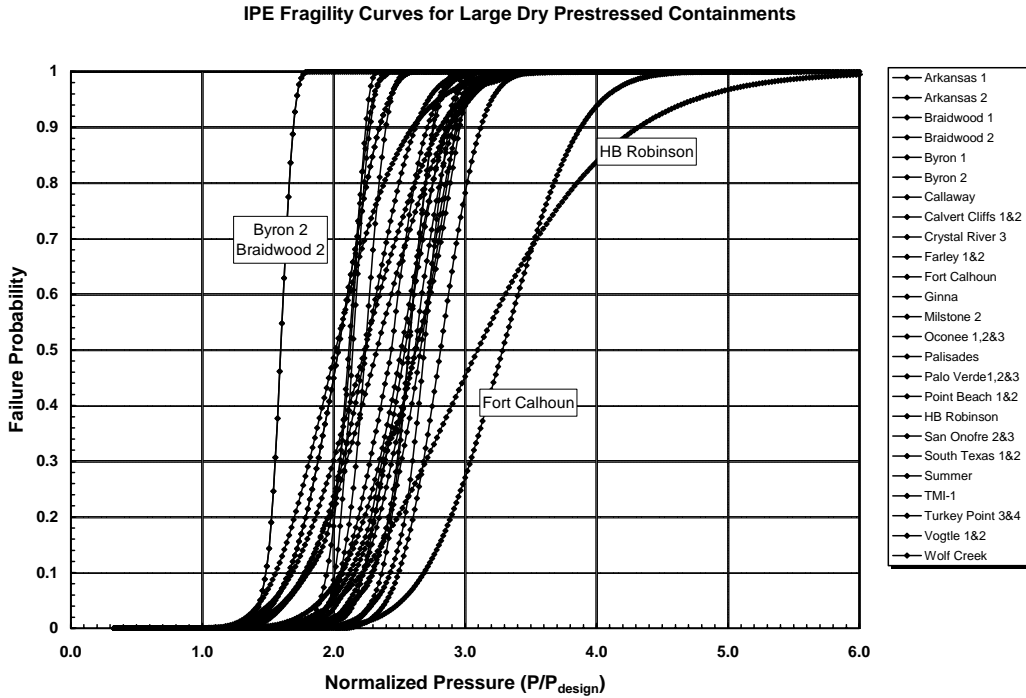


**Figure 14 IPE Fragility Curves for Large Dry Prestressed Concrete Containments**

IPE Fragility Curves for Large Dry Reinforced Concrete Containments

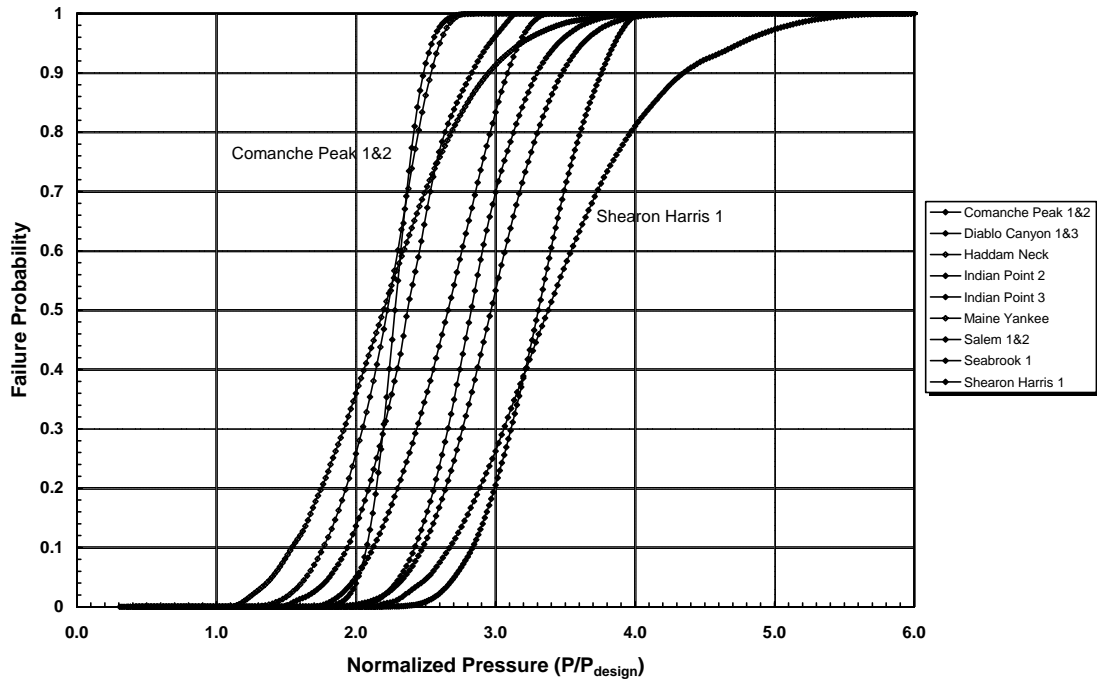


Figure 15 IPE Fragility Curves for Large Dry Reinforced Concrete Containments

IPE Fragility Curves for Large Dry Steel Containments

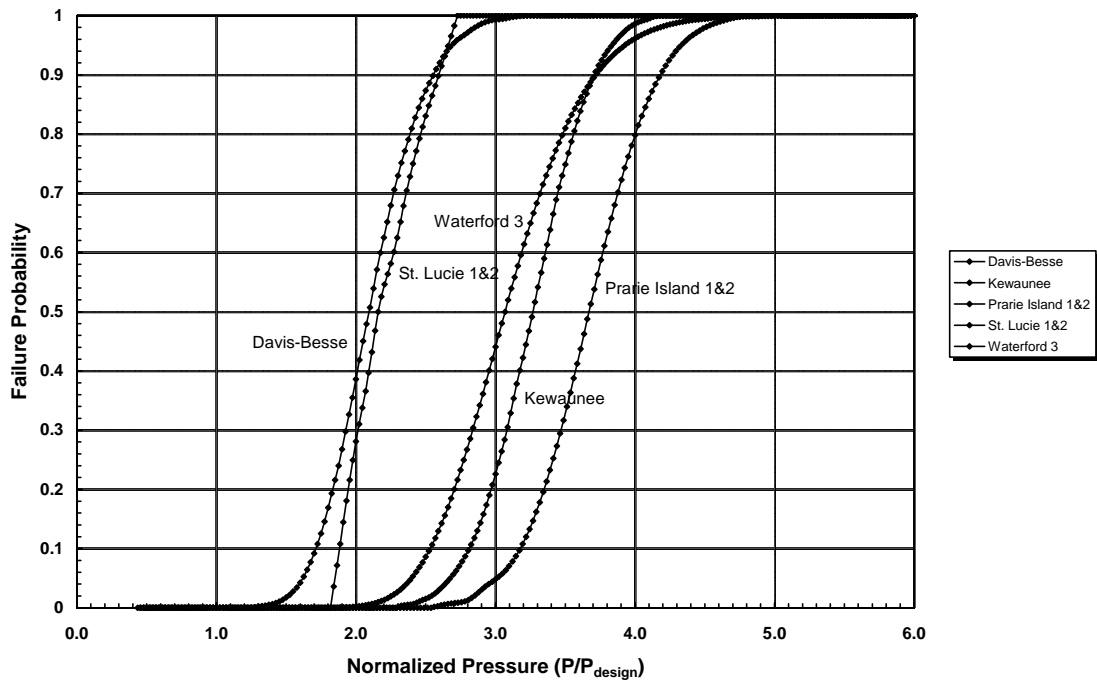


Figure 16 IPE Fragility Curves for Large Dry Steel Containments



IPE Fragility Curves for Ice Condenser Reinforced Concrete and Steel Containments

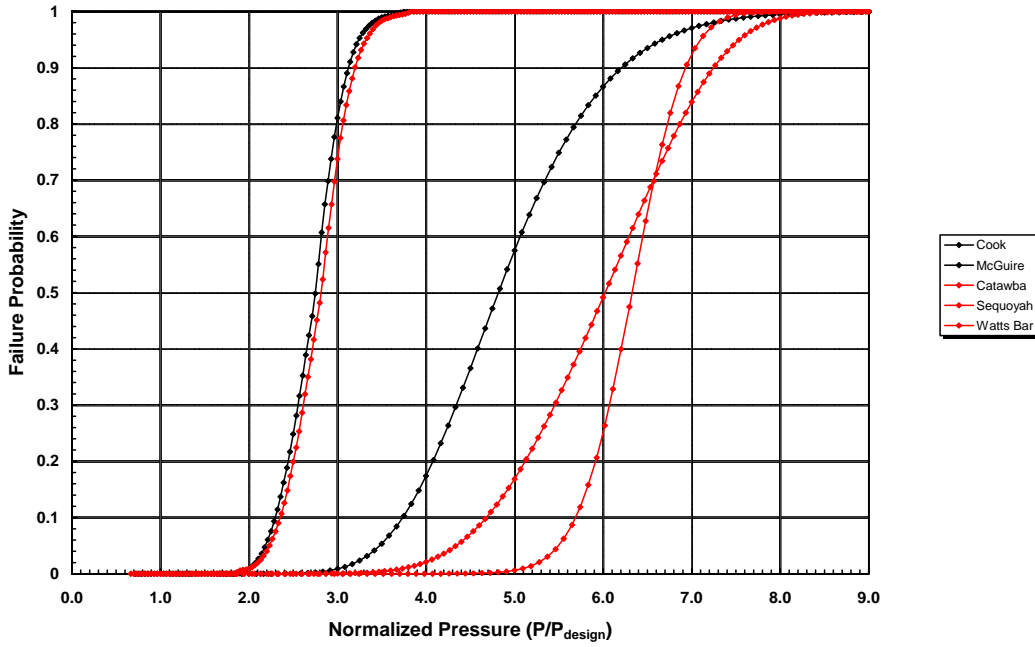


Figure 17 IPE Fragility Curves for Ice Condenser Containments

IPE Fragility Curves for Sub-Atmospheric Reinforced Concrete Containments

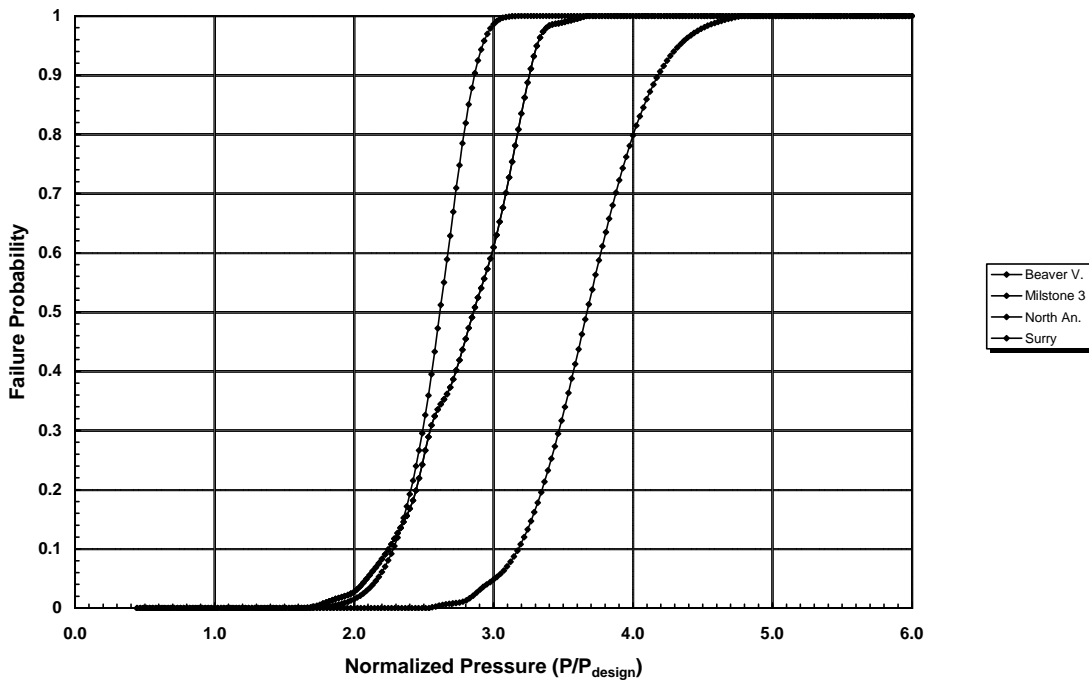


Figure 18 IPE Fragility Curves for Sub-Atmospheric Reinforced Concrete Containments

IPE Fragility Curves for BWR Mark I Containments

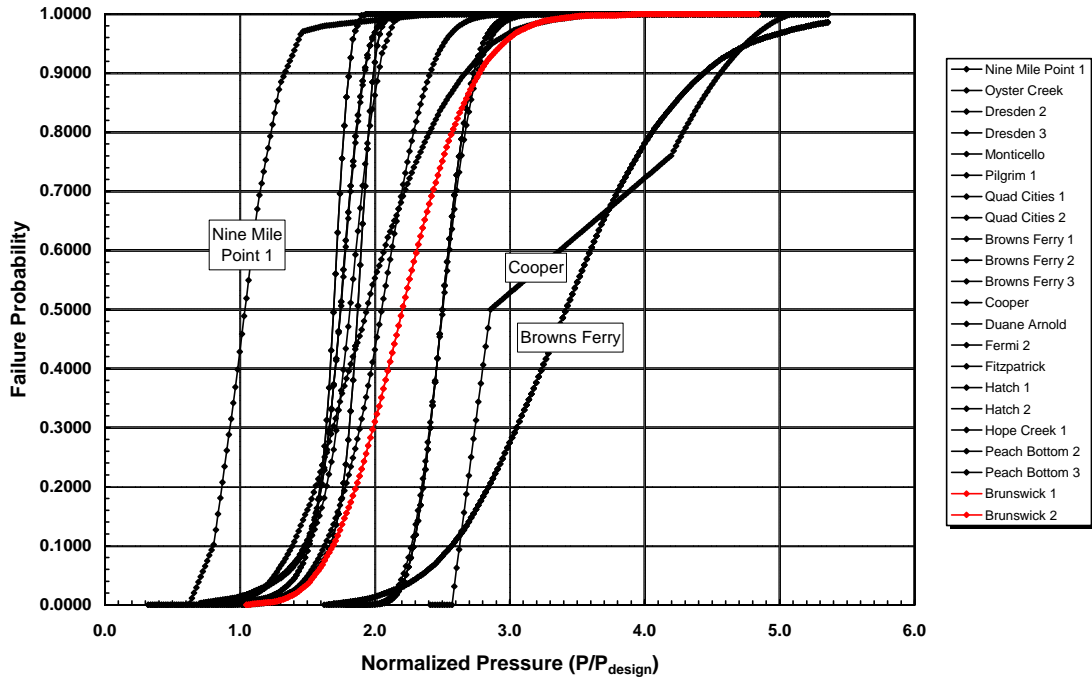


Figure 19 IPE Fragility Curves for BWR Mark I

IPE Fragility Curves for BWR Mark III Containments

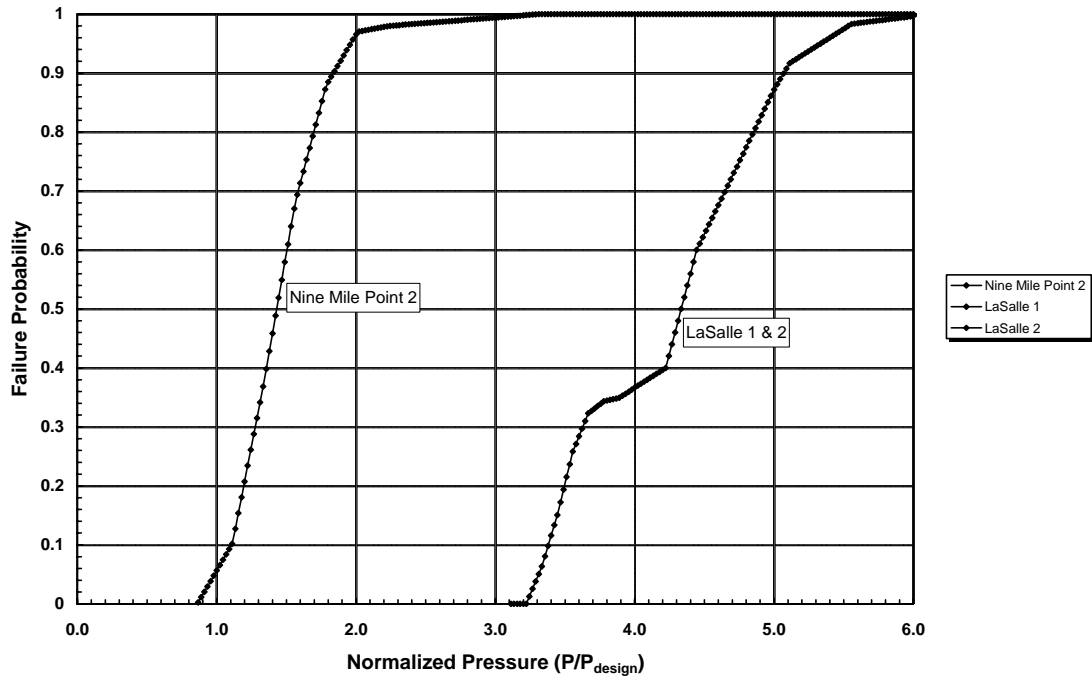
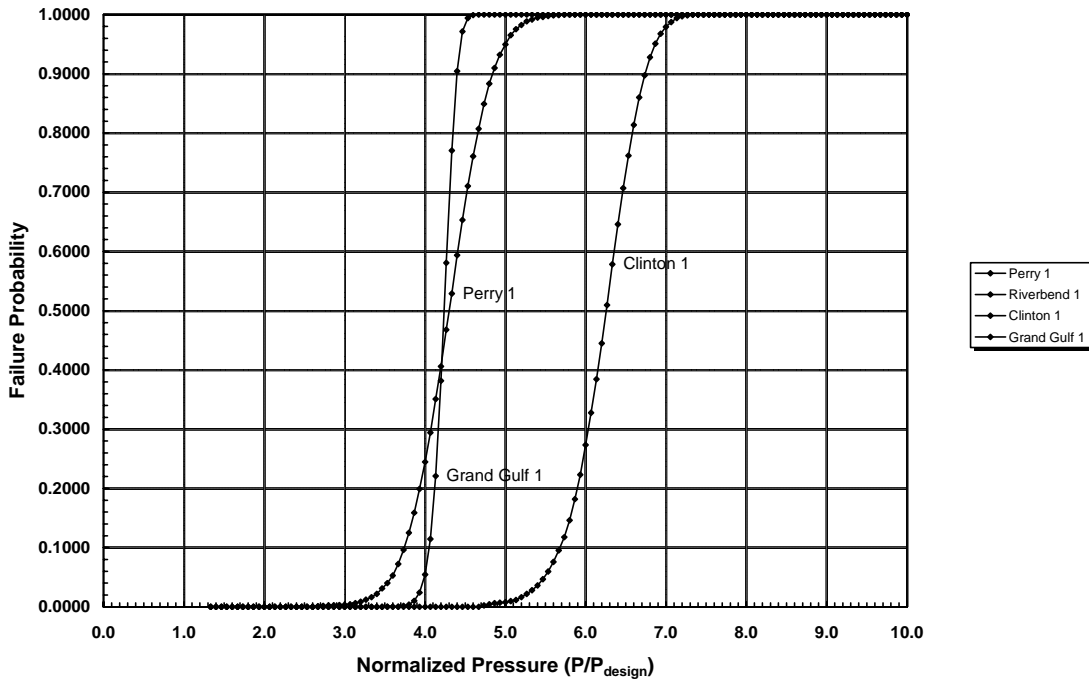


Figure 20 IPE Fragility Curves for BWR Mark II

### IPE Fragility Curves for BWR Mark III Containments



**Figure 21 IPE Fragility Curves for BWR Mark III**

#### *Containment Performance Parameters in Risk Analysis.*

A comprehensive summary and definition of the various containment performance parameters used in risk analysis, e.g. *containment failure probability*, *cumulative containment failure probability or fragility*, *containment failure frequency*, *conditional containment failure probability*,... would be extremely useful. A review of the literature, i.e. a number of reports that either define or use these parameters suggests that the definitions and usage are not always consistent or rigorously applied or interpreted. It is beyond the scope of this current effort to identify or resolve all these uncertainties, but a formal presentation of the subject would be invaluable to the structural and risk communities.

Both NUREG-1150 and the IPEs included estimates of containment failure in terms of the conditional containment failure probability (*CCFP*) and the containment failure frequency (*CFF*). These estimates were based on expert opinion and simplified analyses. The conditional containment failure probability is the probability of containment failure given an accident. The containment failure frequency is the frequency per reactor year of accidents involving containment failure. These quantities are defined as:

$$CCFP = \sum_{i=1}^n \frac{S_i}{CDF} \cdot C_i$$

$$CFF = \sum_{i=1}^n S_i \cdot C_i$$

where *CCFP* is the conditional containment failure probability,

$CFF$  is the containment failure frequency,

$CDF$  is the total core damage frequency,

$S_i$  is the frequency of accident sequence  $i$ ,

$C_i$  is the conditional probability of containment failure given accident sequence  $i$ , and

$n$  is the total number of accident sequences.

Because  $S_i$  and  $C_i$  depend on the particular accident sequences (which vary considerably among the plants), both  $CCFP$  and  $CFF$  can be significantly different for two plants with identical containments.

### 2.3 Background of Containment Testing at Sandia

Given the importance of the containment as one of the cornerstones of the NRC ‘defense-in-depth’ strategy coupled with the lack of data and analysis tools to characterize containment performance to ‘beyond design basis’ loads, the NRC commissioned Sandia to perform a ‘background’ study, completed in 1981, to “develop a methodology for reliably predicting the ultimate capacity of steel and concrete containment structures under loadings caused by accidents and severe environments” [8]. This study included a review of US containment types, a brief summary containment design practices and a review of previous tests of scale models of containment structures and actual containments. At the time of this study, a total of 181 commercial nuclear power reactors were either operating, under construction or proposed, although twenty-one of the proposed plants were either delayed or cancelled. Some of these previous tests are described in Chapter 3.

This review concluded that the ‘large amplitude, nonlinear response of steel containments (had) not been investigated experimentally. The pressure tests of concrete containments indicate(d) that the models behave(d), in a gross sense, as predicted’. The concrete tests indicated, however, the importance of the behavior of the liner and penetrations which were not accurately represented in the models. The tests of actual containments were limited to small overpressures and provided little information on large deformation non-linear response.

Based on this review, an ambitious program was proposed to conduct tests of models of containment structures to failure and determine the suitability of existing analytical methods to predict failure by comparison with the test results. The tests envisioned included static and dynamic internal pressurization and seismic loading. The survey of operating and future US plants showed a large variety of containment types, however, hybrid steel, reinforced and prestressed concrete containments encompassed 75%, so the proposed program focused on these types. Because the scope of this report is, primarily, the end result of the program proposed in 1980, the principles laid out at that time for this program bear repeating:

*“Because it is impractical to test full-size containment structures, scale models will be used. Several requirements are necessary to achieve credible results. Each of the items below is an integral part of this program.*

- *A sound theoretical basis for the model design, the test loading, and interpretation of test data must be established.*
- *The model scale must be chosen such that the characteristics to be determined in the test are accurately represented in the model.*

- *The scale model must be fabricated with sufficient care to insure that failure mechanisms, not present in the prototype, are not introduced into the model.*
- *The test methods must be such that failure modes are not introduced or eliminated in the structure as a result of test procedures or test facilities.*
- *Instrumentation of sufficient accuracy and sensitivity to record all phenomena of interest must be employed.*
- *Adequate analytical support must be incorporated into all phases of the experimental plan.*
- *Repeatability of experimental results must be demonstrated.*

*Because the ultimate capacity and modes of failure of steel or concrete containments cannot be predicted with confidence using existing computer codes, an analytical task that parallels the experimental effort will be undertaken. Qualification of existing codes will be attempted; modifications of existing codes and development of new codes may be required. The end results of this program will be:*

- *Bench-mark data from scale-model tests of selected classes of containments.*
- *A set of qualified computer programs that can be used to determine the ultimate capacity of containment structures.”*

The summary of the experimental and analytical program described in the following sections of this report will describe the extent to which these principles were followed and define the success of the program in meeting the original objectives.

It should also be noted that at the inception of this program, a Peer Review Panel, consisting of representatives from industry, academia, other research laboratories and private consultants, was organized. This panel, the specific make-up of which varied over the course of the program, actively participated in reviewing the research plans and results and provided guidance to the NRC and Sandia on the direction of the program.

### 3 CONTAINMENT MODEL TESTS

#### 3.1 Containment Model Testing for ‘Beyond-Design Basis’ Loading

The background study [8] summarized in Section 1.1.3 identified three types of loading to be considered in the proposed experimental program:

- Static internal pressure
- Dynamic internal pressure
- Seismic loading

While the background study did not explicitly identify temperature loads, the accident sequences resulting in either static or dynamic pressure loading of the containment always result in elevated temperatures inside the containment. As the program evolved, the focus of the experimental work was limited to the response of containments to **severe accident** loading, i.e. those accidents which could lead to substantial core damage. Due to the higher costs and complexity, containment capacity to seismic loads was addressed by analysis [15] and no experiments were proposed at SNL for seismic loading, although some opportunities to participate in tests conducted elsewhere were exploited (see Section 3.7.4).

Severe accidents in the context of containment evaluation can be defined as follows: accidents which cause pressurization and/or temperatures within the containment which exceed the design basis pressure and temperature. In the context of this program, such accidents refer to the quasi-static generation of steam that results from partial core melt contacting water within the containment. When this occurs, and with the volume of the containment essentially fixed, the generation of pressure is assumed to be large enough to eventually breach the containment boundary, resulting in leakage in excess of design specification for the plant. In the authors’ view, most of the containment research community agrees with this basic definition, however, accident definitions begin to diverge when trying to define the pressurization rate because this introduces the controversial concept of an equilibrium leakage rate.

The general principles for the experimental and analytical program conducted at SNL, stated in the background study were listed in Section 1.1.3. The resulting test program carried out by SNL over twenty-plus years, roughly 1980 through 2003, was aimed primarily at **benchmarking** analysis methods, not at proof-testing.

The program was an integrated one of testing models of containment structures and components (both scaled and full-size specimens) coupled with detailed pretest and posttest analyses. Figure 22 shows a timeline of the major containment integrity programs along with other milestone events.

Many modelers or code developers speak of ‘**validating**’ their codes or models by comparing them with experimental data. In practice, most models, particularly those for complex structures and/or loading conditions, are compared to very limited empirical data. While the availability of a fairly extensive suite of experimental data may increase our confidence in the predictive capabilities of our analysis, in most cases, the rigor implied by the term validation is not present. Unfortunately, this is especially true when analysts report on “validation” analyses which are conducted post-test and with data in-hand. Conducting “blind” predictions provides stronger evidence for “validation.” Nevertheless, for purposes of this report, the term ‘**benchmarking**’

1950	WASH-3: Exclusion vs. Confinement
1957	Shippingport Nuclear Power Plant
1971	10 CFR 50, Appendix A: General Design Criteria
1973	WASH-1250: Reactor Safety Study (definition of Severe Accidents)
1973	ASME B&PV Code, Section III, Div. 2 (ACI-359) (concrete containment design rules)
1975	WASH-1400: Rasmussen Report (estimates of containment capacity)
1979	Three Mile Island, Unit 2 Accident
1981	SNL Background Study on Containment Capacity
1982	NRC-sponsored Containment Integrity Program at SNL
1982	1:32-Scale Steel Model Tests
1984	1:8-Scale Steel Model Test
1986	NRC Qualitative Safety Goals
1986	Individual Plant Examination Guidance
1987	1:6-Scale Reinforced Concrete Model Test
~1988	SNL and EPRI/CTL Separate Effects Tests
~1988	Personnel Airlock Test
1988	F4 Phantom Jet Impact Test
~1989	Electrical Penetration Tests
1989	Sizewell-B 1:10-Scale Model Test
1990	NUREG-1150: Risk Study (probabilistic risk assessment, PRA)
1991	NUPEC-NRC Cooperative Containment Research Program at SNL
1994	Containment Bellows Tests
1996	1:10/1:4-Scale Steel Model Test
1996	Watts Bar 1 (latest US commercial nuclear power plant)
2000	1:4-Scale Prestressed Concrete Model Limit State Test
2000	NUPEC 1:10-Scale Seismic Capacity Tests
2001	1:4-Scale Prestressed Concrete Model Structural Failure Test
2005	OECD/NEA/CSNI ISP #48 on Containment Capacity
2006	Containment Integrity at SNL Summary

**Figure 22**      **Timeline for Containment Integrity Research at SNL**

In line with the test program principles, the scale of the models were selected such that some representative features of prototypical containments could be included in the models, and the response mechanisms would simulate the response of the prototypes (more about scaling later).

The analytical efforts focused on evaluating and improving the tools and techniques used in the evaluation of actual containments by applying them to the test models. Additionally, important insights, and a general feel for the state of the industry, were gained through the organization and compilation of round-robin pretest and posttest prediction exercises for three of the largest model tests.

For the severe accident response tests, it was necessary to decide whether both thermal and pressure loads would be applied to the model, either separately or simultaneously, what the pressurization medium should be, and whether the transient characteristics of these loads should be considered. Programmatically, the decisions to perform **static, pneumatic** overpressurization tests at **ambient temperature** were dictated by risk, cost and experimental considerations and previous experience.

The choice of **pneumatic** versus **hydrostatic** pressurization was dictated primarily by the goals of the test program. If ultimate capacity was the primary objective, the tests could have been conducted using water as the pressurization medium (as was done for a number of the tests conducted elsewhere). The minor perturbations in the pressure distribution due to gravity are not significant at ultimate load and can be accounted for by the analysis. Hydrostatic testing is preferable from a safety viewpoint due to the incompressibility of the pressurization medium; however, it raises operational problems and requires protection of sensitive electronics and wiring from the water under high pressure. The containment atmosphere during a severe accident consists of a combination of air, steam, and other by-products of the accident, including hydrogen and particulates (aerosols). The primary program interest is in observing and measuring the structural response of the containment to pressure loads and identifying failure modes. Containment failure (see 3.2.2) includes both functional failure, i.e. leakage, and structural failure, i.e. rupture of the pressure resisting elements. There is not a rigorous distinction between functional and structural failure, and it is conceivable that they might occur simultaneously. Conventional wisdom holds, however, that local, limited failure (e.g. seal failure or liner tearing) and leakage will occur prior to, and at pressures below those required to cause catastrophic structural failure. As a result, detection of leakage which is indicative of a tear in the steel liner or failure of a penetration seal, is a higher priority than measurement of actual leak rates for real containment atmospheres as a function of pressure. The choice of a pressurization medium, then is dictated more by safety and operational considerations and reproduction of the actual containment atmosphere under severe accident conditions is not practical. Pneumatic testing, while inherently more dangerous, present risks that can be managed cost effectively and does not require any unusual measures to protect the instrumentation.

All tests conducted as part of the Sandia program, except one, were conducted using dry nitrogen. Nitrogen gas was chosen as the primary pressurization medium for the model tests primarily for operational considerations. Nitrogen gas has the advantage of being dry, which benefits the performance of the instrumentation, and it allows simpler and more accurate calculation to detect a small leak. Fairly large quantities of nitrogen could be delivered at a remote test site in liquid form with a limited amount of fixed equipment. This decision dictated that careful planning and additional safety precautions were incorporated into the test programs due to the large stored energy and potentially violent nature of a catastrophic failure.

For the final test of the 1:4-Scale Prestressed Concrete Containment Vessel (PCCV), the Structural Failure Mode Test, the vessel was filled 95% with water, and the top 5% volume filled with nitrogen, in order to leverage the nitrogen supply system to achieve higher overall pressurization rate. This is discussed in more detail later (see 3.5.1).



The effects of severe accident **temperature** loads on the structural response of the containment building are primarily limited to (1) the effects of elevated temperatures on the mechanical properties of the materials and (2) the mechanical loads resulting from differential or constrained thermal expansion. The effects of temperature on the material properties can be determined from standard material tests methods. Thermal effects could be incorporated into the evaluation of the prototypical containment vessels without adding the complexity and cost (in terms of generating the thermal environment and protecting the instrumentation) to the PCCV model test. The added complexity and cost of simulating the thermal environments to reproduce these local effects was judged not to be justified for these experiments. It was further concluded that, since there is no unique pressure-temperature relationship for severe accidents, the effects of temperature could be addressed using analytical methods which had been benchmarked against the pressure tests [16]. Therefore, the decision was made to conduct these model tests at **ambient temperature**.

Regarding the stresses imposed by differential thermal expansion, there are only a few locations in a steel and/or concrete containment building where these effects are significant, notably at the junction of the containment wall and the basement or, in the case of the steel lined concrete containments,, the differential thermal expansion between the steel liner and the concrete shell under non-steady state thermal conditions. One further area, not represented in the containment model tests, is the differential expansion between the containment itself and adjacent structures and components, e.g. the shield building, and pipes which penetrate the containment boundary. Polar cranes, supported on the containment wall in some plants, are another example where differential expansion could result in damage to the containment or other internal components, in the event the crane fell from its supports.

In terms of the transient aspect, as noted previously, the pressure and temperature loads resulting from a severe accident can be quite rapid from a thermo-physical perspective (e.g. deflagrations, detonations, etc.), however the typical rates of loading (on the order of tens of seconds to minutes) are essentially static from a structural perspective. As a result, the dynamic aspects can be ignored and the tests can be conducted in a **pseudo-static** manner in the test program with no significant change in the response of the containment.

### 3.2 Modeling Considerations

The testing program that was developed and evolved at Sandia included the three major construction types used in current US containments: free-standing steel containments, steel lined reinforced concrete containments and steel lined prestressed concrete containments. For each type of containment model, the same guiding principles were used in the development of the model design, namely that the models would incorporate representative features of the prototypes, would not knowingly preclude a potential failure mode and would not incorporate details which were unique to the model and not representative of the prototype. While these principles are easy to articulate, their realization in practice is not always simple or straightforward. The scales of the models were chosen to reflect these principles and typically, as a result, the more complex the features were to be incorporated into the model, the larger the scale. As analytical research programs were planned and carried out in conjunction with the testing, an additional goal of the experiments became to determine if any unanticipated structural behaviors would occur.

The Background Study [8] recognized that an important element of an experimental program is repetition of experiments to prove reproducibility of results:

*“It cannot be overemphasized that reproducibility of results must be demonstrated before conclusions can be drawn. For each individual experiment, a sound statistical treatment of all measured data (both control and response) is required prior to considering the*

*experiment complete. The results of this complete experiment must then be demonstrated as reproducible by repetition; i.e., the experiment must be conducted again in as nearly the same manner as possible, limited only by the experimenter's ability and random factors.*

*Random factors will always be present. They may be associated with model fabrication, load application, response measurement, material variability, or other variables. The variations between experiments will produce a scatter in the results of seemingly identical experiments. Therefore, the results are reproducible if the measured response in all attempts fall within an acceptable scatter band. Careful error analysis is necessary to determine an acceptable scatter band. In complicated experiments with multiple responses it is possible that only some responses will be reproducible.”*

Unfortunately, cost and schedule constraints usually prevent repetition of model tests, especially for the type of large-scale, detailed models of complex structures which are the subject of this report. Nevertheless, the principle of reproducibility of results is still important and should be an important consideration in interpreting and applying the results of the tests.

### **3.2.1 Scaling**

In all cases, with some minor exceptions, straight geometric or replica scaling was utilized in the design of the models. This is possible since for most severe accident pressure loading, the rate of pressurization is slow enough that the model responds essentially statically and dynamic effects are not significant. The background study included a fairly thorough review of the scaling laws considered for the test program and a brief review of the scaling issues is warranted at this point in the summary.

Considering all parameters relating to geometry, material properties, loading conditions, the Buckingham Pi Theorem was used to generate a list of non-dimensional pi terms. For a model and prototype system to be equivalent, only the pi terms (and not each individual parameter) have to be identical in both systems. This principle introduces the concept of scale factor for the various parameters in the problem. Inspection of the pi terms yields the scale factors for the various parameters of interest, shown in Table 5.

A replica model is built with the same materials in corresponding model and prototype locations, but is smaller by a geometric scale factor  $\lambda$ . In a replica model, all material properties such as density  $\rho$ , strength  $\sigma$ , and strain rate coefficient  $K_i$  are the same as in the prototype. However, not all phenomena are scaled without distortion in a replica model. Three problem areas are identified in the table. We can't easily scale gravity, short of constructing models on the moon, and if we use the same materials in the model and the prototype, strain-rate dependent properties and viscous damping cannot be modified. For static loading, the latter parameters, and others which are time-dependent, are not critical and do not affect the results. Since gravity affects the dead load stresses, our inability to scale gravity could be important if dead loads are a significant portion of the total load on the model. Typically, severe accident loadings dominate the response of the structures and the differences in response to gravity loading between the model and prototype are not typically significant, but should not be ignored.

**Table 5 Replica Modeling Law to Satisfy Pi Terms**

<b>Parameter</b>	<b>Symbol</b>	<b>Factor</b>
<b>Lengths, displacements</b>	<b>L, x, X</b>	<b><math>\lambda</math></b>
<b>Angles</b>	<b><math>\theta_i</math></b>	<b>1.0</b>
<b>Times, duration</b>	<b>t, T, T<sub>0</sub></b>	<b><math>\lambda</math></b>
<b>Velocities</b>	<b>v, V</b>	<b>1.0</b>
<b>Accelerations</b>	<b>a, A</b>	<b>1/<math>\lambda</math></b>
<b>Stresses</b>	<b><math>\sigma</math></b>	<b>1.0</b>
<b>Densities</b>	<b><math>\rho, \rho_0</math></b>	<b>1.0</b>
<b>Strains</b>	<b><math>\epsilon</math></b>	<b>1.0</b>
<b>Pressures</b>	<b>P, p(t), P<sub>0</sub></b>	<b>1.0</b>
<b>Frequencies</b>	<b><math>\omega</math></b>	<b>1/<math>\lambda</math></b>
<b>Forces</b>	<b>F</b>	<b><math>\lambda^2</math></b>
<b>Number of reinforcing bars</b>	<b>N<sub>i</sub></b>	<b>1.0</b>
<b>Leakage rate</b>	<b>m</b>	<b><math>\lambda^2</math></b>
<b>Acceleration of gravity</b>	<b>g</b>	<b>1/<math>\lambda</math></b>
<b>Strain-rate coefficient</b>	<b>K<sub>i</sub></b>	<b><math>\lambda</math></b>
<b>Equivalent viscous damping</b>	<b><math>\beta_i</math></b>	<b><math>\lambda^2</math></b>

The background study did not address scaling of thermal response since the model tests proposed were conducted at ambient temperature. If future tests or analysis of models include temperature loading, the scale factors for thermal response should be investigated. For example, the scale factor for thermal conductivity will not be 1.0 and the through-wall gradients will be different for the model and the prototype.

It is also important to note that the scale factor for leak rate is  $\lambda^2$ . Leak rates measured from model tests should include consideration of this scale factor when compared to allowable values.

In general, all features of a prototype containment cannot be represented in a scale model. Specific feature such as welds, fasteners (bolts, rebar couplers, tendon anchors, etc.), tolerances in fabrication and construction and other details can only be represented approximately. Each of these features of the prototype must be evaluated to determine its impact on the response and whether its inclusion in the model is necessary. For any realistic model test, compromises, often based only on engineering judgment, are inevitable regarding the fidelity of modeling small details in the structure. Often these compromises result in the elimination of failure modes from the model. The results of model tests should always be interpreted with an understanding of these compromises.

### **3.2.2 Failure**

For pretest and post-test evaluations of the test models, especially the concrete ones, failure predictions have been made based on criteria developed during the early (1980s) phase of the containment research, and refined by large scale tests and supporting analysis. There has been a lack of consistency in the literature over what is meant by ‘failure’ of containments. For the Containment Integrity program at SNL, two working definitions of ‘failure’ have been used. ‘Functional failure’ has been taken to denote a loss of containment function, i.e. a leak rate in excess of the specified minimum leak rate of the containment, usually associated with a loss of

liner integrity of loss of penetration sealing. Functional failure typically occurs when global deformations and strains exceed the elastic limit and/or local strains exceed the material strain limits. Functional failure can include the concepts of 'leak' and 'rupture' used in NUREG-1150. 'Structural failure' denotes the limit of resistance to the applied load and is characterized by large global deformations and extensive material failure. Structural failure includes the concept of 'catastrophic rupture' in NUREG-1150. For the work described in this report, the term "failure" is taken to mean the occurrence of such large deformations (strains) of the liner or of a containment structural element, that a breach of the containment pressure boundary is predicted.

Functional failure criteria have been difficult to define due to a lack of correlation between functional performance parameters (i.e. leak rate) and structural performance parameters (e.g. stress, deformation, strain) which can be measured in an experiment or calculated by analysis (see 2.7.6). Surrogate structural failure criteria have been used in lieu of functional criteria. These surrogate criteria have been based on engineering judgment and experimental results. One of the objectives of the Containment Integrity program at SNL is to provide further insights and, hopefully, improved recommendations for these surrogate criteria.

Current practice for predicting local failure for steel and steel-lined concrete containments for pressure-only loading is based on either the explicit prediction of liner strains high enough to exceed the material strain limits, including consideration of tri-axial strain fields, e.g. the Davis Triaxiality Factor [17], if the finite element mesh is refined enough, or assumes the existence of high strains near a liner discontinuity. Typically, the liner discontinuity is not explicitly modeled or not modeled with a highly refined mesh and strain concentration factors, based on experiment or detailed analysis, are applied to the computed strains. Cherry and Smith [18] provided a comprehensive summary of failure criteria for steel containment analysis. Dameron [19] summarized a range of strain concentration factors for typical details in steel liners of concrete containments. The use of strain concentration factors has been shown to be successful for predicting the behavior and failure of large scale models, and there is evidence that for steel and steel-lined concrete vessels with quasi-static pressurization, tearing will occur when the strain fields in the vicinity of a discontinuity, i.e. the so-called 'near-field' or 'driving' strains, are on the order of 1 to 2%. Obviously, the use of strain concentration factors in lieu of detailed local analysis is dependent on the specific details used in the construction, however, this is not as serious a deficiency as it might appear given the difficulties in defining and modeling the as-built configuration accurately. This suggests that valid surrogate criteria may be developed for both local and global (or near-field) strains.

While the approach for defining surrogate failure criteria for steel or steel-lined concrete containments may be similar, the response upon reaching failure may be dramatically different. For a steel containment, the onset of tearing usually denotes an instability and failure progresses nearly instantaneously to catastrophic rupture. For conventionally reinforced or prestressed concrete containments, the onset of liner tearing can lead to either leakage and gradual depressurization or catastrophic rupture. Arguments regarding the validity of the concept of 'leak-before-break', which find their origin in the design of piping systems, for containment systems are discussed in subsequent sections.

One mode of failure not explicitly considered in the Containment Integrity program is the potential for large displacement of the containment structure relative to adjacent structures and piping which could result in loss of containment or by-pass. Since the model tests did not include these external structures and did not simulate the thermal loading which can lead to large deformations, this failure mode was not represented in the experiments. Nevertheless, this mode could be critical and should be considered in any complete evaluation of containment integrity.

On a practical note, functional failure criteria are not particularly useful for conducting tests to determine the structural capacity of a containment vessel model, especially when the objectives are 1) to generate large inelastic response modes for comparison with analytical predictions, which may be well beyond the levels required to cause functional failure, and 2) to gain some insight into design margins, i.e. the functional and structural capacity beyond the specified design load conditions. The pressurization system is typically designed to allow the model to be pressurized to levels significantly above those expected to cause local strains in the model to exceed the ultimate strain limits of the materials. In some cases, the tests were terminated when the model and the pressurization system were incapable of maintaining or increasing the model pressure-due to excessive leakage or gross rupture. The maximum pressure achieved prior to the termination of the tests should not be confused with the failure pressure, since failure is defined in terms of some acceptance criteria, not the operational inability to maintain pressure in the model.

### **3.3 Steel Containment Model Tests**

A series of scale models of steel containment vessels, of increasing size and complexity were tested at Sandia between 1982 and 1996. Table 6 summarizes the details of the models and the results of the tests. Each series of tests are described in the subsequent sections. Details are provided in the references cited in the table.

#### **3.3.1 NRC 1:32-scale steel models**

The first tests conducted at SNL, in 1983, were on four simplified 1:32-scale models of a cylindrical steel shell with a hemi-spherical head. The models are illustrated in Figures 23 and 24. The containments are typical of a large dry or ice-condenser PWR containment. Two models (SC-0 and SC-1) had no penetrations or stiffeners, one (SC-2) had ten ring stiffeners brazed to the cylinder wall, one (SC-3) had a mock-up of three penetrations (an equipment hatch and two personnel locks) with no gaskets or seals, i.e. the penetrations were welded shut. Details of the tests and supporting analyses are described Horschel in [20] and [21].

The results of these small scale tests demonstrated the value of conducting scale model tests of containments, both for comparison with analytical predictions and for gaining insight into response and failure modes. In general, the results indicated that simple shells, without significant perturbations such as stiffeners and penetrations could withstand pressures causing large strains up to the uniaxial tensile strain limits. The failures initiated near the mid-heights of the cylinders. The presence of even ‘minor’ perturbations or discontinuities resulted in a significant reduction of free field strains with some reduction in the pressure capacity. Pretest analyses gave good comparisons with the global response and the observed failure pressures. The calculated failure pressures of SC-0 and SC-1 was 0.91 MPa with failure occurring at mid-height; for SC-2 the calculated pressure was 0.95 MPa with failure of the stiffener rings; failure of SC-3 was predicted to occur at 0.84 MPa at the sleeve of the equipment hatch (E/H).

One interesting result of these tests was that the calculated initial yield was below the observed yield. At the time this was dismissed as being due to the initial stresses in forming the shells (they were cold-rolled) and the Bauschinger effect. Since the calculations beyond the initial yield joined the experimental results it was not considered a significant effect and this discrepancy was dismissed, however, as shown in the next two sections, this appears to be typical of all the steel containment models tested.

**Table 6 Summary of Results of Experiments for Steel Containment Models**

Test	Scale	Shape	R/t	Pressure Ratio ( $P_d/P_{max}$ )	Global Strain at Failure	Material	Remarks
SNL SCO (12/2/82, 12/12/82)	1:32	Cylinder w/ hemispherical dome	450 (R=549, t=1.22)	0.93*	20%	AISI 1008	Catastrophic rupture and fragmentation initiating at vertical weld seam. [20, 21]
SNL SC1 (4/20-21/83)	1:32	Cylinder w/ hemispherical dome	500 (R=546, t=1.09)	0.76*	6%	AISI 1008	Tearing and leakage next to vertical weld seam.[ 20, 21]
SNL SC2 (7/21/83)  (8/11/83)	1:32	Cylinder w/ hoop stiffeners and hemispherical dome	478 (R=546, t=1.17)	0.93*  0.97*	2.7%  2.5%	AISI 1008	Leakage and tears at cylinder- dome interface; repaired. Retest; catastrophic rupture and fragmentation. [20, 21]
SNL SC3 (11/30/83)	1:32	Cylinder w/ penetrations and hemispherical dome	478 (R=546, t=1.17)	0.83*	14.5%	AISI 1008	Catastrophic rupture initiating at E/H. [20, 21]
SNL 1:8 (11/15- 17/84)	1:8	Cylinder w/ stiffening rings, penetrations and hemispherical dome	448 (R=2134, t=4.76)	4.9  ( $\frac{1.34}{0.27}$ )	3%	SA516, Gr. 70	Catastrophic rupture and fragmentation initiation at stiffener near E/H. [22, 23, 24, 25]
NUPEC/ SNL SCV (12/11/96)	1:10 geom./ 1:4 thick.	Improved BWR Mark II w/ contact structure	135-161 (R=2027- 2900, t=7.5-9.0)	6.0  ( $\frac{4.7}{0.78}$ )	2.0%	SPV490, SGV 480	Tearing and leakage at vertical seam weld and at E/H insert plate weld. [26, 27, 28, 29, 30, 31, 32]

\*Design pressure not specified, maximum pressure (MPa) given.

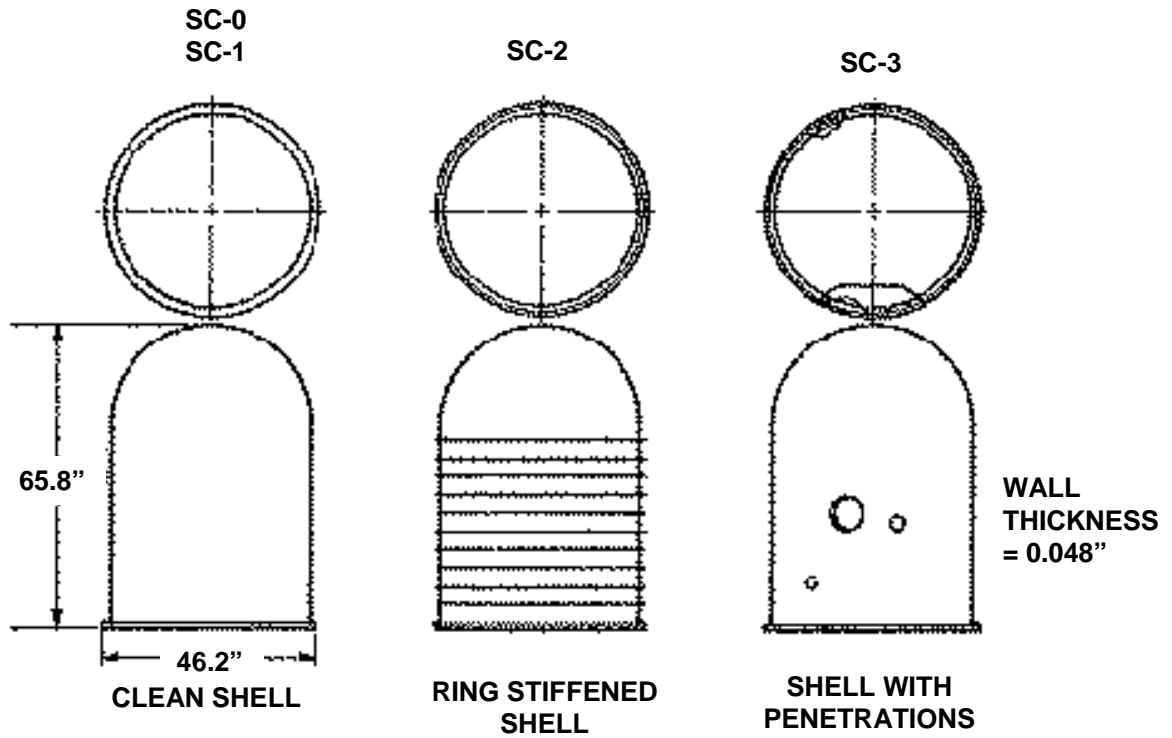


Figure 23 1:32-Scale Steel Containment Vessel Models

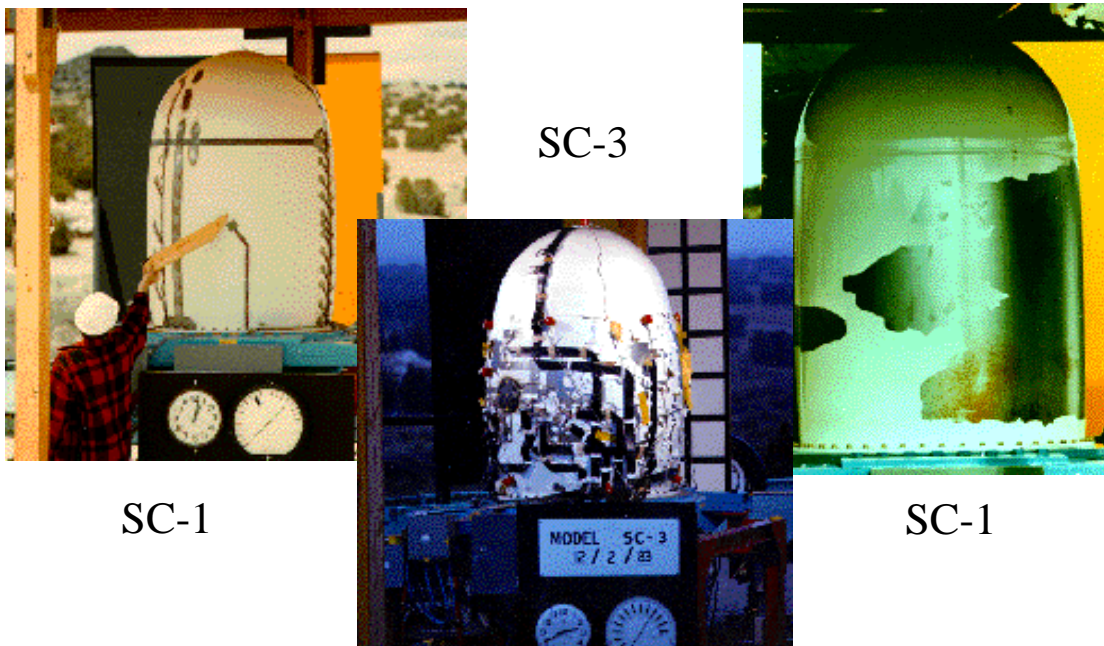


Figure 24 SC-1 and SC-3 Tests

### 3.3.2 NRC 1:8-scale steel containment model

A 1:8-scale model of a free-standing steel containment, which represented some features typical of large dry or ice-condenser PWR containments or a Mark III BWR containment, was the next model tested in the series of tests sponsored by the NRC at Sandia. The model is illustrated in Figure 25 and a picture of the model prior to testing is shown in Figure 26. The model was designed and built according to the ASME B&PV code with a design pressure of 40 psig (.27 MPa). The model included 11 penetrations typical of the prototypical plants including functional representations of the equipment hatch and personnel airlocks. The cylindrical shell was stiffened by external stiffeners with prototypical fabrication details. Details of the model design are provided in [22]. Pretest analysis indicated failure would occur due to ovalization of the E/H and leakage past the seals [23].

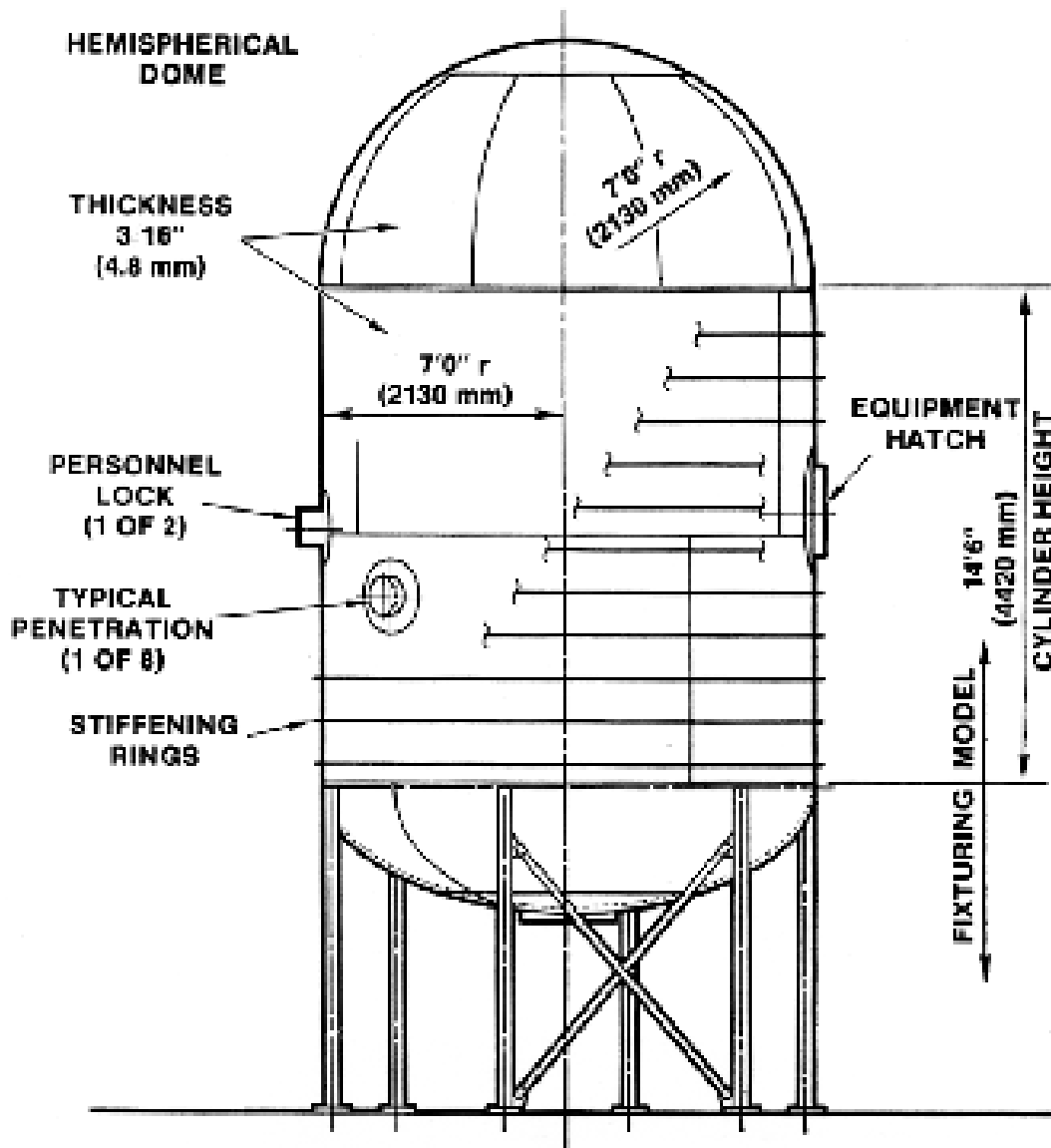


Figure 25 1:8-Scale Steel Containment Model Layout



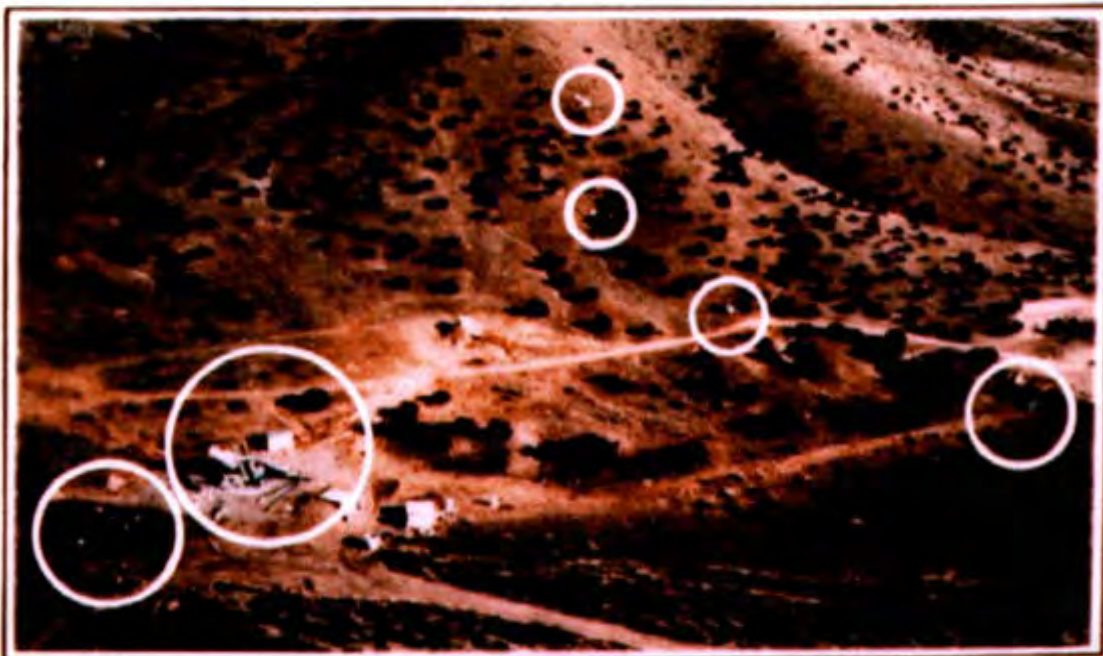


**Figure 26 1:8-Scale Steel Containment Model**

After a series of low pressure tests, the model was tested to failure in late 1984. Pretest analyses predicted failure would occur by ovalization of the equipment hatch sleeve resulting in a failure of the seals and leakage. Before the expected leakage could occur at the hatch, a tear, subsequently discovered as initiating at a stiffener detail adjacent to the E/H, resulted in catastrophic rupture and fragmentation of the vessel. The results of the test are illustrated in the composite Figure 27. The figure shows the predicted and measured response of the model. The posttest picture of the test site shows that fragments of the vessel were thrown over 1500 ft by the violent release of stored energy in the compressed gas. Video of the test was too slow to capture the failure of the vessel, but a wisp of 'steam', associated with escape of the nitrogen gas, was reported as being seen in the vicinity of the E/H immediately prior to vessel rupture.

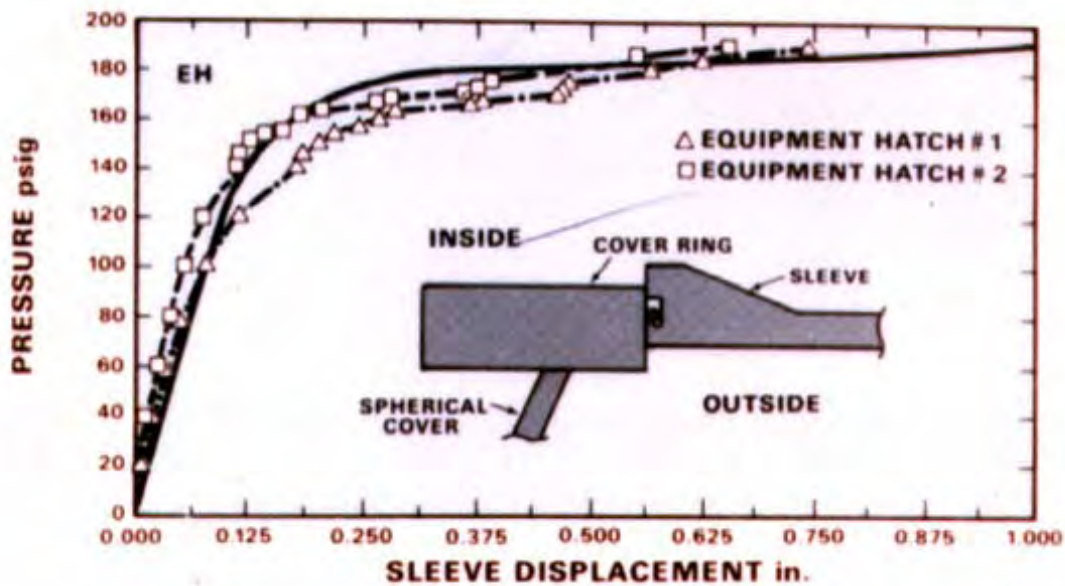


(a) Model with View of EH1 and Cracked Stiffener at 190 psig



(b) Aerial View of Site after Rupture

Figure 27 Results of 1:8-Scale Steel Containment Vessel Model Test



(c) Ovalization Increased Rapidly after Cylinder Membrane Yielding Occurred

	TEST	PREDICTION	POST-TEST ANALYSIS
Capacity [psig]	195	210	200
Failure Mechanism	Rupture	Leakage	Rupture
Location	Near EH1	Past EH1 or EH2 'O' Ring seals	Near EH1 or EH2

(d) Summary of Performance

Figure 27 (cont'd) Results of 1:8-Scale Steel Containment Vessel Model Test

Results of the test were reported by Koenig [24]. Global behavior compared favorably with the predicted response, however, as with the 1:32-scale models, the analysis over-predicted the pressure at which generalized yielding of the shell occurred. Figure 28 compares the predicted and measured free-field hoop strain at the mid-height of the cylinder wall. (The curve denoted 'CP' refers to the hoop strain measured in the vicinity of a constrained penetration.) Again this discrepancy was dismissed as post-yield response approached the predicted behavior.

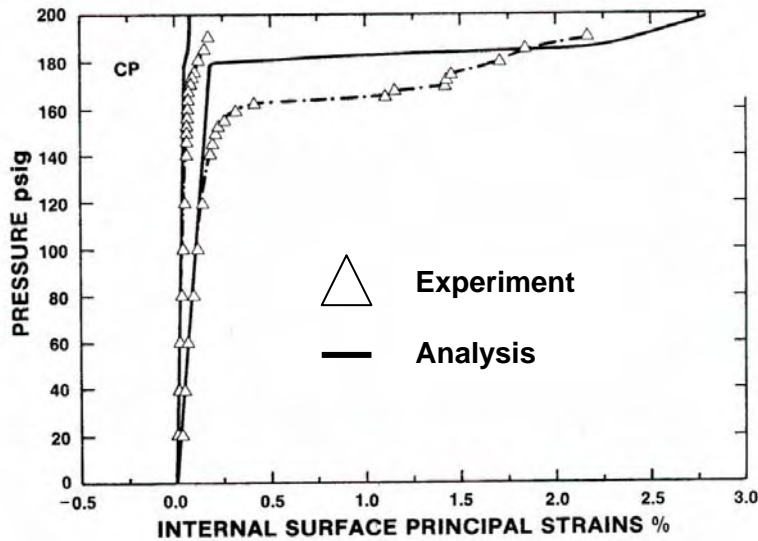


**Figure 28 Comparison of Predicted and Measured Hoop Strains in the 1:8-Scale Steel Containment Vessel Model. [25]**

Posttest analyses confirmed that a high strain concentration at the eccentric intersection of stiffeners around the E/H (Figure 29) was responsible for the tear and subsequent rupture by exceeding the ductile limits of the material. While demonstrating the large excess capacity of the model above the design specification (almost 5 times the design pressure), the test also highlighted the significance of local details in defining the limits of the prototypical containment structure [26].

Two circular samples (1.8 mm uniform thickness, 890 mm diameter) of the actual steel used in the construction of the model were tested by Kernforschungszentrum Karlsruhe, Germany, in a special test fixture that applied oil pressure to one side of the sample, to obtain biaxial stress-strain relationships. Similar tests were conducted on a typical German containment steel: two tests of uniform thickness samples (2 mm thick by 860 mm diameter) and two tests with a circular reinforcement (3.4 mm thick by 132 mm diameter) at the center [27]. Both unreinforced samples failed at 4.3 MPa while the reinforced samples failed at 2.8 and 3.2 MPa, illustrating the dramatic effects of a discontinuity on the capacity.

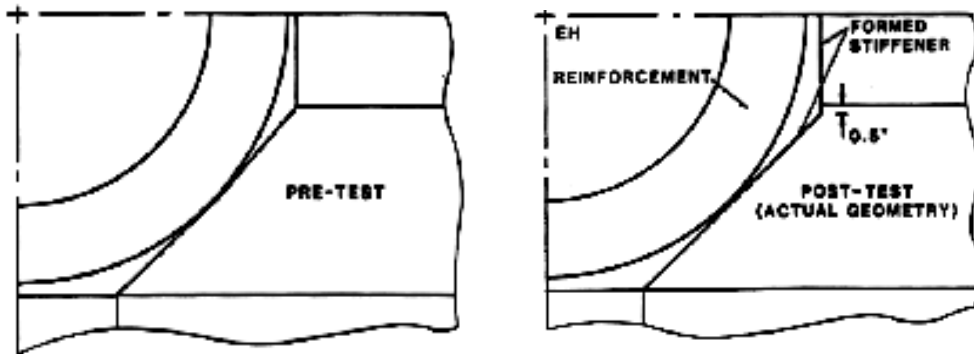


**Figure 29 Pretest Analysis vs. As-built Configuration of Stiffeners at 1:8-Scale Steel Model Equipment Hatch**

### 3.3.3 NUPEC/NRC 1:10/1:4-scale steel containment vessel model

The final steel containment vessel model tested at SNL under the joint sponsorship of the Nuclear Power Engineering Corporation (NUPEC) of Japan and the US NRC was a mixed scale model representative of the containment of an improved BWR Mark II in Japan. The model geometry was scaled 1:10 from the prototype while the shell thickness was scaled 1:4 to facilitate fabrication and to allow the use of prototypical materials. The configuration of the model is illustrated in Figure 30. The portion of the model above the material change interface, which is slightly below the equipment hatch centerline, was fabricated of SGV480, a mild steel, while the lower portion of the model and the reinforcement plate around the penetration were fabricated from high strength SPV490 steel. The conical shape of this structure and the re-entrant curvature at the top head are unique containment design features not tested in previous models. While not identical, this 'knuckle' is also present in Mark I designs. This model included a representation of the top head and the equipment hatch, although these were non-functional (i.e. welded shut) and not a credible leak path. Separate tests of functional drywell and equipment hatches have been conducted in Japan [28, 29]. The design pressure of the prototype containment is 0.31 MPa, whereas the scaled design pressure for this mixed scale model is 0.78 MPa. A separate steel contact structure surrounded the steel containment model during the test. This contact structure was incorporated into the test to represent the confining effect of the concrete shield building surrounding the containment during accident conditions.

The model was fabricated in Japan and shipped to Sandia National Laboratories, Albuquerque, NM, USA for instrumentation and testing. After the model was delivered to Sandia, a 38 mm thick steel (ASTM SA516 Grade 70) contact structure (CS) was installed over the SCV model prior to testing to represent some features of the reactor shield building in the actual plant. A nominal gap of 18 mm was maintained between the SCV model and the CS. Instrumentation of the model consisted of more than 800 channels of strain gages, displacement transducers, temperature and pressure sensors, and an acoustic emission device, in addition to video monitoring.

Luk [30] described the design, fabrications and testing of this model. The high pressure test of the model was conducted on December 11-12, 1996, at Sandia National Laboratories. After approximately 16.5 hours of continuous, monotonic pressurization using nitrogen gas, testing was terminated at a pressure 4.66 MPa or approximately six times the design pressure when a large tear (190 mm) developed adjacent the E/H insert plate weld seam with the main body of the vessel (Figures 31 and 32). Rapid venting of the model was observed and the pressurization system, operating at capacity (37 scm/m, standard cubic meters per minute), was unable to maintain pressure in the model.

Posttest visual inspection of the interior of the model revealed a large tear, approximately 190 mm long, adjacent to the weld at the edge of the equipment hatch reinforcement plate (Fig. 25). The tear appears to have initiated at a point roughly 30 mm below the material change interface (around 8 o'clock when viewed from the inside) in the high strength SPV490 steel shell, and propagated in both directions along the weld seam before it stopped. Interestingly, while the right side of the equipment hatch did not tear, significant necking was observed at a location symmetric with the tear (Fig. 32).

In addition, a small meridional tear, approximately 85 mm long, was found in a vertical weld (at an azimuth of 201°) underneath a semi-circular weld relief opening at the middle stiffening ring (Fig. 33). Some evidence suggests that this small tear might have occurred first but did not grow, and the pressurization system was able to compensate for any leakage through this tear. This tear

also had a counterpart at a similar, diametrically opposed detail. While no tear developed at this location, necking in the weld was observed.

After this initial inspection of the interior of the model, the contact structure was removed to allow inspection of the exterior of the model. In addition to the observations noted above, visual inspection revealed evidence of the pattern of contact between the model and the CS in the form of crushed instrumentation lead wires and transfer of mill markings from the interior of the CS. In addition, concentrated crack patterns in the paint indicated that global strains in the higher strength SPV490 shell were concentrated at the vertical weld seams while the uniformly distributed cracks in the SGV480 shell indicate that the hoop strains were fairly uniform.

More than 97% of the instruments survived the high pressure test. The failed gages, which consisted primarily of those on the exterior of the model, were damaged when the model made contact with the CS. The raw strain data were corrected to compensate for temperature variations and cross-axis strains, and the displacement data were corrected to account for any movement of the center support column to which the displacement transducers were anchored. The complete data record is included in the SCV Test Report [30]. A brief summary of the test data follows.

**Local Response Adjacent To The Equipment Hatch:** An extensive array of single element, strip and rosette strain gages was installed around the equipment hatch to characterize the local strain distribution. Figure 32 shows the locations of a few critical strain gages around the equipment hatch viewed from inside the model. A strip gage (STG-I-EQH-16), adjacent to the upper end of the tear, registered a maximum strain of 4.2%, and the two rosette gages (RSG-I-EQH-12 and -8) above it recorded maximum strains of 3.7% and 2.8%, respectively. The rosette gage (RSG-I-EQH-22) slightly below the lower end of the tear recorded a maximum strain of 1.3%. However, the highest strain reading of 8.7% was recorded by a strip gage (STG-I-EQH-37) at 3 o'clock, just above the material change interface.

**Global Response:** The global response of the SCV model was monitored using free-field strain gages and an array of internal displacement transducers that measured the strains and displacements at several elevations along four cardinal azimuths (0°, 90°, 180°, and 270°). Maximum free-field hoop strains ranging from 1.7 to 2.0% were measured at 4.5 MPa at the upper conical shell section. Hoop strains calculated from the displacement measurements ( $\Delta r/r$ ) were consistent with the strain gage measurements at these locations.

Japanese Improved BWR Mark II supplied by NUPEC

Scale: 1:10 on geometry; 1:4 on thickness

Diameter: 2900 mm (9.5')

Overall Height: 5900 mm (19.5')

Internal Volume: 21 m<sup>3</sup> (740 ft<sup>3</sup>)

Weight: 13,000 kg (28,634 lb)

Design Pressure:

P<sub>da</sub>=0.31 MPa (45 psig)-actual

P<sub>ds</sub>=0.78 MPa (112.5 psig)-scaled

Materials:

SGV480 (F<sub>y</sub>= 265 MPa, 38 ksi) ~ SA-516 Grade 70;

SPV490 (F<sub>y</sub>= 490 MPa,71ksi) ~ SA-537 Class 2

Contact Structure

Weight - 9 metric tons (20,000 lbs)

Material: SA-516-70 (F<sub>y</sub> =38 ksi)

Nominal thickness = 38.1 mm (1.5 in.)

Low Pressure Test: 1.50 P<sub>ds</sub> =1.17 MPa (169 psig)

High Pressure Test Date: Dec. 9 - 13, 1996

Instrumentation:

SCV External: 113 Strain Gages, 6 Displacement Transducers

SCV Internal: 151 Strain Gages, 57 Displacement Transducers

CS: 15 Strain Gages, 10 Gap LVDT's, 59 Contact Probes

Failure Pressure~Mode:

6 P<sub>ds</sub>: 4.7 MPa (676 psig)~tearing and leakage in HAZ of SPV 490 adjacent to E/H insert plate.

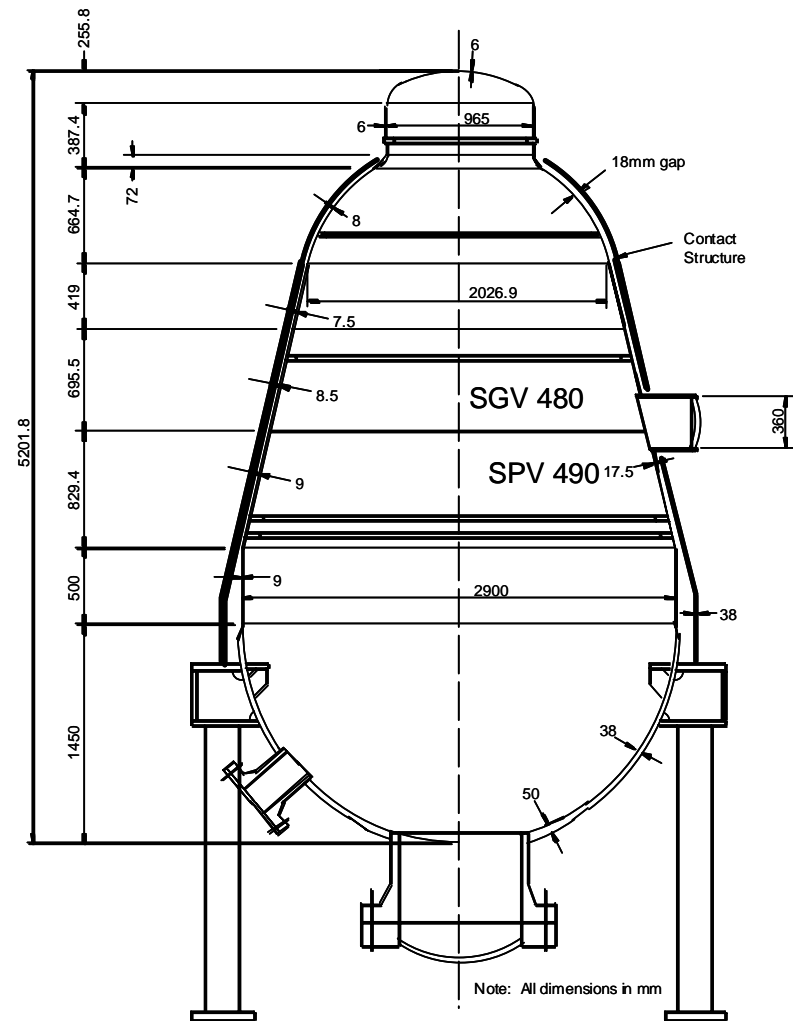
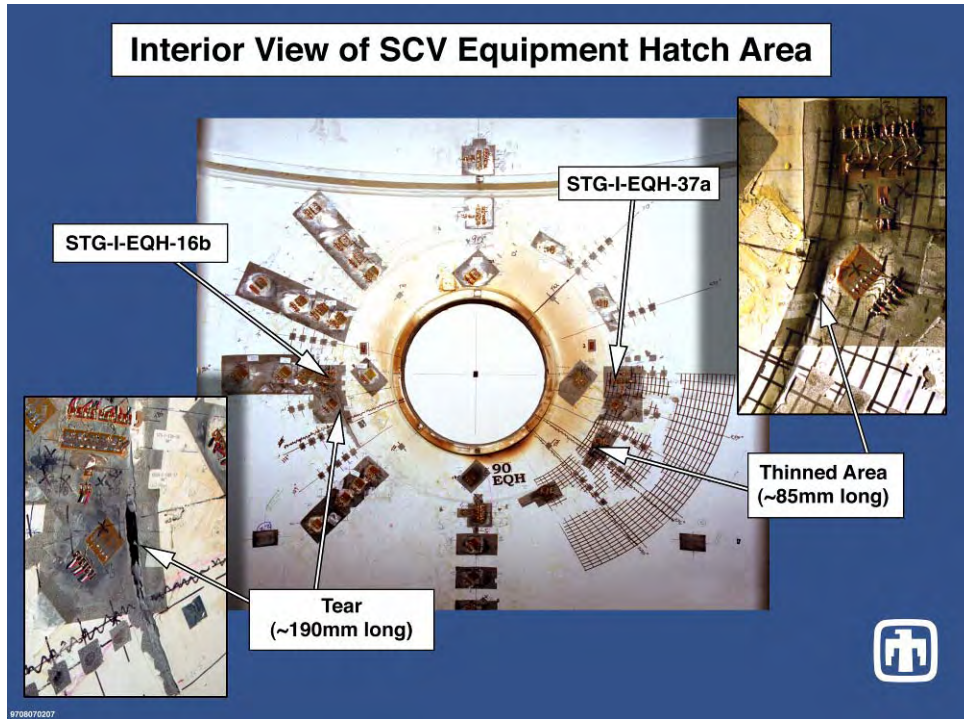
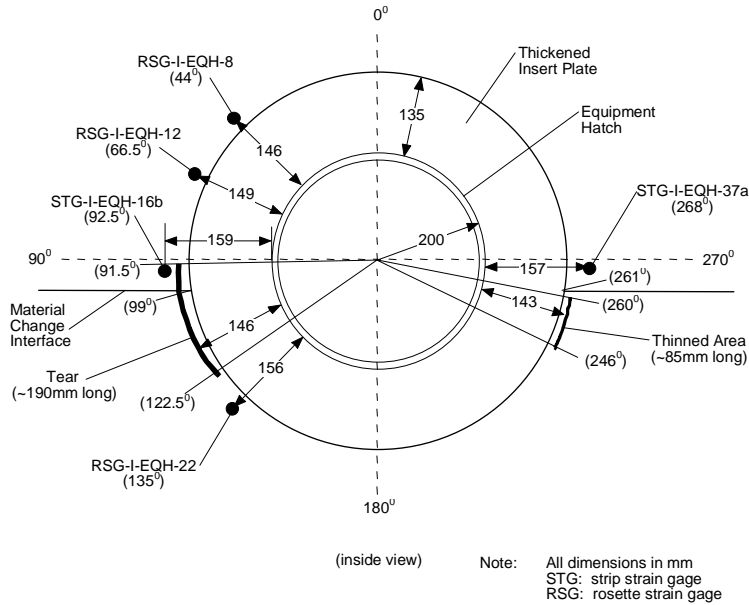


Figure 30 1:10-Scale Steel Containment Model Summary

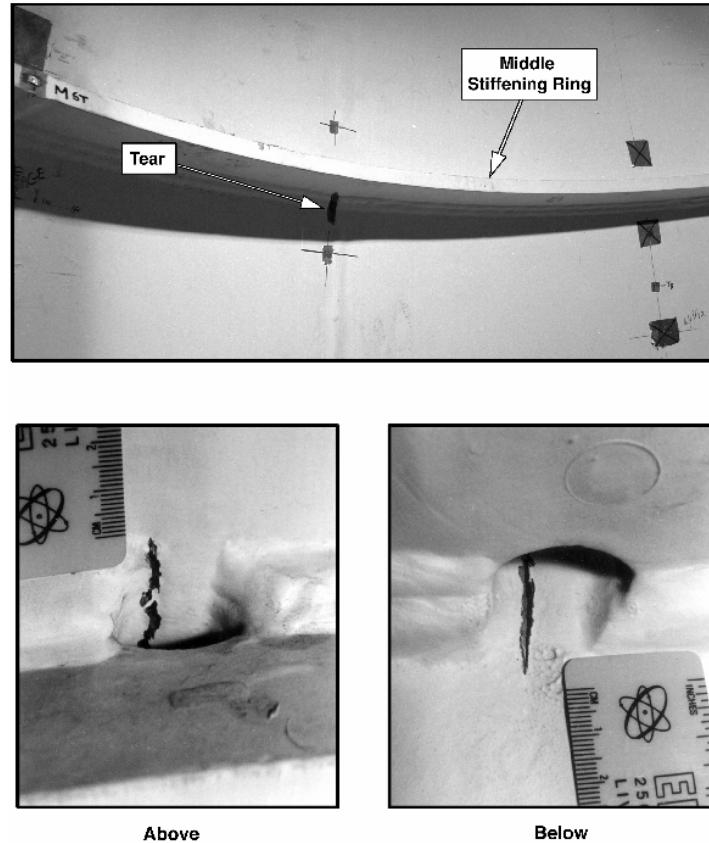


**Figure 31 Posttest View of Tears at E/H, 1:10-Scale Steel Containment Model**



**Figure 32 Posttest Interior View of the 1:10-Scale Steel Model**





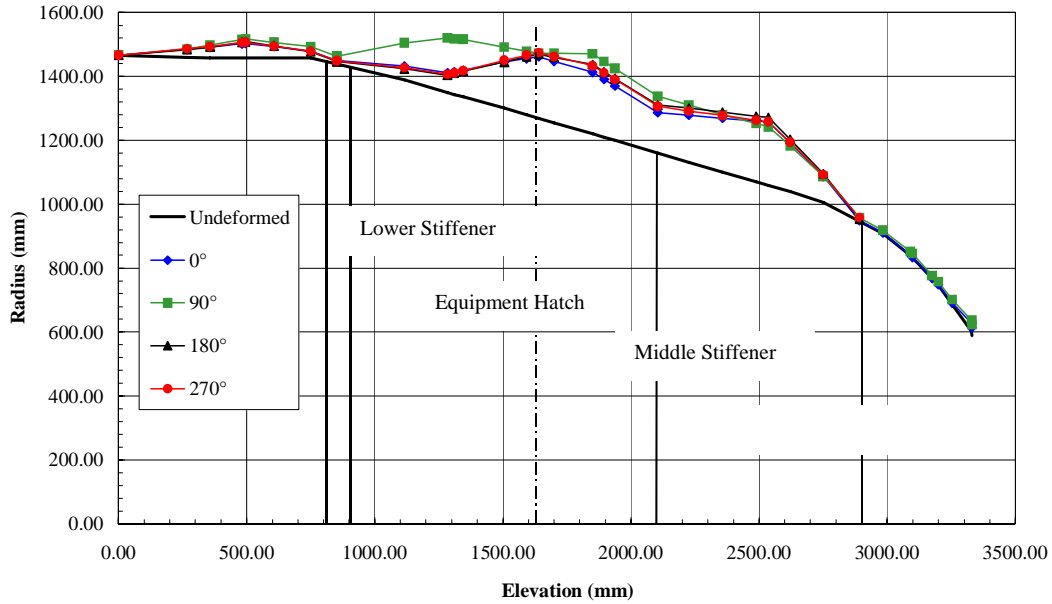
**Figure 33 Tear at Horizontal Stiffener ‘Rat-Hole’, 1:10-Scale Steel Containment Model**

Figure 34 shows the spatial variation of displacements at the cardinal azimuths at 4.5 MPa. It should be noted that the displacement pattern is fairly axisymmetric with the exception of 90°, the azimuth where the equipment hatch is located, where the displacements in the lower conical shell section, below the material change interface, are much larger than at the free-field azimuths (0°, 180°, and 270°). This is of particular interest because this area was actually displaced inward during fabrication of the SCV model and this is the area where the large tear occurred.

In addition to the posttest visual inspection described above, a detailed metallographic evaluation of the SCV model was conducted to characterize the local failure mechanisms and provide some insight into both the global and local response of the model. This detailed evaluation and analysis is described in Reference 33. Briefly, sections were removed from the model surrounding the tears and areas of necking or other obvious structural distress. Fractographic inspection of the failure surfaces indicated that the tearing mechanism was ductile and did not display any evidence of flaws or other defects that might have acted to initiate failure. It was therefore concluded that the model failure resulted from strains exceeding the material strength, and it is possible to characterize failure based on the material properties of the steel.

After this inspection, smaller sections were removed from the model and polished cross-sections normal to the model surface were examined using a scanning electron microscope to characterize the grain structure. Hardness tests were also performed on these polished specimens to look for variations in material properties. A section through the major tear surrounding the equipment hatch is shown in Fig. 35. The results of these inspections revealed changes in the grain structure of the SPV490 material in the heat affected zone (HAZ) surrounding the reinforcement plate weld

and a significant reduction in the hardness of the HAZ and adjacent parent material. Using well-established relationships between hardness and tensile strength, these results indicate a significant reduction in tensile strength along with a corresponding, though less well-defined, reduction in the yield strength of the material. These results indicate that one possible explanation for the strain patterns observed around the equipment hatch and in the weld seams of the SPV490 shell may be due to this localized microstructural alteration and reduced hardness and strength in the HAZ of the SPV490 alloy plate.



**Figure 34 Displacement contours (x10) @ 4.5 MPa**

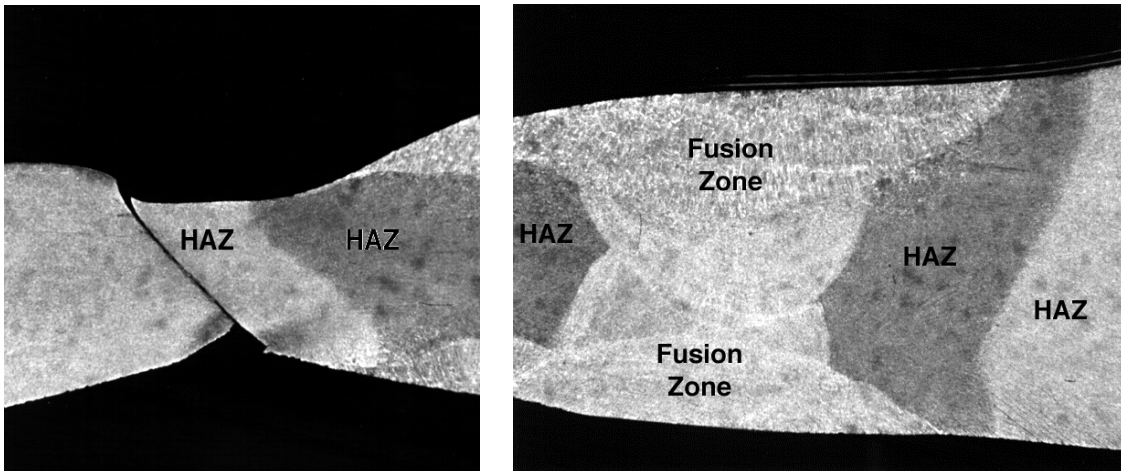


**Figure 35 Cross-section through large tear at equipment hatch**

Pretest predictions of failure pressures, summarized in Table 7, ranged from 5 to 15 times the design pressure with failure modes ranging from ductile material failure to buckling of the top head. These predictions were the result of separate blind analyses performed by a variety of international agencies which were provided with identical design, fabrication and material property data prior to the test [31, 32]. While the lowest predicted failure pressures compared

favorably with the test results, the mechanisms which these predictions were based on were not the apparent cause of the failure. Furthermore, the mechanism giving rise to the small tear was not recognized prior to the test.

**Table 7 Pretest Failure Predictions for 1:10-Scale Steel Containment Model**

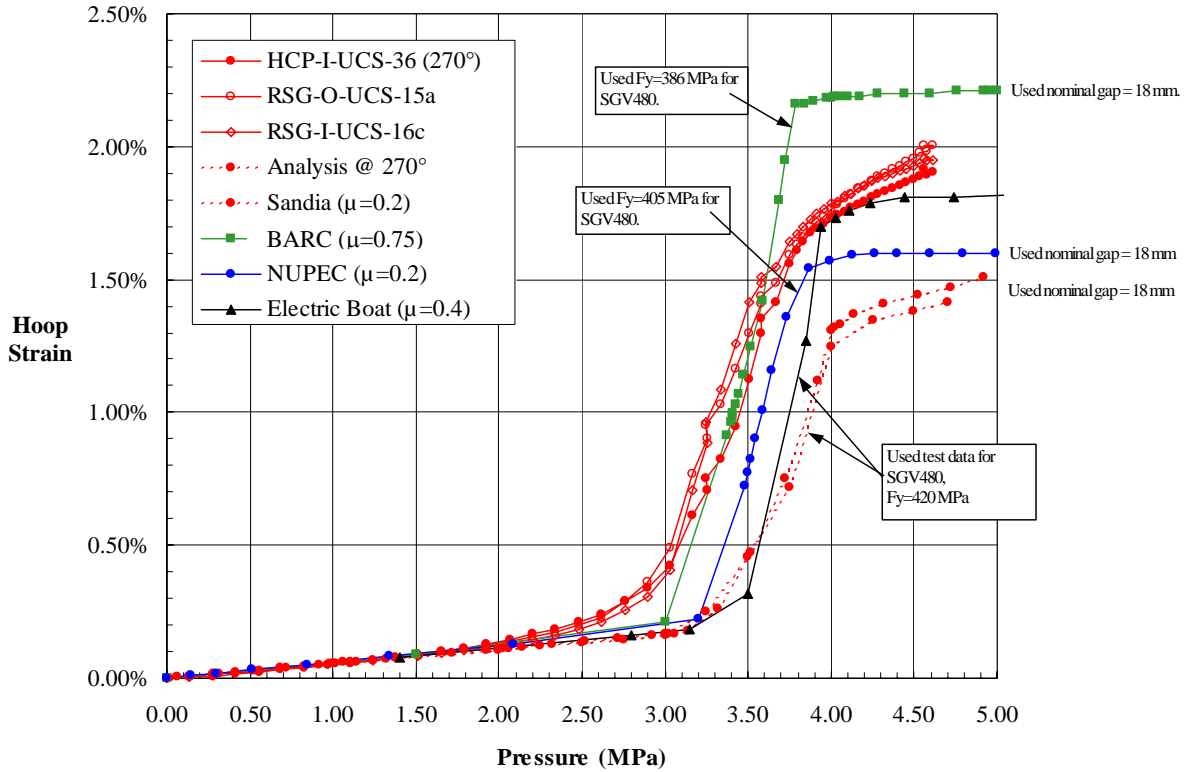
<b>Organization*</b>	<b>Failure Pressure (MPa)</b>	<b>Failure Location</b>	<b>Failure Mode</b>
<b>Test</b>	<b>(4.5) 4.7</b>	<b>(“Rat-hole”) E/H Insert Plate</b>	<b>Material Failure</b>
<b>ANL</b>	<b>4.9-5.5</b>	<b>Knuckle</b>	<b>Material Failure</b>
<b>ANPA</b>	<b>10.9</b>	<b>Drywell Head</b>	<b>Buckling</b>
<b>BARC</b>	<b>11.5-12.0</b>	<b>Drywell Head</b>	<b>Material Failure or Buckling</b>
<b>GD/EB</b>	<b>4.7</b>	<b>Thinned Liner @ E/H</b>	<b>Material Failure</b>
<b>JAERI</b>	<b>&gt;4</b>	<b>Drywell Head</b>	<b>Buckling</b>
<b>NUPEC</b>	<b>4 – 7.3 7.3 – 11.8</b>	<b>Thinned Liner @ E/H Knuckle</b>	<b>Material Failure</b>
<b>SNL</b>	<b>4.5</b>	<b>Thinned Liner @ E/H</b>	<b>Material Failure</b>

\*See Acronyms for Organizations

As with the previous tests, this test demonstrated the large margin in the capacity of the model above the design pressure. Also, as with the previous tests, the importance of details at discontinuities in defining the limits of the vessel capacity was also demonstrated. The exact nature of the local strains and/or stresses which resulted in the tears developing was the subject of extensive posttest investigation and analysis. Furthermore, the contact structure, by arresting or preventing uncontrolled deformation, had some effect on the response of the vessel.

While post-yield response and failure predictions were heavily influenced by modeling of the contact behavior, predictions of global yielding and post-yield behavior prior to contact were very consistent among the participating analysts. It is interesting to note however, that, as in the previous tests, the pressures at which global yielding was predicted were higher than observed during the test. Figure 36 compares predictions of global hoop strain at the mid-height of the vessel with test results. Predictions which based on uniaxial tensile test results of material coupons over-predicted the onset of global yielding by 30 to 50%, whereas those analyses that used (somewhat arbitrarily) a reduced yield strength (e.g. BARC) matched the test results more closely. Furthermore, post-yield predictions and measured response did not converge as in the previous tests. While this discrepancy is much more disturbing than in previous tests, there has been some speculation that it may have be due to the combined effect of residual stresses and the fact that the mixed scale resulted in smaller diameter to thickness ratios than the previous tests or than is typical of the prototype. These results, when taken with similar behavior observed in previous tests, suggest that some factor or factors are not being considered in the analysis. It also suggests that standard material tests using small scale specimens, which are essentially quality assurance tests, may not be adequate for defining material constitutive models for larger scale structures. This issue will be discussed further in Chapter 3.

### Hoop Strain @ UCS, El. 2536



$\mu$  is the assumed coefficient of friction between the SCV and Contact Structure

**Figure 36 Comparison of Pretest Predictions of Hoop Strain with Test Results**

#### 3.3.4 Other Steel Model Tests

Except for the steel containment model tests conducted at SNL, other tests reported in the literature to investigate the capacity of steel containments have focused uniaxial or multi-axial material tests or component tests.

NUPEC conducted a series of small-scale cylindrical pressure vessel tests in support of the 1:10-scale SCV test program. Several tests and investigations were conducted in Germany to investigate the behavior of spherical steel PWR containments to overpressure and hydrogen detonation [37, 38, 39, 40].

#### 3.3.5 Conclusions of Steel Model Tests

With regard to the program objectives, the conclusions overpressurization tests of the steel containment models include the following:

- The tests provided experimental data for checking the capabilities of analytical methods well into the inelastic range of the models.
- In the absence of any other factors (local thinning or the presence of a shield building to restrain deformation) all of the steel models failed catastrophically.

- The onset of global yielding for all of the models occurred at lower pressures, on the order of 10% to 30% lower, than predicted by analyses using material models based on uniaxial tensile test results. While this has been attributed to fabrication effects (e.g. cold-working or welding) or strain-rate effects, no conclusive explanation has been provided.
- Following the onset of yielding, deformation and strains grew rapidly with only a small increase in pressure.
- Failure was initiated at strain concentrations caused by penetrations or stiffeners.
  - The 1:32-scale models without stiffeners or penetrations were able to utilize the full membrane capacity of the model. The hoop strain at the cylinder mid-height for SC0 was estimated to be on the order of 20% prior to failure.
  - Global hoop strains for the models with stiffeners and penetrations were significantly lower at failure than the simple models. With the exception of SC3, the global hoop strains in the 1:32-scale models were between 2.5% to 3%. The maximum global hoop strain was 3% in the 1:8-scale model and 2% in the 1:10/1:4-scale steel model.
- The ratio of ultimate pressure to design pressure was 4.5 for the 1:8-scale model and over 6 for the 1:10/1:4-scale steel model. Design pressures were not specified for the 1:32-scale models.
- The analytical methods used for predicting the global behavior of the model were generally adequate with the exceptions noted. The post-yield response was generally less accurate.
- Pretest predictions for the locations and modes of failure were usually incorrect. As noted by Clauss [25]:

*“An analyst using finite element methods must be able to anticipate the various locations and types of response that can be encountered in shells in order to design a mesh that can be used to accurately calculate the containment response. Localized behavior can have important consequences on the overall containment behavior, as demonstrated by the outcome of the scale model test(s). In particular, any area where there is a potential breakdown of the membrane load carrying action of the structure should be carefully analyzed.”*

In most cases, the analysts did not ‘anticipate’ the correct type or location of the shell discontinuities prior to the test, however, posttest analyses were generally able to reproduce the observed failure mode.

- No general rules regarding material rupture or failure criteria resulted from the tests. Posttest analyses suggest that analyses of local discontinuities using highly refined finite element meshes can yield strain on the order of (or in excess) of the material strain limits from uniaxial tensile tests. These results are heavily dependent on the accuracy of the model (including ‘as-built’ effects), the level of refinement and the experience of the analyst.

### 3.4 Reinforced Concrete Containment Model Tests

Table 8 summarizes the results of tests of scaled reinforced concrete containment models and local specimens used to investigate liner tearing and leakage. A description of the tests follows. Details are provided in the references cited in the table.

Tests of reinforced concrete containment models or models of portions of containments have been conducted elsewhere, although there have been no other large-scale model tests comparable to the test conducted at SNL.

Danisch [41] reported on the plans for conducting pressure tests on a reinforced concrete containment mock-up in Walldorf, Germany. These tests were focused on investigating the performance of a composite liner for the European Pressurized Reactor (EPR). Very little has been reported in the literature on the results of these tests.

Two, nominally, 1:17-scale models were tested hydrostatically in Japan [42, 43]. A rubber bladder was inserted into the models to prevent leakage and the models were tested at room temperature and with a gradient of approximately 45°C across the wall. The results were nearly identical with the models failing at a little more than twice the design pressure.

**Table 8 Summary of Results of Experiments for Reinforced Concrete Containment Models and Liner Tearing and Leakage**

Test	Scale	Shape	R/t	Pressure Ratio ( $P_d/P_{max}$ )	Global Strain at Failure	Liner Material	Remarks
SNL RCCV	1:6	PWR: cylindrical concrete shell w/ steel liner and hemispherical dome and penetrations	13.5 (R=3353 t=248)	3.2 $\left(\frac{1.0}{0.32}\right)$	1.7%	SA414 Gr .D, SA516 Gr. 60	Tearing and leakage at penetration insert plate. [44, 45, 46, 47, 48]
CTL Spec. 2.5	Full	prestressed concrete wall-base juncture	-	2.6*	1.6%	Steel	Several tears at wall-skirt juncture [51]
CTL Spec. 2.4	Full	prestressed concrete wall with penetration	-	2.4*	2.2%	Steel	Large tear at penetration [51,52]
CTL Spec. 3.2	Full	Reinforced wall with penetration	-	2.9*	2.7%	Steel	Severe liner necking next to anchorage [51, 52]
CTL Spec. 2.2	Full	prestressed concrete wall with initial liner flaw	-	-	-	Steel	Ductile extension of Pre-existing flaw [51, 52]
CTL Spec. 3.3	Full	Reinforced	-	-	1.6%	Steel	Strain concentration measured near penetration (4.3% strain) [51, 52]

\*best estimate based on global strains since models were not pressure vessels.

### 3.4.1 NRC 1:6-scale reinforced concrete model

A model of a reinforced concrete containment building, designed and constructed by United Engineers, was tested by Sandia Laboratories in July 1987. It represented a nominal 1:6-scale model of a reinforced concrete PWR containment and was designed according to the ASME code for a design pressure of 0.32 MPa (46 psig). The model, shown in cross-section in Figure 37, consisted of a reinforced concrete shell with steel liner and included functional models of equipment hatches, an airlock and smaller penetrations. Eight layers of primary reinforcing were included in the cylinder wall and the steel liner was anchored to the concrete using headed studs, as in similar prototype containments. Over 1200 channels of instrumentation were installed in the model, the majority consisting of strain gages and displacement transducers. Details of the model construction and instrumentation were described by Horschel [44] and are shown in Figure 38.

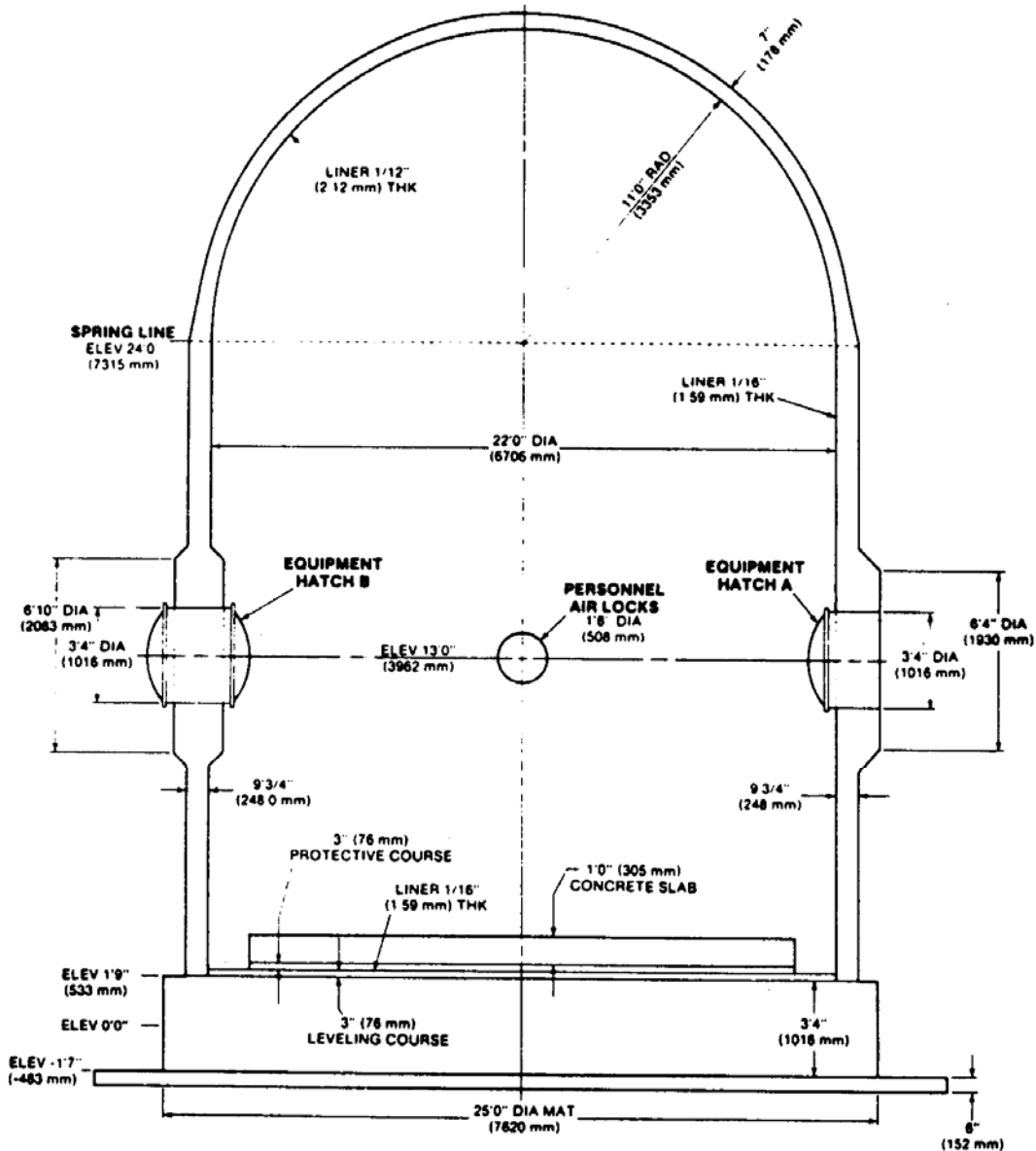


Figure 37 Cross-section of the 1:6-Scale Reinforced Concrete Containment Vessel Model

After a series of low pressure tests, including a Structural Integrity Test and an Integrated Leak Rate Test, the model was tested pneumatically to failure in July 1987. A series of independent pretest calculations predicted failure by various mechanisms including hatch leakage, liner tearing and base shear failures at pressures ranging from 0.90 to 1.31 MPa. [45]

The model was slowly pressurized using nitrogen gas and after 32 hours the test was concluded due to excessive leakage. At 0.96 MPa (140 psig) the leak rate was estimated to be approximately 10 scfm. The leak rate grew to 50 scfm at 0.98 MPa (143 psig) and to over 5000% mass/day or 4000 scfm at 1.0 MPa (145 psig). At this point the pressurization system could not compensate for the leakage of gas through the liner tear and cracked concrete and the test was terminated. The major source of leakage was a 22 inch long tear in the liner plate at a row of studs adjacent to a thickened insert plate assembly, shown in Figure 39. After the test, further inspection revealed a number of smaller (1/8 to 1/2 inch long) liner tears and incipient tears in highly distressed areas as shown in Figure 40. All of these tears were adjacent to liner anchor studs near penetrations [46].



**Figure 38**      **1:6-Scale Reinforced Concrete Containment Model Construction**



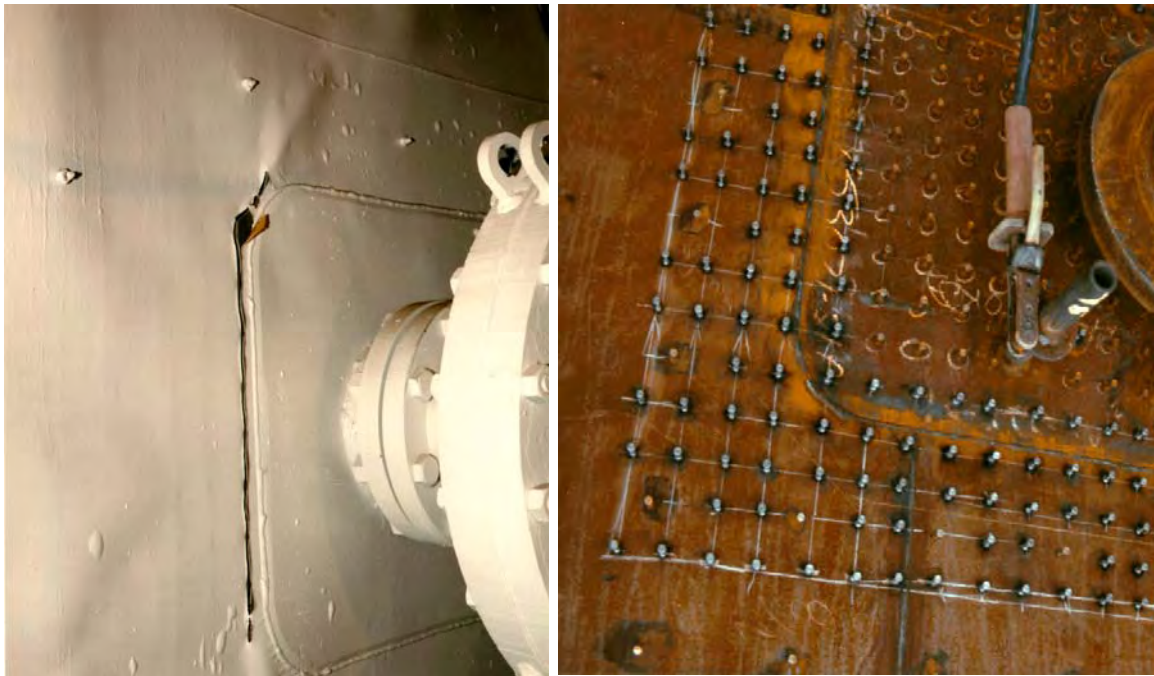
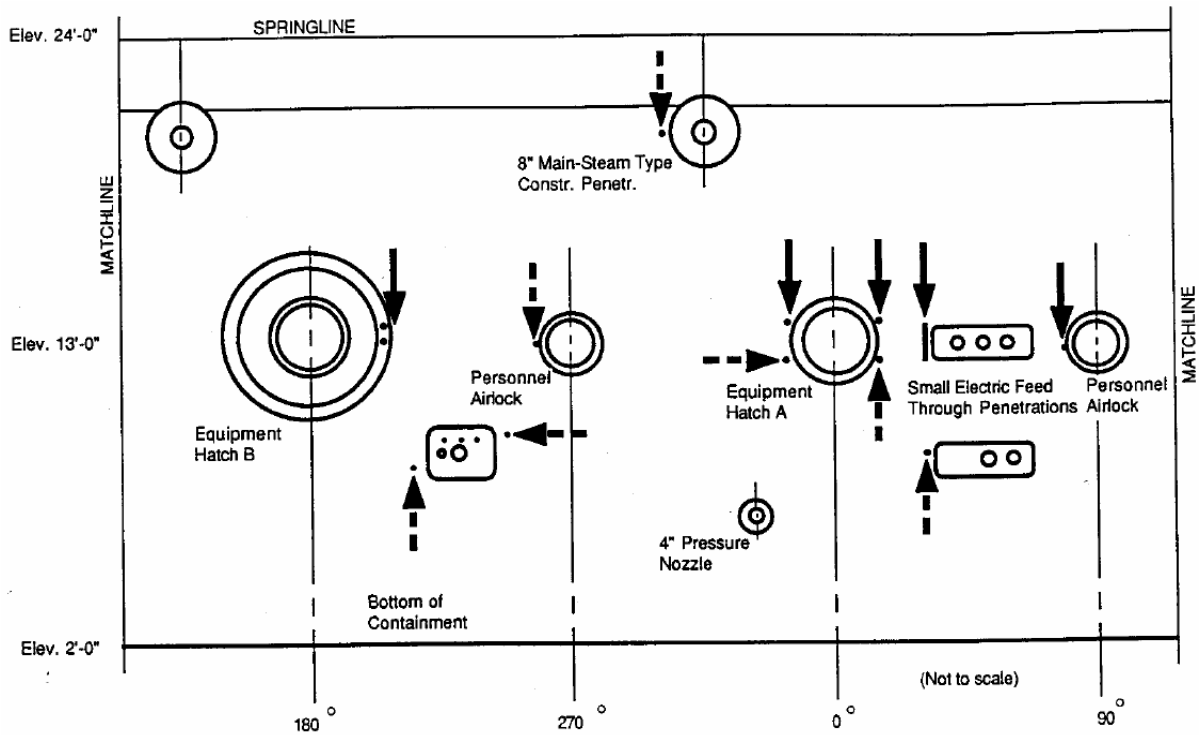


**Figure 39 Major Liner Tear in 1:6-Scale Reinforced Concrete Model**



Locations (Arrows with Solid Lines Had Measurable Leakage; Arrows with Dashed Lines Showed 'Distress,' but Leakage Could not be Confirmed)

**Figure 40 Developed Elevation of the 1:6 Scale RC Model Cylinder showing Liner Tear Locations**

Horschel [46] summarized the major results of the overpressure test:

- No new cracks developed during the high pressure test but cracks in the concrete which had developed during low pressure testing became much wider, up to 1/8 inch.
- Overall response was not perfectly axisymmetric. Maximum radial displacement were on the order of 1-1/2 to 2 inches ( $\Delta R/R \sim 1$  to 1.5%). Free-Field hoop strains measured in the liner and reinforcing at the mid-height of the cylinder were on the order of 1.5 to 2%.
- The peak strains measured in the liner was 8%.
- One of the equipment hatch sleeves was deformed into an oval shape. The change in diameter was on the order of 1.5% in the horizontal direction and minus 1.5% in the vertical direction, comparable to the overall hoop strain.
- A perceptible dishing of the basemat was observed with an average uplift of 3/8-inch at the outer edge.

It should be noted that as a result of tearing of the liner and leakage, the limits on the nonlinear structural response and the ultimate structural capacity, i.e. catastrophic rupture, were not challenged. While some consideration was given to ‘sealing’ and re-pressurizing the model, this was not done and efforts focused on understanding the local liner and penetration behavior. It was generally conceded that catastrophic failure could not occur and the structural capacity limits were well above the limits on the liner and penetrations.

Posttest analysis confirmed the presence of large strain concentrations at the locations shown in Figure 40 which are very similar to details in prototypical plant construction. Figure 41 shows the results of an analysis of the strains in the liner at the location of the major tear. This analysis suggests maximum strains were near the material strain limits at the time of failure.

Pretest predictions of global response compared favorably to the test results, however, as with the previous steel containment model tests, the mechanism which defined the limit state of the model was not recognized prior to the test by many of the analysts. Some analysts presented a list of candidate liner tearing locations and associated leakage pressure range and, in this way, were able to reasonably predict the test failure pressures and locations. These predictions, however, still relied substantially on judgment in addition to the analytical tools involved [48]. Following the post-test examination, it was postulated that the many small tearing locations may have occurred within a narrow pressure range (which was predicted by analysis), but that the tear near the rectangular insert plate dominated because this tear had a propensity to lengthen along a constant elevated strain field. Thus with only slight increase in pressure, this tear and the associated leak size grew large while other tears did not. While the conditions that gave rise to tearing of the liner were recognized, it was, **and still is**, the case that the ability to model the behavior of the liner after the tear initiated and predict the subsequent leakage rate is beyond our current analytical capabilities.

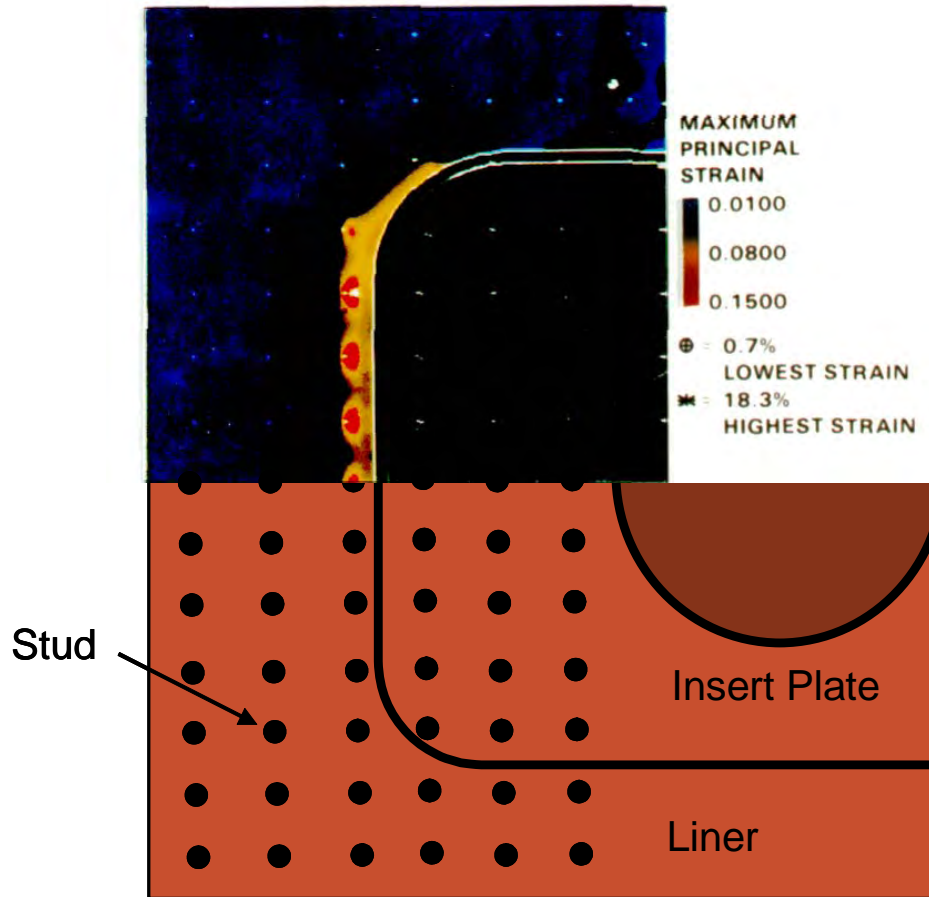


**Figure 41** Posttest Analysis of 1:6-Scale RC Model Liner at 1.0 MPa (145 psig)

Following the test and posttest analyses, Von Rieseman [49] summarized the ‘state of knowledge’ on the behavior of steel liners. His key observations included:

- Prior to the test, while “the possibility of local liner failure was recognized as a major uncertainty”, little effort was invested into understanding the behavior of the liner. There was “a false sense of security” that the anchor studs would fail before the liner tore. Also, while the presence of strain concentrations at the penetrations were recognized, the belief was that the high ductility of the liner material would be adequate to prevent tearing.
- The strength of the cylinder wall-basemat intersection was underestimated. Pretest analyses over-predicted the deformations in this area and as a result predicted this as the most likely location for liner tearing to occur [50].

### 3.4.2 *Separate Effects Tests for Reinforced Concrete Model*

In the years following the 1:6 Scale RCCV model test, SNL conducted analytical [53] and experimental [54, 55] investigation of the strain concentrations and mechanisms leading up to and causing liner tear. The analytical work consisted of local models “driven” by boundary conditions taken from global analysis models. Similar studies were undertaken by EPRI [51] (see 3.4.3).

The experimental work at SNL consisted of uniaxial tests of a series of specimens that simulated certain features of the 1:6-scale model liner. These specimens were instrumented with strain

gages and photo-elastic coatings. One series of six tests, shown in Figure 42(a) were conducted by applying a varying preload to the liner and then applying a separate load to the concrete block to shear the stud anchors. These tests showed that at low preloads, the studs failed while at higher preloads the liner failed.

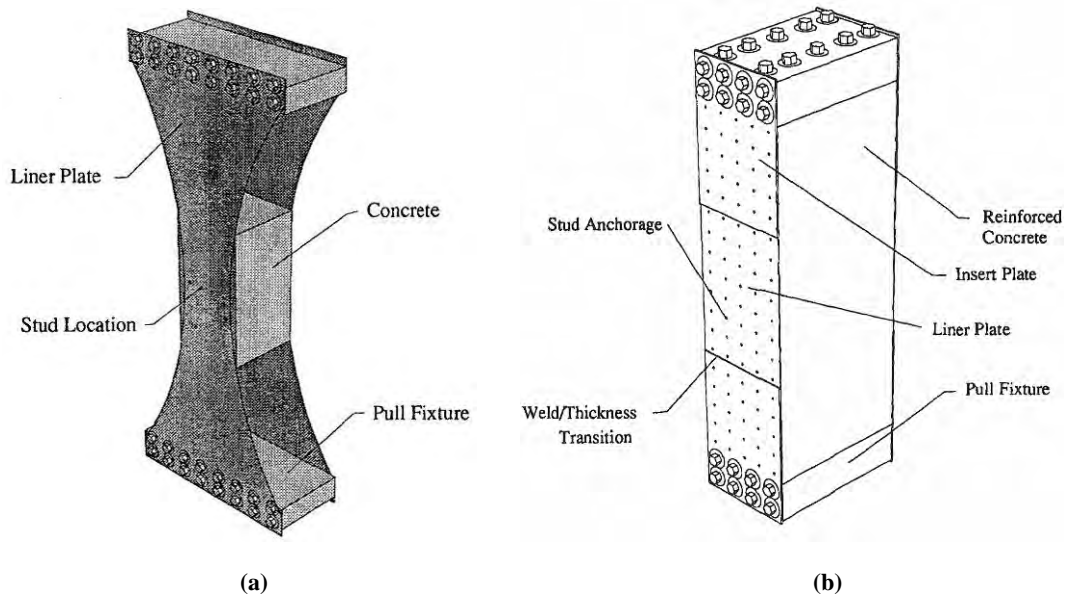


**Figure 42 Separate Effects Test Liner Specimens**

A second series of tests were conducted in an attempt to reproduce the liner tearing mechanism observed in the 1:6-scale R/C containment model. The test specimen, shown in Figure 42(b), included the liner and insert plate with the anchor studs, reinforcing and concrete to represent a section through the wall. While the liner tore in the same relative location, these tests did not replicate the behavior observed in the 1:6-scale model. The elongation required to tear the liner was much higher, attributed to the lack of lateral restraint.

The primary value of these tests was to demonstrate that the liner failure mechanism observed in the 1:6-scale R/C model test was not an artifact of the model and to provide insights into the sources/mechanisms giving rise to strain concentrations in the liner, including:

1. thickness change
2. liner-to-concrete anchor geometry
3. strain magnification across a concrete crack, either in-plane with the liner, or in shear if the crack is a “dislocation” associated with a local “hard spot” in the concrete wall due to a reinforced penetration or thickened wall segment.

Each of these strain concentrations can act independently or can compound each other if they are coincident. The thickness change concentration also tends to be exacerbated by presence of a weld, which does not yield at the same stress as the base metal and so adds to the strain concentration in the base metal. Though this work added to the understanding of causes of liner tears, these results have never been implemented into a prediction methodology as part of the SNL research.

### 3.4.3 CTL/EPRI Tests

As part of a 6-year EPRI sponsored concrete containment research program, a variety of containment panel tests (models of typical containment wall sections) were performed at full scale at Construction Technology Laboratories in Skokie Illinois [51]. These experiments further demonstrated that strong liner strain concentrations exist near penetrations and other discontinuities. These tests, when combined with the results of the Sandia full model test, provide some evidence the existence of liner strain concentrations and a liner tearing, ‘leak before break’ failure mode for concrete containments.

All together, nine specimens were designed, constructed and tested, starting with simple, unlined R/C wall panel elements, and then including steel lined R/C test units that included complex details liner connection and penetration details found in typical R/C and P/C containments in the U.S. Figure 43 shows a schematic depicting the test specimen planning strategy, i.e., to choose small portions of containment walls and load these panels with the biaxial conditions they might experience in a containment subjected to overpressure. This biaxial loading consisted of direct loading applied to individual rebars and applied to liner edges, and also some out-of-plane loading for specimens with discontinuities. The loading was planned by using axisymmetric analysis of the typical R/C and P/C containments shown in Figure 44. Some details of the more important tests are shown in Figures 45 through 47. The overall failure mode and equivalent failure pressure information for Specimens 2.2, 2.4, 2.5, 3.2, and 3.3 were summarized in Table 8. These specimens all focused on the existence and causes of liner strain concentrations and liner tearing, and all tended to support the hypothesis of ‘leak before break’ failure mode for concrete containments.

These tests, combined with the results of the Sandia 1:6-scale model test (global deformation results and local liner strain results near penetrations) and Sizewell B 1:10-scale model test (global deformation results) (see 3.5.2) were used to form the basis of a liner tearing and leakage prediction methodology that was used for the containment portions of a number of Individual Plant Examinations in the early 1990s. Though the database of liner tearing geometries and measured strains at failure is not exhaustive, the methodology does represent the first attempt at developing a systematic approach to containment leakage prediction. The basic approach, which is described in more detail in Analysis Methods sections of Chapter 3, introduces global strain as a ‘driving strain’ to which are applied strain concentration factors to produce a local strain that can then be compared directly to a liner failure criteria. The research also represented one of the first attempts to quantify pressurized gas leakage through cracks, and quantify the associated growth in leak rate with the growth of tear size in the liner. These early steps toward a leak prediction methodology are described in [56]. An illustration of the basic assumptions for leakage through liner tears in concrete containments is shown in Figure 48. The phenomena illustrated here were studied with the leak rate measurements performed on EPRI/CTL Specimen 2.2. Some developmental, but extensive, work quantifying the flow of pressurized gas through cracked concrete has been reported in Canada by Rizkalla, et al [57].

**Typical Prestressed Containment**

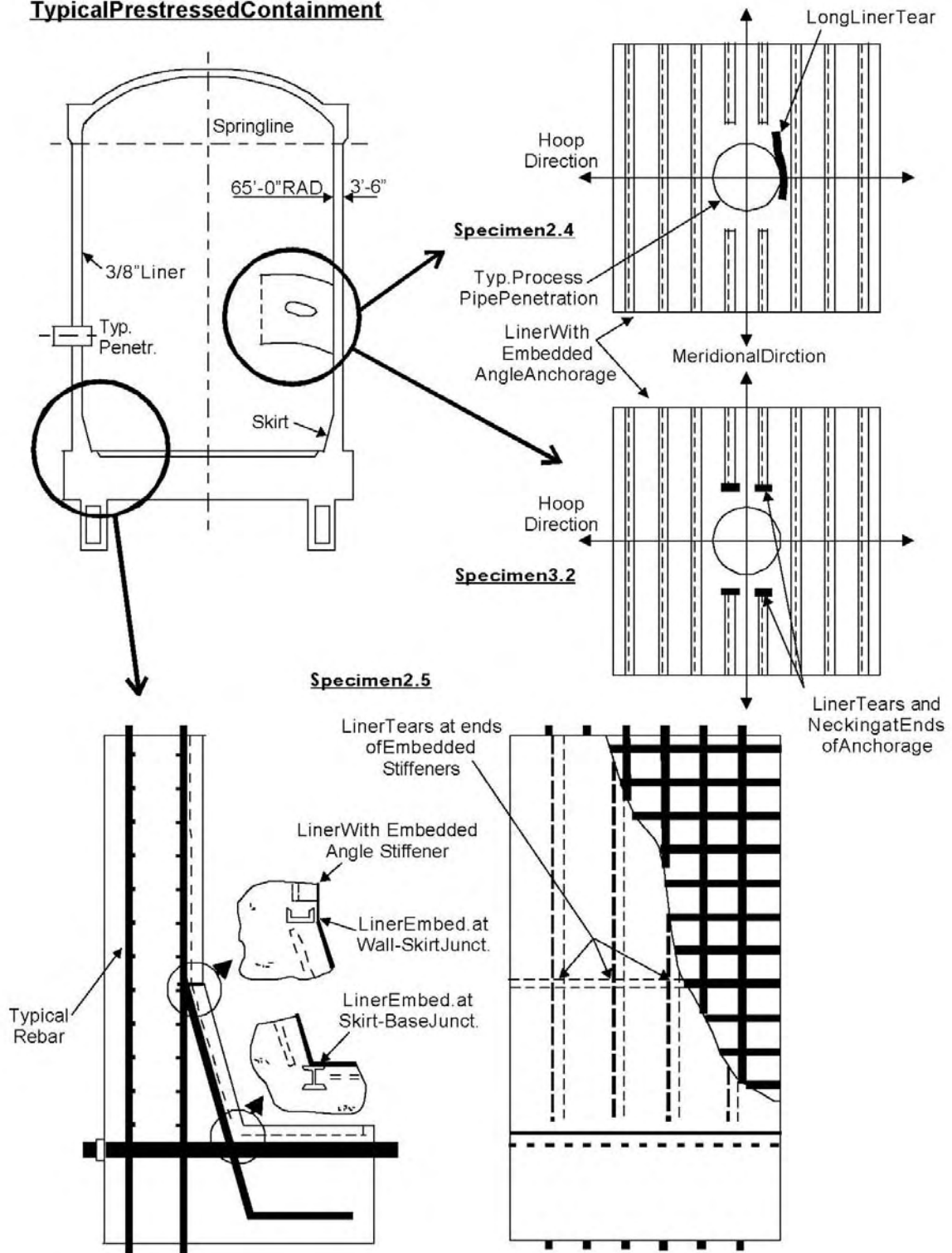


**Figure 43** Containment Wall Panel Specimen Test Strategy for EPRI/CTL Tests [51]

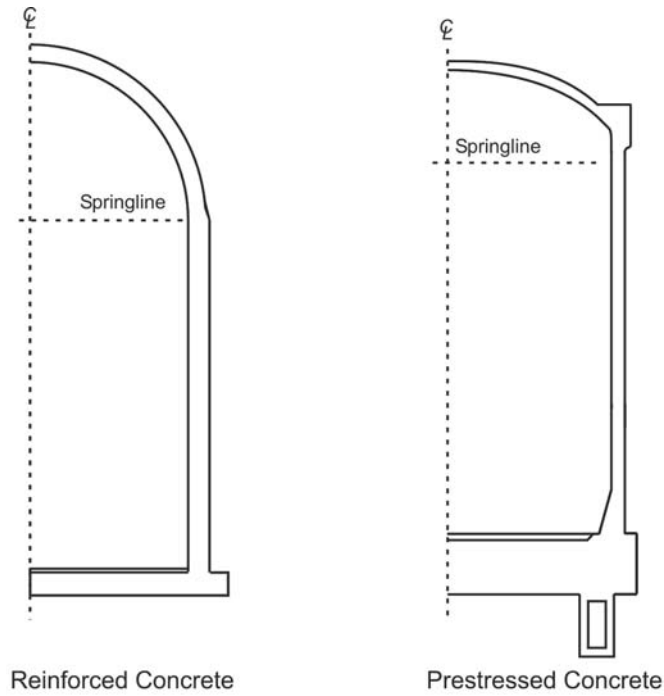


**Figure 44** Typical R/C, P/C Containment Geometries used in EPRI Global Analyses [51]

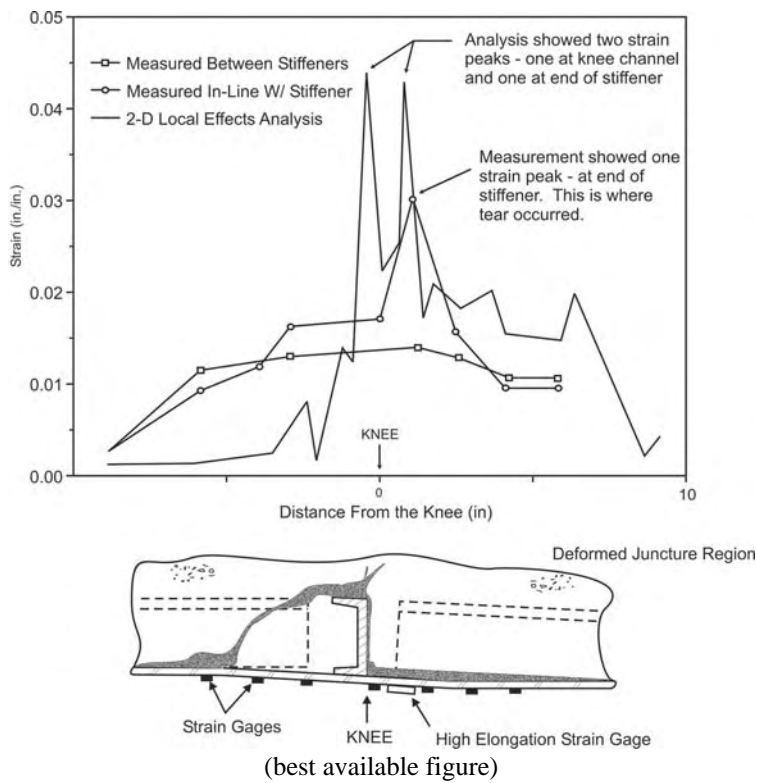


**Figure 45** Liner Vertical Strains Measured (and Analyzed) in EPRI/CTL Specimen 2.5, Wall-Skirt Junction of a Typical P/C Containment

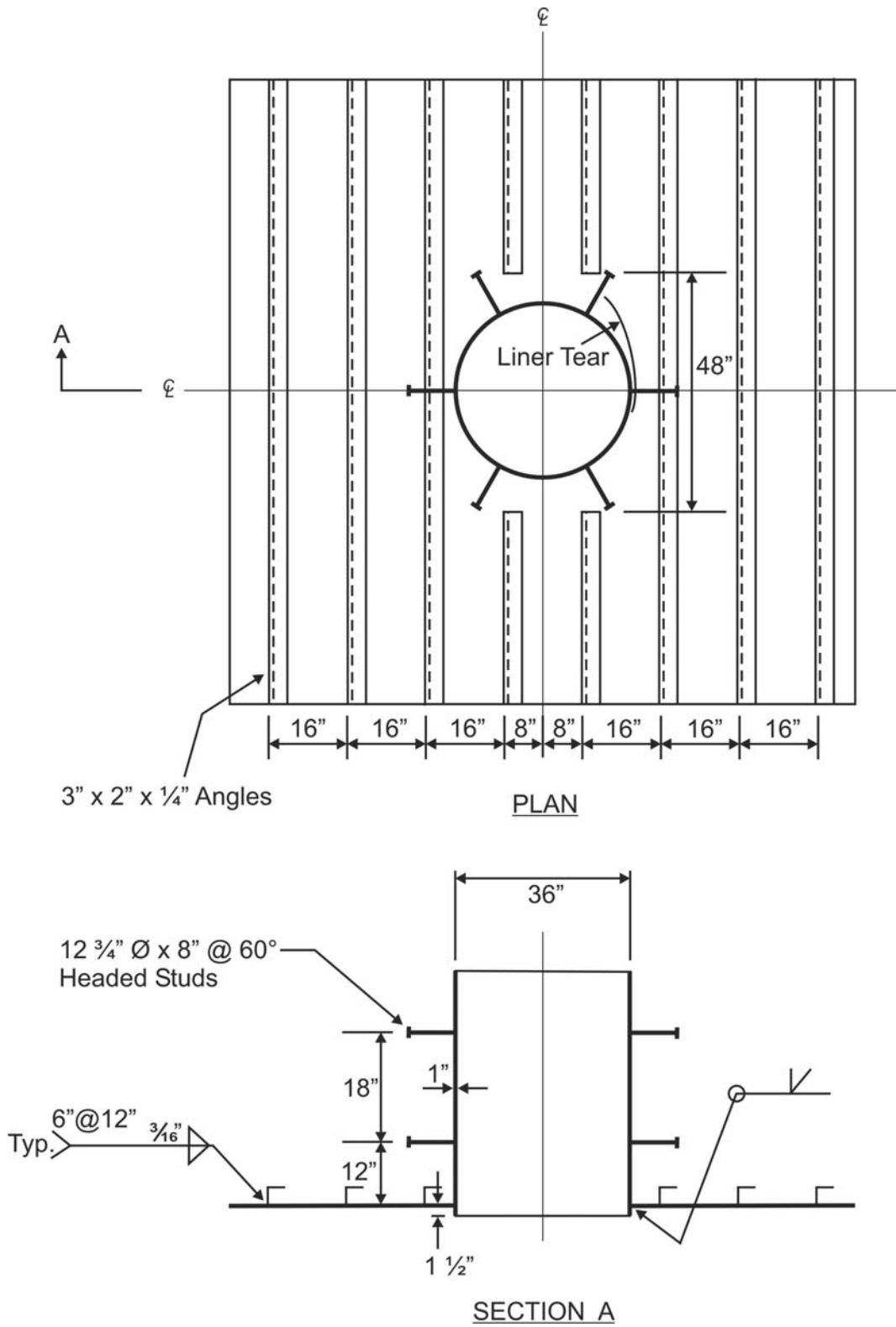


**Figure 46 Liner Plate Details for EPRI/CTL Specimen 2.4**



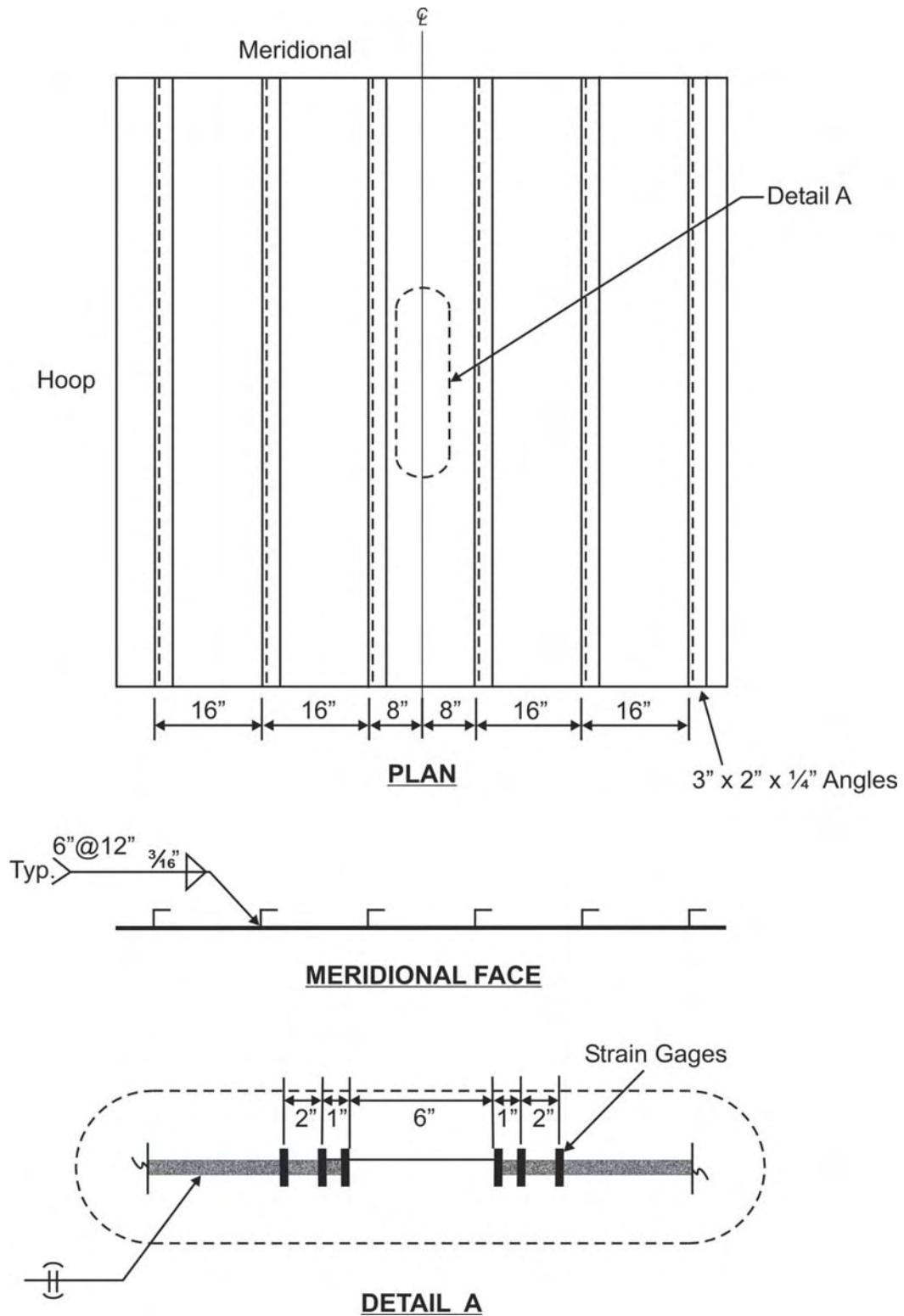


**Figure 47 Liner Plate Details for EPRI/CTL Specimen 2.2, Which Studied Leak Rates Through an Advancing Liner Crack Tip**

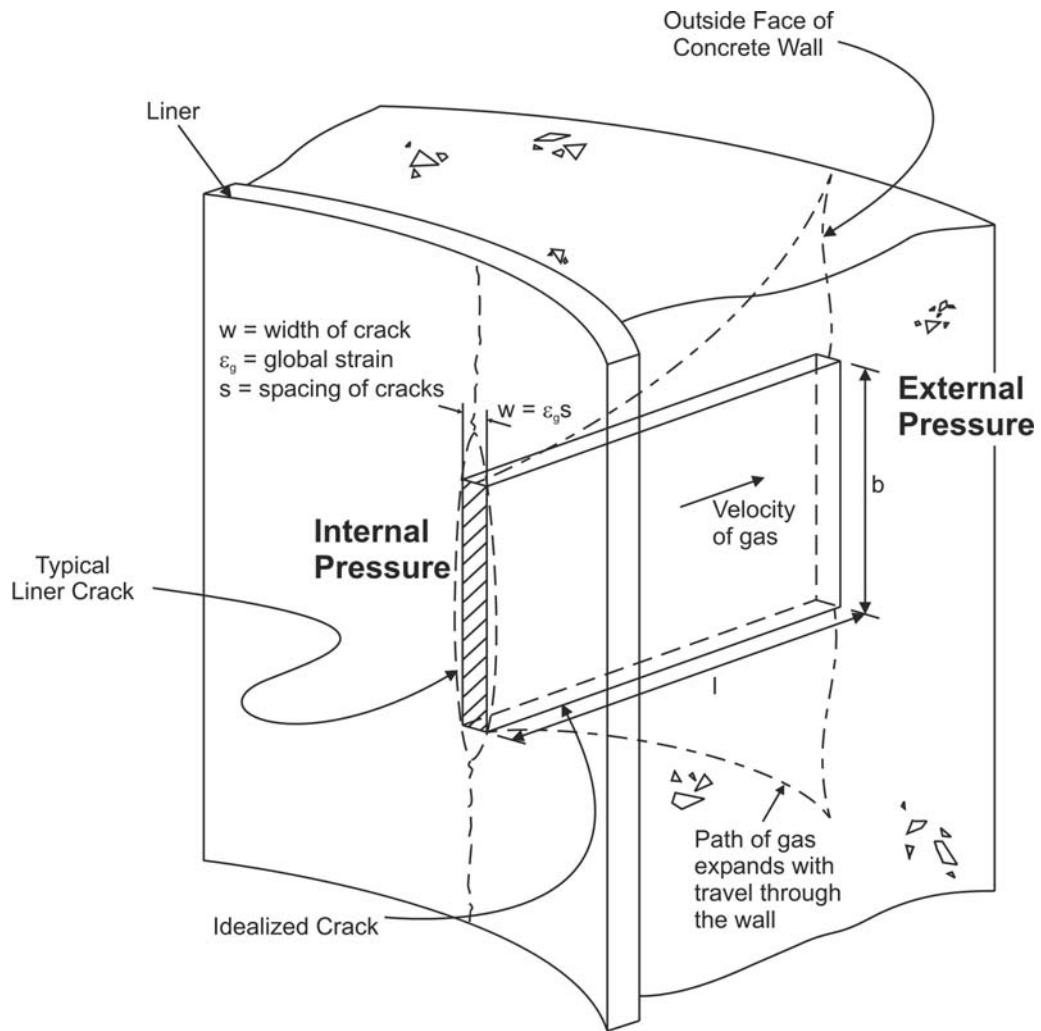


Figure 48 Idealization of Flow of Pressurized Gas Through a Liner Tear [56]

### 3.5 Prestressed Concrete Containment Models

A number of scale model tests of prestressed concrete reactor pressure vessel and containment vessel models have been conducted. Table 9 is a list of the major tests and includes a brief comparison of the results. References to ongoing or recent tests are also included even though the results of these tests may not be available. This section will focus on the 1:4-scale prestressed containment vessel model tested by SNL for then US NRC and NUPEC and analyses conducted in support of the 1:10-scale model of the Sizewell B prestressed concrete containment tested in the UK. A brief description of the other tests concludes this section.

**Table 9 Summary of Results of Experiments for Prestressed Concrete Containment Models**

Test	Scale	Shape	R/t	Pressure Ratio	Global Strain at Failure	Liner Material	Remarks
<b>Pressure Vessel Tests</b>							
Fort St. Vrain G.A. Model 1, USA	1:4.5	Cylinder	5	3.5,2.5	0.22%	Steel	[58] Liner tear / leakage occurred.
Wylfa Vessel, U.K.	1:12	Sphere	5	See remark	0.1%	Rubber	2.7 pressure ratio reached with no leakage [58]
Oldbury Vessel, U.K.	1:8	Cylinder		3	0.4%	Steel	[58] Liner tear / leakage occurred
"	1:12	Sphere	5	2 - 3	0.4%	Rubber	
"	1:8	Cylinder	3.5	2 - 3	-	Steel	Shear-type failure artificially induced [58]
1000 MWe HTGR G.A. Model 2, USA	1:4	Cylinder	2.4	2	0.06%	Steel	Liner tear / leakage occurred
<b>Containment Model Tests</b>							
Indian Model	1:12	(CANDU)	20	1.9	-	1mm steel liner	Liner tearing and leakage esp. around penetration [59]
Polish Model	1:10	(CANDU)	20	1.9	-	1mm steel liner	Liner tearing and leakage esp. around penetration [60]
Canadian Model	1:14	Gentilly-2: 4-buttress w/ ring buttress	12.6	8.6	-	none (hydrostatic)	Vertical and hoop tendon rupture. [61, 62, 63, 64]
Sizewell-B (CEGB)	1:10	Sizewell-B	8.6	2.4	-	Rubber bladder (hydrostatic)	Basemat bending failure [65-70]
EPR Model (Civaux Test)	?	Cylinder, inner containment	6.7	0.65 *	-	unlined and partial composite liner	[71]
NUPEC/NRC PCCV (SNL)	1:4	Large, dry PWR: 2-buttress cylinder w/ hemispherical dome	16.5	0.39* 3.6	-- 1.4%	SGV 410	LST: Liner tear/leakage SFMT: Tendon rupture and through-wall rupture [72-76]

\*Design pressure (MPa).

#### 3.5.1 NUPEC/NRC Prestressed Concrete Containment Vessel (PCCV) Model Test

As part of a Cooperative Containment Research Program that was co-sponsored and jointly funded by the Nuclear Power Engineering Corporation (NUPEC) of Japan and the U.S. Nuclear Regulatory Commission (NRC), Office of Nuclear Regulatory Research, Sandia National

Laboratories (SNL) conducted a 1:4-scale model of a large, dry PWR prestressed concrete containment vessel. The PCCV model was a 1:4-scale model of the prestressed concrete containment vessel (PCCV) of an actual nuclear power plant in Japan, Ohi-3 (Figure 49). Ohi-3 is an 1127 MWe Pressurized Water Reactor (PWR) unit, one of four units comprising the Ohi Nuclear Power station located in Fukui Prefecture, owned and operated by Kansai Electric Power Company.



**Figure 49 Ohi Nuclear Power Station, Ohi-cho, Fukui, Japan**

The design pressure,  $P_d$ , for the model and the prototype is 0.39 MPa. The features and scale of the PCCV model were chosen so that the response of the model would mimic the global behavior of the prototype and local details, particularly those around penetrations, would be represented. The model includes a steel liner anchored to the concrete shell by semi-continuous structural shapes (T's). Conventional reinforcing ratios match the prototype and prestressing tendons match 1-to-1 with the prototype. The un-bonded prestressing system consists of three, seven-wire strands per hairpin tendon, anchored in the basemat and identical, 360° hoop tendons anchored in opposing vertical buttresses. The overall geometry and dimensions of the PCCV model are shown in Figure 50. Figure 51 shows the sequence of the model construction from erection of the liner, to installation of the prestressing tendon ducts to placement of the concrete wall and dome. Figure 52 shows the completed model. Details of the design, including the design drawings, and construction are reported in the PCCV test report [72]

Model construction commenced at the Containment Technology Test Facility at Sandia National Laboratories on January 3, 1997. Concurrent with the construction of the model, Sandia installed nearly 1500 transducers to monitor the strain, displacement, forces, temperatures and pressures in the model. These transducers were monitored by a data acquisition system (DAS) which provided for near-continuous scanning of all transducers while providing real time display of any sensor channel. In addition to this suite of instrumentation, an independent acoustic monitoring system and internal and external video and still cameras were used to record the response of the model during pressure testing.

Construction and instrumentation of the PCCV model was completed on June 25, 2000. Prior to the completion of construction, tensioning of the model prestressing tendons commenced March 8, 2000 after the majority of the model transducers had been installed and certified. Initial model response was recorded on March 3 and monitored continuously through the prestressing operations and pressure testing.

Prestressing levels for the model tendons were selected so that the net anchor forces (considering all losses due to anchor seating, elastic deformation, creep, shrinkage and relaxation) at the time of the Limit State Test matched those expected in the prototype after 40 years of service. One further adjustment was made by increasing the vertical tendon stress level to account for the additional gravity load in the prototype, which is lost in the geometric scaling. Eight instrumented tendons and load cells at the ends of 1/6th of the model tendons were monitored continuously during prestressing. Unfortunately over half of the strain gages installed on the tendons were damaged during prestressing operations, nevertheless, enough survived to provide useful data on the tendon response during prestressing and pressurization tests. Since all model sensors were scanned during and after prestressing, the overall response of the model to prestressing forces as well as ambient thermal response and time dependent effects was also recorded.

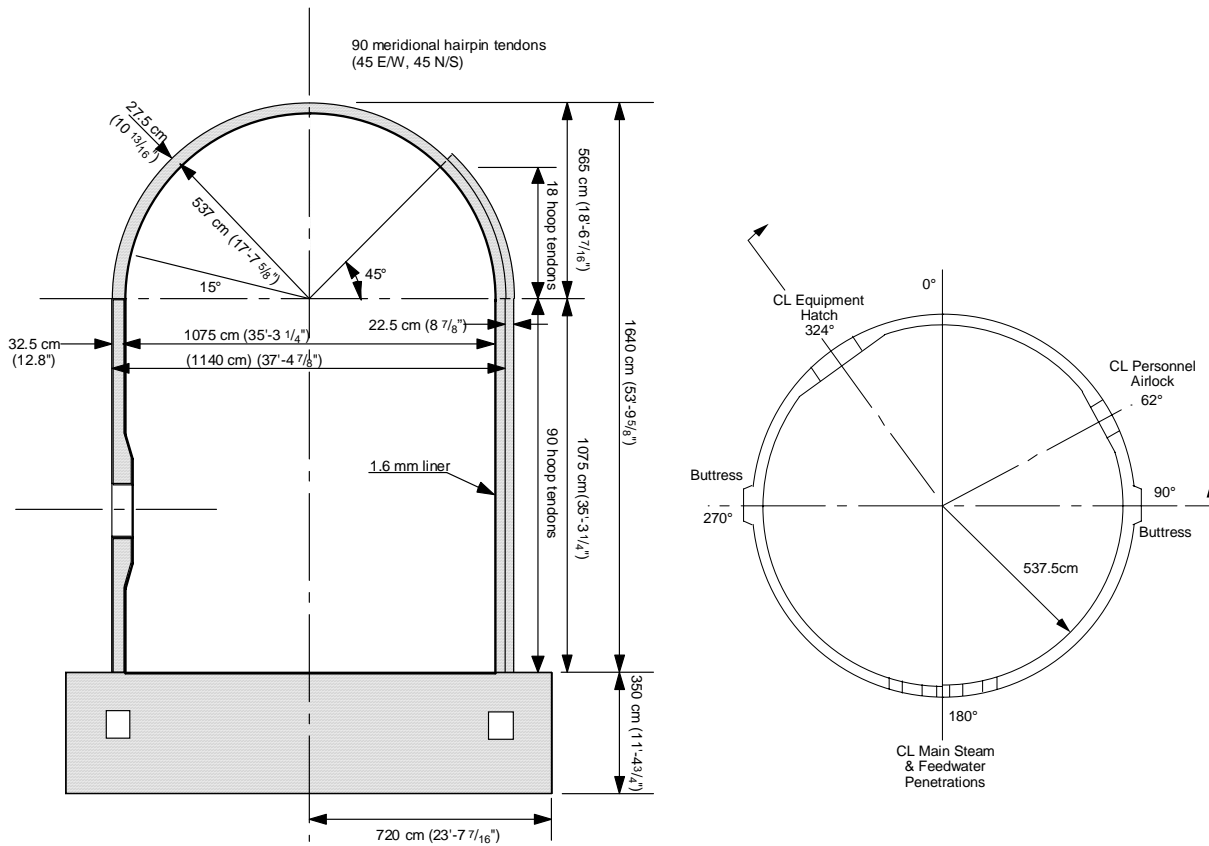


**Figure 50 PCCV Model Elevation and Cross-Section**

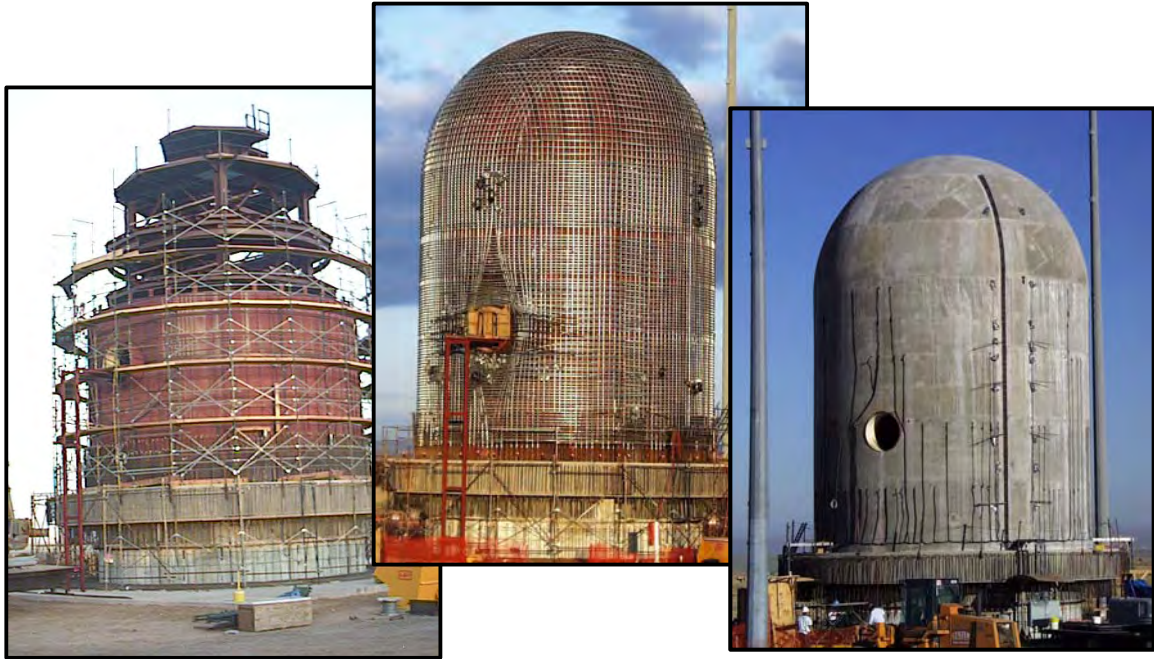


**Figure 51 PCCV Model Construction**



**Figure 52 Completed PCCV Model**

### 3.5.1.1 Pressure Tests

The final test sequence for the PCCV model is shown in Figure 53. Pressure testing of the model consisted of a series of static overpressurization tests of increasing magnitude, beginning with the System Functionality Test (SFT) to  $0.5P_d$  (0.2 MPa) on July 18-20, 2000. This test was conducted to confirm the operation of all test and data acquisition systems, verify that the model was leak tight and calibrate the leak detection/measurement system. It also provided some preliminary response data on the model. The next tests were a combined Structural Integrity and Integrated Leak Rate Test (SIT/ILRT). The PCCV model was pressurized to  $1.125P_d$  (0.44 MPa) on September 12, 2000 and after holding pressure for approximately 1 hour, the model was depressurized to  $0.9 P_d$  (0.36 MPa) and held at this pressure for 24 hours. During this period a leak rate of less than 0.1% mass/day was calculated, essentially demonstrating that the model was leak-tight. While holding at the ILRT Pressure, a limited amount of crack mapping was performed. Cracks widths were not measured.

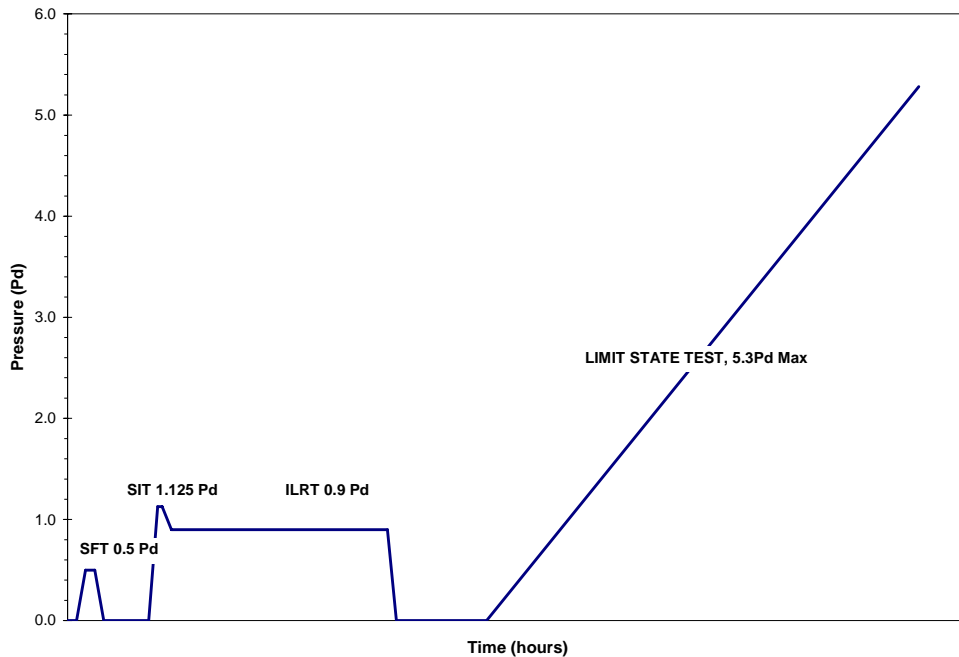
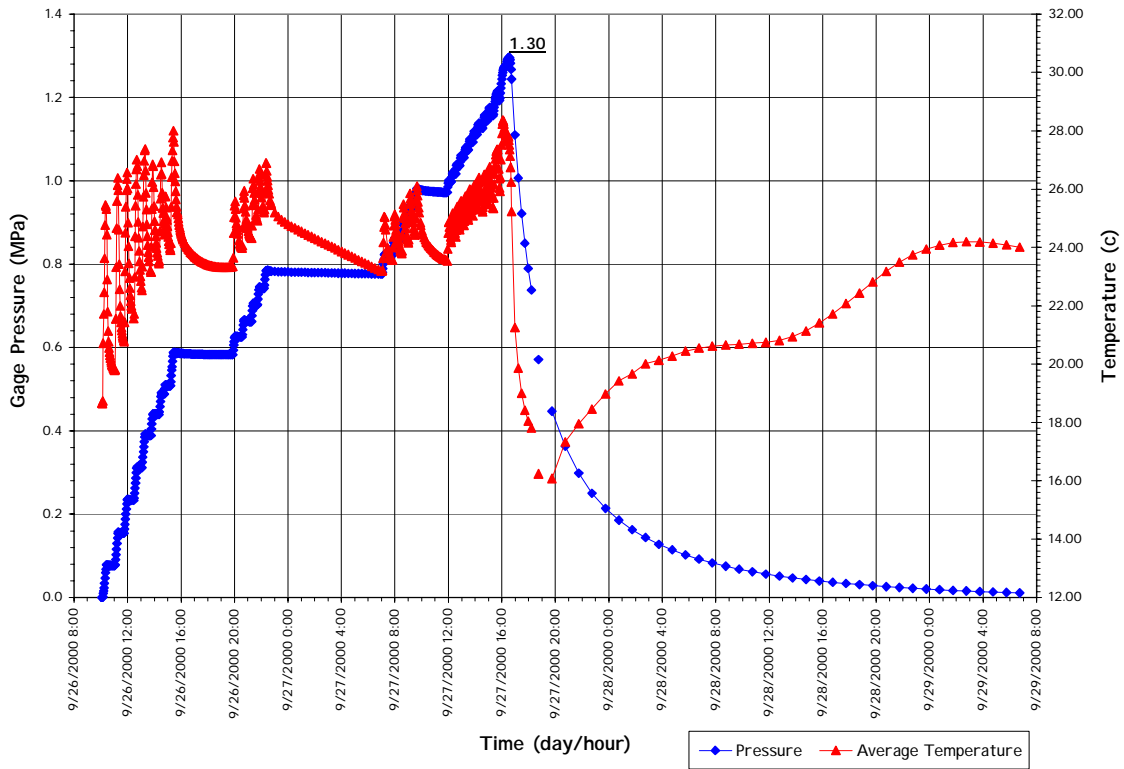


**Figure 53 PCCV Pressurization Plan Sequence (not to scale)**

#### *Limit State Test*

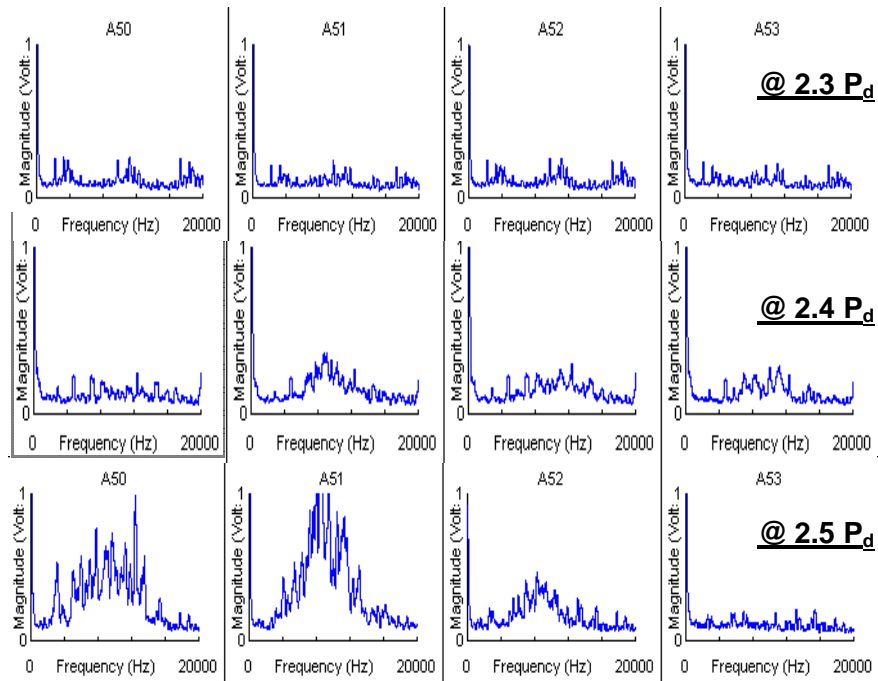
The Limit State Test (LST) was designed to fulfill the primary objectives of the PCCV test program, i.e. to investigate the response of representative models of nuclear containment structures to pressure loading beyond the design basis accident and to compare analytical predictions to measured behavior. The LST was conducted after the SIT and ILRT were completed and the data from these tests evaluated. The PCCV model was depressurized between the SIT/ILRT and the LST. The LST began at 10:00 AM, Tuesday, September, 26, 2000 and continued, without depressurization, until the test was terminated just before 5:00 PM on Wednesday, September 27. The LST pressure and temperature time histories are shown in Figure 54. The model was pressurized in increments of approximately  $0.2P_d$  to  $1.5 P_d$  (0.08 to 0.6 MPa) when a leak check was conducted yielding a leak rate of 0.48% mass/day. Pressurization of the

model continued, in increments of approximately  $0.1P_d$ , to  $2.0P_d$  (0.78 MPa) when a second leak check resulted in a calculated leak rate of 0.003%, i.e. essentially zero. Pressurization of the model resumed in increments of  $0.1P_d$  to  $2.5P_d$  (0.98 MPa). At  $2.4P_d$  (0.94 MPa) the acoustic system operator reported hearing a change in the acoustic output which might indicate that “something had happened”. Plots of the output of the four internal acoustic sensors surrounding the E/H at 2.3, 2.4 and  $2.5 P_d$  are shown in Figure 55. The model was isolated for a third leak check and after approximately 1-1/2 hours, a fairly stable leak rate of 1.63% mass per day was calculated, indicating that the model was leaking, most likely from a tear in the liner in the vicinity of the equipment hatch. The average hoop strain at  $2.5P_d$ , coinciding with the onset of liner tearing and leakage was 0.18%.



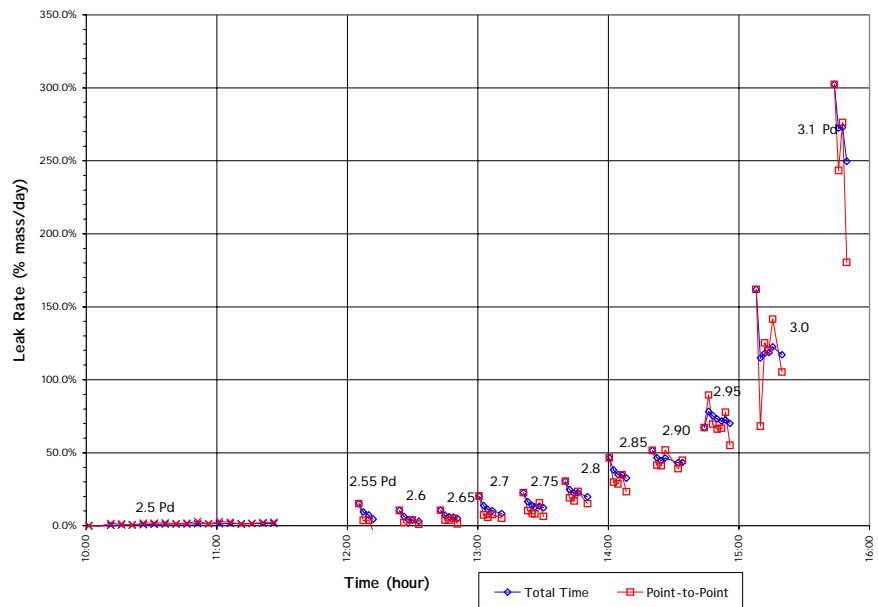
**Figure 54 Limit State Test Pressure and Average Temperature**



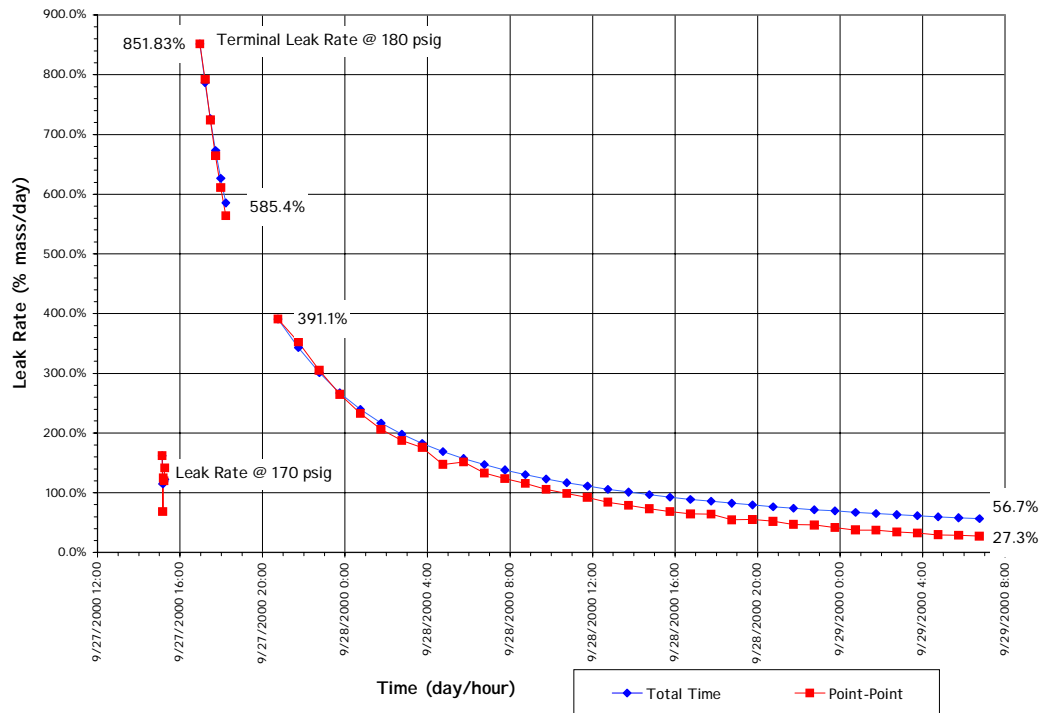


**Figure 55 Internal Acoustic Sensor Signals @ the Equipment Hatch**

After concluding that the model had functionally failed between 2.4 and 2.5 Pd, the next goal was to continue to pressurize the model as high as possible to collect data on the inelastic response of the structure and to observe, if possible, a structural failure mode. Pressurization continued in increments of 0.05 Pd. The pressure was increased to slightly over 3.3 Pd before the leak rate exceeded the capacity of the pressurization system and the test was terminated. Estimated leak rates during the final pressurization and depressurization phases are shown in Figures 56 and 57.



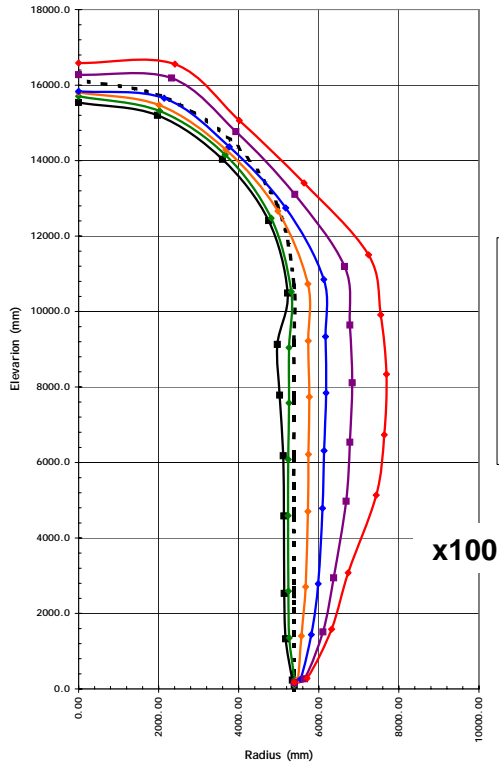
**Figure 56 LST - Estimated Leak Rates (2.5-3.1 Pd)**



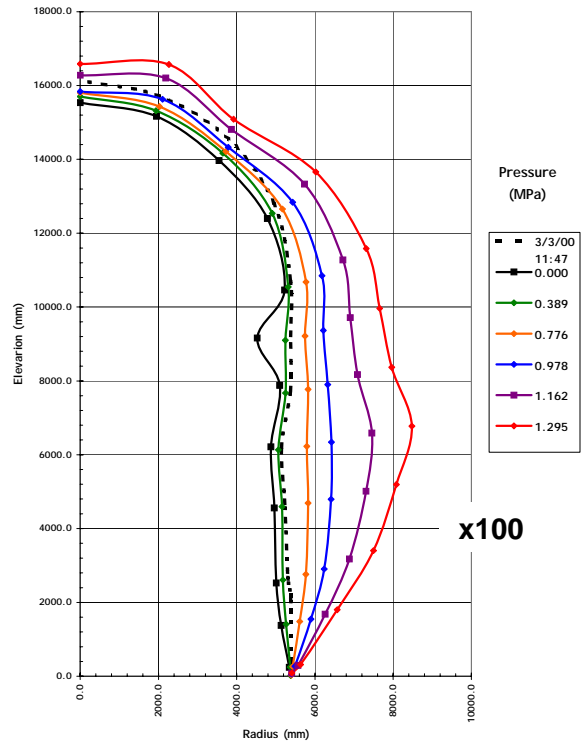
**Figure 57 LST Estimated Terminal Leak Rates**

Figure 58 shows the displacement profiles (exaggerated by a factor of 100) at Azimuths 135°, representing the axisymmetric response, and 324°, at the centerline of the equipment hatch. The profiles are based on interior measurements of the model surface prior to prestressing (3/3/00, 11:47am) and at multiples of the design pressure 0Pd, 1.0Pd (0.389 MPa), 2.0Pd (0.776 MPa), 2.5Pd (0.978 MPa), 3.0Pd (1.162 MPa) and 3.3Pd (1.295 MPa). The profile at 324° illustrates the buckling of the liner which occurred at Elev. 9200 due to prestressing. This bulge in the liner disappeared when the model was initially pressurized and did not affect the capacity of the liner. At maximum pressure local liner strains approached 6.5% and global hoop strains (computed from the radial displacement) at the mid-height of the cylinder averaged 0.4%.

While large local liner strains were measured and the liner was torn in several locations (see Figure 59), the remainder of the structure appeared to have suffered very little damage with the exception of more extensive concrete cracking at some locations. Figures 60 and 61 show two of the large tears near the equipment hatch, along with photographs of the liner anchor details at these locations taken during construction of the model. There was no indication of tendon or rebar failure and the data showed that no tendon strains exceed the elastic limit while only a few dozen rebar strain gages showed strains in excess of 1%.



(135°)  
Figure 58



(324°)  
LST - Deformation @ Az. 135° and 324° (Z and L)

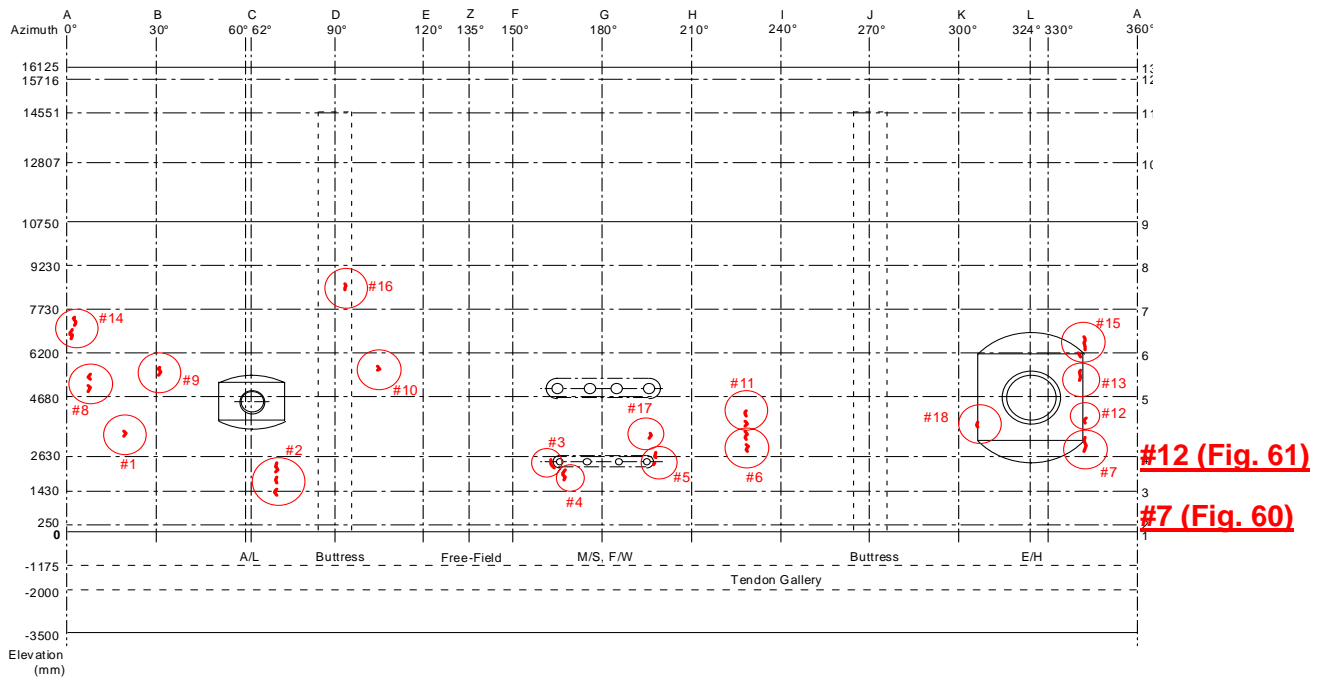
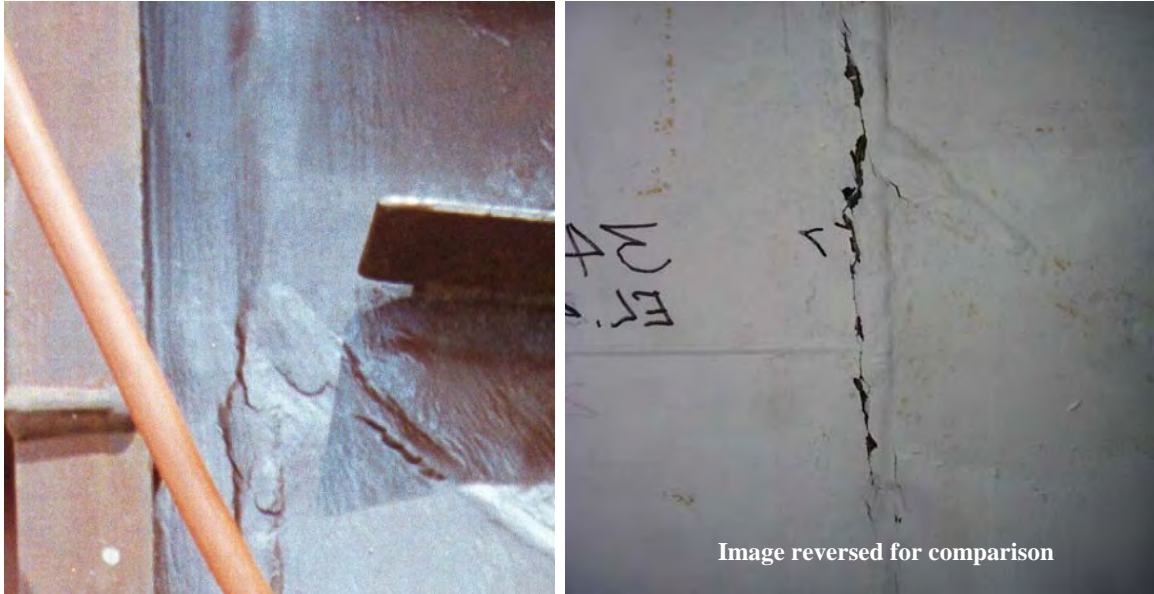
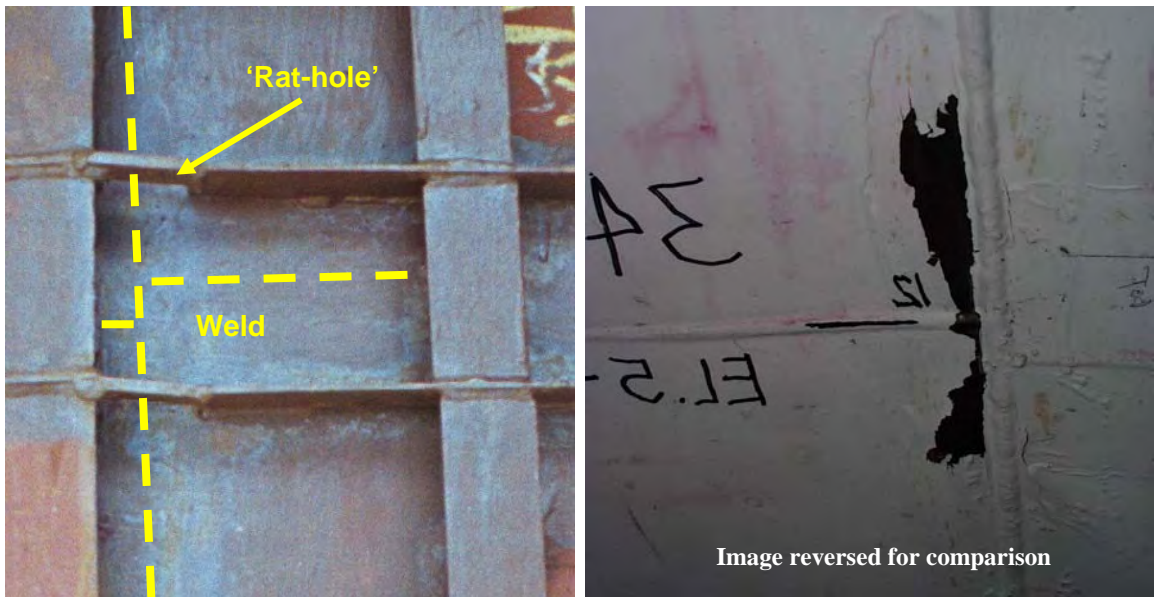


Figure 59 Post-LST Liner Tears



**Figure 60**      **Tear #7 at Equipment Hatch**



**Figure 61**      **Tear #12 at Equipment Hatch**

*Structural Failure Mode Test*

Almost immediately after the completion of the LST, it was recognized that while the PCCV model had demonstrated its capacity to resist pressures well above the design pressure and confirmed, arguably, liner tearing and leaking as the functional failure mode, the test objectives were not fully met with respect to observing large inelastic deformations, for comparison with analyses, and witnessing the structural failure mode of the PCCV model. NUPEC and NRC approved a concept proposed by SNL to seal the interior surface of the liner with an elastomeric membrane, fill the model with water to 1.5m (5 ft.) from the dome apex, approximately 97% of

the interior, and re-pressurize the remaining gas pocket with nitrogen until the model failed or pressure could not be maintained.

The Structural Failure Mode Test (SFMT) began shortly after 10:00 AM on Wednesday, November 14, 2001. The model was continuously pressurized at a rate of approximately 0.035 MPa/min (5 psi/min). All active sensors (approximately 500) were continuously scanned at intervals of approximately 30 seconds and video cameras were continuously recording the response of the model. As the pressure was increased, evidence of leakage was visible by increasing wetting of the concrete surface. At 10:38 AM, the effective pressure in the model equaled the peak pressure achieved during the LST, 3.3 Pd. At approximately 10:39 AM, the acoustic system recorded a very high noise level event which was interpreted as the breaking of a tendon wire. At this point in the test, events occurred very quickly. Shortly after detecting the wire break, a small spray of water was observed at approximately 0° azimuth and additional tendon wire breaks were detected by the acoustic system with increasing frequency. The rate of pressurization was decreasing and the nitrogen flow rate was increased to maintain the pressurization rate. Pressurization of the model continued until a second spray of water was observed and then, suddenly, at 10:46:12, at an effective pressure of 3.63 Pd (1.42 MPa or 206.4 psig) the PCCV model ruptured violently at ~6° azimuth near the mid-height of the cylinder. Four external video cameras recorded the rupture of the model and the moment of rupture is captured in Figure 62. The condition of the model after the SFMT, viewed from 0°, is shown in Figure 63.

The radial displacement of the model at Az. 135°, Elevation 6200 during the LST and SFMT is illustrated in Figure 64. (The SFMT response was 'offset' in this figure by adding the residual displacement at the end of the LST to facilitate comparison.) This figure demonstrates that the hoop stiffness during the SFMT is essentially identical to the post-cracking stiffness during and after the LST. It also shows that the SFMT displacement is nearly identical to the LST displacement at the maximum LST pressure, suggesting that, if the LST could have been continued, the response would have been almost the same as that measured during the SFMT. It thereby confirms the assumption that, again with the exception of the liner and cracking of the concrete, the model was essentially undamaged by the LST.



(a) 0° Azimuth

(b) 90° Azimuth



(a) 180° Azimuth

(b) 270° Azimuth

Figure 62 SFMT: Rupture of the PCCV Model



Figure 63 PCCV Model after the Structural Failure Mode Test

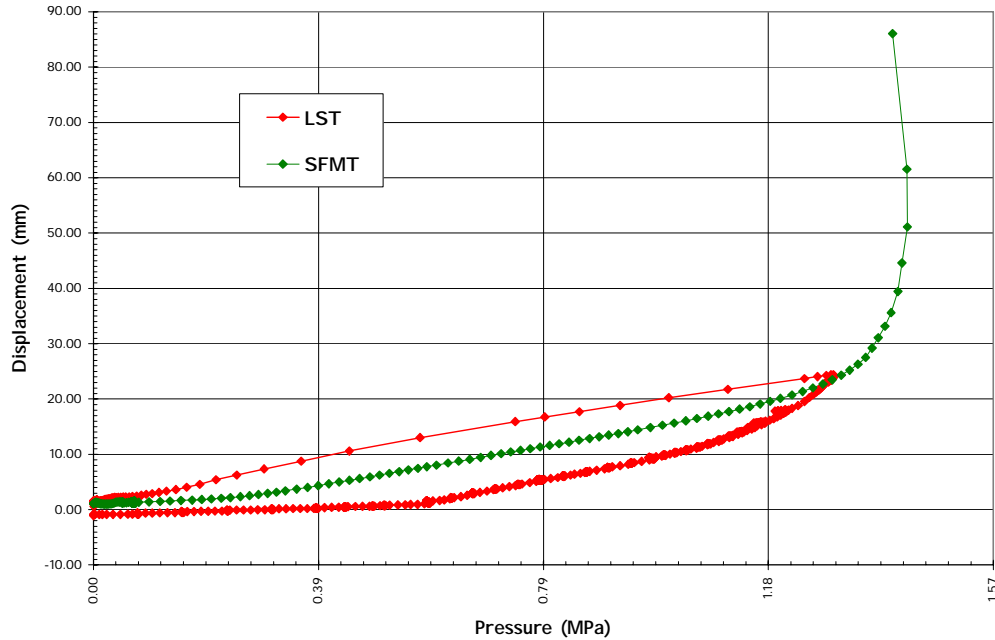


**Figure 64 SFMT – Radial Displacement at Az. 135°, El. 6200**

The acoustic monitoring system used during the LST was also employed for the SFMT minus the interior sensors which were removed to allow the elastomeric liner to be installed. Since the SFMT was not focused on detecting liner tearing/leaks, this was not a significant compromise. The focus of the acoustic system during the SFMT was to detect tendon wire breaks and any other events which might indicate structural damage. Fifty seven wire break or probable wire break events were identified between 10:39:47 and rupture of the model at 10:46:12. Figure 65 plots the time history of all the wire break events along with the effective pressure time history and radial displacement time history. It is readily apparent that the frequency and magnitude of the wire break events increases just prior to rupture.

The displacement profiles at Azimuths 135° and 324° during the SFMT are shown in Figures 66 and 67. Since the displacement transducers used during the LST were removed and replaced by water-proof transducers for the SFMT, the initial profile was taken as that prior to prestressing. In Figures 66(a) and 67(a), the displacement profiles are plotted for the hydrostatic pressure (0.18 MPa) and multiples of the design pressure, approximately 1.0Pd (0.389 MPa), 2.0Pd (0.776 MPa), 2.5Pd (0.978 MPa), 3.0Pd (1.162 MPa), 3.5Pd (1.295 MPa) and the peak pressure of 3.63Pd (1.42 MPa). The maximum average hoop strain at the peak pressure of 3.63 Pd was 1.02%. The profiles are expanded between 3.0Pd and 3.63Pd in Figures 66(b) and 67(b). These figures also show that after reaching the peak pressure, the model continued to expand significantly, even though the pressure decreased to 3.57Pd (1.40 MPa) yielding a maximum hoop strain of 1.65% just prior to rupture.

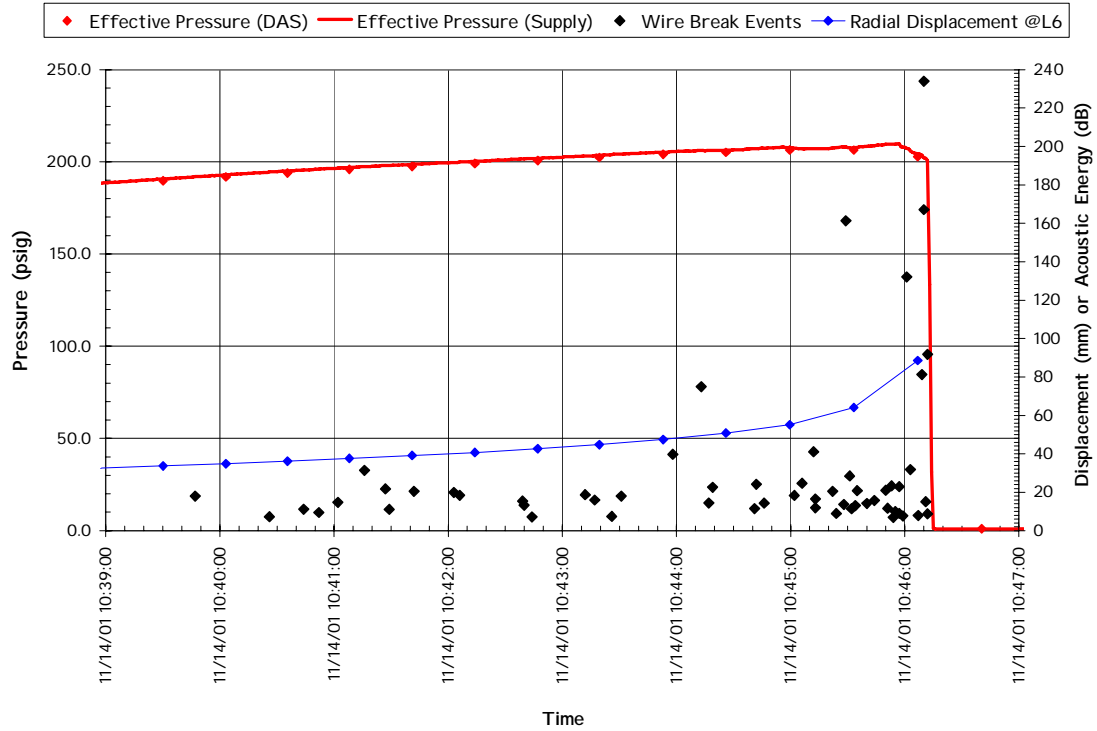
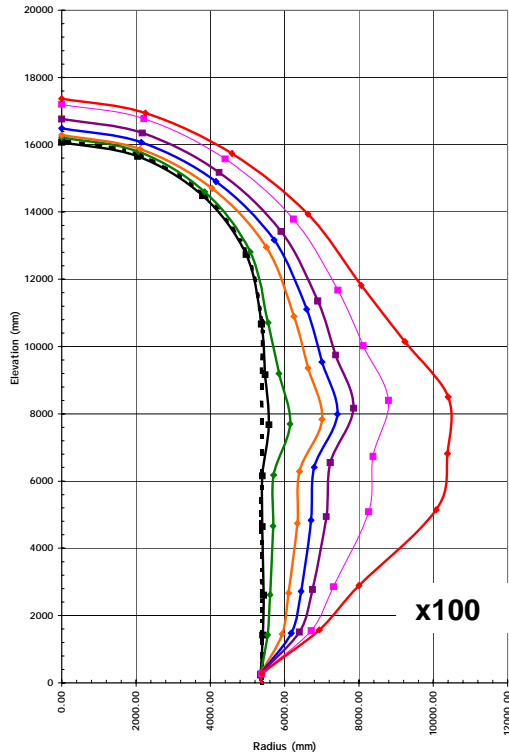
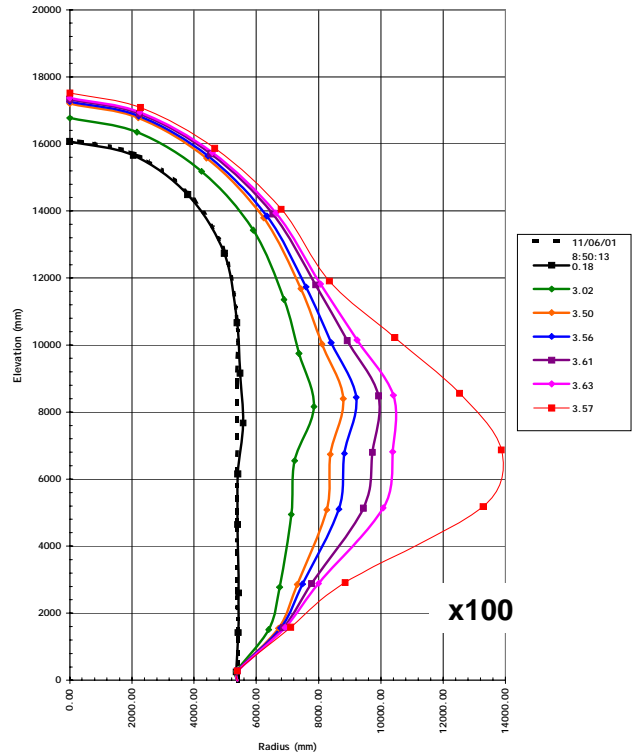


**Figure 65 SFMT Wire Break Events vs. Pressure vs. Displacement**

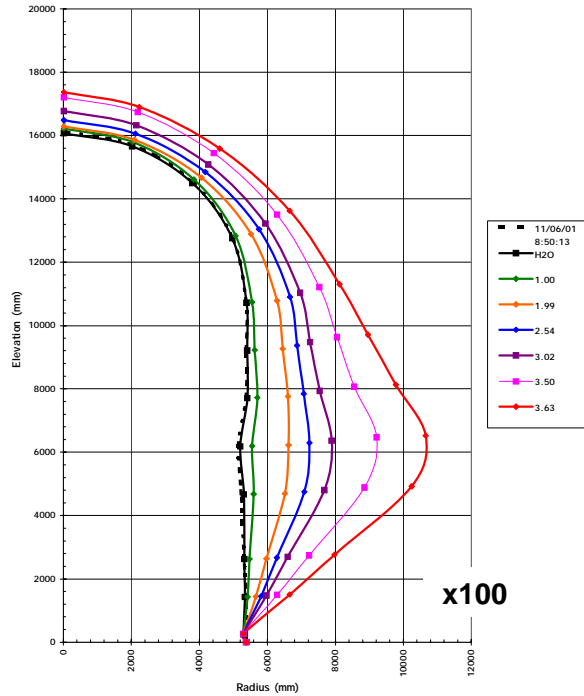


**(a)  $0P_d$  to  $3.63P_d$   
Figure 66**

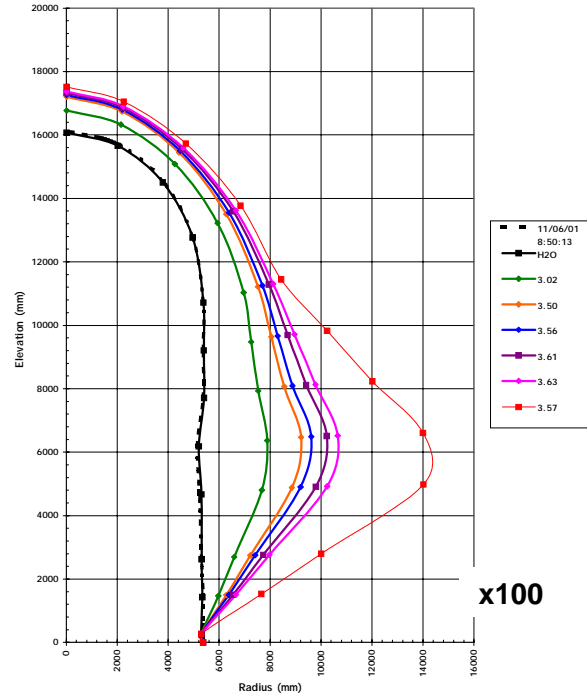


**(b)  $3.0P_d$  to  $3.63P_d$   
SFMT - Deformation @ Az.  $135^\circ$  (Z)**





(a)  $0P_d$  to  $3.63P_d$   
Figure 67



(b)  $3.0P_d$  to  $3.63P_d$   
SFMT - Deformation @ Az.  $324^\circ$  (L)

### 3.5.1.2 Analysis

#### *Pretest Analysis*

The principal objectives of the pretest analyses were to (1) validate analytical methods for predicting global structural response of a prestressed concrete containment, (2) gain insight into potential structural failure modes of a prestressed concrete containment, and (3) support planning of test procedures and instrumentation. The pretest prediction analyses were completed many months prior to the LST in order to document and publish the predictions prior to the test [73]. Because the pretest analysis predictions were needed well in advance, they did not include certain as-built features, actual measured prestressing and associated losses, nor creep and temperature effects. Prestress values, losses due to friction, anchor set, and concrete creep were approximated from the assumptions used in the PCCV model design.

A list of possible failure modes and failure locations was developed in the preliminary analysis phase prior to conducting the analyses. Some of the potential failure modes were specifically addressed by the global analysis while others were addressed by local models. Preliminary analyses suggested that liner failure at the mid-height of the cylinder near a penetration and a shear/bending failure at the base of the cylinder wall had significant probability of occurring. The basic ‘workhorse’ of the Pretest analysis was an axisymmetric model (Figure 68). The model represents the  $135^\circ$  azimuth which was assumed to be typical of a “free-field” azimuth, away from buttresses or penetrations. Local models were developed for: the Equipment Hatch region (Figure 69), the Personnel Airlock region, and the Main Steam Penetration region. A detailed 3D model of the entire cylinder mid-height region (3DCM) was also developed to investigate tendon behavior in the cylinder and 3D effects that drive the local strain concentrations near the penetrations (Figure 70). The ABAQUS [77] general purpose finite element program along with the ANACAP-U [78] concrete and steel constitutive modeling program were used for all analysis.

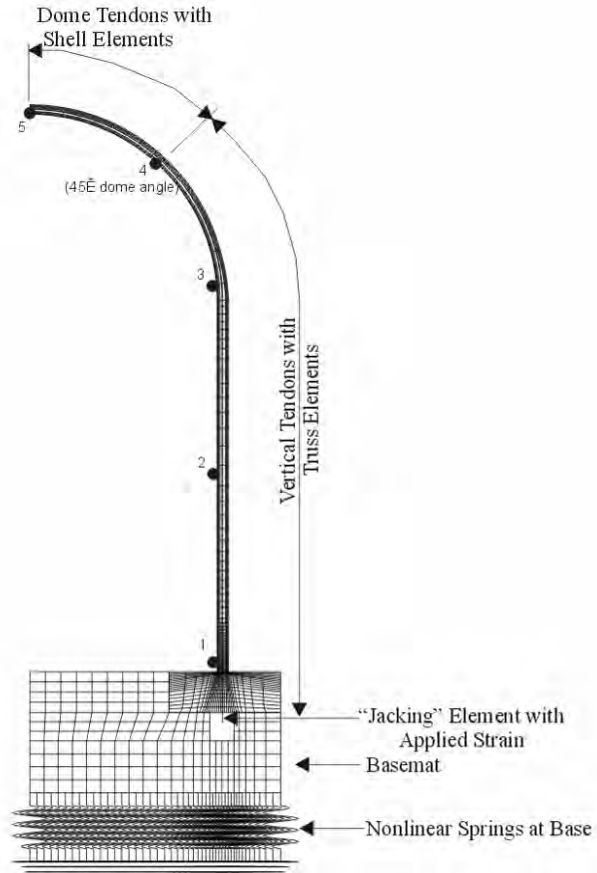


**Figure 68** Axisymmetric Model of 1:4-scale PCCV

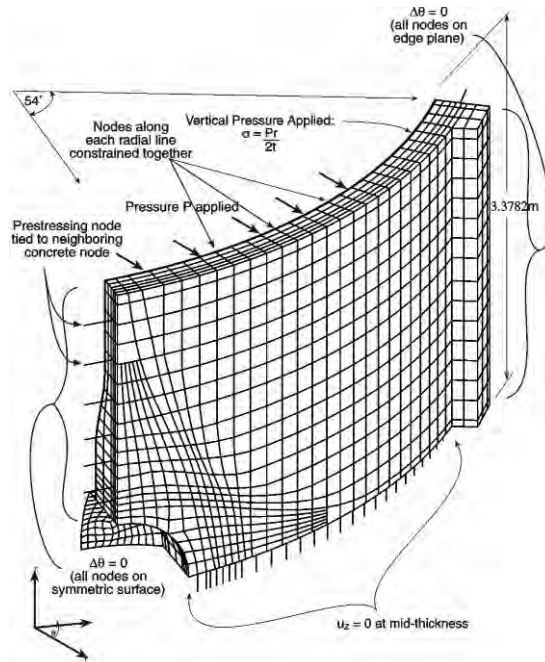


**Figure 69** Local Model of Equipment Hatch

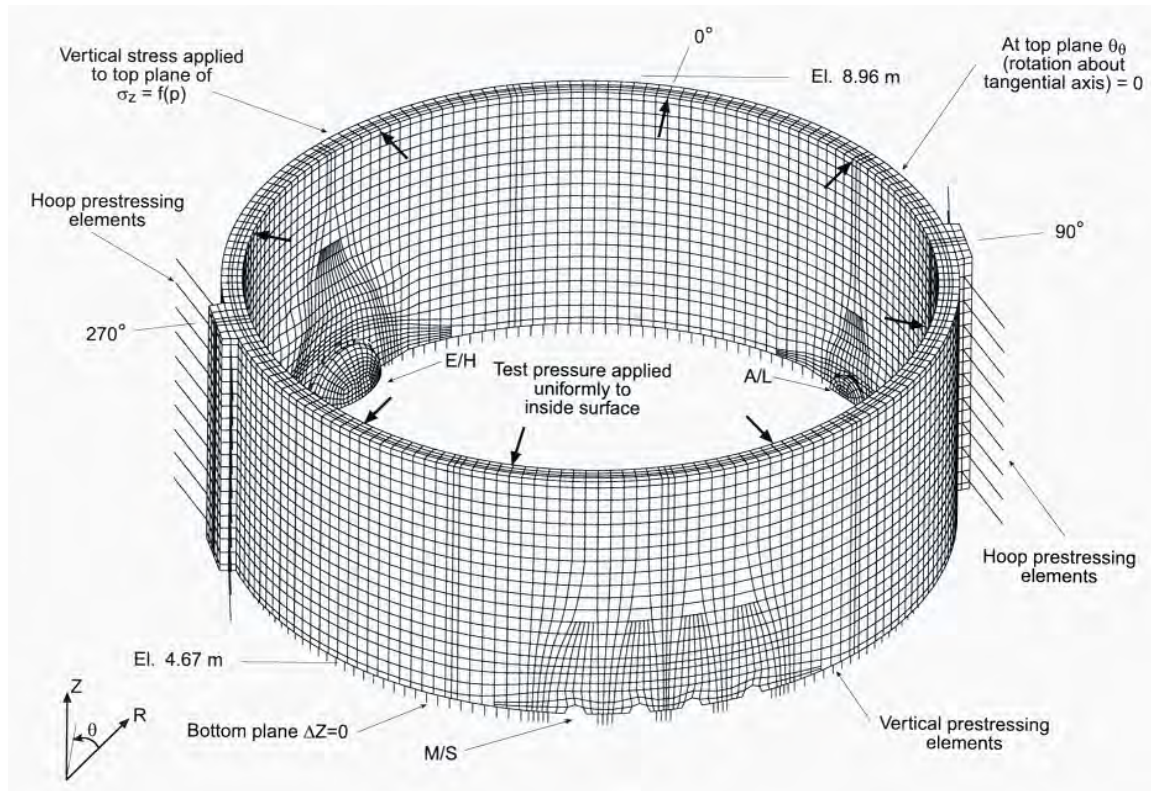


**Figure 70 Three-Dimensional Cylinder Mid-Height Model (#DCM)**

The results of the Pretest analyses include the following

- The model deforms radially out more at 4.68 m (cylinder mid-height) than at 8.96 m, which is the same trend as in the axisymmetric model.
- The largest hoop expansion occurs at the Equipment Hatch, and the "free-field displacement" (displacement at 0° and 180°) are slightly less and are approximately equal to each other.
- At pressures greater than  $3.0P_d$  the radial displacements at 135° (and elsewhere) become somewhat larger in the 3DCM model than in the axisymmetric analysis, while below  $3.0P_d$ , the axisymmetric analysis agrees well with the 135° azimuth of the 3DCM model.
- There is significant local circumferential bending adjacent to each buttress.
- There are significant strain concentrations at terminations or step-downs in rebar patterns.
- There are significant strain concentrations near hatches and near the edges of wall embossments.
- Using a strain-based failure criteria which considers the triaxiality of stress and a reduction in ductility in the vicinity of a weld, the liner failure strain was 0.16. The failure pressure at which a local analysis computed effective plastic strain that reached the failure strain, was  $3.2P_d$  or 1.3MPa. The location for this liner-tearing failure was near the Equipment Hatch (E/H), adjacent to a vertical liner anchor that terminated near the liner insert plate transition.

- The 3DCM model with its detailed tendon representation, predicted rupture of hoop tendons closest to the E/H at a model pressure of about  $3.5P_d$ . However, this mode was predicted to be precluded by the liner tearing and leakage failure mode.

#### *Pretest Round-Robin Analysis*

Prior to pressure testing the scale models, a number of regulatory and research organizations were invited to participate in a pretest Round Robin analysis to perform predictive modeling of the response of scale models to overpressurization. Seventeen organizations responded and agreed to participate in the pretest PCCV Round Robin analysis activities:

AECL	Atomic Energy of Canada Limited	Canada
ANL	Argonne National Laboratory	U.S.
CEA	Commissariat a l'Énergie Atomique	France
EDF	Électricité de France	France
Glasgow	University of Glasgow	U.K.
HSE	Health and Safety Executive	U.K.
IBRAE	Nuclear Safety Institute	Russia
INER	Institute of Nuclear Energy Research	Republic of China
IPSN	Institut de Protection et de Sûreté Nucléaire	France
JAERI	Japan Atomic Energy Research Institute	Japan
JAPC	The Japan Atomic Power Company	Japan
KINS	Korea Institute of Nuclear Safety	Korea
KOPEC	Korea Power Engineering Company	Korea
NUPEC	Nuclear Power Engineering Corporation	Japan
PRIN	Principia Ingenieros Consultores, S.A.	Spain
RINSC	Russia International Nuclear Safety Center	Russia
SNL	Sandia National Laboratories/ANATECH	U.S.

The purpose of the Round Robin effort was to provide a forum for researchers in this area, and the industry in general, to apply current (state-of-the-art) analysis methodologies to predicting the response and capacity of the PCCV model. Each participant was supplied with the same basic information, including the design drawings of the PCCV model and the material properties of the structural components. Each participant used his own chosen analytical methods and performed independent analyses. Participants were asked to submit response histories at 55 Standard Output Locations along with predicting the most likely failure mode and pressure. Luk [74] compiled the results along with the individual participant reports and these were discussed in a pretest workshop in October, 1999.

Figure 71 shows the predicted radial displacement at the mid-height of the cylinder wall where the maximum response is expected. Table 10 summarizes these estimates and predictions of the pressure for various milestones (onset of cracking, yielding, etc.) leading up to failure. Comparing the results of the various analyses, the following observations can be made:

- Predictions of elastic response were, for the most part, very consistent up to the onset of global yielding (hoop) which appears to occur around  $2.5 P_d$  or about 1.0 MPa. Predictions of response diverge significantly beyond this point with responses varying by a factor of three to five or more at a given pressure.
- There are considerable differences in the predictions of some local strains, such as those close to a penetration, after global yielding has occurred.

- Nevertheless, the predicted capacity of the model is fairly consistently bounded at 4 to 5  $P_d$ . For failure predictions based on material failure of the steel components (liner, rebar or tendons), the average predicted pressure at failure is 3.6  $P_d$  or 1.46 MPa.
- Approximately half the participants predicted failure based on structural failure, i.e., rupture of rebar or tendons, while approximately half the participants predicted functional failure from excessive leakage through a tear in the liner and/or cracks in the concrete. No one predicted a shear failure or leakage through the penetrations.

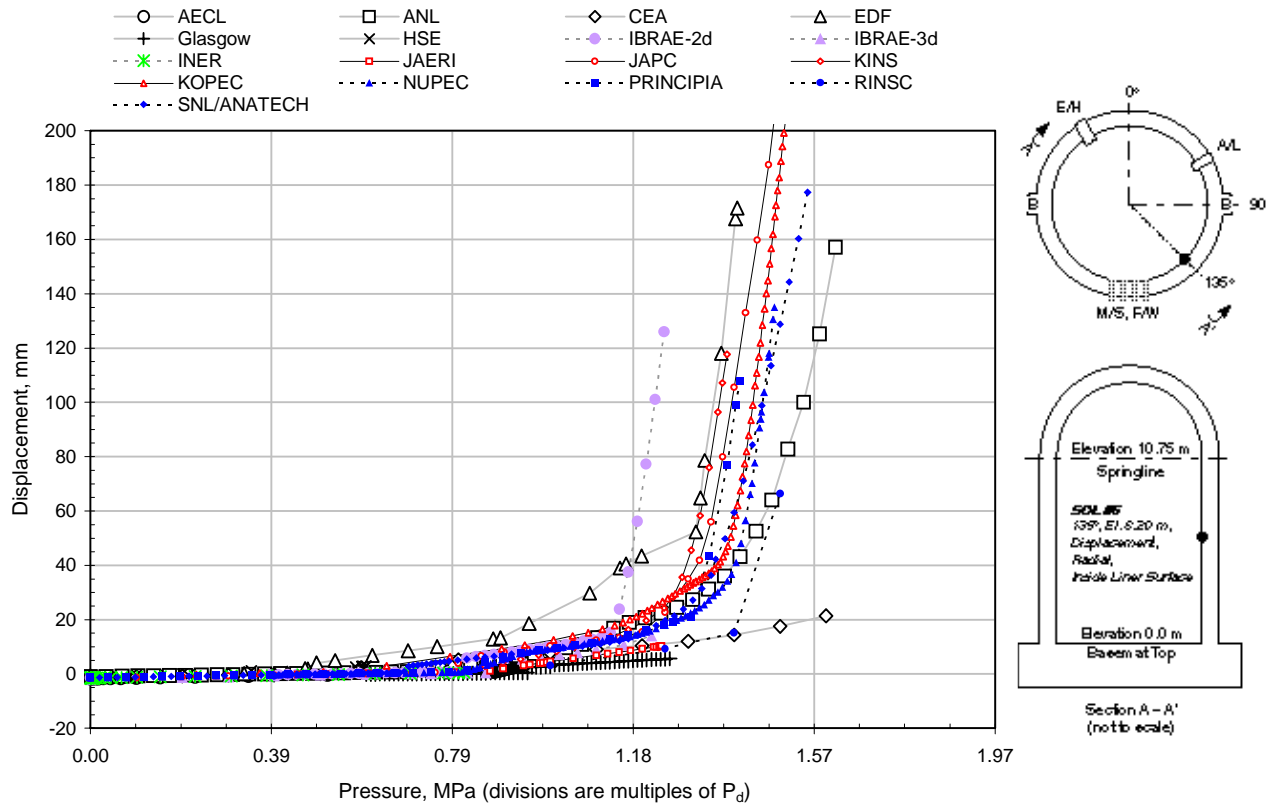


**Figure 71 Radial Displacement at Cylinder Wall Mid-height (SOL 6)**

**Table 10 Summary of PCCV RR Pretest Results**

<b>Participant*</b>	<b>Pressure (MPa)</b>	<b>Failure Mode</b>
ANL	1.51-1.62	local liner tear/hoop tendon failure @ El. 6.4 m
AECL	0.94-1.24	complete cracking/axisymmetric yield
CEA	1.60-1.70	numerically unstable
EDF	1.95	
INER	0.81	
JAERI	—	buckling @ dome or local fracture by bending in cylinder
JAPC	1.45-1.55	hoop tendon/rebar/liner rupture @ El. 7 m
KINS	1.25-1.44	tendon rupture
KOPEC	1.30-1.51	tendon rupture (@3.55% strain)
HSE/NNC	1.98	liner tear w/ extensive concrete cracking @ buttress
NUPEC	1.49-1.57	tendon rupture
IBRAE	1.26	tendon rupture
Principia	1.30	tendon yielding
RINSC	1.50	hoop failure of vessel
ANATECH/SNL	1.25	liner tearing (16%) @ Equipment Hatch
	1.40	tendon rupture
<b>Limit State Test</b>	<b>0.98</b>	<b>1.5% mass/day leak through liner tear @ E/H</b>
	<b>1.30</b>	<b>limit of pressurization capacity</b>
<b>Structural Failure Test</b>	<b>1.42</b>	<b>hoop tendon rupture</b>

*Posttest Analysis*

The post-test analysis represents the third phase of a comprehensive PCCV analysis effort. The principal objectives of the post-test analyses were: (1) to provide insights to improve the analytical methods for predicting the structural response and failure modes of a prestressed concrete containment, and (2) to evaluate by analysis any phenomena or failure mode observed during the test that had not been explicitly predicted by analysis. Comparisons between measured behavior and predicted behavior of the liner, concrete, rebar, and tendons, a variety of failure modes and locations were investigated. Pretest and post-LST analysis results were also compared to the SFMT data and additional analyses, to provide some insight into the mechanisms leading to the structural failure.

Extensive additional studies were also performed for the posttest 3DCM analysis. A modeling assumption, found to be at significant variance with observed test behavior, was the representation of friction in the tendon modeling.

Posttest analyses were also performed for the penetration sub-models. Liner strains measured in the vicinity of the E/H penetration collar were much lower than predicted by pretest analysis. Since the predicted high strain locations were fundamental to the failure predictions, significant effort was spent reanalyzing the E/H model after the test. Posttest analysis showed that by preventing relative slip between liner and concrete, the overall behavior of the system (concrete

strains, tendon strains, liner strains away from the hatch) remained the same, but the elevated strains close to the collar (the thicker insert plate surrounding the penetration sleeve) were eliminated. The results of a detailed liner ‘rat-hole’ (see Figure 61) analysis show that the elevated strain associated with this detail, and similar details, is enough to exceed the liner tearing strain criteria. Considering both the effects of a discrete crack and elevated local strains at the rat-hole, a liner tear could have been predicted to occur as early as  $2.8 P_d$ .

Posttest analysis of the SFMT showed that good simulation of the PCCV global behavior through and including tendon rupture is possible with a 3D shell model as shown in Figure 72. The main limitations of the shell model were a lack of local liner strain concentration prediction and a lack of accuracy in the predictions of local wall-base-juncture behavior. However, accuracy in global behavior prediction did not seem to be lost when a bonded tendon assumption was used. The SFMT model provided additional insight as to how the structural failure likely developed. The additional hoop reinforcing surrounding the Equipment Hatch penetration (an increase of approximately 50% over the reinforcing in the free-field) is terminated near the  $6^\circ$  azimuth of the cylinder wall. At  $3.49 P_d$  (1.36 MPa), the wall and tendon hoop strains at Azimuth  $0^\circ$  to  $6^\circ$  (Figure 72) are approximately 4%, higher than all other azimuths. Assuming a maximum tendon strain of 4%, the first hoop tendon rupture occurs at this pressure. The analysis subsequently shows neighboring tendons rupturing and deformations spreading quickly along this azimuth. By  $3.65 P_d$  (1.42 MPa), the analysis shows rupture to have spread over a vertical distance of approximately 6 m. This is consistent with the behavior observed during the test.

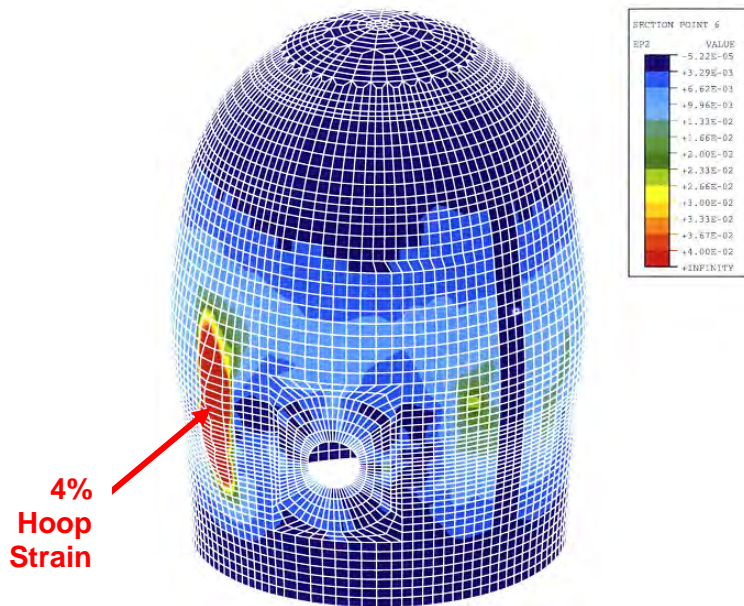


**Figure 72 Posttest Analysis of SFMT at Rupture (~1.38MPa)**

The PCCV test showed that the response quantity driving the limit state of the vessel is radial expansion of the cylinder. This response must be predicted correctly in order to reliably predict vessel capacity and, at least approximately, the local response mechanisms (local liner strains, penetration ovalization, etc.) that are driven by the cylinder expansion. This, and other steel-lined concrete vessel tests, show that many competing strain concentrations occur around the mid-height of the cylinder. Although it is difficult to predict which local liner detail will tear first, and although some particular response quantities, like basemat uplift, were not predicted exactly by the pretest analysis of the PCCV model, the average radial expansion or hoop strain of the

cylinder was predicted very accurately by the axisymmetric analysis. The axisymmetric analysis also predicted the cylinder wall-base flexure and shear response, another critical response mode, accurately. Even though the hoop stiffness/strength of most containments is not uniform along the circumference, these results suggest that a **minimum requirement for containment overpressure evaluation should certainly be a robust axisymmetric analysis.** A ‘robust’ analysis consists of an accurate representation of the structural elements and material properties in a numerically-stable nonlinear finite element solution. Analytical robustness is quality of a solution which exhibits a degree of insensitivity to numerical solution strategy and control parameters, i.e. the solution is primarily dependent on the structure def

The lessons learned which may be most instructive are those related to tendon friction behavior. As a result of this project, the best calculation methods recommended for tendon friction modeling are, in descending order of preference, 1) an advanced contact friction surface between the tendons and the concrete, 2) pre-set friction ties applied in one direction during prestressing and then added in the other direction during pressurization and, 3) if neither of these methods are practical within the scope of the calculation, it is best to start with an “average” stress level (using a friction loss design formula), but assume uniform stress distribution in the tendons throughout pressurization, i.e., an unbonded tendon assumption, and finally 4) same as 3, but using a bonded tendon assumption. It should be recognized for method 4, however, that this can lead to a premature prediction of tendon rupture, because the tendon strain increments during pressurization will match the hoop strain increments of the vessel wall one-to-one, and this was not observed to be the case during the PCCV LST.

The relevance of this work to full size U.S. Containments is highly significant. All of the analysis methods tried, calibrated, and validated are applicable to full-scale structures. The posttest work also provides a reasonably simple liner-only mesh approach for predicting local strains near weld seams, and the test itself underscores the need for continuous back-up bars on all liner seam welds as required in the ASME code.

#### *OECD/NEA/CSNI International Standard Problem #48 on Containment Capacity*

While no formal posttest Round Robin analysis was conducted as part of the NUPEC/NRC Cooperative Containment Program, an informal meeting of the participants was held at SNL following the LST. This forum included a comprehensive discussion of the results of the LST and a critical review of the pretest analyses. While the results of this meeting were never formally documented, many of the participants presented the results of their posttest analyses in a variety of technical forums including the SMiRT and ICONS conferences. These discussions also contributed to the technical impetus for conducting the SFMT due to a general consensus that the data from the LST was inadequate to benchmark analyses for large inelastic deformations.

One question which remained following the PCCV test was how temperature loading might have affected the results of the test. In an attempt to answer, or at the least shed some light on, this question, a proposal was made to the Committee on the Safety of Nuclear Installations (CSNI) of the Nuclear Energy Agency (NEA), Organization for Economic Cooperation and Development (OECD), to sponsor an international standard problem (ISP) to investigate the role of temperature on Containment Capacity. The proposal was accepted and at the planning meeting for held in Stockholm in November, 2002. Two questions were posed which summarize the objectives of the ISP:

- With addition of temperature, would the onset of leakage occur later in the pressure history and, possibly, closer to the burst pressure?



- How would including the effect(s) of accident temperatures change the prediction of failure location and failure mode?

Eleven organizations (or teams), including several participants in the Pretest Round Robin analysis, participated in the ISP:

BE/HSE/NNC	British Energy Nuclear Installations Inspectorate/Health & Safety Executive NNC Ltd.	UK
EDF	Électricité de France	France
EGP	Energoprojekt Praha, UJV Rez. Div.	Czech Rep.
FORTUM	Fortum Nuclear Services Ltd.	Finland
GRS	Gesellschaft für Anlagen und Reaktorsicherheit mbH	Germany
IRSN/CEA	Institut de Radioprotection et de Sûreté Nucléaire Commissariat a l'Énergie Atomique	France
JPRG	Japan PCCV Research Group	Japan
KAERI	Korea Atomic Energy Research Institute	Korea
KOPEC	Korea Power Engineering Company	Korea
NRC/SNL/DEA	US Nuclear Regulatory Commission Sandia National Laboratories David Evans and Associates	US
SCANSCOT	Scanscot Technology	Sweden

The ISP consisted of four phases:

- Phase 1: Data Collection and Identification
- Phase 2: Calculation of the Limit State Test (LST), i.e. static pressure loading
- Phase 3: Calculation of response to both Thermal and Mechanical Loadings
- Phase 4: Reporting Workshop

The results of the ISP were reported in [79]. Following the Phase 2 calculations which comprised a posttest analysis of the LST, two cases of combined thermal and pressure analysis were considered:

- Case 1: Saturated Steam Conditions (mandatory for all Phase 3 participants) (Figure 73)
  - Monotonically increasing static pressure and temperature (saturated steam).
- Case 2: Station Blackout Scenario (Figure 74)
  - A representative severe-accident scenario for a four-loop PWR including vessel failure and hydrogen detonation

The results of the ISP are summarized in Table 11. While there was no clear consensus regarding the effect of temperature on the failure mode and pressure, some observations could be made.

*With addition of temperature, would the onset of leakage occur later in the pressure history and, possibly, closer to the burst pressure?*

- Results predict failure at both lower and higher pressure when temperature is considered.
- The margin between leak and rupture does not appear to change significantly
- Change in 'failure' pressures are generally small (<10%).
- Consideration of 'realistic' severe accident scenario (Case 2) yields lower 'failure' pressure than saturated steam conditions.
- Effects of material degradation are significant for 'realistic' severe accident scenarios.

*How would including the effect(s) of accident temperatures change the prediction of failure location and failure mode?*

- While leak or rupture pressures are not significantly changed, displacements are significantly greater, especially when considering material property degradation.
  - Case 1: Vertical displacements increase
  - Case 2: Radial displacements increase
- Failure at penetrations appear more likely, and may control, under combined pressure and temperature loading.

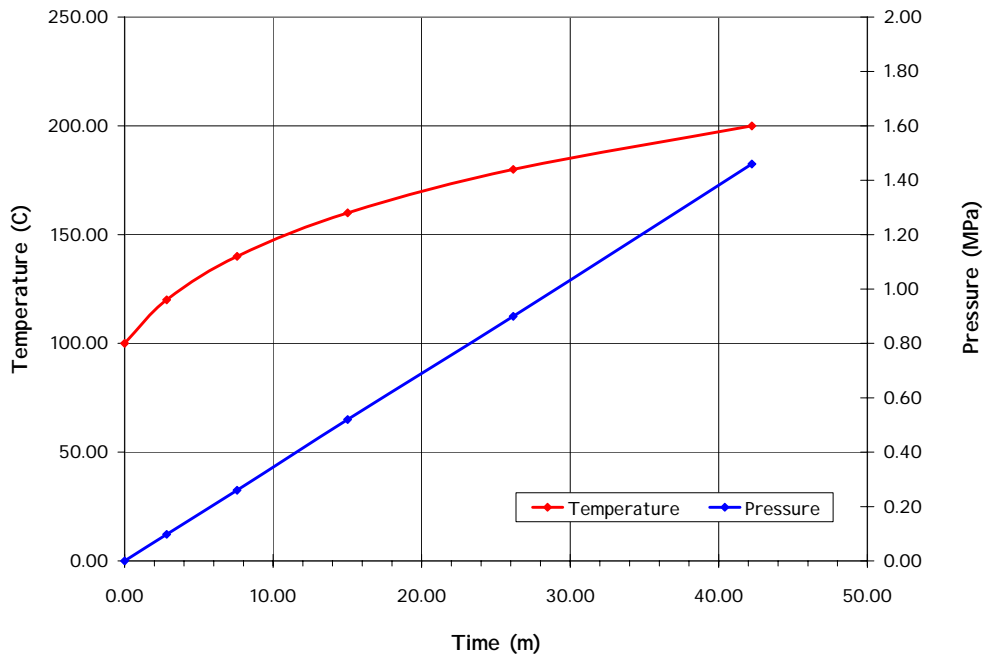


**Figure 73 Case 1 Saturated Steam Pseudo-Time History**

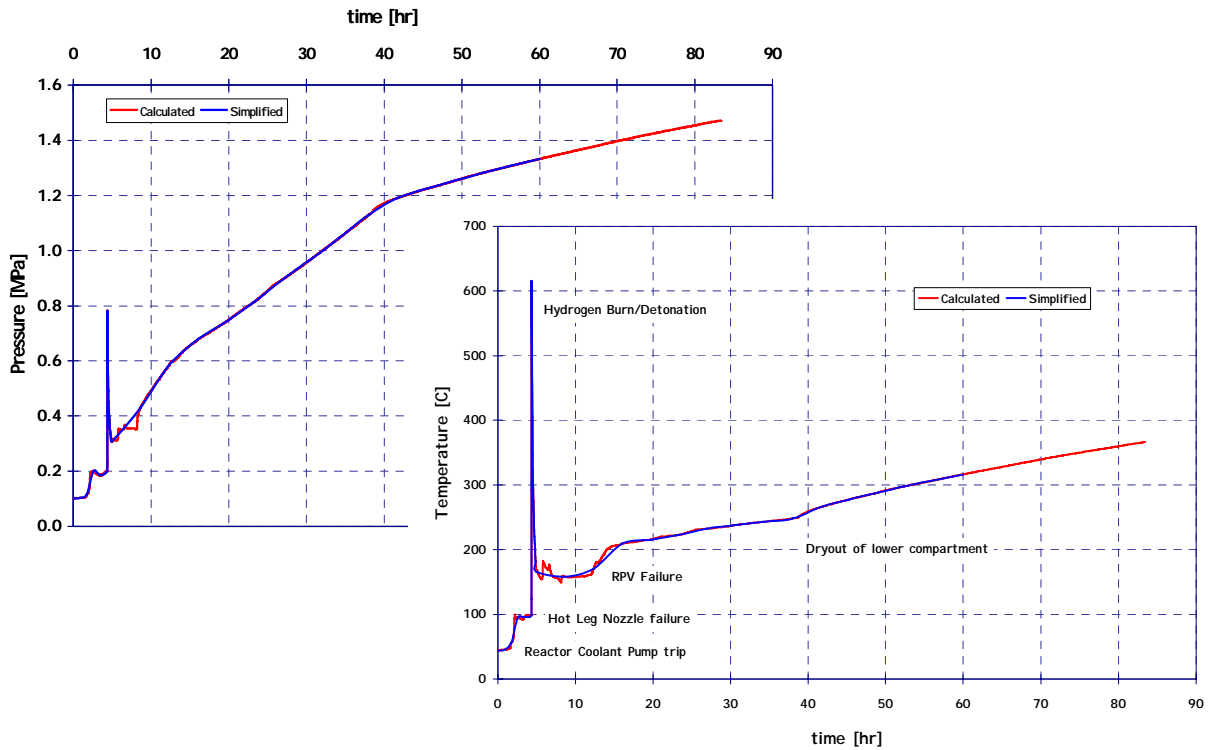


**Figure 74 Case 2 Station Black-Out Time History**

**Table 11 Summary of ISP 48 Results**

**Pressure Only**

	<b><u>Pressure (MPa)</u></b>				
	<b>Liner Tearing</b>	<b>Pressure @ Failure</b>	<b>Hoop Strain</b>	<b>Radial Disp.</b>	<b>Criteria</b>
<b>LST</b>	0.98		0.17%		Liner tear, 1% leak
<b>SFMT</b>		1.42	1.4%		Tendon rupture
<b>BE/HSE/NNS</b>	1.10	1.40	0.12%	39 mm	Liner tearing
<b>Fortum</b>	1.30	1.60		12mm	
<b>JPRG</b>					Failure does not occur
<b>NRC/SNL/DEA</b>	1.33	1.33	0.74%	40mm	Liner tearing
<b>Scanscot</b>	1.3	1.38	2.1%	91mm	Tendon rupture

**Pressure plus Temperature**

	<b><u>Pressure (MPa)</u></b>				
	<b>Liner Tearing</b>	<b>Pressure @ Failure</b>	<b>Hoop Strain</b>	<b>Radial Disp.</b>	<b>Criteria</b>
<b>BE/HSE/NNS</b>	1.25	1.40 1.50	0.18%	39 mm	Liner tearing Tendon rupture
<b>EGP</b>	1.15	1.25	0.3%	16mm	
<b>Fortum</b>	1.40	1.69		17mm	Tendon rupture
<b>GRS (Case 1)</b>	1.40	1.40	1.5%	85mm	Liner tearing
<b>(Case 2)</b>		>1.30	0.4%	23mm	
<b>JPRG</b>					Failure does not occur
<b>KOPEC (Case 1)</b>	1.20	–		114mm	Tendon rupture
<b>(Case 2)</b>	0.41				
<b>NRC/SNL/DEA</b>	1.28	1.28	1.11%	60mm	Multiple liner tears
<b>Scanscot (Case 1)</b>	1.3	1.45	3%	134mm	Tendon rupture
<b>(Case 2)</b>	1.33	>1.33	0.75%	54mm	

**3.5.2 1:10-scale prestressed concrete model (Sizewell-B)**

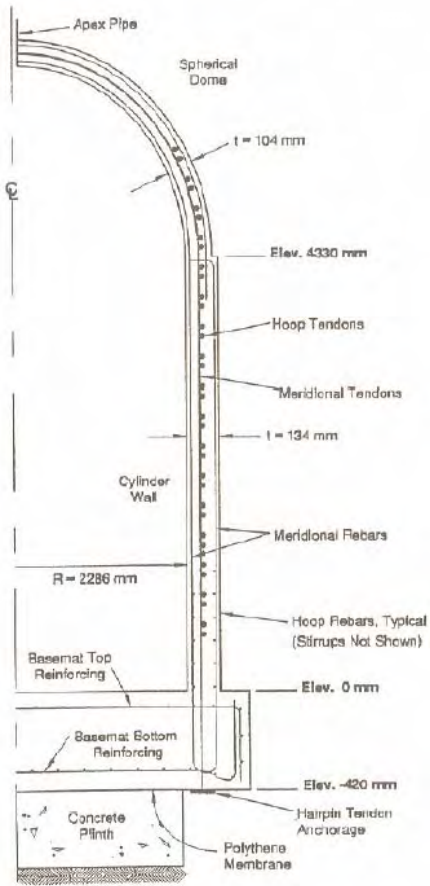
In July, 1989 a test was conducted for a 1:10-scale model of a prestressed concrete containment vessel by the Central Electricity Generating Board (CEGB) in the United Kingdom. This model of the Sizewell-B NPP containment structure utilized seven-wire strands in plastic sheaths to represent the vertical hairpin and hoop tendons. The vertical tendons were anchored below the basemat, and the 240° hoop tendons were anchored in two of the three vertical buttresses. The model was unlined (although a bladder was inserted in the model to prevent leakage) and included an equipment hatch penetration. Instrumentation included rebar, tendon and concrete strain measurements, and measure of displacements and tendon anchor forces. The model was tested hydrostatically. The NRC, through an agreement with the United Kingdom Atomic Energy

Authority (UKAEA), participated in the test program with SNL and ANATECH providing technical support to the NRC [80, 81].

As with other model tests with international participation, the principal objectives were to use blind pretest analyses to critically evaluate analytical methods for predicting global structural response, and gain insight into potential structural failure modes of a PCCV. The geometry of the model is shown in Figure 75. The model was tested with four loading cycles to 1.15 x design pressure, followed by one ultimate pressure test. Design pressure of the model was 0.345 MPa (50 psig). The model behavior was observed to be primarily elastic during the low pressure tests, except that the basemat uplift response was somewhat larger at the end of the fourth low pressure test than after the first, indicating the occurrence of inelastic damage to the basemat or wall-base region, or both. During the high pressure test, a maximum pressure of 0.834 MPa (121 psig) was reached at the model base (2.4 x design pressure). Failure occurred when excessive bending of the basemat slab led to rounding of the underside of the basemat, model tilting and potential instability, spalling of basemat under-surface concrete, and termination of the test. Upon post test inspection, model failure was postulated to have been associated with the basemat spallation and the resulting loss of bond in basemat bottom reinforcement as illustrated in the sketch of Figure 76. Another interesting result was the observation that the tendons, constructed with wire strand sheathed in plastic coating (not conventional post-tensioning that is free to slide in metal ducts) showed evidence of significant friction, and by parametric analysis, this was shown to influence model behavior. Evidence of this is shown in Figure 77 in which the tendon strain measurements on hoop tendons indicate higher strains, the further a gage is located from the tendon anchorage. A tendon behaving in frictionless fashion would not exhibit these strain gradients.

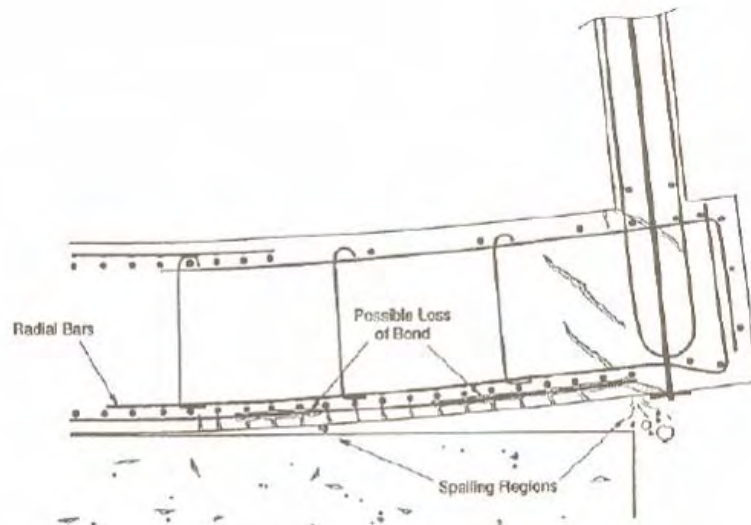
The maximum radial displacement (not including tilting of the model) was 13.5 mm, but basemat uplift exceeded 30 mm. So only a small amount of rebar and tendon yielding occurred in the cylinder, while extensive inelastic behavior occurred in the basemat.

Pretest analysis consisted primarily of axisymmetric analysis, but two different parametric assumptions were used for the tendons—a bonded tendon assumption and an unbonded (frictionless) tendon assumption. While the cylinder expansion predictions were not significantly influenced by the vertical tendon friction assumption (and showed good agreement with test measurements), the analysis results with the bonded tendon assumption compared better with the basemat bending and uplift response than the results with frictionless tendons. A sampling of pretest analysis results versus experiment are shown in Figure 78. So as with other experiments, axisymmetric modeling resulted in satisfactory prediction of containment cylinder global response, the modeling was unsatisfactory for predicting local and 3D effects such as rebar debonding, very localized concrete spallation, and behavior near penetrations.



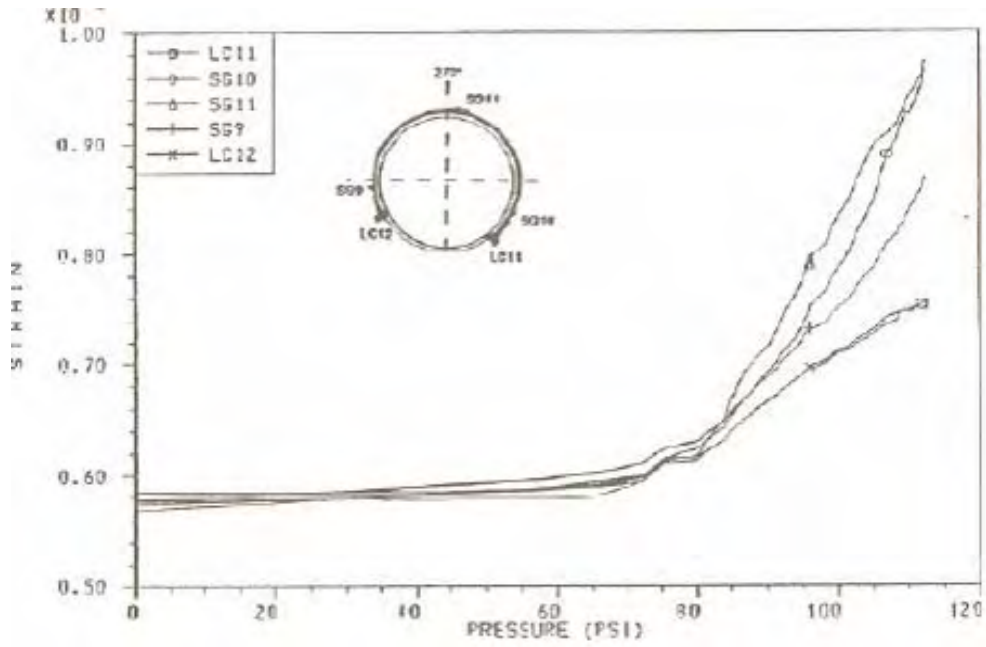
(best figure available)

**Figure 75 Schematic of 1:10 Scale Sizewell Model**



(best figure available)

**Figure 76 Section View of Posttest Condition of the 1:10-Scale Model**



(best figure available)

**Figure 77 Hoop Tendon Gage Data Near Cylinder Mid-height**

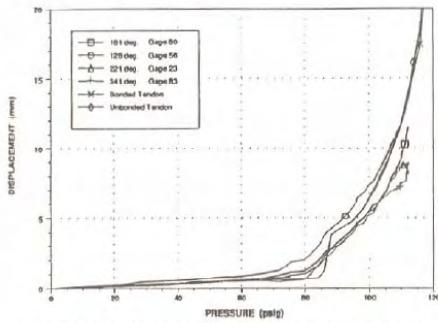


Figure 4. Comparison of Pretest Analyses vs. Experiment for Radial Displacements at Cylinder Midheight

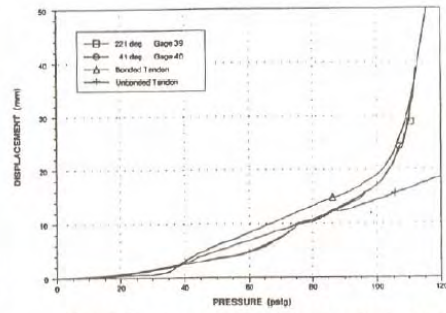


Figure 5. Comparison of Pretest Analyses vs. Experiment for Basemat Uplift Displacement

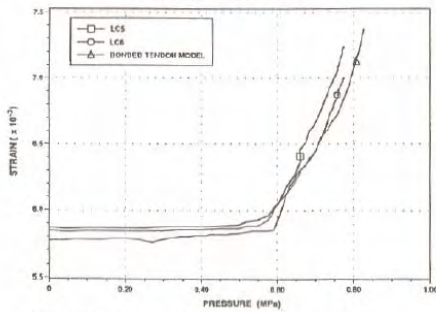


Figure 6. Comparison of Pretest Analyses vs. Experiment for Hoop Tendon Strain Near Cylinder Midheight

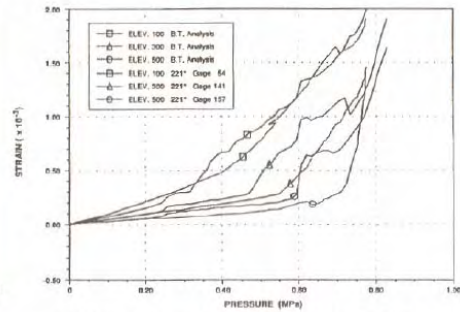


Figure 7. Comparison of Pretest Analyses vs. Experiment for Meridional Rebar Strains, Inside Surface, Base of Wall, Measured From Top of Basemat

(best figure available)

**Figure 78 Comparison of Pretest Analyses vs. Experiment Results for 1:10 Scale P/C Model**

### 3.5.3 *Other Prestressed Concrete Containment Model Tests*

A number of large concrete pressure vessels were tested to failure in the late 1960's and 1970's as part of research to proof-test concrete reactor vessels used in high temperature gas-cooled reactors. While these tests were not of containments and so involved larger wall thicknesses and higher pressures than are seen in containments, this body of research helped shape more modern evaluation methods used today on containments. Some of these vessels, particularly those with steel liners exhibited liner tearing and leakage failures, while a few of the tests ended in major through-wall shear failures of either the cylinder wall or the top head.

#### 3.5.3.1 1:12-scale prestressed concrete model (India) [59]

A 1:12 scale model was constructed in India using micro-concrete and annealed wire to represent the reinforcing and prestressing wire for the tendons. The inside of the model was coated with a type of vinyl paint similar to that used in the prototype. The model included six non-functional penetrations. The model leaked at a pressure of 0.13 MPa (19.5 psig), lower than the design pressure of 0.17 MPa (25 psig), due to excessive cracking.

#### 3.5.3.2 1:10-scale prestressed concrete model (Poland) [60]

A test of a 1:10-scale model of a prestressed containment vessel was conducted in Poland in the late 1970s. The prestressing tendons consisted of two, unbonded, 6 mm wires anchored in six buttresses for the hoop tendons and a ring buttress at the springline for the dome and hoop tendons. The model also included a steel liner and representation of an equipment hatch and airlock. The model was tested using air to 80% of the design pressure followed by dynamic testing to determine frequencies and mode shapes and finally a hydrostatic test to failure. Instrumentation consisted of liner, rebar and concrete strains, displacements and tendon anchor loads.

During the final pressure test, large radial cracks developed around the equipment hatch penetration, ultimately leading to liner tearing and leakage. Pretest predictions based on the capacity of the reinforcing and tendons slightly overestimated the capacity of model and did not anticipate the cracking patterns and ultimate response modes.

#### 3.5.3.3 1:14-scale prestressed concrete CANDU model (Canada) [61, 62, 63, 64]

A 1:14-scale model of a prestressed containment vessel was tested in Canada in the 1970s. Wall thicknesses were scaled at approximately 1:8 to accommodate reinforcing. The prestressing consisted of grouted, seven wire strands with the hoop tendons anchored in four vertical buttresses and the vertical and dome tendons anchored in the ring girder. The model was unlined (although a plastic liner was used to prevent leakage after cracking of the concrete) and included an access hatch penetration. Instrumentation consisted of rebar, tendon and concrete strains, displacements and crack widths. Testing to failure was performed using water as the pressurization medium.

Failure occurred when the plastic liner ruptured and leaked following a progressive sequence of structural events beginning with cracking and bearing failures at the buttresses, large deflections and cracking in the cylinder, tendon rupture and, finally spalling and ejection of the concrete. The authors concluded that the pretest predictions of response compared favorably with the test results with the exception of under-predicting the deflections.



#### 3.5.3.4 Large-scale prestressed concrete model (EPR, France/Germany, Civaux)

A large-scale model of the inner containment for the European Pressurized Reactor was constructed and tested in late 1997 at Civaux, France. The model consisted of a horizontal section of the cylindrical containment section including conventional reinforcing and prestressing steel capped by stiff slabs. Portions of the model were unlined, while other portions included an innovative composite liner. After a series of leak tests with air and steam at LOCA conditions, the model was tested to failure hydrostatically. Unfortunately, the results of the test have not been published.

### 3.6 Component (Penetration) Tests

In reporting on the results of the 1:8-scale steel containment vessel model test, Clauss [25] made the following observation:

*“The level of analysis that will be required to provide these answers will depend largely on the results of investigations into the leakage characteristics of containment penetrations that are now in progress. If these studies identify penetrations or seal geometries that are likely to leak prior to the onset of membrane yielding, the structural analyses of containments to be used for consequence analyses can be relatively simple. However, preliminary indications are that leakage from penetrations will not occur below the membrane yield pressure. If this is the case, predictions for leakage and rupture would require structural analyses to be carried out to pressures greater than the membrane yield pressure, and the analyses would therefore be similar in complexity to those conducted for the 1:8-scale steel model.”*

As noted previously, the containment system consists of several elements. In addition to the primary structure, these include various components such as the mechanical (hatches, piping) and electrical (instrumentation and controls) penetrations. For US containments there are a large variety of designs [91, 92] and not all can be tested. Since the variety of penetration designs could not be incorporated into the model tests, a series of tests of a variety of penetrations types were conducted to determine their leakage characteristics under severe accident conditions. Parks and Clauss summarized the research on penetration performance [82].

#### 3.6.1 Compression Seals & Gaskets [83, 84]

Compression seals and gaskets are used in many operable penetrations such as equipment hatches, personnel air locks and drywell heads. Aged and un-aged gaskets of ethylene propylene (EPDM), silicone and neoprene were tested at SNL [83] and the Idaho National Engineering Laboratory (INEL). The gaskets were tested up to pressures of (0.98 to 1.10 MPa (143 to 160 psig) and temperatures up to 370°C (700°F). The test indicated that failure, i.e. leakage, was independent of aging and that the silicone seals failed at lower temperatures in steam than in air or nitrogen, while EPDM was not affected by the pressurization medium.

#### 3.6.2 Electrical Penetration Assemblies [85]

Electrical penetration assemblies are used to provide a leak-tight feed-through into the containment building for power, control and instrumentation cables. Electrical penetrations, in addition to serving as a closure, in most cases will have to function ‘electrically’ during a severe accident and this function must also be evaluated. Three different commercial penetration designs were tested at SNL at pressures of 0.51 to 1.07 MPa (75 to 155 psia) and temperature from 180 to 370°C (360°F to 700°F) for up to 10 days. None of the penetrations assemblies tested failed.

The authors of the test report, however, cautioned against assuming that all electrical penetration assemblies would perform identically to the three tested.

### 3.6.3 Personnel Airlocks [86, 87]

A full size personnel airlock (Figure 79), originally fabricated for the cancelled Callaway Unit 2, was tested by CBI Research Corporation under contract to SNL. [86, 87]. Double EPDM gaskets provided the seal between each door and the bulkhead. The airlock was designed for an external pressure of 0.41 MPa (60 psig) and a maximum temperature of 170°C (340°F). It was tested to a pressure of 2.07 MPa (300 psig) and a temperature of 204°C (400°F) without failure. The inner door leaked when subjected to a pressure of 0.07 MPa (10 psig) at °C (650°F), although the outer door did not leak. Again, the authors of the test report cautioned against extrapolating the results of this test to all airlocks, since designs can vary significantly.

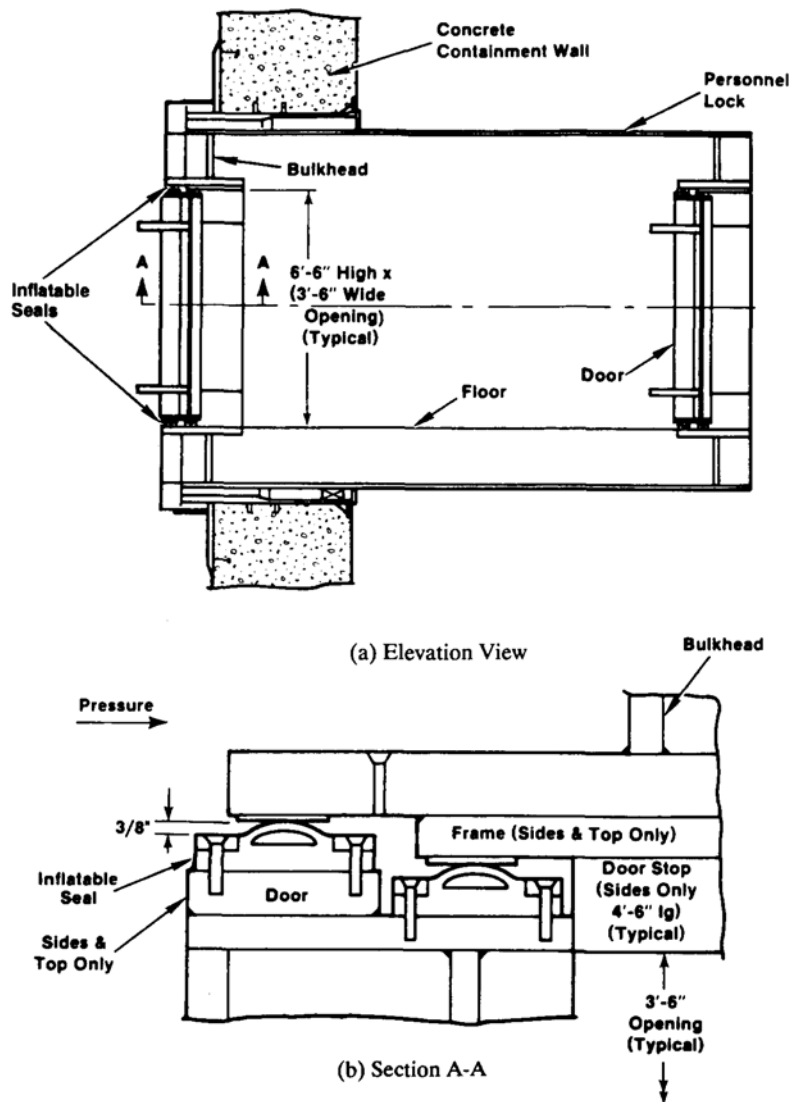


Figure 79 Typical applications of inflatable seals in personnel airlock doors [82]

### 3.6.4 Inflatable Seals [88]

A series of test of un-aged and aged EPDM inflatable seals were conducted at SNL. Inflatable seals are used to seal personnel airlock and escape lock doors at approximately 10% of US PWR or Mark III BWR containments (Figure 80). In operation the seals are maintained at a constant internal pressure of 0.34 to 0.69 MPa (50 to 100 psig). (It should be noted that inflatable seals will leak at containment pressures greater than the seal pressure.) The tests were conducted to determine the combination of temperature and pressure which would result in significant leakage past the seals. The tests showed that, regardless of seal design, aging or operating pressure, the seals did not leak until the containment pressure exceeded the normal operating seal pressure. There was evidence of breakdown in the seal material at temperatures above 176°C (350°F).

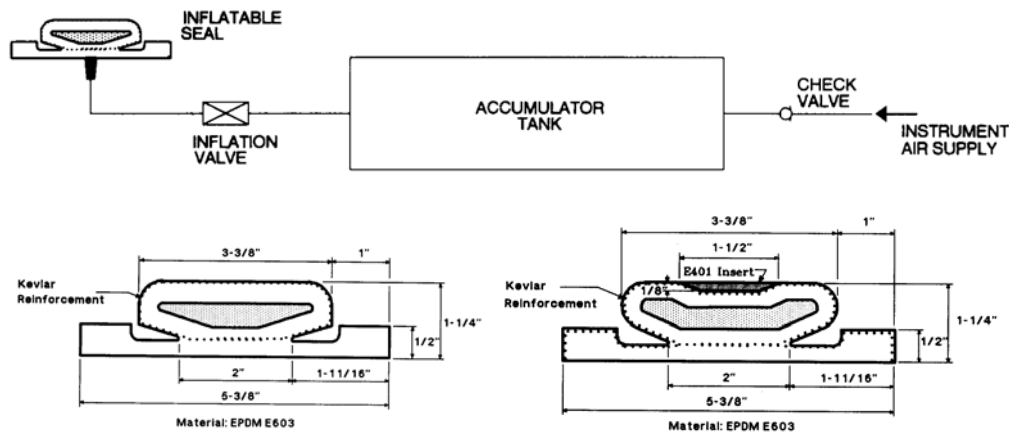


Figure 80 Inflatable Seal Schematic and Typical Designs [82]

### 3.6.5 Equipment Hatch, Drywell Head [89, 90]

A series of tests were conducted on the pressure unseating equipment hatch included in the 1:6-scale reinforced concrete containment model (see 2.4.1). An analytical method was proposed to predict the pressure at which significant leakage would first occur and the subsequent rate of leakage for pressures and temperatures beyond this level. The tests showed that the leak initiation pressure could be predicted reasonably well by the analytical model; however the subsequent leak rate could not be predicted with confidence. Also, since only the hatch was pressurized, the effect of global structural deformation, i.e. ovalization of the hatch sleeve, was not represented in the tests or the analyses.

For pressure unseating equipment hatches [89] and for BWR drywell heads [90], analytical techniques depend on knowledge of the force of the connecting or tie-down bolts. In most cases this is not known and must be estimated. Even knowing the torque used to tighten the bolt is not in itself adequate in calculating the force in the connection.

The increase in the horizontal diameter of an equipment hatch may be approximated [45], and this will provide some insight into whether there may be leakage past the seals. Note that in the 1:8-scale steel test [24] considerable ovalization occurred in the test.

### 3.6.6 Bellows [93, 94]

Bellows are employed at most process piping penetrations in steel containments (Figure 81) to minimize the loads imposed by the pipe on the steel shell. Bellows are also used at the fuel transfer tube penetration in all concrete containments.

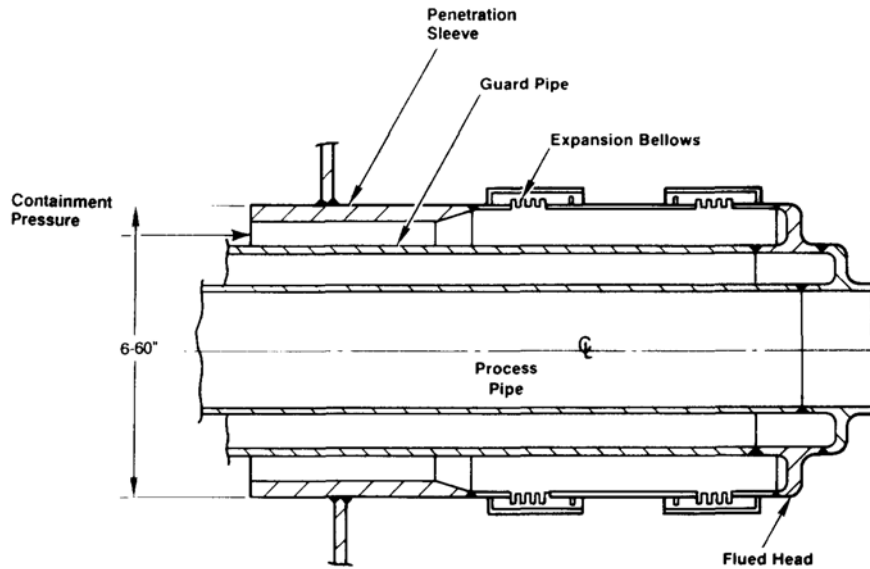


**Figure 81** Typical application of process piping bellows [82]

Two series of bellows pressurization tests were conducted at SNL:

- Thirteen 'like new' bellows were tested under various combinations of internal pressure and temperature, axial and lateral loading. Two specimens were single-ply bellows and 11 were double-ply bellows.
- Six bellows (One single ply, 5 two-ply) were corroded by exposure to magnesium chloride to produce transgranular stress corrosion cracking before testing.

Figure 82 shows an un-corroded specimen before and after testing.

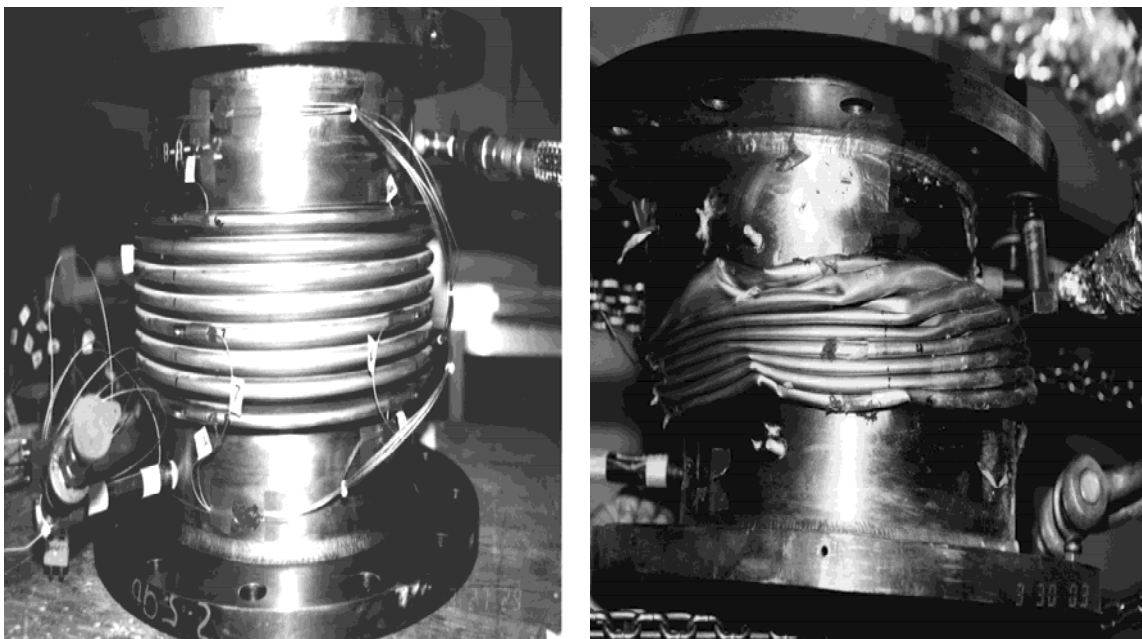


**Figure 82** Bellow Test

The containment bellows tests concluded that:

- “Like-new” specimens withstood the full range of compression (i.e. full metal-to-metal contact) or elongation before leakage occurred.
- Corroded specimens:
  - When only one ply of a two ply bellow was corroded, the bellows were capable of resisting extreme loading conditions similar to the bellows in a ‘like-new’ condition.
  - Three corroded bellows were leak tight before loading. They withstood severe deformations before developing leaks.
  - The corroded bellows that were not leak-tight before loading exhibited an increasing leak rate during loading. The leak rate depended heavily on the corroded condition of the bellows.

### **3.7 Related Containment Research Activities**

#### **3.7.1 Containment Performance Goals**

In 1990, the NRC staff proposed a safety policy goal for Advanced Light Water Reactors (ALWRs) that required a conditional containment failure probability of 0.1 (10%) or less for severe accident conditions.<sup>4</sup> In lieu of performing a full probabilistic assessment of the loads and containment behavior, the staff proposed an alternative, deterministic acceptance criteria for steel containments:

*“The containment should maintain its role as a reliable leak tight barrier by ensuring that containment stresses do not exceed ASME Service in Level C limits ....”*

The NRC tasked SNL with evaluating this alternative criteria and, since Service Level C limits only apply to steel containments, to investigate if similar criteria could be defined for reinforced and prestressed concrete containments. A panel of four experts in containment design was enlisted to advise the NRC and SNL in defining the scope of this program and reviewing the results. Klamerus, et. al. [12] reported on the results of this program.

The approach chosen to investigate these questions consisted of designing six simplified surrogate containments to ASME code requirements and investigating their performance to severe accident loading conditions. The surrogate containments investigated were:

- One reinforced concrete containment
- One prestressed concrete containment
- Four steel containments
  - Cylinder with hemispherical dome and torispherical base, SA-537 Cl. 2
  - Cylinder with hemispherical dome and torispherical base, SA-516 Gr. 70

---

<sup>4</sup> SECY-90-016

- Sphere, SA-537 Cl. 2
- Sphere, SA-516 Gr. 70

The same volume and design pressure, 45 psig, was used for each of the surrogate containments. The resulting designs were then each analyzed to determine the failure pressure under thermal loading conditions of 400°F and 600°F. The failure criteria used in these analyses was 2% global hoop strain for the reinforced concrete and steel containments and 1% global hoop strain for the prestressed containment.

It should be noted here that these were relatively simplistic ‘models’ and criteria and did not take into account the effect of local strain concentrations and penetration details. Failure criteria were not explicit in terms of the mode of failure, but suggested ‘incipient leakage’ and did not attempt to differentiate between leak and catastrophic rupture. The study also did not have the advantages of the insights gained in the subsequent containment model tests. Nevertheless, the results provide some insights on containment performance criteria, and it might be valuable to revisit these questions with the benefit of the subsequent research.

The primary ‘conclusions’ or insights gained from this study include the following:

- Current ASME design practices and requirements for concrete containment are based on yield criteria. Similarly, although steel containment designs are usually governed by some fraction of the ultimate allowable stress [  $S_{mc} \cong 1.1(S_u/4)$  ], the ASME Level C allowable are, in fact, based on (code specified) yield. As a result, the concrete design requirements specified in Section III, Division 2 and the alternative Safety Goal criteria based on the Level C allowable for steel containment have some equivalence. The margin to yield computed for both the concrete and steel surrogate containment were approximately equal, roughly 1.7 times the design pressure. This suggested that concrete code requirements possess a similar level of margin to yield as that provided by the alternative Level C allowable criteria currently in place for steel containments.
- A similar evaluation of failure pressures also suggested a level of equivalence between the Service Level C requirements for steel containments and the requirements for Section III, Division 2 for concrete containments.
- When severe accident conditions (in this case based on an ongoing NRC study on Direct Containment Heating) were convolved with the containment failure probabilities (based on assumed variations on median failure pressures and Monte Carlo simulation), the resulting CCFPs were less than 0.02 (2%). Alternately, the severe accident pressure of twice the design pressure was required for the CCFP to exceed the safety goal of 10%. A CCFP of 50% corresponded to a pressure load of  $3P_d$ .

These results suggest that alternative criteria based on ASME code design requirements satisfy the Commission’s safety policy goal. This conclusion, however, should be confirmed by more rigorous analysis and utilize the results of the latest containment experimental research results.

### ***3.7.2 Degraded Containment Capacity Analyses***

Since corrosion damage in the containment has been found in over one-third of the current US fleet of operating nuclear power plants, and it is expected that incidences of corrosion damage will increase as the fleet ages, the NRC tasked SNL to investigate how corrosion degrades the capacity of the containment to resist design and severe accident pressures. Along with experimental work on the effect of corrosion on the tensile behavior of steel coupons, Cherry and

Smith [18] performed detailed finite element analyses of containments, in this case the plants studied in NUREG-1150, with corrosion damage representative of observed conditions. They considered the following situations:

- Steel Ice Condenser (Sequoyah)
  - Local thinning of steel shell at wall-basemat junction, upper floor and ice basket.
- Steel Mark I (Peach Bottom)
  - Local thinning of the steel shell at the knuckle, sand pocket and torus.
- Large, Dry Reinforced Concrete Containment (Surry)
  - Local thinning of the steel liner at the wall basemat junction, mid-height of the cylinder wall and at the equipment hatch.
- Large, Dry Prestressed Concrete Containment (Zion)
  - Local thinning of the steel liner at the wall basemat junction, mid-height of the cylinder wall and at the equipment hatch.
  - Corrosion of prestressing and loss of prestressing simulated [95].

In all cases of corrosion of the steel shell or liner, corrosion was modeled as local thinning of the liner with no additional factors (e.g. local material degradation, local cracks, etc.) considered. This assumption was made as a result of the tensile tests on the corroded steel coupons which showed that corrosion could essentially be represented as a loss of cross-section.

The results of the steel liner and shell analyses showed that if corrosion damage occurs in a highly stressed region of the structure, the pressure capacity of the structure would be reduced. On the other hand, corrosion in non-highly stressed areas, assuming it did not penetrate the entire thickness, was found to not have any significant effect on the capacity of the containment.

As noted previously, Cherry and Smith [18] included a fairly detailed discussion of failure criteria for steel shells and liners. While Cherry and Smith addressed this problem deterministically, a companion study conducted by Ellingwood and Cherry [96] considered it from a probabilistic perspective.

Smith [95] investigated the effects of corrosion damage on prestressing tendons and loss of effective prestress by performing finite element analyses of the containment without damage and with varying levels of damage to the tendons. He concluded that the loss of vertical prestress had no effect on containment capacity. (This result is consistent with the behavior of the 1:4-scale PCCV model test.) He further concluded that loss of hoop prestress had little effect on the ultimate capacity of the containment as long as the strength of the tendons was not degraded. It is not clear how this hypothetical condition would manifest itself. Only loss of the hoop tendons themselves had any effect on the ultimate capacity and this was proportional to the number of tendons lost, especially if the losses occurred in the highly stressed regions near the mid-height of the cylinder.

### ***3.7.3 Risk-Informed Assessment of Degraded Containment Capacity***

Sandia is completing a study, to be published as a NUREG/CR, to assess containment degradation from a risk-informed perspective. Reg. Guide 1.174 [98] describes a risk-based approach for

evaluating changes in a plant’s licensing basis, which could include damage or degradation of the containment boundary. Spencer and Petti have built on the previous analytical work by Cherry and Smith by investigating the risk-significance of hypothetical occurrences of corrosion in the steel shell and liner the NUREG-1150 plants in terms of Large Early Release Frequency (LERF). LERF is used in Reg. Guide 1.174 as a quantitative surrogate risk metric for the Quantitative Health Objective specified in the Commissions Safety Policy Goal Statement. Small increases in LERF (Region II and III in Figure 83) are not considered risk significant.

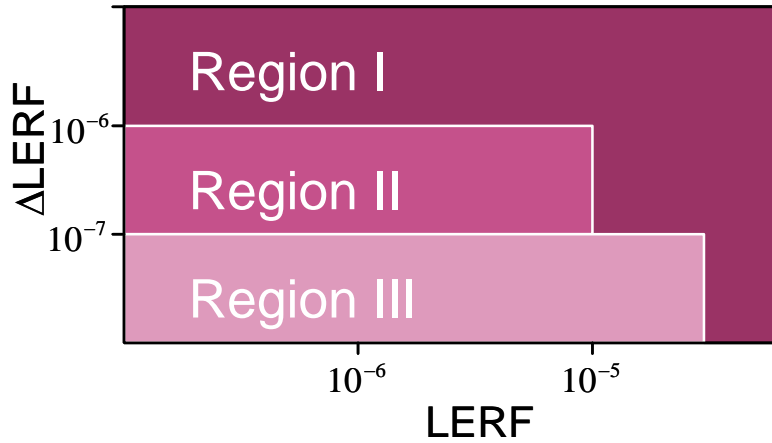


**Figure 83 Acceptance Guidelines for Large Early Release Frequency**

Finite element models were used, along with Latin Hypercube sampling of up to 30 model parameters, to generate fragility curves for various containment pressure failure modes. Figure 84 shows an example of the original and degraded (due to liner corrosion) fragility curves for the Surry containment.

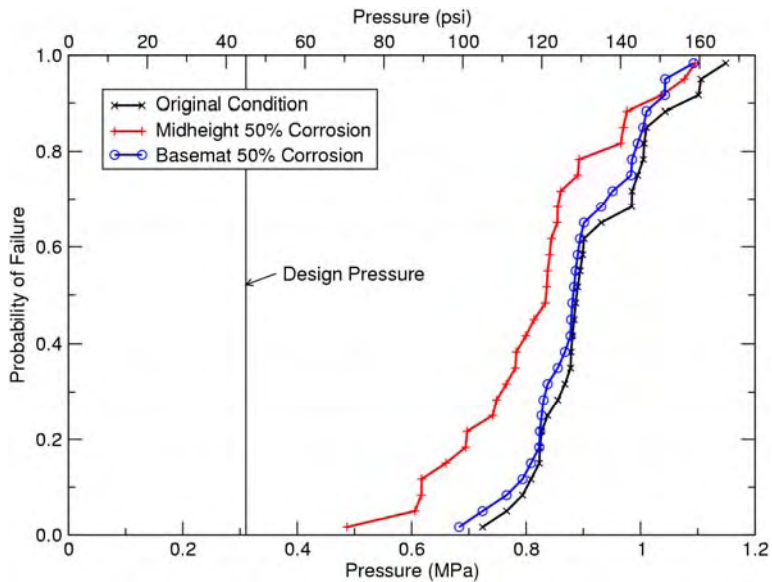


**Figure 84 Leak Fragility for Surry Containment with Liner Corrosion**



The degraded fragility curves for all failure modes are combined and conditional cumulative failure probability curves for leak, rupture and catastrophic rupture were used in revised Level 1 PRA analyses to determine the effect on LERF.

The analyses resulted in both a positive and negative change in LERF ( $\Delta$ LERF), however, these analyses were not intended to be used to determine the risk-significance, with subsequent implications for inspection and/or repair, for actual occurrences of corrosion or damage in real containments. Rather, the study provides an approach and demonstrates how risk-informed decision making might be applied to real occurrences. The study also suggests that alternate risk metrics might be more appropriate for making decisions regarding individual systems, structures or components.

### ***3.7.4 Seismic Capacity Tests and Analyses***

During the first 15 years of the SNL containment research program, no special consideration or research was applied to the seismic behavior or performance of containments. Seismic reinforcement that is added to containments was included in scale model designs, but the objectives of the tests did not include seismic behavior. The first large scale investigations for seismic behavior of containments were performed starting in the late 1980s in Japan. These were carried out by NUPEC, using the large-scale shaking table at the Tadotsu Engineering Laboratory. These tests were sponsored by the Ministry of Economy, Trade and Industry (METI) of Japan, but the NRC and SNL had a participatory role, particularly in conducting pre- and post-test analysis [99]. These analyses were conducted by SNL with analytical support by ANATECH Corp. [100, 101]. Tests of both an RCCV and a PCCV (1:10 scale) were performed, and the project was completed in March, 2000. An interesting aspect of the tests was that many different earthquake records and magnitudes were applied to the same model specimen, starting with small ground motions and building up to larger motions, which eventually failed the structures. So the effects of accumulating damage to the structures became an important part of the observed and analyzed behavior. Ultimately, this caused both advantages and disadvantages to the process of interpreting the shake table testing and analysis results, because while the tests qualitatively demonstrated significant changes in structure dynamic behavior with the accumulation of damage, these effects were difficult to quantify or analytically simulate because to introduce them required analysis of each and every shake table record in cumulative fashion. As with any large scale shake table test, there were also difficulties with delivering the intended ground motion signature, when the stiffness and mass of the shake table apparatus and test specimen both have significant influence on the motion that actually occurs at the shake table-specimen interface.

The Tadotsu experiments served dual goals set by the project sponsors, namely, those of proof testing, and those of benchmarking for improving analytical methods. Although there may be lack of agreement as to how comprehensively these goals were met, the tests did succeed in calling attention to the importance of the amount and the dynamic character of seismic energy delivered to a containment structure, and the role that concrete containment cracking plays in containment dynamic response. These issues are largely ignored in containment seismic design, and perhaps need to be considered in future design practice.

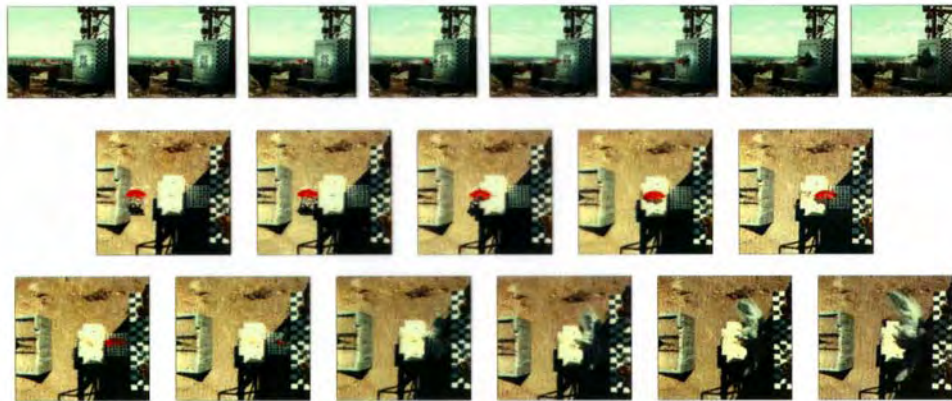
### ***3.7.5 Impact Tests and Analyses***

In addition to the programs described in this report which address the capacity of nuclear power plant containment structures to resist beyond-design basis loads resulting from severe accidents and seismic events, SNL has performed a number of experimental and analytical programs to investigate the response of structures (not necessarily containments) to impact loads which may result from failures of equipment such as turbines, tornado-generated missiles and aircraft. It is

beyond the scope of this report to describe these programs in detail; however, a brief description of the major programs, with references for further details, is included for completeness.

### 3.7.5.1 Turbine Missile Tests

A series of tests were conducted for the Electric Power Research Institute (EPRI) at SNL's rocket sled track to accelerate full-scale quarter segments of turbine rotor disk into concrete containment wall targets and turbine casings [102, 103].



**Missile mass 147 kg, velocity 13.1 m/sec; Panel mass 153 tonnes, thickness 1.37m**  
(best available figure)

**Figure 85 Turbine Missile Test Sequence**

### 3.7.5.2 Full-Scale Aircraft Impact Test at SNL

A full-scale F4 Phantom jet was accelerated to 210 m/s (496 mph) to impact a ballistic pendulum, comprised of a 3.6 m (12 ft) thick reinforced concrete block on air bearings. This test was conducted for the Kabori Research Complex, Tokyo, Japan. The purpose of the test was to measure the impulse of the aircraft impacting a rigid mass. The results of the test have been used to benchmark analytical models for aircraft loading time histories [104].

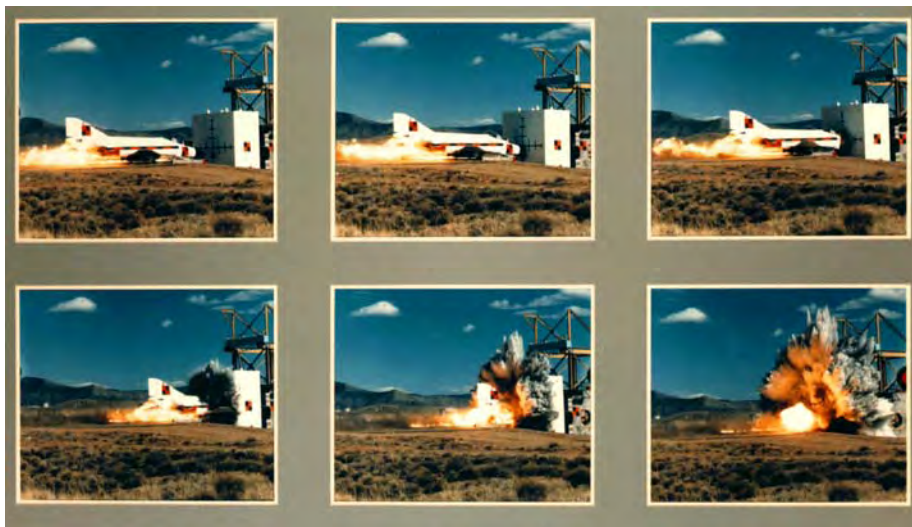


**Figure 86 Full-Scale Aircraft Impact Test Sequence**

### 3.7.5.3 Full Scale Engine Tests

Full-scale jet engine tests were conducted at SNL to observe the penetration and damage response of concrete wall panels of varying thickness, reinforcing and with and without steel liners. These tests were also conducted at Sandia's rocket sled track for the Kobori Research Complex. [105, 106].

### 3.7.5.4 'Water-Slug' Tests

The previous tests investigated the behavior of rigid missiles impacting flexible or 'soft' targets and flexible missiles impacting rigid targets. In order to understand the full spectrum of loading conditions, SNL conducted a series of impact tests for soft missiles on flexible targets. In these tests, a thin aluminum cylinder was filled with water, referred to as the 'water slug', and accelerated to impact a reinforced concrete panel. Tests were conducted varying the 'water slug' size and impact velocity. The results of these tests and the analyses conducted to simulate the tests were published in a limited distribution report.



**Figure 87** 'Water Slug' Test Sequence

### 3.7.6 Leakage Tests

As described in Chapter 2, containment performance criteria are qualitatively and quantitatively described in terms of a leakage rate. However, experimental models and analyses typically measure containment response to pressure loading in terms of stress, strain or displacement. Two primary containment leakage modes have been identified: by-pass leakage through penetrations, typically at the seals, and tearing or rupture of the steel shell or liner. Experimental and analytical investigations of penetration leakage were discussed in Section 3.6. Experimental results of steel containments suggest that, in most cases, material failure in the steel shell progresses rapidly from leakage to rupture. In the case of concrete containments, however, the transition between large local material strains to material failure, manifested as a tear or hole, coupled with cracking in the concrete and fluid mechanics of the gas flow through the tear and the cracked concrete is currently beyond ability to model. This problem can be de-coupled into the problem of predicting the progression of material failure in the steel and the problem of gas flow through cracked

concrete. Castro [56] proposed a model for predicting the size of tears in a steel liner (see Section 3.4.3), however, this model has yet to be benchmarked against test data. Various researchers have investigated the fluid mechanics problem experimentally and have proposed analytical models to simulate the observed behavior.

Salmon, Cuesta, and Pardoen [108] provide a good summary of relevant research on leakage through cracked concrete that may be applicable to containments; however, this research, to date, has not been implemented directly into SNL containment research.

The flow rate of air through concrete depends upon the air permeability, the thickness of the concrete, and the pressure gradient applied. The flow rate appears to be inversely proportional to the slab thickness and directly proportional to the pressure difference across the slab. A literature review covering the past 30 years examined published works on air permeability measurements in concrete. Most of the works reviewed dealt with gas flow and permeability measurements in undamaged concrete. But there is work that deals with gas flow through cracks, and some of this may be applicable to concrete containments.

Rizkalla et al. [57] proposed a mathematical expression for the rate of pressurized air flow through idealized cracks. In their work, Rizkalla et al. simulated the membrane stresses in a concrete containment structure subjected to large internal pressures by tensioning the longitudinal reinforcement which protrude along the ends of the test specimen. Steady-state differential air pressures were created by controlling the pressurized air to the upstream chamber of the specimen, while maintaining the downstream pressure at atmospheric pressure. Rizkalla refined the proposed equation for flow rate by using the experimental data obtained from several concrete specimens subjected to uniform tensile stresses. Although these data are valuable, it is doubtful whether they are applicable to seismic induced shear cracks, or out-of-plane bending cracks.

Mayrhofer et al. [109] investigated the airflow through cracked reinforced concrete. This effort was aimed at determining the gas impermeability of shelter roof slabs loaded to their maximum carrying capacity with uniform pressure. The out-of plane pressure load causes the slabs to bend. Gas impermeability for the slabs was defined by the ability to maintain a minimum overpressure of 0.5 to 1.0 millibar. Square slabs with length dimensions of 114 cm (45 in) and 300 cm (118 in), 0.14% and 0.3% reinforcement by area, and a thickness of 17.8 cm (7 in) were used in the experiments. The slabs were pressure loaded statically in monotonically increasing load steps. Airflow was measured upon completely unloading the structure after each load step. Data presented included static load-deformation curves, crack patterns, and airflow-overpressure curves. A mathematical expression to correlate slab deflection with gas permeability was described in detail. A correlation between deformation and permeability was possible because the loading and resulting crack patterns in all slabs were similar.

Suzuki et al investigated the gas leakage rate through cracks in both reinforced and unreinforced concrete [110]. Sensitivity studies on the leakage rate due to the kind of fine aggregate and the size of the coarse aggregate were performed. Suzuki's test were limited to concrete crack widths less than 0.5 mm, and differential pressures less than 250 kPa (36.2 psi). Although limited in samples for reinforced concrete, Suzuki's recommended flow equations based on his empirical data may be used as a benchmark.

Okamoto and others performed an experiment on a three-dimensional one-tenth-scale specimen based on a part of a prototype boiling-water reactor nuclear power plant [111]. The study was conducted to measure the air-leakage as a function of lateral load, or shear cracks. The specimen was subjected to nine static load cycles up to and beyond the specimen design bases. Leakage rate data were obtained at both the peak, and upon removal of the load at each cycle.

Greiner and Ramm [112] performed a series of experiments on both reinforced concrete and unreinforced concrete in an effort to derive an equation for the leak rates of air as a function of crack width and overpressure. Their efforts were limited to the following parameter ranges:

1. crack width, 0.20 mm to 1.30 mm (0.008 in to 0.05 in)
2. overpressure at the beginning of the crack, 0.10 MPa to 0.80 MPa; (14.5 psi to 116 psi)
3. fine aggregate particle size, # 8 (2.36 mm) , #16 (1.18mm) and #32 (0.6mm).

They concluded that for unreinforced concrete, their proposed flow equations were good for the experimentally proven ranges, while for reinforced concrete, their predicted flow equations were conservative (i.e., measured flows were less than those predicted).

Dameron, et al [113] evaluated leak test results that were available in the open literature, and suggested a methodology for calculation of leak rates in lined concrete containment vessels. As part of their research, Dameron, et al were required to estimate the flow rate through the concrete containment vessel. They used the method developed by Rizkalla in calculating the measured leak rates, and found good agreement between the measured values and the calculated values for micro-concrete.

Riva, et al [114] performed a single experiment on a reinforced concrete slab subjected to differential pressure and uniaxial tension. In their experiment, they compared the measured leak rates with those calculated using the leak formulae available in the literature. Riva concluded that, among the formulations considered:

1. the leak rate prediction formula given by Rizkalla et al. provides the best fit to his experimental data,
2. the leak rate prediction formula given by Greiner and Ramm [112] would be more suitable for higher differential pressures, 0.1MPa (14.5 psi);
3. the Poiseuille equation generally overestimates the leak rate, and
4. the expressions by Suzuki et al. [110] obtained the best results for the smallest pressure gradient (0.01 MPa) (14.5 psi).

In summary, the literature review indicates that there are very little data on the permeability of cracked reinforced concrete or on earthquake damaged reinforced concrete. Data that are available include that published on gas permeability in undamaged concrete, that published by various researches on concrete subjected to uniaxial tension, and that of Farrar and Girrens on the single shear wall tested to below its design capacity. The experimental data available on cracked concrete were directly applicable for reinforced concrete containments that are subjected to high internal pressure loads.

## 4 ASSESSMENT OF CONTAINMENT PRESSURE CAPACITY

No assessment of containment pressure capacity can be formulated without definition of what constitutes containment failure. And there still remains a lack of consensus on the definitions of failure modes, so it is appropriate to begin this chapter by summarizing the definitions from the authors' perspective. These definitions are generally supported by the observed behavior. For the Sandia program, failure of the models has been defined in terms of functional failure, that is, the inability of the containment to meet its primary functional objective of maintaining a pressure boundary to prevent the release of radioactive materials to the environment or 'leakage'. This may coincide with the common understanding of failure as gross structural failure or 'bursting', i.e. the limit state of the primary load resisting system. In many cases however, functional failure may occur well below the loading limits of the structure. Alternately, the difference between 'leakage' and 'bursting' has been described as the difference between local loss of function at a discrete location and loss of structural integrity. Experience has shown that steel containments may exhibit 'bursting' or gross structural failure while reinforced concrete containments with steel liners would exhibit 'leakage' or local functional failure. The data on failure of prestressed concrete containments is inadequate to draw unequivocal conclusions regarding failure although 'leakage' appears to be the most likely limit state.

This difference between functional and structural failure has led some researchers to include features in the model to allow loading beyond the functional limits of the model, e.g. the inclusion of resilient bladders to prevent leakage of the pressurization medium, usually water. One problem with including these model artifacts is that they may tend to mask real functional failure modes which could occur in prototypical plants. Since the objective of Sandia's program has been to investigate representative behavior of actual containments, the decision was made not to 'mask' the functional failure modes and to rely on the primary containment function as the definition of failure.

The following sections briefly describe the research conducted at Sandia and elsewhere for each of the main containment types, as well as the components, with an emphasis on the results as they pertain to assessment of containment pressure capacity.

### 4.1 Insights from Containment Testing

As previously described, the Sandia containment test program was geared toward conducting experiments to gain insight on, and "benchmark," analytical methods for calculating containment response and capacity. None of the tests were "proof tests." Nevertheless, the implications and insights on containment overpressure behavior provided directly by the tests should not be completely discounted. The design of each of the large scale containment tests (especially the 1:6-scale RCCV, mixed scale SCV, and 1:4-scale PCV) was performed using, then current, containment design codes and procedures, and the test structures were designed as pressure vessels. They were not designed simply by geometric scaling. This means that it is probably reasonable to draw some general conclusions from trends observed from these tests. These conclusions would include, for example, the following.

- **Scale Effects:** The results of the tests clearly demonstrate the necessity of conducting model tests at a scale large enough to:
  - a. utilize materials which exhibit the characteristics of the materials used in the prototype,

- b. allow the design details and construction methods used in the prototype to be represented in the model, and
  - c. avoid non-representative details and as-built conditions to be present in the model.
- **Material Properties:** As a corollary to the previous point, it is worth making a few observations regarding the data from tests used to define the properties of the construction materials. Typically, the properties are obtained from standardized tests of small or representative samples of the materials used in the construction of the model. These test methods have, as their primary purpose, the function of assuring that the materials used in the construction meet a minimum quality standard. Experience has shown that if these minimum standards are met, the structure will meet the design requirements. This is subtly, but significantly, different from characterizing the *in-situ* properties of a structure's constitutive elements.

Nevertheless, these standardized test results are usually all that is available, and most engineers would be happy to have actual material data rather than minimum specified properties. The difficulty arises when the properties of these sample tests are used to develop mathematical material models for use in analysis, especially when these material models include inelastic behavior and failure conditions, to predict the response of structures well beyond their design limits.

The 1:4-scale PCCV model tests clearly demonstrated that the tendons failed shortly after the cylinder wall and measured tendon strains were approximately 1%, much less than the 4 to 7% strain obtained from laboratory tests of tendon specimens. Similarly, the measured (and calculated) liner strains at the pressure level when the liner tore were well below the ultimate strain of the liner coupons, even when considering local strain concentrations.

This raises the question, then, of whether current standard material test methods are being used to perform a function for which they were not originally intended and if they are adequate for the task. If not, can alternate test methods be devised which might provide a better basis for constitutive models? (Another way of looking at this is to consider that there have been significant advances in the computational methods used to simulate structural response. However, there has been no comparable advance in measurement and characterization of the material models on which these computational methods depend.)

A second question related to the material properties is what type and amount of data is considered adequate for calculating the response of actual containments? A fairly extensive suite of material tests were typically conducted in conjunction with the model tests, and actual properties were used in all cases. It is not clear that this level of information would be available for all containments. If it is not, the quality of the capacity predictions may be reduced with a corresponding increase in uncertainty.

- **Loading:** The reasons for conducting static, pneumatic over-pressurization tests at ambient temperature were discussed in Section 2.1. While the tests were successful in obtaining data on the response to pressurization and, secondarily, to prestressing, the application and interpretation of these results should recognize the fact that the test load is not a faithful representation of the complex loading environment which will exist during a severe accident. The effects of temperature, the temporal relationship between pressure

and temperature, the composition of the internal atmosphere and the rate of loading may all have an effect on the response and failure modes and the sequence of these events should be considered in any evaluation of containment capacity.

Other containment model tests attempted to consider some or all of these aspects of severe accident loads. Future efforts should consider evaluating the effects of these other loads on the response of the prototype, and the results of these efforts may indicate the need for additional testing which includes these loads.

- **Failure Criteria:** Nevertheless, the test did provide some insight into issues which should be considered in establishing failure criteria for actual containments.

First, the primary functional failure criteria defined in terms of a maximum leak rate, cannot be applied directly to conventional mechanistic models of containment structures, which output response in terms of displacement, strain, force, stress, etc. As a result design philosophies have focused on limiting these response variables to ensure that no leakage occurs. Further study of the relationship between leakage and structural response may provide some insights which could be applied to regulations and design requirements based on functional criteria.

Secondly, predictions of containment capacity have often been based on the structural capacity of the components used in the construction. For example, using the ultimate strength or elongation of samples of the prestressing tendons, liner, rebar, etc. as the limit criteria. The model tests have demonstrated, as noted in the discussion on material properties, that the strain levels measured at failure can be much less than the limiting values obtained from standard tests of sample specimens. The test results should provide some guidance to the development of appropriate failure criteria to be used in future capacity calculations.

- **Leak Rate Measurements:** SITs/ILRTs conducted in accordance with the specified procedures, demonstrated the difficulty of measuring leak rates with the accuracy required to guarantee that they do not exceed the specified limits. Even with the relatively simple, controlled structure represented by the PCCV model, and the extensive suite of instruments available during testing, it was not possible to accurately measure leak rates on the order of 0.1% mass/day. An apparent leak rate of 0.5% mass/day at 1.5P<sub>a</sub> during the LST was due to thermal expansion of the model in response to ambient temperature changes and direct heating of the model. In light of these results, a review of leak rate measurement methods and the leak rate test criteria should be considered.

## 4.2 Insights from Containment Analysis

In reporting on the results of the 1:8-scale steel containment vessel model test, Clauss [25] made the following observation:

*“The analysis of a nuclear containment subject to loads arising during a severe accident can be divided into two distinct steps. The first step consists of solving for the strains and displacements at different pressure (and temperature) levels. Implicit in this first step is an analyst's ability to identify which sections of the containment are critical and the amount of detail that must be included in an analytical model to obtain accurate results. The next step consists of inferring structural performance (by evaluating criteria for leakage and rupture) from the predicted strains and displacements in the model, as well as other parameters, such as thermal and radiation aging of seals, and aerosols.”*



While the SNL containment test series provide insight into the behavior and capacity of actual containments, it should always be kept in mind that actual containments are much more complex than even the most detailed model tested. Conclusions about the capacity of actual containments can only be made from a reasoned evaluation of the test data and the results of detailed analysis of the actual containments using experimentally validated methods. Full size or large-scale component tests were planned to complement, and increase the understanding of, the capacity of the containment boundary, especially where complex geometries challenge the ability to perform reliable numerical simulations (e.g. bellows, electrical penetrations) or to verify these predictions.

The results of this research, both experimental and analytical, have been and probably will continue to be used to characterize the behavior of actual containment structures. This behavior can then be used in risk analyses. The step from predicting deformation response to performing a risk analysis is not necessarily straightforward. Depending on the risk analysis model, the containment performance may have to be input as a leakage or as a function of the loads, or a probability function. If the risk analyses indicate that the containment is dominating the risk, then it is also possible to go back to the containment analyses and "sharpen the pencil," to improve the results. One must realize that, for example, performing a full 3-D non-linear analysis of the containment system including all of the details of the as-built containment system is expensive, and not necessarily required. But suffice it to say that there still is work required in using the results of the containment analyses. Examples of how one might go about utilizing deterministic response analyses results in a probabilistic risk assessment have been developed in EPRI sponsored research of the late 1980's. A summary of this methodology is provided in Section 4.5 which discusses current practice, and 'what we know versus what we don't know.'

One of the key difficulties of a probabilistic framework is, again, the lack of extensive data on the size of leaks that develop after liner tears or other form of rupture occurs in the containment. Some data is available, and this was used to the extent possible in the EPRI probabilistic leak prediction approach, but most of the containment research, both experimental and analytical, has been focused on prediction of the first liner tear or rupture. Another difficulty with developing a probabilistic framework occurs when the analyses indicate a weak feature of the containment system. That item may become a candidate for retrofit, thus dramatically changing the containments risk characteristics. Also, analysis results can be used to write improved code requirements and to enhance new designs, which could significantly influence risk assessment.

### **4.3 Analysis Goals**

Since one of the main objectives of containment integrity research programs has been the validation of analytical methods, most of this research has had a significant analysis component. These efforts can be grouped into the categories: global containment response, local response near stiffness discontinuities, and the prediction of failure and its consequences.

#### ***4.3.1 Global Response Prediction***

Global response prediction can be further subdivided into containment types, namely steel versus concrete containments, because of the significantly different requirements for the corresponding analytical tools.

Global response analyses of steel containments have been conducted by researchers throughout the world [21] in conjunction with tests of steel containments and pressure vessels. Basic methods of analysis have been in place for as much as three decades, i.e. since the development of reliable shell element formulations and steel plasticity models in finite element programs. However, steel containment analysis research has provided extensive lessons learned as to how to

apply these tools to containments. A detailed summary of these insights and lessons is provided in [46, 53]. Issues that analysts continue to find challenging are the accurate prediction of onset of yield, made complicated by the three dimensionality of the stress state, and the prediction of pressure versus deformation in the final stages of loading, i.e., on the “descending branch” of the load versus deformation response curve.

Tools for modeling steel and concrete containments have a more recent history due to the lack in the early 1980's of a generally accepted concrete finite element program. The Three Mile Island accident highlighted the need for capability to analyze concrete containments for beyond design basis pressure loads. This need triggered analytical research in the US and elsewhere to develop and improve concrete analysis software. One such research program which started in 1983 and ran for 7 years was the EPRI-sponsored containment research program. This effort had an experimental program and an analytical one and was aimed at developing not only a usable tool, but also an experimentally verified one. The analysis tool evolving from this work was ABAQUS-EPGEN [115], a general purpose F.E. program with special-purpose concrete and rebar sub-elements, and ANACAP-U, a user-supplied concrete constitutive modeling module. ANACAP-U is based on the smeared-crack approach to concrete modeling. The ability of the software to predict global containment response was tested and verified with pre-test analysis exercises performed on the Sandia 1:6 scale reinforced concrete containment model pressure tested to failure in 1987 [44, 46], the CEGB's 1:10 scale prestressed concrete containment model pressure tested to failure in 1991 in the United Kingdom [65], and on the Sandia 1:4 Scale Prestressed Concrete Containment model pressure tested to failure [72] in 1999/2001. Similar constitutive model development efforts were conducted and have successfully predicted global containment model test response for the following software tools: DIANA, ADINA, CASTEM, NEPTUNE, NFAP, PAFEC, BOSOR5 and ANSYS. Prediction of global, free-field containment response has, therefore, been reasonably well established as long as analyses are performed with validated tools and by sufficiently experienced analysts.

#### ***4.3.2 Local Response Prediction***

Prediction of the response near stiffness discontinuities and the local deformation states of containment components such as the liner, rebar, or prestressing tendons is more difficult and has less widespread experimental verification. The first large scale tests of local concrete containment details were those of the EPRI program in which wall panel tests of different geometries and different discontinuities (penetrations and other details) were stressed biaxially as they would be in a containment subjected to overpressure. Local discontinuities have also been tested in other component test programs and by detailed instrumentation of these details within various global containment tests. Prediction of strain concentrations near these details in steel containments is made more difficult by the presence of welds (and heat affected zones), residual stresses associated with rolling and fabrication, and incomplete knowledge of actual plastic behavior of materials, particularly under three dimensional states of stress. Local response prediction in concrete containments involves all of these difficulties (all of these are present in the liner alone) and others stemming from liner/concrete/rebar interactions, and difficulties in modeling the shearing response of concrete [50]. Nevertheless significant advances in local and component modeling have been made by various researchers and a few of these are examined later in this chapter. Accurate representation of the local response is now generally accepted to be reasonably good provided analysts have sufficient time and resources to devote to the modeling effort, a proviso not often satisfied in the design of new facilities.

### 4.3.3 Failure Prediction

This last analytical research area is, perhaps, the least mature, and in some ways the most debatable in the containment research community. It is immature because it involves the combination of the most refined analytical techniques and constitutive modeling, the latest information on failure criteria, and often reliance on engineering judgment. The last of these is difficult to codify or otherwise disseminate to the containment analysis community.

The failure criteria define a threshold environment which is the pressure and temperature at which leakage or rupture is imminent. In a LWR containment building, there are a number of potential failure mechanisms, or release paths. The release paths we have considered are described in Table 12. Separate structural calculations may have to be made for each release path, each with its own unique modeling requirements.

One of the reasons for the immaturity of the failure prediction part of containment analysis is the difficulty with measuring and even defining failure. Experiments on complete containments provide a wealth of global and local response information that is available for analytical correlation and validation, but these tests only fail in one, or at most a few, locations. Further, it is nearly impossible to precisely gage an exact fracture location so knowledge of the strains that exist just before fracture remains limited and therefore controversial.

**Table 12 Release Paths in LWR Containments**

<b>Rupture of Containment wall or shell</b>
<b>Leakage past Sealing Surfaces (Operable Penetrations)</b>
<ul style="list-style-type: none"> <li>○ <b>Pressure Seating Equipment Hatches</b></li> <li>○ <b>Pressure Unseating Hatches (Drywell Heads, Equipment Hatches)</b></li> <li>○ <b>Personnel Air Locks</b></li> </ul>
<b>Leakage past Purge and Vent Valves</b>
<b>Leakage from Electrical Penetration Assemblies</b>
<b>Leakage due to Failure of a Bellows (Expansion Joint)</b>

Also adding to the debate in this area is the disagreement amongst analysts, especially for concrete containments, and practitioners over "just how good is good enough". For example, prediction of the failure pressure of the 1:6 scale reinforced concrete was made within a relatively narrow band, but the prediction of the location consisted of a relatively long list of potential "hot spots"[45]. Once global hoop strains of between 1% and 2% are reached, most researchers and analysts are reasonably certain that containments will fail, and some say that this knowledge may be complete enough. Others, however, argue that failure locations and failure sequence have highly varying consequences on risk, on potential release of radionuclide's, and on mitigation measures; therefore, reducing these uncertainties justifies the furtherance of containment analysis research.

For steel containments, the failure criteria, and the implementation of it by way of analysis is a little more straightforward and universally accepted. The rupture criterion for steel shells is tensile instability. For steel containments, tensile instability will generally occur when the strain is near the material's ultimate strain. Thus, rupture will occur if, at any point on the pressure boundary, the equivalent strain exceeds the material's ultimate strain (the strain at maximum load for a uniaxial tensile test). If the strain is due primarily to bending, somewhat higher strain may be allowable (to account for crack growth through the thickness).

Through-wall cracks in a steel containment resulting from quasi-static internal pressurization will grow in a stable fashion or a short period of time until a critical length is reached, at which point rupture occurs. The stored energy in a containment at the rupture pressure is so great that venting through the growing crack does not cause a significant drop in pressure before the critical crack length is reached. Consequently, the stresses at the crack tip are not relieved and the crack cannot be arrested. It is concluded that a through-wall crack that would cause a venting of the containment precluding rupture is extremely unlikely. Therefore, the rupture criterion represents any shell failure.

#### **4.4 Analytical Research Findings**

The authors have concluded from the analytical research that the only approach to reliably predict the nonlinear response, especially for the complex geometry of containments, is with nonlinear finite element analysis. There is a restricted class of general purpose computer codes that has the features needed to represent the mechanics of large strain and large deformation typical of containment response. Based on comparisons of calculated response with experimental data, features of analysis that are needed to obtain reliable results are listed below.

##### **4.4.1 Steel Containment Analysis**

The experimental results and nonlinear analyses of scale models has demonstrated that the post-yield behavior cannot be extrapolated from linear analyses. Linear analyses cannot account for the effects of load redistribution, plastic flow, or the shape of the stress-strain curve for steel. For instance, at the base of a cylinder where radial displacement is constrained, an elastic stress concentration associated with bending is observed. The stress at the base is nearly twice that at mid-height while the response is still elastic. Yielding occurs near the base of the cylinder well below the general yield pressure, but the stress and strain do not increase appreciably until general yield occurs. Then, as the pressure is increased beyond general yield, the strains at mid-height increase more rapidly than those at the base. In the scale model tests, rupture was always associated with high strains near the cylinder mid-height. Failures have been unrelated to the stress concentration at the base of the cylinder.

##### **4.4.1.1 Material Modeling**

The stress-strain relationship for each type of steel should be represented by a multi-linear curve up to at least the ultimate strain. Minimum specified properties are not normally representative of the actual materials; properties may vary as a function of heat (i.e., production run) and thickness. The specified properties for the material also give little indication of the shape of the stress-strain curve. Variations of properties within a particular heat are negligible. However, the temperature dependence of the yield strength, tensile strength, and work hardening slopes of steels can have an important effect on performance, and should be represented in the material model.

Material properties should be determined from uniaxial tensile tests on the actual fabrication materials if at all possible. However, using the uniaxial yield stress has been found to over-

predict the pressure at first yield. Such uncertainties in predictions are still being studied, but one potential reason for this is the residual stresses of fabrication. Of course, these factors introduce uncertainty into the predictions for structural performance. One of the best ways to reduce uncertainties is to “test” analyst decision-making by analyzing one of the existing steel containment tests prior to starting analytical study of an actual containment. Lessons learned through this process are likely to greatly improve the reliability of the response prediction.

Prediction of failure of steel plate material should be based on strain measurements in coupon tests and on consideration of the triaxiality of the stress state. A failure criteria that includes triaxial stress considerations proposed in [17] has been used in much of the containment analysis research described herein.

#### 4.4.1.2 Geometric Nonlinearities

Second-order and large-rotation terms need to be included in the strain-displacement relations. The stiffness matrix should be updated to reflect the changes in geometry, including thinning of the wall. Distributed forces should be formed on the basis of current geometry (i.e., loads from pressure should remain normal to the surface).

#### 4.4.1.3 Element Formulation

Thin shell elements appear to work well for steel containment analysis. Elements should be benchmarked against known solutions before being used for the first time in a predictive analysis.

The effects of elevated temperature were not incorporated into the scale model structural tests, and therefore, the analytical methods are not benchmarked for elevated temperature. Nevertheless, the authors feel that the effects of elevated temperature can be handled by most general-purpose finite element codes. See for example [77]. The main difficulty is in determining the actual temperature profiles in the shell and the penetrations.

### 4.4.2 *Concrete Containment Analysis*

Reliably predicting the threshold environment for leakage or failure of a concrete containment requires accurately calculating the post-yield response. Nonlinear 3D calculations for the structural response are also necessary for local stiffness discontinuities and penetrations if liner tearing and leakage is to be accurately predicted. Methods for performing such analyses will almost certainly require the use of sub-models of local regions rather than a 2D or 3D analysis of the entire containment. Local sub-models can be loaded via specified boundary displacements generated from coarser global analyses. These boundary conditions need to include the effects of the interaction of the penetration or discontinuity with the free-field structure. For example, penetration regions have been observed to displace smaller radial distances than the free-field, causing out-of-plane relative motion between the penetration and the free-field [46, 47].

For equipment hatches and drywell heads, the structural response parameters used in the seal leakage criterion developed in [82] characterizes approaches applicable to calculating the response. However, to predict leakage from many types of penetrations, the nonlinear response of the supporting wall must be known.

#### 4.4.2.1 Material Modeling

Pertinent details for modeling steel materials were discussed previously under "Steel Containment Analysis". These factors must also be included in reinforced and prestressed concrete

containment analyses for modeling the liner. In particular, the strain hardening of liner steels in the yield plateau requires careful verification of the strains in the nonlinear response range.

Concrete constitutive models should include tensile cracking (normally treated as occurring in the principal stress directions at the integration points). Alternatively, the concrete can be treated as a no-tension material in analyses aimed at predicting global response. Some method for simulating post-cracking shear retention should also be included. Shear retention is particularly important at the wall base, and numerical solutions in this region are found to be sensitive to the shear retention algorithm used. Description of these methods, and a reasonable assessment of the current “state of the practice” in concrete modeling is available from the report on Round-Robin pretest analyses of the 1:4 Scale PCCV Model [74].

While most of the concrete elements in a computational grid will probably experience no compressive stress at high pressures, a few elements at the outer wall base and along the top of the basemat will experience compression, sometimes large enough to exceed  $f_c'$ . Thus, it is important to properly model concrete crushing. An elastic/perfectly plastic stress-strain curve has shown reasonable results in most cases, but inclusion of strain-softening is preferred for completeness. (Although, the associated plasticity algorithm is more complex.) As complex behavior is to be expected at the wall base, it is important that the concrete compressive yield algorithm properly treat the effective stress and strain calculation. Compressive yield is more likely to be reached by the combination of vertical compressive stress and shear stress rather than any one component stress reaching  $f_c'$ . This condition is essential for predicting potential wall-base shear failure.

#### 4.4.2.2 Geometric Nonlinearities and Other Issues

Contrary to the recommendations for steel containment analysis, it has been found that the second order and large rotation terms need not be included in the strain-displacement relations for concrete containment analyses. The stiffness matrix need not be updated to reflect the changes in geometry or thinning of the wall, as it is in steel shells. This recommendation carries with it some practical advantages, especially for modeling such complexities as prestressing tendons. Restricting the solution to small-displacement theory provides some options as to approximate formulations for friction and other effects. The effects of elevated temperature discussed previously are also relevant to concrete containments, and these are described later in this chapter.

#### 4.4.3 *Comparison of Analyses Methods Used for Predicting Model Behavior with US Containment Design Practice*

Design practices for US containment designs were discussed in Section 2.2.2. The authors are not aware of any standard for analysis of containment for design loads or for response to beyond design basis loads. A comprehensive survey of the FSARs and IPEs, would be required to ‘establish’ or characterize current practice, however this is beyond the scope of the current effort. Presumably most designs utilize conventional linear elastic analysis methods, either simplified, closed-form analytic solutions or elastic finite element analysis methods. The liner plate is not considered a structural element for design.

It was not until the 1980s that containment failure analyses were conducted for overpressure conditions. Because of the highly nonlinear behavior of concrete containment structures, the analytical requirements for failure analysis differ significantly from those for design analysis. The absence of containment failure analysis from general practice has been due mainly to the demanding analytical requirements involved. It was not until the Three Mile Island (TMI) accident, which created the need for better understanding of containment overpressure behavior, that such investigations were undertaken.

#### **4.4.4 Temperature Effects**

The subject of temperature remains largely an untested issue with regard to global containment behavior. This is due to the experimental difficulties involved with scale modeling of elevated temperatures. Conclusions about global behavior must be taken primarily from analytical studies. Experiments have, however, been conducted for local structural details and penetrations by both SNL in the NRC research and CTL in the EPRI research. Results of the analytical and experimental studies are summarized below.

Studies of temperature effects in the EPRI research included a test of a prestressed containment specimen (specimen 2.6 in the CTL test series 10), a reinforced containment specimen (specimen 2.7), and analyses of these specimens. Typical prestressed and reinforced geometries have also been investigated by analysis for combined pressure and global temperature up to 204°C (400°F), plus the addition of a local temperature spike simulating a local hydrogen burn.

The specimen tests and analyses were aimed at inducing thermal buckling in the liner. The results of that work showed that temperatures in the ranges predicted to occur (by NUREG-1150, for example, 177° to 204°C (350° to 400°F)) have only a small effect on the ultimate pressure capacity of both reinforced and prestressed containment structures because the cracked concrete carries no tension regardless of temperature. Also, temperatures in this range have only a minor effect on typical rebar properties.

The increase in temperature changes the liner stress-strain behavior in the low pressure range, but the end results near failure are essentially the same as in the pressure only cases. The addition of local temperature spikes to the temperature history cause small local liner-concrete separation (a precursor to liner buckling) in prestressed containments. However, this is not so in reinforced containments. The tendency for liner buckling in prestressed containments is viable only for temperatures about 204°C (400°F) and pressures at or below design pressures; this may not be a plausible combination, thus effectively eliminating liner buckling as a realistic concern.

The liner buckling findings were suggested by the experiments mentioned above. In both prestressed and reinforced containments subjected to elevated temperature, the liner experiences compressive yield at low pressures, but eventually develop tension at higher pressures regardless of added temperature. Similar conclusions have been reached by other researchers, such as Wesley et al., at NTS/Structural Mechanics Associates. It was concluded for reinforced concrete containments that temperature effects are primarily limited to steel material properties.

If temperatures were developed in the range of 370° to 427°C (700° to 800°F) and existed long enough to heat up the embedded rebar or tendons, ultimate pressure capacities would be dramatically reduced because of degradation of the modulus and yield strength of the steel elements. With regard to liner tearing and leakage, the effect of temperature can delay tearing until slightly higher pressures, but at temperatures of 204°C (400°F) and below, it is generally believed that the effect is not enough to change the characteristic of leakage before catastrophic burst for gradual pressurization. Once liner yield is reached during pressurization, the global structure strain would need to be approximately 0.2% larger with a 204°C (400°F) temperature to cause the same global liner strain that would occur without temperature. The effect of temperature on leakage pressure predictions is easily handled by incorporating temperature distribution into a global containment analysis such as that recommended herein.

As described earlier, until recently, the NRC/SNL containment research program did not focus heavily on the application of temperature as a severe accident loading condition for the containment structures. (Testing of seals, gaskets, electrical penetration assemblies, personnel

airlocks and equipment hatch models were conducted at temperatures associated with severe accidents.) But as an off-shoot of the 1:4 Scale PCCV test work and post-test analysis, NRC/SNL participated in the International Standard Problem (ISP 48) on containment integrity and providing assistance to NEA/CNSI in distributing data and interpretations from the PCCV model test to participants in an analysis exercise [79]. The main focus of the workshop was to take first steps toward addressing fundamental questions about temperature effects on PCCVs that were not addressed in previous research programs, namely:

- a. With the addition of temperature, would the onset of leakage occur later in the pressure history and, possibly, closer to the burst pressure?
- b. How would including the effect(s) of accident temperatures change the prediction of failure location and failure mode?

Two thermal analysis cases (Figures 88 and 89) were selected as representative challenges to typical containments:

- Case (1) a Saturated Steam Condition, basically, adding a temperature to each pressure step from the original PCCV pressure analysis, and
- Case (2) an accident safety case, essentially a Station Blackout scenario, with a hydrogen burn at about 4-1/2 hours into the event.

The thermal-mechanical analysis was approached in two steps: 1) add temperature to the mechanical solution without consideration of material property degradation due to temperature, and 2) temperature and material property degradation. Analysis results were presented for these cases individually to gain better understanding of the behavior differences and the causes of failure, when temperature is introduced. The primary tool for the ISP Exercise was axisymmetric modeling, so while the temperature behavior discussions emphasize global behavior, the effects of temperature on local behavior were also examined.



ISP 48 Phase 3, Case 1, Loading

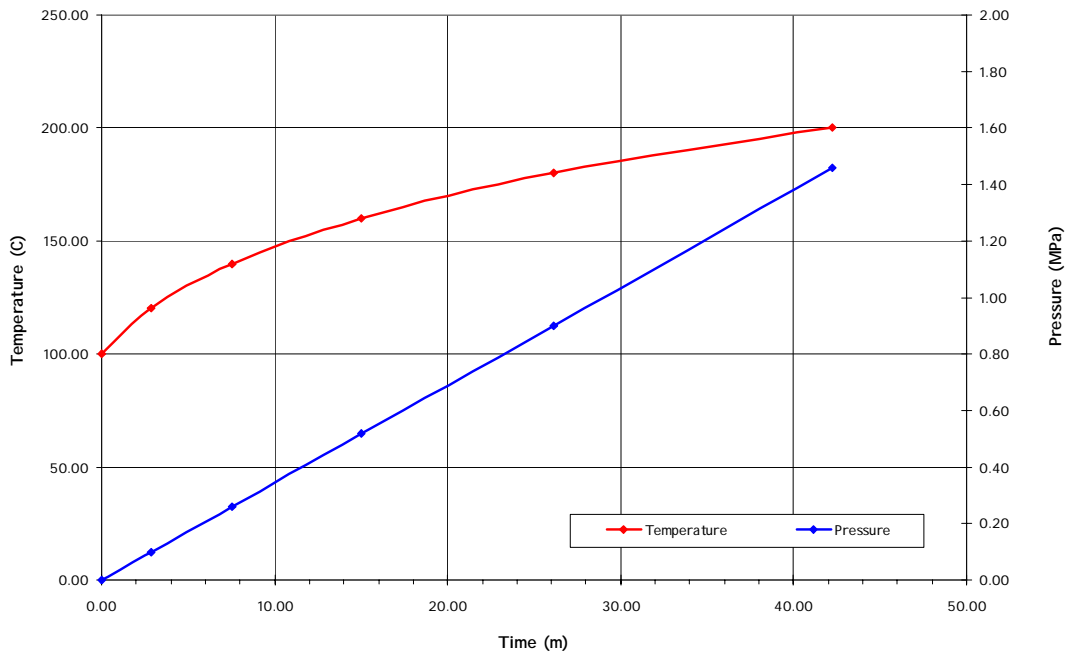


Figure 88 ISP 48 Phase 3, Case 1 Loading and Temperature

ISP 48 Phase 3, Case 2, Loading

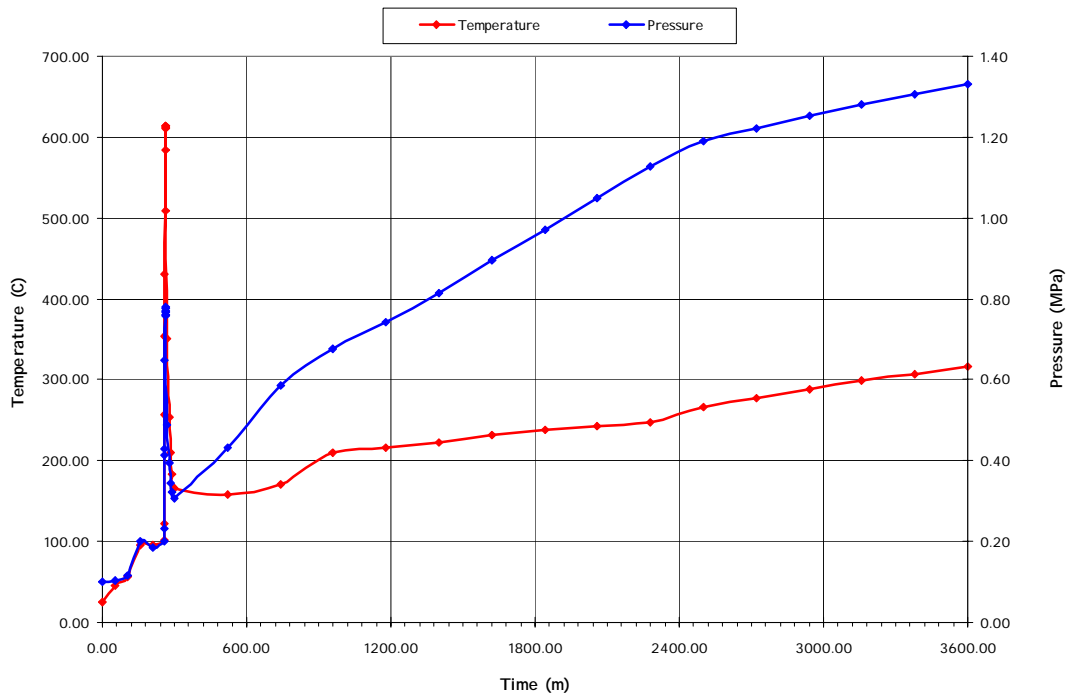


Figure 89 ISP 48 Phase 3, Case 2 Loading and Temperature

The following procedures and assumptions are recommended for thermal analysis of concrete containments.

1. Perform a Heat Transfer analysis. (In some programs like ABAQUS, this means all elements relevant for thermal analysis need to be changed to diffusive heat transfer element types which only have temperature degrees of freedom.)

Thermal boundary conditions are imposed at the outer surface of the cylinder and dome wall consisting of “free convection with air. The heat transfer coefficient,  $h$ , varies with temperature according to the following relationship:

$$h = 0.00382(\Delta T)^{1/3} \text{ lb}_f/\text{in-s-}^\circ\text{F} \quad (\text{T in } ^\circ\text{F}) \text{ for a full scale containment analysis,}$$

The boundary condition on the basemat foundation consists of heat conduction with soil with a sink temperature. An example of a heat transfer coefficient developed for the horizontal surface of the foundation in contact with soil is:

$$h = 5.76 \times 10^{-5} \text{ lb}_f/\text{in-s-}^\circ\text{F} \text{ for a full scale containment.}$$

For Temperature Case 2, a steady state heat transfer analysis step would precede a dynamic heat transfer analysis with the time history temperature input. The steady state heat transfer step is used to bring the model up to an ambient/operating temperature of 25°C. Figure 90 shows the location of the prescribed thermal boundary conditions for the axisymmetric model of the PCCV.

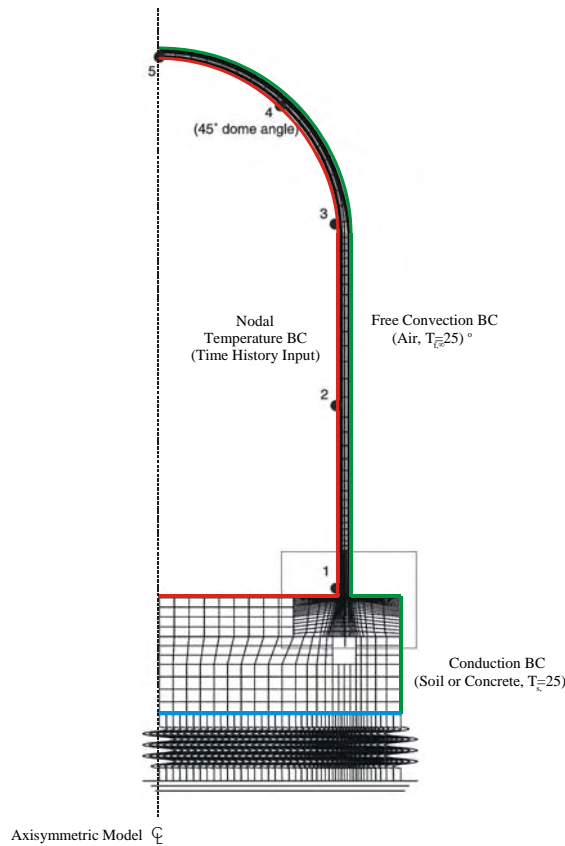


**Figure 90 Axisymmetric Model Thermal Boundary Conditions**

A literature review was conducted to develop reasonable concrete thermal properties, and for degradation of concrete and steel material properties. References [116] through [123] proved useful in support of this study. Though there are scores of publications on these subjects, the references cited are considered to be a reasonably representative sample of the general literature. A summary of conclusions that were found relevant to concrete containments is as follows.

#### Density

Use the average density of the concrete. For the PCCV at the time of construction was reported as 2186 kgf/m<sup>3</sup> for the nominal 300 kgf/cm<sup>3</sup> (used in the basemat) and 2176 kgf/m<sup>3</sup> for the nominal 450 kgf/cm<sup>3</sup> (used in the tendon gallery, wall and dome). Using a nominal 2% by volume of reinforcing steel and other embedments, a nominal value of 2290 kgf/m<sup>3</sup> was used for the PCCV thermal analysis.

#### Specific Heat

Specific Heat of ordinary concrete at normal temperatures can vary from: 0.50 to 1.13  $kJ\ kg^{-1}K^{-1}$ . A value of 0.879  $kJ\ kg^{-1}K^{-1}$  was used in the analysis of the PCCV model.

Generally it is assumed that changes in aggregate, mix, and age do not have a significant effect on this, but moisture content does have a significant effect. Reducing moisture content from 25 to 12.5% by volume can reduce overall specific heat by 25%; the authors have assumed moisture content in the containment wall will be relatively low. At high temperatures, specific heat can go up considerably, approximately doubling from 150°C to 500°C; however, the authors assumed a constant value of specific heat since the very high temperature is of relatively short duration.

#### Thermal Conductivity

Assuming igneous amorphous aggregate leads to the following:

Thermal conductivity = 1.0 – 1.6  $Wm^{-1}C^{-1}$  (1.4  $Wm^{-1}C^{-1}$  was used in the analysis.)

This is not significantly variable with temperature, but tends to decrease by ~10% to 30% between 20°C and 200°C.

#### Thermal Spalling of Concrete

Thermally induced spalling may occur in either quiescent or violent fashion, and the probability increases at higher heating rates. A primary cause of this is moisture content; the greater the moisture the greater the spalling potential. High steel reinforcement ratios can also increase spalling potential.

#### Strength

Significant reductions in strength occur when  $T > 300^\circ C$ , and at 690°C, strength can be assumed to reduce by about 80%. On reaching this conclusion, it is noted there is a lot of scatter in experimental results, owing to different test conditions and to the composition of various concretes and aggregates. But for conventional aggregates, the following observations have been made:

- between 80 and 90°C reductions range from 10 to 35%

- between 90 and 200°C, compressive strength ranges from continuing decrease to even slight increase.
- from 200°C and higher, there is continuous decrease.
- rich mixes show greater reduction in strength
- different water-cement ratios have little effect
- there is also a significant time of exposure factor
- there is some specimen shape and size effect. Small specimens lose more strength than large ones.
- Poisson's ratio also drops from about 0.2 to 0.1 at 400°C
- tensile strength decreases showed similar trends as the compressive strength decreases
- modulus of elasticity reductions also showed similar trends as strength losses, but overall reductions are less. Tends to follow the square-root relationship commonly used.

The choice of generic properties to use for analysis has been based on an approximate "median" of literature data; a smooth curve for strength degradation versus temperature was estimated below and plotted in Figure 91.

Concrete Strength Ratio,  $S_{Rc} = \exp^{- (T / 632)^{1.8}}$  where T is in degrees C.

Further, in lieu of more precise data, it appears reasonable to continue to base the modulus on the standard ACI formula:  $E = 57,000\sqrt{fc'}$  (English Units) such that a Modulus Reduction Ratio can be defined as:

$$M_R = (S_{Rc})^{\frac{1}{2}}$$

It should be noted that the peak strain at which the concrete compressive strength limit is reached also shifts with increasing temperature. While at 25C, this strain is approximately 0.002, it can reach two to three times this value at high temperatures.

Temperature variation of steel is also important for the highest temperatures. This variation has been idealized based on curves provided in the literature:

Steel Yield Strength Ratio,  $S_{Rs} = \exp^{- ((T - 340) / 300)^{1.9}}$  where T is in degrees C.

$$S_{Rs} = 1.0, T \leq 340C$$

For steel, the Young's Modulus follows the yield strength one-to-one, rather than the square-root relationship found in concrete. The steel yield strength reduction is shown in Figure 92.

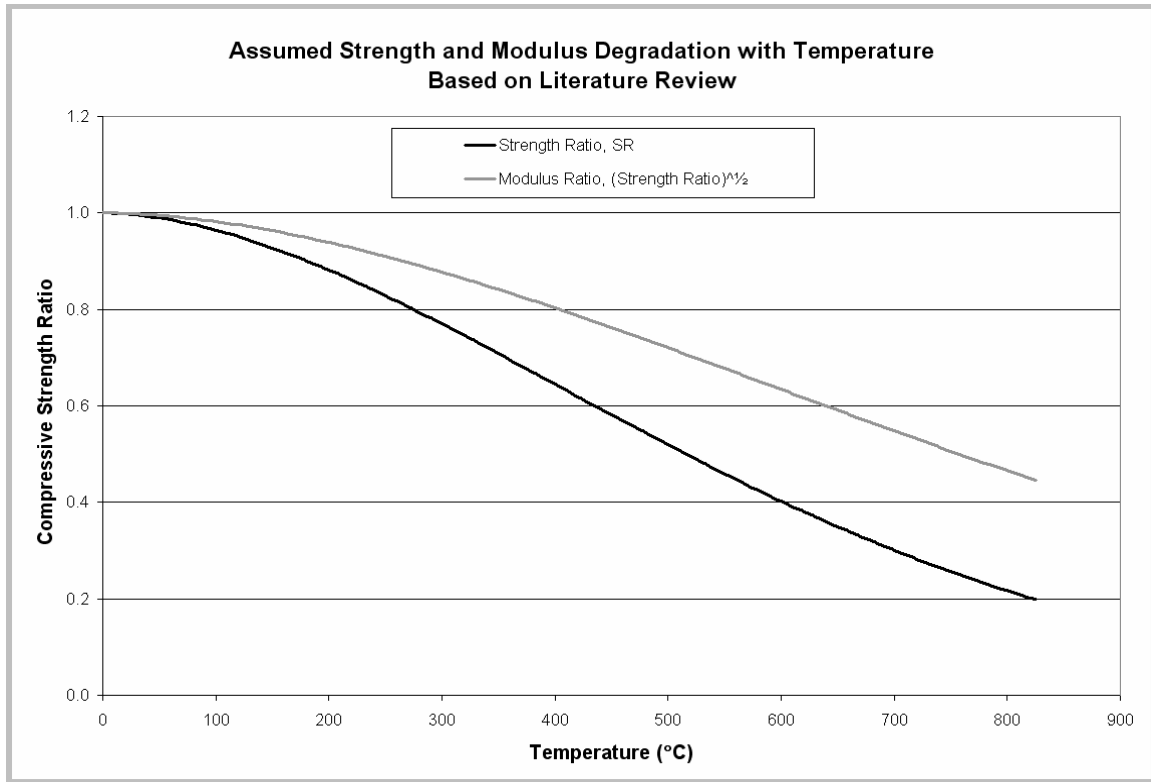


**Figure 91 Concrete Compression Strength Ratio vs. Temperature**

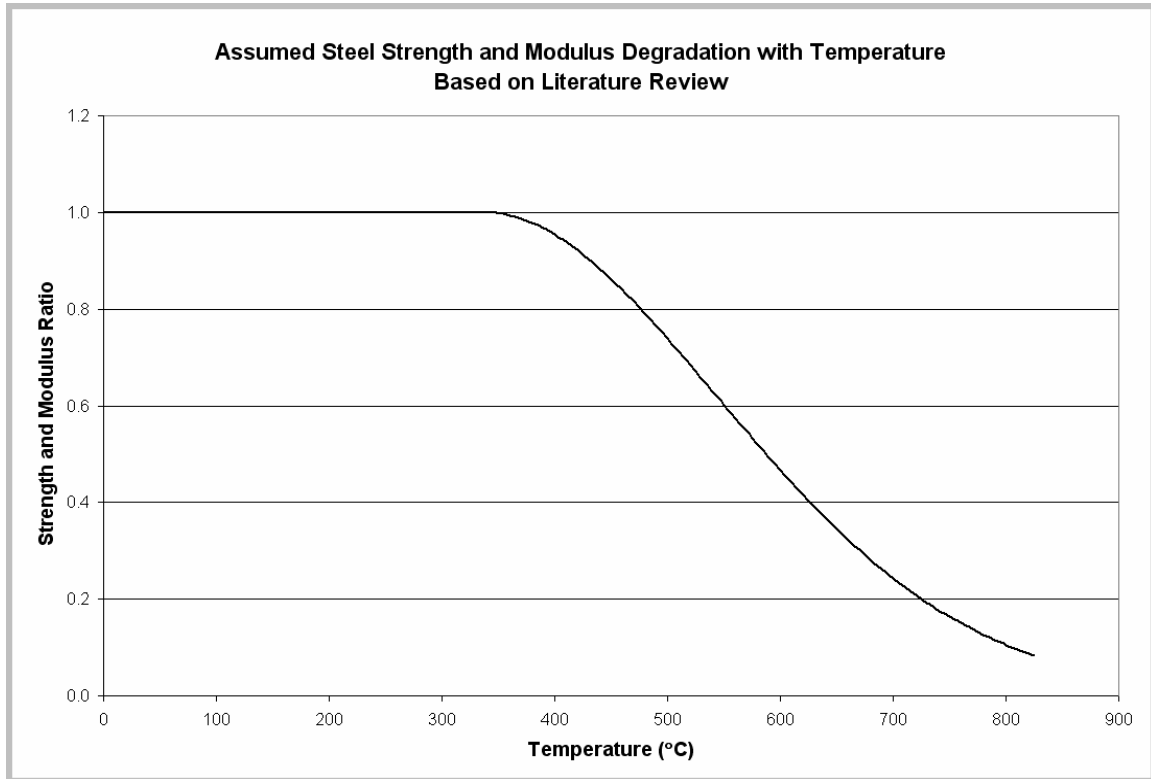


**Figure 92 Steel Yield Strength and Modulus Ratio vs. Temperature**

## 4.5 Recommendations for Prototype Containment Capacity Estimates

### 4.5.1 Current Practice

Standard Review Plan Sections 3.8.1.II.4.j provides general guidance for determining ultimate capacity of concrete containment. It requires that a licensee submit a report to the NRC providing details of the analysis, failure design criteria, and behavior of the liner under postulated conditions. ASME Section III, Division 2 does not provide any guidance for determining ultimate capacity of containment. IPEs of different plants use differing criteria for determining the ultimate capacity and probability. Neither the SRP nor ASME Code provide specific guidelines for determining containment ultimate capacity.

For concrete containments, a few of the plants' IPEs followed a methodology developed by EPRI and ANATECH in the late 1980s, early 1990s, which provided a framework not only for making deterministic failure prediction analysis, but also extended these results to a PRA framework, compatible with NUREG-1150. These procedures, covered in detail in [98], are summarized here in an attempt to identify 'what we do know and don't know' about containment failure/leakage prediction.

A deterministic leakage prediction criterion was postulated based on the fundamental assumption for concrete containments that quasi-static pressurization would lead to a leakage rate that is in equilibrium with the gradual pressurization rate. But this criterion does not provide information on the effect of rapid pressurization on failure sequences and the evolution of failure modes, or the conditional probability of the catastrophic burst (ultimate) failure mode. All of these scenarios were presented in NUREG 1150 along with NRC's direction to plant owners that they needed to be considered in the IPEs.

An EPRI deterministic leakage prediction methodology provides guidelines for global axisymmetric analysis, and local strain concentration factors near stiffness discontinuities such as thickened liners, penetrations, and liner anchorages. It was developed using detailed local analyses and the body of experimental research described in Chapter 2. Along with predicting where liner tears would occur, a formula was adopted for quantifying liner tear size (leak area) [56, 57] as shown in Figure 48. So these guidelines estimate where liner rupture can occur and at what pressure levels. This implies that rapid pressurization could trigger more than one failure location with the possibility of exceeding (at elevated pressures) the definition of leakage, defined to be a leakage path with a depressurization time of two hours or greater (NUREG 1150). (For depressurization within two hours, the containment is defined to experience either rupture or burst failure.) Within the context of NUREG 1150 for severe accident risk evaluation, a containment failure criterion is meaningful only in a probabilistic sense.

Extending the methodology to PRA, the process of predicting failure locations was separated into two parts: 1) identifying and quantifying the probabilities associated with locations with large peak strains, and 2) determining relative probabilities between leak size categories defined by assigning specific leak areas to individual liner tears.

The EPRI Probabilistic Leakage Prediction Methodology (PLPM) developed assigned randomness and uncertainty ranges to the ability to predict global liner strain, strain concentration factors, and liner strain failure criteria. Applying these, and assuming lognormal distribution of the parameters, determined the probability of failure at given locations. Then these probabilities from all locations were combined and this determines the probability of a total leak area exceeding a particular size as defined in NUREG 1150. Three leak area cutoffs are designated: a slow leak characterized by a flow area less than 0.1 ft<sup>2</sup> (subsequently revised to 0.3 to 0.5 ft<sup>2</sup>), a

moderate rupture of flow area greater than 1 ft<sup>2</sup>, and a catastrophic rupture characterized by a flow area of 10 ft<sup>2</sup>. The probabilities of liner tears at possible locations are combined to determine the total size of flow areas, within a probabilistic framework. For example, an equipment hatch may have four possible tear initiation points (at locations symmetric around the penetration). If the area of a single tear is 0.09 ft<sup>2</sup>, then one tear would create a flow area defined as a *leak*. However, if several of these tears and tears at other penetrations (or ‘hot spots’) occurred, the flow area would reach more than 1 ft<sup>2</sup>, which is a *rupture*. Clearly, the probability that at least one tear will occur is higher than that of many tears occurring, and algorithms for calculating probabilities of multiple tears were developed based on standard probability theory.

In the EPRI work, the liner tearing and leakage prediction methods were demonstrated by application to two large dry concrete containments, chosen to be typical of a prestressed and a reinforced concrete US containment. (These examples are shown in Figure 44 earlier in this report.) These predictions and the log normally distributed variations on these predictions are then combined and ‘binned’ as conditional probabilities that a leakage, rupture, or catastrophic rupture occurs, given that a leak of any size has already occurred. At low pressures, small leakage is the dominant mode and so has a conditional probability of nearly 1.0. At high pressures, only reachable by rapid pressurization which may leapfrog the leakage mode, rupture conditional probability eventually surpasses leakage. This should not be confused with probability of failure; this is entirely separate as shown in Figure 93. This is simply the probability of the first liner tearing occurring. One way of visualizing the relationship between failure probability and the conditional leakage/rupture calculation is by plotting, as shown in Figure 94. The plot represents the probability of a leakage, rupture, or catastrophic rupture mode, given non-occurrence of the other modes. In the physical sense, the non-occurrence of modes other than small ‘leakage’ are attributed to rapid pressurization.

To apply NUREG 1150, some simplifying assumptions are made: 1) any pressurization scenario must be categorized as either gradual or rapid pressurization. More research would be required to characterize these, but for simplicity in the IPEs, it was postulated that general pressurization after vessel breach is slow, but steam explosion or hydrogen detonations are rapid; 2) for slow pressurizations, all event tree sequences end in leakage – for all other pressurizations, the conditional probabilities of leak, rupture, or catastrophic rupture are used.

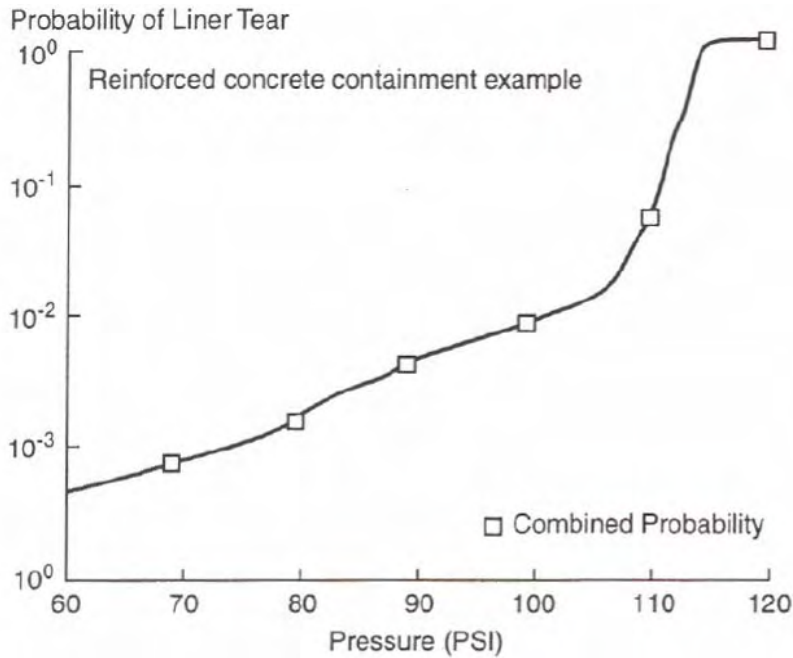


**Figure 93 Combined Probability of Liner Tear by PLPM Software for the Reinforced Concrete Containment Example**

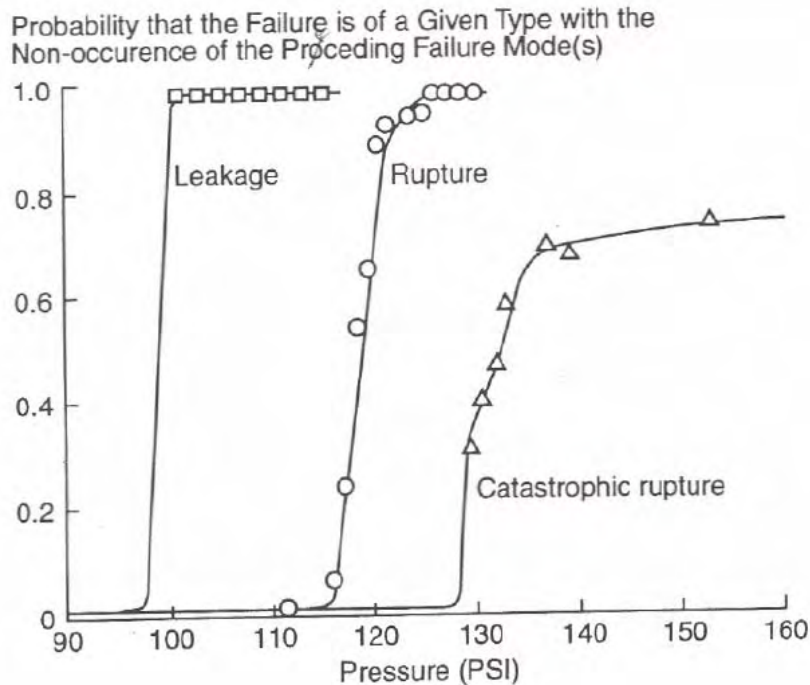


**Figure 94 Probability of either Leakage, Rupture, or Catastrophic Rupture Occurring given that failure has occurred for Reinforced Concrete Containment**

In reviewing this methodology now 15 years after it was developed, it is clear that some liberal doses of engineering judgment were required to develop the PRA assessments using the limited data available, and the work heavily relies on the concept of equilibrium leakage, which may not



yet have consensus within the industry. Nevertheless, the methodology does provide a framework for PRA for containments that allows implementation of sophisticated, deterministic containment response analysis, and so in the author's opinion is an advancement over containment failure prediction based solely on expert elicitation and hand calculation. What is needed to increase the reliability of the method is significantly more data quantifying the development and growth of liner-tear/leak-areas after initial liner tear occurs, and how the size of these tears relate to total leakage in the containment. A peer review of the procedure and an expert elicitation of the lognormal distribution parameters would also seem appropriate. Neither the SRP nor the ASME Code provide specific guidelines for determining containment ultimate capacity.

#### ***4.5.2 Recommendations for Design and Performance***

With the inception of the idea of equilibrium leakage, especially for concrete containments, most groups have focused on the prediction of the onset of liner tearing as the "failure performance" criteria for containments. They have accomplished this by improving and refining advanced structural analysis techniques, and computing very localized liner strains with greater and greater precision. However, to our knowledge, these studies have not included fracture mechanics refinements to estimate crack size and trajectory. These exclusions are due to the complexity of the liner-concrete-anchorage interaction.

As described in an earlier discussion, the fundamental gap in knowledge for estimating release risks during loss of coolant accidents is in estimating leak areas and leakage rates. In order to interface with regulatory requirements, leak areas and leakage rates must eventually be addressed. Some preliminary work has been conducted in this area by different groups. But the subject of estimating leak rates through liner tears and cracked concrete is particularly complex.

Nevertheless, based on existing work in this area, some fundamental conclusions can be drawn regarding leakage through cracks in concrete containments. In most cases, if liner tearing occurs in a region experiencing far-field rebar yield, leakage rates can be assumed to be governed by the liner tear aperture itself. This will not be greatly affected by any obstruction to the leak path posed by the concrete. Such a conclusion is supported by experiments performed. At the University of Alberta, EPRI leak rate experiments, and leak rate measurements taken from the SNL 1:6-scale model.

To illustrate this further, for a concrete containment undergoing global hoop strain of 0.5% at the barrel mid-height (still well within its ultimate barrel capacity) and using a concrete cracking strain of  $100 \times 10^{-6}$ , the sum of all the primary crack widths around the circumference of the barrel of 45.7 m (150-ft) diameter containment is 71cm (28 in). At 1.3% strain, as was the case when the 1:6-scale containment liner tears occurred, the sum of concrete crack widths in a full-scale containment is 1.8 m (72 in). Once the liner tears at far field strains of this magnitude, it is clear that the leak paths through the concrete will be quite large and the obstruction to flow through the concrete will be negligible in comparison to the throttling of flow through a small liner aperture. With the EPRI approach described earlier, approximate leak area and leak rate prediction rules have been established based on the Canadian tests, an EPRI test, and the 1:6-scale containment measurements.

Areas where further work is needed to link the Containment Capacity research to design practice include:

- Liner welding rules and anchorage details and their role in containment performance

- Containment performance in terms of leak rate in a format useful for PRA work that can be used for IPE and system analysis.

#### **4.5.3 Recommendations for Containment Capacity Analysis**

Detailed guidelines for developing finite element models of steel and concrete containments are provided in the Appendix, but a general discussion of recommendations for containment capacity analysis is provided here.

The analyst should be focused on making a best estimate prediction. Consistent with the supposition that leakage is not likely prior to the onset of general yielding, some methods can be eliminated as candidates for predicting containment performance. For instance, a failure criterion often used in the past is based on rupture occurring at general yield of 1% strain. Simple axisymmetric models, either finite element or closed form formulations, could be used in conjunction with such a failure criteria. But such simplifications may tend to underestimate the rupture pressure and provide conservative predictions of maximum pressure capacity.

##### **4.5.3.1 Steel Containments**

In order to evaluate shell rupture, at least two structural models, one including an equipment hatch or a personnel airlock and one modeling the general shell behavior is necessary. It has been learned that it is important to include details of any local breakdown in the membrane action of the shell or stiffeners. In the 1:8 scale steel model, for example, the strength of the stiffeners was reduced by an eccentricity in the stiffener pattern around the equipment hatches, which caused primary bending in the stiffener. As a result, when the stiffener failed, the load was transferred into the shell, and the shell failed at a lower pressure than expected. When the analytical program is considered, the analyst needs to identify eccentricities and other small details that affect the capacity and the failure mechanism of in-service steel containments.

Ensuring that the model has been properly discretized depends largely on the analyst's ability to anticipate the type of behavior (i.e., membrane action, bending, shear, etc.) that will occur in any given location. In this respect, a thorough understanding of the differences in element formulations is needed. For example, bending occurs at discontinuities such as intersections between penetrations and pipes and the containment shell. It occurs where there are changes in the shell geometry and thickness.

The analyst must exercise considerable engineering judgment in constructing the model and discretizing a finite element mesh. The element choices must be assessed by verifying that the solutions do not violate fundamental mechanics (for example, force equilibrium), and perhaps even with sensitivity studies with element size and order as the parameters.

Predictions for leakage from pressure seating equipment hatches can be based in part on the same three-dimensional model of the shell and equipment hatch used in the analysis for rupture. In order to accurately predict ovalization of the sleeve, the stiffener pattern around an equipment hatch must be modeled explicitly.

##### **4.5.3.2 Concrete Containments**

Calculations show that substantial hoop cracking can occur in a reinforced concrete containment between 70% and 90% of the design pressure, depending on the percentage of steel. Therefore, a reinforced containment, unlike a prestressed containment, will experience extensive cracking before the design pressure is reached. When a reinforced containment cracks, the main

reinforcement is stressed only to approximately 30% of its yield, whereas tendon reinforcement in a prestressed containment is at 80% or 90% of yield when the concrete cracks.

This, combined with the fact that conventional rebar has greater ductility than prestressing tendons, gives reinforced containments an after-cracking pressure capability range that is significantly larger than in prestressed containments. This implies that leakage before catastrophic rupture is more likely to occur in a reinforced containment than in a prestressed containment.

On the other hand, some typical details of prestressed containment designs include stronger liner anchorages and more severe stiffness discontinuities than in reinforced containment designs, as evidenced by the EPRI-sponsored Construction Technology Laboratories (CTL) specimen test series. Therefore, with the site specific nature of containment designs, it is not possible to generalize what pressures cause leakage in prestressed containments as compared to reinforced containments. The relative behavior of the two containment types can be summarized by Figures 95 and 96 that show the stress-strain behavior of the primary load carrying elements for reinforced and prestressed concrete containments, respectively.

The liner and rebar behavior is basically the same in both cases except that, in the prestressed case, the liner and rebar stresses remain compressive until approximately 1.4 times the design pressure (shown as 1.4 DP on Figure 96). The significance of the figures lie in the relative positions of the liner yield range versus the yield range of the primary load carrying components and the ultimate strain capacity of the materials. The S-shaped curves shown represent the general shape and relative location of the expected probability of leakage and probability of catastrophic rupture curves.

After liner yielding, the probability of leakage becomes significant due to liner strain concentrations. It should be noted that it is not until much larger global strain (and pressure) that the probability of catastrophic rupture becomes significant. And in conjunction with this, if the failure pressure is approached from below in quasi-static fashion, the range of pressure needed for catastrophic rupture might never be reached.

There are two major issues involved in developing the finite element models for concrete containments: determining what geometric detail of a containment need to be represented and establishing proper mesh discretization. Here again, the models need to be consistent with the failure criteria and the analytical methods that are adopted.

In a global analysis (such as a global axisymmetric or 3D analysis) it is not necessary, nor is it recommended, to predict liner strain concentrations across cracks or at liner embedment discontinuities. These strain concentrations are predicted with special local techniques rather than in a global model. In the main wall and dome regions, use of 8-node elements with quadratic displacements along element sides allows relatively large element spacing. For cracking analyses, higher order elements with lower order integration (i.e., 8-node quadrilaterals with 2x2 integration) are preferred because of their superior numerical behavior under cracking conditions. Finer element integration typically leads to poorer convergence characteristics because of the significant increase in unique cracking states that can occur in any given element.

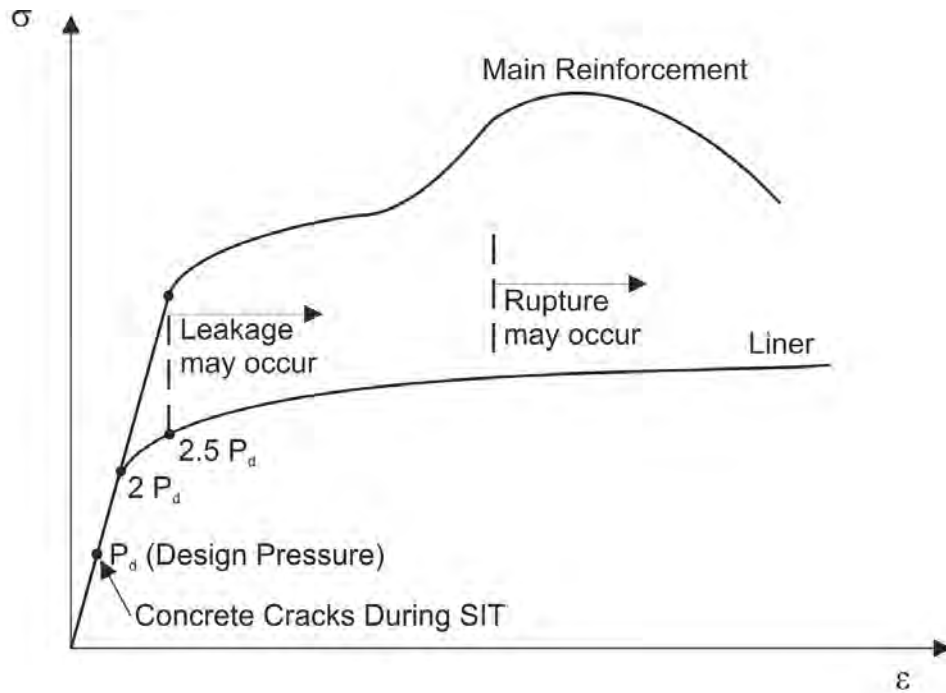


**Figure 95** Idealization of Reinforced Concrete Containment Behavior

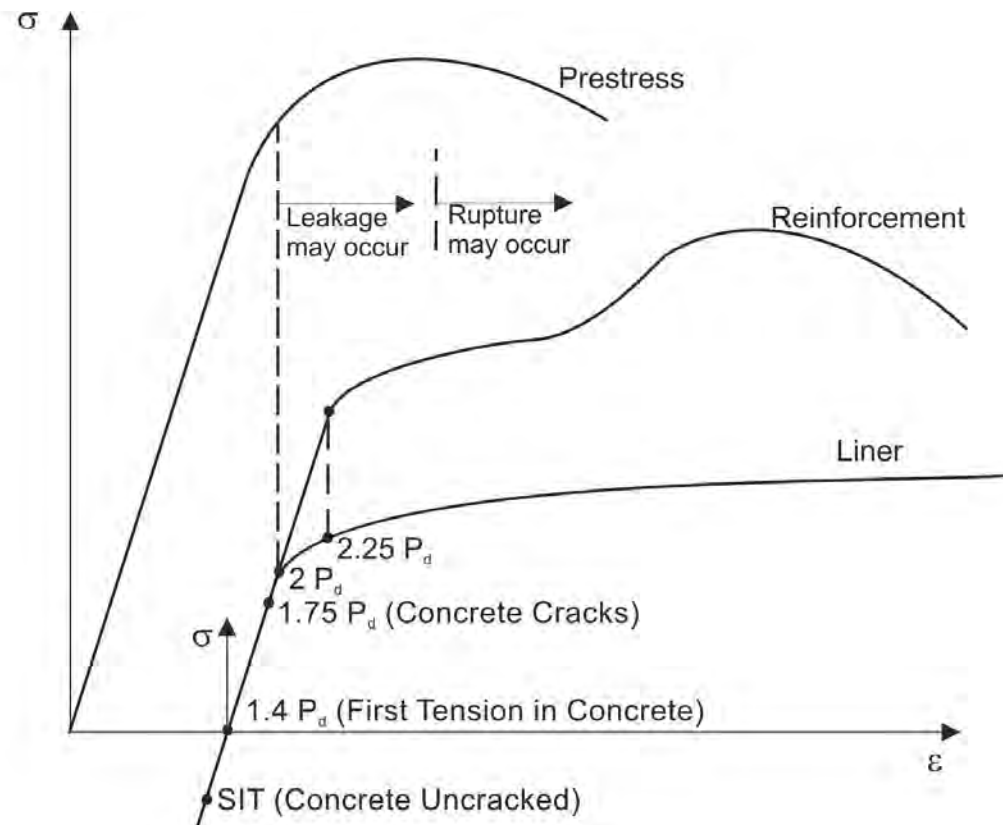


**Figure 96** Idealization of Prestressed Concrete Containment Behavior

The modeling of rebars in a finite element code varies widely from code to code. Displacement compatibilities between the rebars and the concrete require that the rebars be represented by the same displacement shape functions as the continuum element in which they reside. This is not generally observed in all computer codes. Another difficulty is the translation of rebar drawings to computer code input. For 2D axisymmetric grids, rebar modeling is relatively straightforward. However, for 3D continuum analysis, the rebar arrangements are very complex. As such, it is virtually impossible to develop computer input without preprocessing software.

The present state of the art of modeling and analysis of concrete structures consists of finite element computer codes in which: (a) plain concrete and steel reinforcement are modeled as two materials joined together as structural elements; (b) plain concrete material models account for compressive plasticity and tensile cracking (smeared over the element) with post-cracking tension stiffening and shear retention capabilities; or (c) reinforcement is treated as simple tension-compression members fully bonded to the concrete.

Accurate predictions of the threshold environment for leakage or failure of a concrete containment requires accurate calculation of post-yield response. Nonlinear 3D calculations for the structural response are also necessary for local stiffness discontinuities and penetrations if liner tearing and leakage is to be accurately predicted. Methods for performing such analyses will almost certainly require the use of sub-models of local regions rather than 3D analysis of entire containments. Local sub-models can be driven by boundary conditions generated from coarse global analyses. These boundary conditions need to include the effects of the interaction of the penetration, or discontinuity with the free field structure. For example, penetration regions have been observed to move less radially outward than the free field, causing out-of-plane relative motion between the penetration and the free field.

Other more detailed guidelines may be found in the Appendix.

#### **4.6 Conclusions from Containment Model Tests**

Some general conclusions on predicting containment behavior can be made from the series of containment vessel model tests that were described in Chapter 2:

- Although establishing a generic margin of safety was not the purpose of the SNL program, the steel models have pressure capacities on the order of 4-6 times the design pressure [46]. The reinforced concrete models have pressure capacities significantly larger than the design pressure. The margin to failure, on the order of 2.5 to 3.5 times the design pressure, is lower than in the steel containments.
- Global, free-field strains on the order of 2-3% for steel and 1.5 to 2% for reinforced and 0.5 to 1.0% for prestressed concrete can be achieved before failure or rupture.
- Model (and presumably prototype) capacities are limited by high strains arising at local discontinuities which are present in both the model and the prototype.
- In the absence of a 'backup' structure, steel containment model capacities tend to be limited by gross structural failure or 'rupture'. (The 1:10-scale NUPEC steel model developed a tear and leaked after the model had apparently made contact with the surrounding shell.) Due to the inherent structural redundancy of the liner and concrete system, steel lined concrete containments appear to be limited by functional failure (leakage). While the behavior that leads to tearing of the steel vessel or the steel liner is similar, i.e. local exceedence of the ductility limits of the steel at geometric

discontinuities, the subsequent response of the vessels differs due to the presence of the surrounding structure. It should be noted, however, that many tests conducted on concrete pressure vessels have, typically, used hydrostatic pressurization. (Often this decision is made because of the likelihood of a liner tearing/leakage failure mode when using a steel liner). Hydrostatic testing significantly decreases the probability of a catastrophic rupture of the pressure vessel because sudden local expansions of a portion of the vessel results in a rapid drop in driving pressure.

- It seems reasonable to assume that with the added complexity of the actual containments, there is a higher probability that these local strain risers are present in, and possibly more severe than in any of the models tested. As a result, the capacities of the model, can, at best, be interpreted as an upper bound on capacity of prototypical containments.
- Analytical methods currently used are adequate to predict global response into the inelastic regime. One caveat on this statement is the discrepancy between predictions and observations of global yielding. Further investigation is required to understand the nature of this discrepancy (e.g. residual stresses, etc.) and its significance for calculation of prototypical containment capacities.
- Prediction of local failure mechanisms are highly dependent on the experience of the analyst, on the availability of accurate as-built information (geometry and material properties) at discontinuities, and on fabrication processes. Even if this information is available (not typical for actual containments) the prediction, a priori, of local failures is at best an uncertain proposition. The large scale model tests have, however, educated and sensitized the community to the types of details which may be critical in limiting containment capacities, and, hopefully, have improved the reliability of the predictions.
- These conclusions are predicated on failure of the containment structure. Any evaluation of the capacity of an actual containment must be based on the entire system, including mechanical and electrical penetrations and other potential leak paths.

## **4.7 Issues for Future Consideration**

### **4.7.1 Leakage**

A great deal has been learned about containment behavior and containment analysis methods in the last two decades of containment research, but questions still remain. One of the most important behavior questions is that it is not known with certainty whether a leakage failure will reach an equilibrium state or if it will lead to a catastrophic failure. The arguments for each follow below.

**Equilibrium Leakage:** For steel containments, testing has shown that equilibrium leakage will probably not occur unless the expanding vessel has a structural redundancy such as a "contact structure" as in the recent US NRC/Sandia SCV test. The equilibrium leakage concept for concrete containments first introduced in WASH-1400 [2] and related work has been covered in numerous reports over the last decade. With this in mind, a quasi-static pressurization failure scenario for concrete containments is as follows. As a concrete containment building (either reinforced or prestressed) begins to expand in response to quasi-static pressurization, liner strain concentrations occur at local stiffness discontinuities. The strain concentrations can be strong or weak depending on the type of discontinuity and the type of liner to concrete anchorage system. The strength of the discontinuity affects the level of global strain needed to tear the liner. These global

strains have been found (from testing and analysis) to range from 0.2% (just above yield) to about 2%. With regards to the weakest discontinuities, 2% global strain is still well within the ultimate capabilities of the concrete containment reinforcement; thus, a liner tear is deemed to be almost certain to occur. Once the strain concentration causes a tear to initiate, the tear will not grow beyond the size required to maintain equilibrium between pressure increase and leakage. This is because: (a) the structure's residual stiffness at initial rupture is sufficiently large to restrain the liner from rapid expansion, and (b) the liner tearing is a stable fracture process due to the highly redundant crack arrest mechanism offered by the concrete backing. This leads to the conclusion that liner crack growth beyond the equilibrium leak area requires further pressure rise.

**No Equilibrium Leakage:** The high pressure expulsion of molten material from the reactor vessel, the deflagration of combustible gases, and the rapid generation of steam through the interaction of molten fuel with water in the containment are phenomena that could lead to pressure rises in the containment over a period of a fraction of a second. While this pressure rise time is still effectively quasi-static, there is some concern that the rapid rise time would not allow large enough tears to develop. This would lead to a more severe failure of the liner. While the general consensus supports giving a high probability to the occurrence of leakage, for certain pressurization rates, more severe failure modes involving higher pressures may also be reached.

#### **4.7.2 Other Considerations**

Many aspects of containment integrity have still not been addressed in the various containment integrity research programs. Some of these topics are listed below:

- The behavior of the containment under elevated temperature and pressure loads has not been thoroughly investigated. Most of the containment tests have ignored the effects of temperature on the material properties and thermal induced stresses associated with elevated temperatures.
- The effect of aerosols within the containment atmosphere during an accident has not been investigated. Aerosols may plug holes in the containment that may lead to a higher pressure capability, but have the potential to change the mode of failure from a possible benign mode to a burst mode. This applies to unlined concrete containments and lined containments when the liner has failed.
- Seismic loadings coupled with severe accident loads have not been investigated in any detail.
- Liner-anchorage-concrete interaction is significant in determining how liners tear in concrete containments. These phenomena are still not fully understood.
  - Under what conditions will stud or other anchorage shear failure occur rather than liner tearing?
  - How is the failure mode of the liner-anchorage system affected by scaling? For example, it could be affected by the ratio of liner thickness to stud diameter and by membrane loading of the liner (before the development of high stud shear forces).
  - To what extent is the magnitude of liner strain concentrations affected by friction and bond between the concrete and liner? An example of this could be by

differential radial motion at a major concrete crack, or by stud or anchorage spacing.

- How is the magnitude of liner strain concentrations and the resulting tear length and trajectory affected by the size and shape of insert plates? What is the best way to extend the current analysis techniques to predict tear areas?

Investigation and validation of methods for evaluating other potential failure modes is still needed. Shear failure is particularly difficult to evaluate; there is no generally recognized, reliable method of determining shear capacity of a reinforced concrete section under simultaneous application of tensile load and bending moment. Failure of large rebars where they are bent around penetrations, as occurred in an EPRI test [47], are also of some concern. The effects of cold working on the available ductility to these bars should be studied further. Rates of pressurization and effects of temperature must be considered in more detail. At high rates of pressurization, there is a possibility that sequential failure modes could occur; that is, for very high rates of pressurization, liner tearing may not arrest the pressure buildup within the containment, and another failure mode could occur at slightly higher pressure. This is the basic reason for emphasizing the development and validation of analysis methods. A reliable evaluation of containment performance must be based on careful, detailed analysis of the specific containment geometry and loading of interest.



**This page intentionally blank**

## 5 REFERENCES

1. Haskin, F.E., A. L. Camp, S. A. Hodge and D. A. Powers, "Perspectives on Reactor Safety", NUREG/CR-6042, Rev. 2, SAND93-0971, Sandia National Laboratories, Albuquerque, NM, March, 2002.
2. U.S. Atomic Energy Commission, "Summary Report of Reactor Safeguards Committee," WASH-3, 1950.
3. "The Safety of Nuclear Power Reactors (Light Water-Cooled) and Related Facilities," Final Draft, WASH-1250, US Atomic Energy Commission, July, 1973.
4. "Reactor Safety Study, An Assessment of Accident Risks in US Commercial Nuclear Power Plants," Draft WASH-1400, US Atomic Energy Commission, 1974; Final, NUREG-75/014, 1975.
5. U. S. Code of Federal Regulations, "Individual Plant Examination for Severe Accident Vulnerabilities," Title 10, Part 50.54, (f) Generic Letter 88- 20, Nov 23, 1988.
6. U. S. Nuclear Regulatory Commission, "Individual Plant Examination: Submittal Guidance," NUREG-1335, August 1989.
7. "Severe Accident Risks: An Assessment of Five U.S. Nuclear Power Plants", NUREG-1150, U.S. Nuclear Regulatory Commission, Washington, DC, December 1990.
8. Blejwas, T. E., et. al., "Background Study and Preliminary Plans for a Program on the Safety Margins of containments," NUREG/CR-2549, SAND82-0324, Sandia National Laboratories, Albuquerque, NM, May 1982.
9. Spencer, B. W., and J. A. Smith, "Containment Query Utility, Version 1.3.1", Sandia National Laboratories, Albuquerque, NM, July, 2003
10. ASME Boiler and Pressure Vessel Code, Section III, Division I-Subsection NE, *Nuclear Power Plant Components-Class MC Components* and Section III, Division 2, *Code for Concrete Reactor Vessels and Containments*, The American Society of Mechanical Engineers, New York, NY.
11. Stevenson, J. D. ed., "Structural Analysis and Design of Nuclear Plant Facilities", Manual No. 58, American Society of Civil Engineers, New York, NY, 1980.
12. Klamerus, E. W., et. al., "Containment Performance of Prototypical Reactor Containments Subjected to Severe Accident Conditions", NUREG/CR-6433, SAND96-2445, Sandia National Laboratories, Albuquerque, NM, November, 1996.
13. Brown, T. D., et al, "Integrated Risk Assessment for the LaSalle Unit 2 Nuclear Power Plant: Phenomenology and Risk Uncertainty Evaluation Program (PRUEP)," NUREG/CR-5305, SAND90-2 765, Sandia National Laboratories, 1992.
14. "Evaluation of Severe Accident Risks: Quantification of Major Input Parameters, Experts Determination of Structural Response Issues", NUREG/CR-4551, Vol. 2, Part 3, SAND86-1309, Sandia National Laboratories, Albuquerque, NM, March, 1992.

15. Amin, M. P., P. K. Agrawal and T. J. Ahl, "An Analytical Study of the Seismic Threat to Containment Integrity", NUREG/CR-5098, SAND88-7018, Sandia National Laboratories, 1989.
16. Miller, J. D., "Analysis of Shell-Rupture Failure Due to Hypothetical Elevated-Temperature Pressurization of the Sequoyah Unit 1 Steel Containment Building," NUREG/CR-5405, SAND89-1650, Sandia National Laboratories, Albuquerque, NM, February 1990.
17. Manjoine, M. J., "Ductility Indices at Elevated Temperatures," *Transactions of the ASME Journal of Engineering Materials and Technology*, April 1975.
18. Cherry, J. L. and Smith, J. A., "Capacity of Steel and Concrete Containment Vessels with Corrosion Damage," NUREG/CR-6706, SAND2000-1735, Sandia National Laboratories, Albuquerque, NM, February, 2001.
19. Dameron, R. A., R. S. Dunham and Y. R. Rashid, "Methods for Ultimate Load Analysis of Concrete Containments, Phase 3: Developing Criteria and Guidelines for Predicting Concrete Containment Leakage", ANATECH report to EPRI, EPRI NP626OSD, February, 1989.
20. Horschel, D. S., and Clauss, D. B., "The Response of Steel Containment Models to Internal Pressurization," *Structural Engineering in Nuclear Facilities*, J. J. Ucciferro: Editor, Raleigh, North Carolina, September 1984, Vol. 1, pp. 534-553.
21. Horschel, D. S., and Blejwas, T. E., "An Analytical Investigation of the Response of Steel Containment Models to Internal Pressurization," *Proceedings of the 7th International Conference on Structural Mechanics in Reactor Technology*, Volume J, Chicago, August 1983, Paper J 6/4, pp. 297-304.
22. Reese, R. T., and Horschel, D. S., "Design and Fabrication of a 1:8-Scale Steel Containment Model," NUREG/CR-3647, SAND84-0048, Sandia National Laboratories, Albuquerque, NM, February 1985.
23. Clauss, D. B., "Pretest Predictions for the Response of a 1:8-Scale Steel LWR Containment Building Model to Static Overpressurization", NUREG/CR-4137, SAND85-0175, Sandia National Laboratories, June, 1985
24. Koenig, L. N., "Experimental Results for a 1:8-Scale Steel Model Nuclear Power Plant Containment Pressurized to Failure," NUREG/CR-4216, SAND85-0790, Sandia National Laboratories, Albuquerque, NM, December 1986.
25. Clauss, D. B., "Comparison of Analytical Predictions and Experimental Results for a 1:8-Scale Steel Containment Model Pressurized to Failure", NUREG/CR-4209, SAND85-0679 (Albuquerque: Sandia National Laboratories, July 1985).
26. Greimann, L., et. al., "An Evaluation of the Effects of Design Details on the Capacity of LWR Steel Containment Buildings", NUREG/CR-4870, SAND87-7066, Sandia National Laboratories, Albuquerque, NM, May 1987.

27. Goeller, B., Krieg, R., and Mesemer, G., "Failure at Reinforced Sections of Spherical Steel Containment Under Excessive Internal Pressure", *Proceedings of the 8th International Conference on Structural Mechanics in Reactor Technology*, Paper No. J 3/6, pp. 107-112, Brussels, Belgium, August, 1985.
28. Hirao, K., et. al., "Pressure Test of the Typical Vessels Flange under Pressure Loading", *Proceedings of the 11th International Conference on Structural Mechanics in Reactor Technology*, Tokyo, Japan, August 18-23, 1991, Paper No. JO2/4, pp. 25-30.
29. Arai, S., Matsumoto, T., etc., "Pressurization Test on the Equipment Hatch Model," *Proceedings of the 14th International Conference on Structural Mechanics in Reactor Technology*, Lyon, France, August 18-22, 1997.
30. Luk, V. K., M. F. Hessheimer, G. S. Rightley, L. D. Lambert and E. W. Klamerus, "Design, Instrumentation, and Testing of a Steel Containment Vessel Model", NUREG/CR-5679, SAND98-2701, Sandia National Laboratories, Albuquerque, NM, January 1999.
31. Porter, V. L., P. A. Carter and S. W. Key, Pretest Analysis of the Steel Containment Vessel Model, NUREG/CR-6516, SAND96-2877, Sandia National Laboratories, Albuquerque, NM, January, 1999.
32. Luk, V. K., and E. W. Klamerus, Round Robin Pretest Analysis of a Steel Containment Vessel Model and Contact Structure Assembly Subject to Static Internal Pressurization, NUREG/CR-6517, SAND96-2899, Sandia National Laboratories, Albuquerque, NM, August, 1998.
33. Van Den Avyle, J. A., and K. H. Eckelmeyer, "Posttest Metallurgical Evaluation Results for the Steel Containment Vessel (SCV) High Pressure Test", SAND98-2702, Sandia National Laboratories, Albuquerque, NM, August, 1999.
34. Luk, V. K., and E. W. Klamerus, "Round Robin Posttest Analysis of a Steel Containment Vessel Model", NUREG/CR-5678, SAND98-700, Sandia National Laboratories, Albuquerque, NM, January, 2000.
35. Ludwigsen, J. S., V. K. Luk, M. F. Hessheimer, and J. F. Costello, "Posttest Analyses of the Steel Containment Vessel Model", NUREG/CR-6649, SAND99-2954, Sandia National Laboratories, Albuquerque, NM, February 2000.
36. Not Used
37. Krieg, R., et al, "Spherical Steel Containments of Pressurized Water Reactors under Accident Conditions, Investigation Program and First Results, *Nuclear Engineering and Design*, 82, 77, 1984.
38. Goller, B., et al, "On the Failure of Spherical Steel Containments under Excessive Internal Pressure," *Nuclear Engineering and Design*, 100, 205, 1987.
39. Krieg, R., et al, "Limit Strains for Severe Accident Conditions, Description of an European Research Program and First Results, SMiRT 16, Washington 2001, paper P01/2.

40. Dolensky B., B. Goller, R. Krieg, "Assessment of Loading and Response of a Spherical PWR Steel Containment to a Postulated Hydrogen Detonation," Proceedings of the seminar on Containment of Nuclear Reactors held in conjunction with 16th International Conference on SMiRT, August 2001, Albuquerque.
41. Danisch, R, et. al., "Containment Mock-up Tests at Waldorf, Germany", Transactions of the 15<sup>th</sup> SMiRT Conference, Paper H06/4, Seoul, ROK, August, 1999.
42. Aoyagi, Y., et al, Behaviours of Reinforced Concrete Containment Models Under Thermal Gradient and Internal Pressure," Transactions of the 5th SMiRT, Paper 5415, Berlin, August 1979.
43. Uchida, T., et al, 'Behavior of Reinforced Concrete Containment Models Under the Combined Action of Internal Pressure and Lateral Force," Transactions of the 5<sup>th</sup> SMiRT, Paper 5414, Berlin, August 1979.
44. Horschel, D. S., "Design, Construction, and Instrumentation of a 1:6-Scale Reinforced Concrete Containment Building," NUREG/CR-5083, SAND88-0030, Sandia National Laboratories, Albuquerque NM, August 1988.
45. Clauss, D. B., "Round Robin Pretest Analyses of a 1:6-Scale Reinforced Concrete Containment Model Subject to Static Internal Overpressurization," NUREG/CR-4913, SAND87-0891, Sandia National Laboratories, Albuquerque, NM, April 1987.
46. Horschel, D. S., "Experimental Results from Pressure Testing a 1:6-Scale Nuclear Power Plant Containment," NUREG/CR-5121, SAND88-0906, Sandia National Laboratories, Albuquerque NM, January 1992.
47. Weatherby, J. R., "Posttest Analysis of a 1:6-Scale Reinforced concrete Reactor Containment Building," NUREG/CR-5476, SAND89-2603, Sandia National Laboratories, Albuquerque NM, February 1990.
48. Clauss, D. B., "Round Robin Analysis of the Behavior of a 1:6-Scale Reinforced Concrete Containment Model Pressurized to Failure: Posttest Evaluations", NUREG/CR-5341, SAND89-0349, Sandia National Laboratories, Albuquerque, NM, 1989.
49. von Rieseemann, W. A., and M. B. Parks, "Current state of knowledge on the behavior of steel liners in concrete containments subjected to overpressurization loads", Nuclear Engineering and Design, 157 (1995), pp. 481-487.
50. Walther, H. P., "Evaluation of Behavior and Radial Shear Strength of a Reinforced Concrete Containment Structure," NUREG/CR-5674, SAND91-7058, Sandia National Laboratories, Albuquerque, NM, January 1992.
51. Hanson, N., "Concrete Containment Tests, Phase 2: Structural Elements with Liner Plates-Final Report," EPRI NP-4867-M, Electric Power Research Institute, Palo Alto, 1987.
52. Dunham, R. S., Rashid, Y. R., Yuan, K. A. and Lu, Y. M., "Methods for Ultimate Load Analysis of Concrete Containments," EPRI NP-4046, Electric Power Research Institute, Palo Alto, 1985.

53. Weatherby, J. R. and Clauss, D. B., "Investigation of Liner Tearing Near Penetrations in a Reinforced Concrete Containment Under Severe Accident Loads," *Proceedings of the 10th International Conference on Structural Mechanics in Reactor Technology*, Anaheim, California, USA, August 14-18, 1989, Paper H025.
54. Lambert, L. D., "Posttest Destructive Examination of the Steel Liner in a 1:6-Scale Reactor Containment Model", NUREG/CR-5961, SAND92-1721, Sandia National Laboratories, February, 1993.
55. Spletzer, B. L., L. D. Lambert, V. L. Bergman and J. R. Weatherby, "Separate Effects Testing and Analyses to Investigate Liner Tearing of the 1:6-Scale Reinforced Concrete Containment Building, NUREG/CR-6184, SAND92-1720, Sandia National Laboratories, June, 1995.
56. Castro, J. C., R. A. Dameron, R. S. Dunham, Y. R. Rashid, "A Probabilistic Approach for Predicting Concrete Containment Leakage," ANATECH Final Report to EPRI, TR-102176 (Tier 1), March 1993.
57. Rizkalla, S.H, Lau, B.L., and S.H. Simmonds, "Air Leakage Characteristics in Reinforced Concrete," *Journal of Structural Engineering*, American Society of Civil Engineers, Vol. 110, No. 5., 1984.
58. The Institute of Civil Engineers, *Conference on Prestressed Concrete Pressure Vessels*," at Church House, Westminster, SWI, March 1967.
59. Appa Rao, T. V. S. R., Behaviour of Concrete Nuclear Containment Structures Up to Ultimate Failure With Special Reference to MAPP-1 Containment", *Inelastic Behaviour*, Report 4-SM-THEME75, Madros, India: Structural Engineering Research Centre, 1975.
60. Donten, K., M. Knauff, A. Sadowski, and W. Scibak: "Tests on a Model of Prestressed Reactor Containment," *Archiwum Inzynierii Ladowej*, vol. XXVI, no. 1/1980, pp. 231-245 (also *Proceedings of the 5th International Conference on Structural Mechanics in Reactor Technology*, Scibac, Berlin, Germany, August 13-17, 1979, Paper J 4/8).
61. MacGregor, J. G., S. H. Simmonds, and S. H. Rizkalla, "Test of a Prestressed Concrete Secondary Containment Structure," University of Alberta, Dept. of Civil Engineering Structural Engineering Report No. 85, 1980 (also *Proceedings of the 5th International Conference on Structural Mechanics in Reactor Technology* , Scibac, Berlin, Germany, August 13-17, 1979, Papers J3/2, J3/5 and J 4/2).
62. Atchison, I. J., G. J. K. Asmis, and F.R. Campbell, "Behaviour of Concrete Containment under Over-Pressure Conditions," *Transactions of the 5th SMiRT*, Paper No. 531 2, Berlin, August 1979.
63. Rizkalla, S., S. H. Simmonds, and J. G. MacGregor, 'A Test of a Model of a Thin-Walled Prestressed Concrete Secondary Containment Structure,' *Transactions of the 5th SMiRT*, Paper No. 5412, Berlin, August 1979.
64. Murray, D. W., L. Chitnuyanondh, and C. Wong, 'Modelling and Predicting Behavior of Prestressed Concrete Secondary Containment Structures Using BOSOR5.' *Transactions of the 5th SMiRT*, Paper 5315, Berlin, August 1979.

65. Smith, J. C. W., "Sizewell 'B' Power Station, A Brief Assessment of the Results of the 1/10th Scale Model Pressure Tests", PWR/89/117, Nuclear Design Associates, Knutsford, Cheshire, England, September 1989.
66. "Sizewell 'B' Scale Model Containment Pre-test Analysis", Ove Arup & Partners, London, England, April 1989.
67. "Sizewell 'B' Power Station, One-tenth Scale Containment Model, Comparison of Analyses with Test Results", Nuclear Design Associates, Knutsford, Cheshire, England, October 1990
68. Palfrey, J., "A Comparison of the Results of the 1/10th Scale Containment Model Test with Non-Linear Axisymmetric Analyses, Sizewell 'B' Power Station Reactor Building", PWR/89/124, SXB-IC-096523, Issue B, Vol. 1 & 2, Nuclear Design Associates, Knutsford, Cheshire, England, March 1990.
69. Smith, J. C. W., "Sizewell 'B' Power Station, Report on the Proceedings of the 1'10th Scale Containment Model Workshop", PWR/92/156, Nuclear Design Associates, Knutsford, Cheshire, England, June 1992.
70. Palfrey, J., "Sizewell 'B' Power Station, One-tenth Scale Containment Model, Examinations of Base Reinforcement and Tendon Ducts", PWR/94/195, Nuclear Design Associates, Knutsford, Cheshire, England, March 1994
71. Danisch, R., L'Huby, Y., "Containment Design of the European Pressurized Water Reactor (EPR)", *Advanced Reactor Safety (ARS '97)*, American Nuclear Society Annual Meeting, Orlando, Florida, June 1-5, 1997.
72. Hessheimer, M. F., Klamerus, E. W., Rightley, G. S., Lambert, L. D. and Dameron, R. A., "Overpressurization Test of a 1:4-Scale Prestressed Concrete Containment Vessel Model", NUREG/CR-6810, SAND2003-0840P, Sandia National Laboratories, Albuquerque NM, March, 2003.
73. Dameron, R. A., L. Zhang, Y. R. Rashid, and M. S. Vargas, "Pretest Analysis of a 1:4-Scale Prestressed Concrete Containment Vessel Model", NUREG/CR-6685, SAND2000-2093, ANATECH Corporation, San Diego, CA and Sandia National Laboratories, Albuquerque, NM, October, 2000.
74. Luk, V. K., "Pretest Round Robin Analysis of a Prestressed Concrete Containment Vessel Model", NUREG/CR-6678, SAND00-1535, Sandia National Laboratories, Albuquerque, NM, August, 2000.
75. Dameron, R. A., Hanson, B. E., Parker, D. R., and Rashid, Y. R., "Posttest Analysis of a 1:4 Scale Prestressed Concrete Containment Vessel Model", NUREG/CR-6809, SAND2003-0839P, ANA-01-0330, ANATECH Corporation, San Diego, CA and Sandia National Laboratories, Albuquerque, NM, March, 2003.
76. Hessheimer, M. F., and E. Mathet, "International Standard Problem No. 48, Containment Capacity, NEA/CSNI/R(2005)5, OECD Nuclear Energy Agency, Paris, FR, September, 2005.

77. ABAQUS Users Manual, Version 5.8, 1998. Providence, RI: Hibbitt, Karlsson & Sorensen, Inc.
78. ANACAP-U User's Manual, Version 2.5, September, 1997. San Diego, CA: ANATECH Corp.
79. Hessheimer, M. F. and E. Mathet, "International Standard Problem 48, Containment Capacity, Synthesis Report", Organization for Economic Co-operation and Development, Nuclear Energy Agency, Committee on the Safety of Nuclear Installations, NEA/CSNI/R(2005)5, Paris, September, 2005.
80. Dameron, R. and Y. R. Rashid, "Post-Test Report on Testing and Analysis of the Sizewell-B 1:10-Scale Containment Model", NUREG/CR-5825, SAND92-7064, ANATECH Research Corp., San Diego, CA, February 1991.
81. Dameron, R. A., Y. R. Rashid and M. B. Parks, "Comparison of Pre-Test Analyses with the Sizewell-B 1:10 Scale Prestressed Concrete Containment Test," SMiRT 11, Vol. H Paper H10 (August, 1991), Tokyo, Japan.
82. Parks, M. B. and Clauss, D. B., "Performance of containment penetrations under severe accident loading," *Nuclear Engineering and Design*, No. 134, 1992, pp. 177-197.
83. Brinson, D. A. and Graves, G. A., "Evaluation of seals for Mechanical Penetrations of Containment Buildings", NUREG/CR-5096, SAND88-7016, , Sandia National Laboratories, Albuquerque, August 1988.
84. Bridges, T. L., "Containment Penetration Elastomer Seal Leak Rate Tests," NUREG/CR-533, SAND87-7118, , Sandia National Laboratories, Albuquerque, July 1987.
85. Clauss, D. B., "Severe Accident Testing of Electrical Penetration Assemblies," NUREG/CR-5334, SAND89-0327, , Sandia National Laboratories, Albuquerque, November 1989.
86. Clauss, D. B., "An Evaluation of the Leakage Potential of a Personnel Air Lock Subject to Severe Accident Loads," *Proceedings of the 9th International Conference on Structural Mechanics in Reactor Technology*, Volume J. Lausanne, Switzerland, August 1987, pp. 147-152.
87. Julien, J. T. and Peters, S. W., "Leak and Structural Test of a Personnel Air Lock for LWR Containments Subjected to Pressure and Temperature Beyond Design Limits," NUREG/CR-5118, SAND88-7155, Sandia National Laboratories, Albuquerque, May 1989.
88. Parks, M. B., "Leakage behavior of inflatable seals subject to severe accident conditions," *Nuclear Engineering and Design*, No. 137, 1991, pp 175-186.
89. Parks, M. B., Walther, H. P. and Lambert, L. D., "Experiments to Determine the Leakage Behavior of Pressure-Unseating Equipment Hatches," *Proceedings of the 11th International Conference on Structural Mechanics in Reactor Technology*, Tokyo, Japan, August 18-23, 1991, Paper No. FO 3/4, pp. 49-54.



90. Kulak, R. F. et. al., "Structural Response of Large Penetrations and Closures for Containment Vessels Subjected to Loadings Beyond Design Basis," NUREG/CR-4064, SAND84-7177, ANL-84-41, , Sandia National Laboratories, Albuquerque, February 1985.
91. Bump, T. R., et. al., "Characterization of Nuclear Reactor Containment Penetrations-Preliminary Report," NUREG/CR-3855, SAND84-7139, Sandia National Laboratories, Albuquerque, NM, June 1984.
92. Shackelford, M. H., Bump, T. R., Seidensticker, R. W., "Characterization of Nuclear Reactor Containment Penetrations-Final Report," NUREG/CR-3855, SAND84-7180, Sandia National Laboratories, Albuquerque, NM, February 1985.
93. Lambert, L. D. and Parks, M. B., "Experimental Results from Containment Piping Bellows Subjected to Severe Accident Conditions, Volume 1: Results from Bellows Tested in 'Like-New' Conditions," NUREG/CR-6154, SAND94-1711, Sandia National Laboratories, Albuquerque, September 1994.
94. Lambert, L. D. and Parks, M. B., "Experimental Results from Containment Piping Bellows Subjected to Severe Accident Conditions, Volume 2: Results from Bellows Tested in Corroded Conditions," NUREG/CR-6154, SAND94-1711, Sandia National Laboratories, Albuquerque, October 1995.
95. Smith, J. A., "Capacity of Prestressed Concrete Containment Vessels with Prestressing Loss," SAND2001-1762, Sandia National Laboratories, Albuquerque, NM, September, 2001.
96. Ellingwood, B. R. and Cherry, J. L., "Fragility Modeling of Aging Containment Metallic Pressure Boundaries," NUREG/CR-6631, ORNL/SUB/99-SP638V, Oak Ridge National Laboratory, Oak Ridge, TN, August, 1999.
97. Not Used
98. US Nuclear Regulatory Commission, Regulatory Guide 1.174, "An Approach for Using Probabilistic Risk Assessment in Risk-Informed Decisions on Plant-Specific Changes to the Licensing Basis", Washington, DC, November, 2002.
99. Youichi, S., H. Kiyoshi, N. Susumu, S. Kunihiro, T. Kazuaki, E. Hiroaki, A. Hiroshi, "Seismic Proving Test of a Prestressed Concrete Containment Vessel (PCCV)," Proceedings of the Seminar on Containment of Nuclear Reactors held in conjunction with 16th SMiRT, August, 2001, Albuquerque.
100. James, R., Y. Rashid, J. Cherry, N. Chokshi, S. Tsurumaki, "Analytic Simulation of the Seismic Failure of a Reinforced Concrete Containment Vessel Model," SMiRT 16.
101. James, R. J., et al., "Seismic Analysis of a Prestressed Concrete Containment Vessel Model," NUREG/CR-6639, SAND99-1464, March 1999
102. Woodfin, F. L., "Full-Scale Turbine Missile Concrete Impact Experiments", EPRI NP-2745, Sandia National Laboratories, Albuquerque, NM, February, 1983

103. Yoshimura, H. R., and J. T. Schauman, "Full-Scale Turbine Missile Casing Tests", EPRI NP-2741, Sandia National Laboratories, Albuquerque, NM, January, 1983.
104. Sugano, T., et al, " Full-scale aircraft impact test for evaluation of impact force", Nuclear Engineering and Design, N. 140, pp 373-385, Elsevier, 1993.
105. Sugano, T., et al, "Local damage to reinforced concrete structures caused by impact of aircraft engine missiles, Part 1. Test program, method and results", Nuclear Engineering and Design, N. 140, pp 387-406, Elsevier, 1993.
106. Sugano, T., et al, "Local damage to reinforced concrete structures caused by impact of aircraft engine missiles, Part 2. Evaluation of test results", Nuclear Engineering and Design, N. 140, pp 407-423, Elsevier, 1993
107. Not Used
108. Salmon, M. W., Isabel Cuesta Garcia and Gerard Pardoen, "Experimental Program for Determining Leak Rates in Unlined Concrete Shear Walls Subjected to Beyond Design Basis Earthquakes," SMiRT18.
109. Mayrhofer, Chr., Korner, W., and W. Brugger, "Gas Impermeability of Reinforced Concrete Slabs Supported on Four Sides. Part 2, " Foreign Technology Division Wright-Patterson AFB Report, FTD-ID(RS) T-0085-88., 1988.
110. Suzuki, T., Takiguchi, K., and H. Hotta, "Leakage of Gas Through Concrete Cracks," Nuclear Engineering and Design, 133 (1991), pp. 121-130, 1992.
111. Okamoto, K., Hayakawa, S., and Kamimura, R., "Experimental Study of Air Leakage from Cracks in Reinforced Walls," Nuclear Engineering and Design, 156 (1995) pp. 159-165, 1995.
112. Greiner, U., and Ramm, W., "Air Leakage Characteristics in Cracked Concrete," Nuclear Engineering and Design, 156 (1995), pp. 167-172, 1995.
113. Dameron, R.A, Rashid, Y.R., and Tang, H.T., 1995., "Leak Area and Leakage Rate Prediction for Probabilistic Risk Assessment of Concrete Containments Under Severe Core Conditions," Nuclear Engineering and Design, 156 (1995), pp. 173-179, 1995.
114. Riva, P, Brusa, L, Contri, P, and L. Imperato, "Prediction of Air and Steam Leak Rate through Cracked Reinforced Concrete Panels," Nuclear Engineering and Design, 192 (1999) pp. 13-30.
115. Hibbitt, H. D., et al., "ABAQUS-EPGEN - A General Purpose Finite Element Code with Emphasis on Nonlinear Applications" *Nuclear Engineering and Design*, Volume 77, 1984, pp. 271-298.
116. Bazant, Z.P., Kaplan, M.F., "Concrete at High Temperatures – Material Properties and Mathematical Models," Concrete Design and Construction Series, Longman Group Limited, 1996.

117. Khoury, G.A., "Compressive Strength of Concrete at High Temperatures: a Reassessment," Magazine of Concrete Research, 1992, 44, No. 161, Dec., pp. 291-309.
118. Bamforth, P.B., "The Long-Term Properties of Concrete Used in Prestressed Concrete Pressure Vessels," Taywood Engineering Ltd., Southall, Middlesex, "Inspection and Structural Validation of Nuclear Power Generation Plant," held in London, 11/25/93.
119. Freskakis, G.N., et al, "Strength Properties of Concrete at Elevated Temperatures," Civil Engineering Nuclear Power, Vol.1, ASCE National Convention, Boston. April, 1979.
120. DeFish-Price, C., et-al (Rockwell International Report), "Effects of Long-Term Exposure to Elevated Temperatures on the Mechanical Properties of Hanford Concrete," a construction Technology Laboratories Report for the U.S. Department of Energy Under Contract DE-AC06-77RL01030, October, 1981.
121. Abrams, M. S., "Compressive Strength of Concrete at Temperatures to 1600F," Temperature and Concrete, ACI SP-25, American Concrete Institute, pp. 33-58 (1971).
122. Zoldners, N. G., "Thermal Properties of Concrete Under Sustained Elevated Temperatures: ACI SP-25, American Concrete Institute, p. 1-32 (1971).
123. Sanad, A. M., "Development of Generalised Stress-Strain Relationships for the Grillage Models of Cardington Concrete Slab," University of Edinburgh, School of Civil & Environmental Engineering, PIT Project Report, December, 1999.

#### Additional References

Okrent, D., *Nuclear Reactor Safety, On the History of the Regulatory Process*, the University of Wisconsin Press, 1981.

Clauss, D. B., Horschel, D. S. and Blejwas, T. E., "Insights into the Behavior of LWR Steel Containment Buildings during Severe Accidents," *Nuclear Engineering and Design*, No. 100, 1987, pp. 189-204.

Parks, M. B., Horschel, D. S., and von Riesemann, W. A., "Summary of NRC-Sponsored Research on Containment Integrity," *Proceedings of the 11th International Conference on Structural Mechanics in Reactor Technology*, August 18-23, 1991, Tokyo, Japan.

Horschel, D. S., Ludwigsen, J. S., Parks, M. B., Lambert, L. D., Dameron, R. A. and Rashid, Y. R., "Insights Into The Behavior of Nuclear Power Plant Containments During Severe Accidents," SAND90-0119, NPRW-CON90-1, Sandia National Laboratories, Albuquerque, NM, June 1993.

Dameron, R. A., et al., "Methods for Ultimate Load Analysis of Concrete Containments, 4th Phase: Concrete Containment Leakage Predictions - A Probabilistic Approach with Applications to NUREG-1150", ERPI RP-2172-1, Electric Power Research Institute, Palo Alto.

Tang, H. T., Dameron, R. A. and Rashid, Y. R., "Probabilistic Evaluation of Concrete Containment Capacity for Beyond Design Basis Internal Pressures", *Nuclear Engineering and Design*, 157 (1995) pp. 455-467.

Hessheimer M. F., R. A. Dameron and W. A. von Rieseemann, "A Summary of Containment Integrity Research," Presented at the Seminar on Containment of Nuclear Reactors held in conjunction with the 14th International Conference on Structural Mechanics in Reactor Technology (SMiRT 14), Saclay, France, August 15-26, 1997

**This page intentionally blank**

## Appendix – Containment Capacity Analysis Guidelines

### A.1 Introduction

This Appendix provides guidelines which analysts may use in performing analysis to determine the capacity of containment structures to withstand loads beyond their design basis. These guidelines address only overpressurization in combination with elevated temperature, i.e. the scenarios associated with severe accidents. These guidelines come directly out of experience and lessons learned from the Sandia containment research program, both direct experience from Sandia (and contractor) analysis, and the shared experience of international participants in round-robin analyses.

In general, containment structural analysts need to develop a model that represents the geometry, structural details and material properties which are ‘important’ to the response regime being analyzed and to the goals of the analysis. With continuing advances in computational power, the trend (and temptation of analysts) may be to model containments with more elements, more detail, and more comprehensiveness than ever before. But there remain real limits on what the state-of-the-art in material models can simulate and, generally, very real limits on the experimental data which is needed for interpreting and verifying the quality of complex model representations.

*“Everything should be made as simple as possible, but no simpler!”- Albert Einstein*

Though cliché, this is still probably the best philosophy, but also the biggest challenge, for containment analysis. Any analysis effort should include at least the following four steps:

1. Planning and identifying the goals of the analysis;
2. Developing model(s);
3. Calculating the response;
4. Interpreting and checking the results.

This Appendix is structured around these four key steps. And although the topics presented here are discussed separately, these overall tasks must also be well integrated. Failure criteria must be consistent with the geometric details in the model(s) and the physical phenomena (i.e., plasticity, large deformations, etc.) accounted for in the calculations. Failure criteria have been proposed, and calculation methods are described here, as well as the geometric details that should be considered to be consistent with the proposed criteria. It also must be decided how predictions for containment performance will be used, because this strongly influences choices of methods and modeling details.

### A.2 Analysis Goals and Planning

The first step in choosing an analysis method is to ask how the results will be used, i.e. what question the analysis will answer or what decisions will be made based on the results. For most containment capacity analyses, the results will be used to answer questions regarding safety margins and may be used in Level 2 PRA analyses and risk-informed licensing decisions.

The answer to this question affects selection of the tools and methods, which are important features of the work. For example, analysis of containments for the specified design loads can

usually be done with elastic or mildly nonlinear analysis since the code-specified design limits on stresses are usually constrain the response to the elastic regime. But predictions of containment response to severe accidents or ultimate capacity typically require capabilities for simulation far into the nonlinear range of response. Both the load limits, in terms of pressure and temperature, and the modes of response or failure are important for severe accident risk assessments and emergency preparedness planning. For example, in the event of a severe accident, the consequences of an early containment failure typically are greater than those of a late failure and the consequences of rupture are worse than those of leakage. Since the elastic analysis methods used in design are well understood (note the near uniformity the Round Robin predictions of response in the elastic regime[32, 34, 42, 45, 74, 79]) and have been benchmarked against the experiments, this appendix will focus on methods of analysis for severe accident loading and capacity/failure mode predictions. It should also be noted that the level of confidence in analyses of the non-linear response or capacity of the containment is less, or conversely the uncertainty is greater, than design or elastic response analyses.

Analysis planning and goals should be established as follows.

- a. Identify the loads to be applied.
  - Typically, severe accident containment loads consist of both transient pressure and thermal loading.
  - In some cases, the pressure transient may be considered independent of the thermal load because the peak pressure may not occur simultaneously with significant thermal loading. (See Section A.5.3 for guidelines regarding what constitutes “significant.”)
  - The transient nature of the pressure and thermal loading is usually ignored since the duration of the loading is usually longer than the period of the structure. As a result, static analysis methods are usually adequate.
  - While these simplifications are usually valid, the analyst should review their validity in planning the analysis approach.
- b. Conduct an initial “failure/vulnerability review”.
  - Identify potential failure locations and modes and the types of models needed to simulate them.
  - It is helpful to discriminate between functional failure modes, i.e. loss of containment integrity or leakage, which is generally progressive and structural failure modes which can occur rapidly. The primary value of discriminating between these modes of failure is in determining the risk significance of any given mode. Usually, this is beyond the scope of the structural analysis, but is important to the interpretation and application of the analysis results.
  - Failure modes and thresholds of ‘engineered components’ such as penetration assemblies, may rely on some level of analysis, but are typically determined by testing. This appendix focuses on recommendations for the analysis of the structure that comprises the primary containment boundary.

- c. Define the engineering significance of the failure prediction. For example, is the goal to determine the margin of safety between the design pressure and the pressure at which a loss of containment integrity occurs.
- d. Determine if the focus the analysis is on making a best estimate prediction or on a 'conservative' lower bound estimate. Typically, containment analyses have been deterministic due to the complexity of performing detailed non-linear structural analyses. Estimates of uncertainty or probability of failure have been based on engineering judgment or multiple simplified analyses which are usually restricted to considering model parameter uncertainty.

This last item has consequences on choices of material properties (i.e., using actual properties, when available, rather than design-spec properties, etc.), and choices on modeling parameters, such as friction, foundation spring stiffness, etc.

It is crucial to not underestimate the importance of planning the analysis. The obvious, but often overlooked, fact is that only those features of the structure or modes of response/failure that are included in the model will be represented in the results. Experience has shown that the critical response or failure modes of the real structure are often not considered important or overlooked and not included in the model. As a result, analysis planning should also make use of judgment and experience on containment behavior.

For example for a prestressed concrete containment, since it appears likely that measurable leakage will not occur prior to the onset of general yielding; simplified methods can be used to predict containment performance. A failure criterion based on an average hoop strain of 1 to 2 % appears reasonable based on the (limited) experimental data. Simple axisymmetric models, either finite element or closed form formulations, could be used in conjunction with such a failure criteria. While this method may tend to underestimate the rupture pressure, yet, it could be acceptable if it can be demonstrated that significant leakage occurs (past penetration seals, bellows, or isolation valves, for example) at a lower pressure. If leakage does not occur before general yielding, a method based on a simple model and failure criteria like that described above is not adequate. This is due to it not allowing for the possibility of leakage which can occur at a local tear, and preclude the occurrence of rupture.

### **A.3 Simulation Code Selection**

Containment capacity analyses require the use of a robust, general-purpose finite element code. There are a large number of code that meet the basic requirements and the selection of a particular code often depends on features that make the development of the model, the definition of the material constitutive models and the analysis of the results more efficient and convenient for the analyst.

It is not appropriate to recommend or endorse any particular finite element code in this report, however, the required or desirable features should include the following:

- Solution algorithm appropriate for simulating nonlinear response
- Suitable element library (including rebar for concrete containments)
- Appropriate material models that work for all needed element types (either resident in the program, or having an interface for user-supplied models)
- Capability to apply prestress (for a PCCV)



- Numerically robust Contact Simulation (only for some specific modeling procedures)
- Track record of performance for this class of problems

More specific requirements on element types and material modeling are provided later in this Appendix. The last item, “track record of performance,” is included to stress the need to test finite element programs for new applications (at least new to the user). Sometimes, while a program may have theoretically sound published capabilities, in practice, it may prove difficult to advance solutions far into the nonlinear response range.

## **A.4 Model Development**

### **A.4.1 Geometric Considerations**

One of the primary modeling decisions to be made is to determine the scope or extent of the simulation model and which elements of the real structure can be ignored or simplified without affecting the analysis goals. Decisions made in this step are a continuation of the model planning and goal setting, particularly the “failure/vulnerability review.” The geometric considerations which enter into this step include:

#### **a. Global versus Local models**

- Probably the most fundamental decision to be made is whether to construct a detailed global model which incorporates all of the relevant features of structure or a simplified global model which captures the global behavior combined with sub-models to capture the local behavior. With ongoing increases in computing capacities and simulation codes that can take advantage of these capacities, there may be (is) a tendency or temptation to construct the most detailed, three-dimensional model possible. If these modeling capabilities are used judiciously this can provide a very accurate simulation, however, the potential complexities can often mask the underlying mechanisms and can also introduce model artifacts.
- This decision is tightly coupled with the choice of a global or local failure criterion. It should be obvious that all failures initiate at the local level, but experience has shown it is much more difficult to identify and simulate local response, which is often driven or influenced by as-built conditions, than the global response of the structure.

#### **b. What structure “idealizations” can be made without loss of achieving analysis goals?**

- Typically small penetrations can reasonably be ignored in terms of their effect on overall containment response.
- Typically basemat irregularities, such as reactor cavities or access tunnels for control mechanisms, can be ignored.
- Typically, the gravity effects of containment internal structures and adjacent external structures can be ignored due to the high stiffness of the basemat.

These last two simplifications should be carefully reviewed if a relatively flexible basemat is encountered.

- c. What symmetries in the structure can be exploited? If existing symmetries can be exploited, a finer mesh can usually be used than would be possible in a full, 3D model.
- Bi-symmetric about one plane or Quarter-symmetry about two orthogonal planes?
  - Wedge or Sector symmetry, i.e. can a ‘slice’ or repeating sector (e.g. 30°) of the structure represent the response of the entire structure
  - Axisymmetric? A majority of the containment structures currently in use or proposed can be fairly represented by an axisymmetric model. This makes sense since a uniform shell is more efficient in resisting internal pressure than an irregular structure. The axi-symmetry of the containment is usually compromised, however, by constructability and operational considerations. Nevertheless, idealizing the structure as axisymmetric is usually possible and reasonable. Sources of non-axisymmetric behavior include
    - Major openings (usually the Equipment Hatch and Personnel Airlocks)
    - Hoop tendon buttresses
    - Dome tendon layout (part of which is often rectilinear)
    - Basemat rebar layout (part of which is often rectilinear)

It should be noted that apparent geometric symmetries can often mask underlying asymmetries in the structure, such as changes in stiffness associated with variations in reinforcing in concrete containments or local thickening or stiffeners in steel structures.

- d. Interaction with adjacent structures or components.
- Is there a shield structure or other adjacent structure that could restrict containment “growth”?
  - Can the pipe penetrations and equipment supports accommodate differential movement (both radial and vertical)?

As discussed in section A.4.1, there are two major issues involved in developing the finite element models: determining what geometric detail of a containment need to be represented and establishing proper mesh discretization. As part of the last two decades of Sandia containment research, many containments have been analyzed, and for the Sandia large scale model tests, many analyses were conducted by round-robin participants. In most cases, to complete a thorough set of predictions of behavior to overpressure, several different model types are developed and analyzed for each containment. These modeling decisions made for the Sandia Containment model tests are summarized in Table A-1.

**Table A-1 Summary of Analytical Model Types Used for Containment Studies**

Test	Scale	Shape	R/t	Press. Ratio	Global Models	Local Models	Remarks
SNL SCO (12/2/82, 12/12/82)	1:32	Cylinder w/ hemispherical dome	450 (R=549, t=1.22)	0.93*	Axisymm.		
SNL SC1 (4/20- 21/83)	1:32	Cylinder w/ hemispherical dome	500 (R=546, t=1.09)	0.76*	Axisymm.		
SNL SC2 (7/21/83)  (8/11/83)	1:32	Cylinder w/ hoop stiffeners and hemispherical dome	478 (R=546, t=1.17)	0.93*  0.97*	Axisymm.  Axisymm.		
SNL SC3 (11/30/83)	1:32	Cylinder w/ penetrations and hemispherical dome	478 (R=546, t=1.17)	0.83*	Axisymm.		
SNL 1:8 (11/15- 17/84)	1:8	Cylinder w/ stiffening rings, penetrations and hemispherical dome	448 (R=2134, t=4.76)	4.9	3D Sector	3D of Local Stiffener Detail	
NUPEC SCV (12/11/96)	1:10 geom./ 1:4 thick.	Improved BWR Mark II w/ contact structure	135-161 (R=2027- 2900, t=7.5-9.0)	6.0	3D Sector	3D E/H	
SNL RCCV	1:6	PWR: cylindrical concrete shell w/ steel liner and hemispherical dome	13.5 (R=3353 t=248)	3.2	Axisymm.; 3D coarse global (half symmetry)	2D Wall- base junction; 3D E/H; 3D P/A	PRETEST
SNL RCCV	1:6	“ “ “	13.5 (R=3353 t=248)	3.2	Axisymm.	3D of small penetration group	POST-TEST
Sizewell-B	1:10	Sizewell-B	8.6	2.4	Axisymm.; 3D coarse global (half symmetry)		
NUPEC PCCV NUPEC PCCV	1:4	Large, dry PWR: 2-buttress cylinder w/ hemispherical dome	16.5	3.2	Axisymm.; 3DCM	3D E/H; 3D P/A; 3D M/S Pen.	PRETEST
NUPEC PCCV NUPEC PCCV	1:4	“ “ “	16.5	3.6	Axisymm.; 3DCM; 3D-Shell	3D E/H; 3D M/S; 3D tendon ring slice; liner rat-hole	POST- TEST/SFMT

\*Design pressure not specified, maximum pressure (MPa) given.

The model types used include: axisymmetric, 3D global, 3D sector, 2D local, and 3D local models of various details. As evidenced from this work and the round-robin participant submittals, the minimum analytical assessment of containments is achieved with an axisymmetric model. (Some analysts choose to use a 3D sector model if the program used does not have a full suite of axisymmetric element types, but the analyses, and the results obtained are essentially equivalent.) Some argue that a 3D model is also needed to capture the non-axisymmetric features of containment response. Setting this minimum standard depends on how the results are to be used.

#### *A.4.1.1 Special Considerations for Steel Containments*

The overall geometry of steel containments ranges from relatively complex (e.g. BWR Mark I) to relatively simple (e.g. the free standing steel cylinder for a large, dry PWR). The modeling of the basic shell geometry is relatively straight forward. The primary considerations for modeling steel containments are the representation of transition regions (changes in basic geometry such as at the wall-base junction, the springline or knuckle regions or changes in shell thickness) that may give rise to bending stresses and discontinuities such as penetrations, supports and stiffeners. Some representative models are shown in Figure A-1.

One fundamental question in developing the model of a steel containment is whether shell or solid elements will be used to represent the structure. Typically, shell elements are adequate for representing thin-shell steel structures. Certain discontinuities in the structure, however, such as local eccentricities or where other sharp gradients in strain occur, may require the use of solid elements. Usually, solid elements are only used where perceived to be necessary since there is a penalty, in terms of degrees of freedom, to be paid to achieve the resolution required. Thermal loading considerations may also dictate whether shell or solid elements are required. Shell elements do not have the capability of simulating steep thermal gradients through thick sections. Normally, the through thickness gradient is a less significant effect than the average increase in material temperature.

The test programs illustrated the importance of including accurate representation of the details that may result in local breakdown in the membrane action of the shell or stiffeners. For example, in the 1:8-scale steel model, an eccentricity in the stiffener pattern around the equipment hatch was responsible for introducing primary bending into the stiffener. As a result, when the stiffener failed, the load was transferred into the shell, and the shell failed at a lower pressure than expected. Similarly, the 'rat-hole' detail in the hoop stiffener in the 1:10-scale NUPEC model resulted in a local strain concentration which resulted in a tear. The analyst needs to be sensitive to the presence of details that may introduce local strain concentrations and decide if these features are significant enough to include in the analysis.

These features may be included in a single model, but more commonly a simplified representation of the structure is used to analyze the general shell behavior and sub-models are used to investigate local discontinuities. Each approach has advantages and disadvantages. A detailed, comprehensive model may require some level of simplification to manage the model size while the boundary conditions for sub-models may reduce the accuracy of the model if not applied properly.

Typically, it is not practical to include highly localized details, such as local weld geometry (and associated variations in material properties for the weld metal and heat affected zones), even in sub-models, although tests have shown that failure may initiate at these locations. Similarly, since most steel containment structures are not stress relieved after cold work (rolling or forging), there may be considerable residual stresses which are not represented in the finite element models. These effects are usually addressed in the interpretation and evaluation of the analysis results and in the selection of failure criteria.

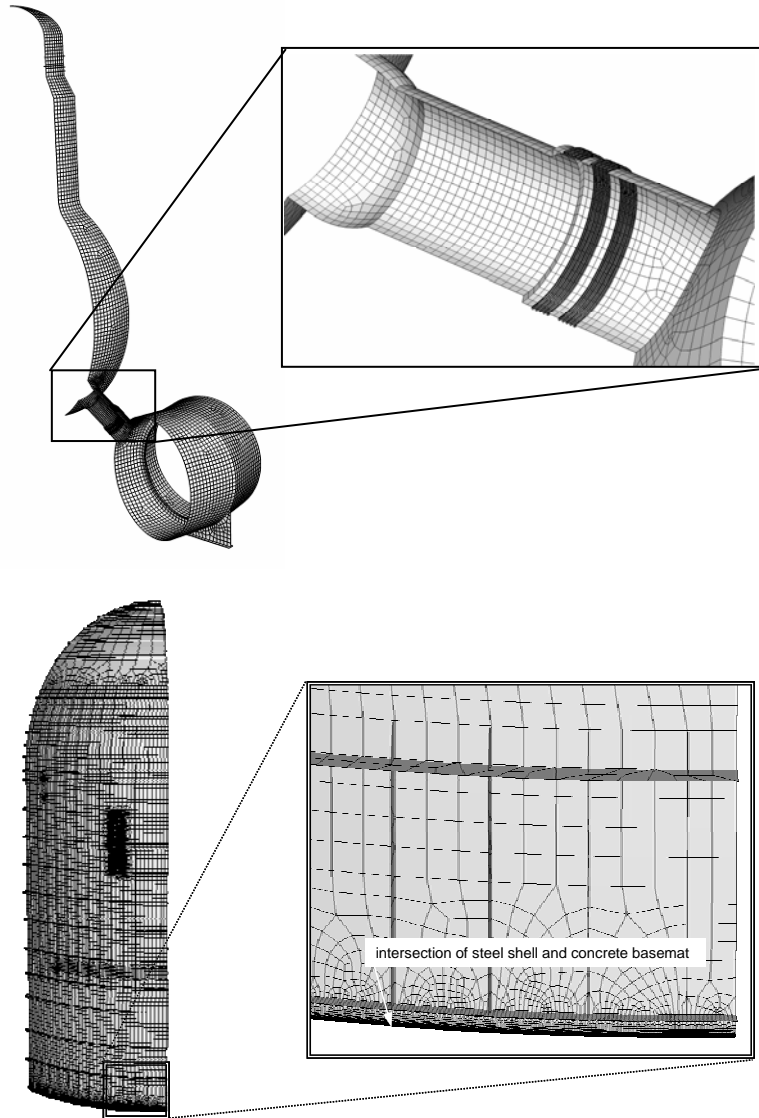


**Figure A-1 Examples of Steel Containment Models [97]**

Predictions for leakage from operable penetrations such as pressure seating equipment hatches can be based in part on the same three-dimensional model of the shell and equipment hatch used in the analysis for structural response. The results of these analyses are typically used in analytic solutions of bolt and/or seal behavior or compared to empirical results. In order to accurately predict ovalization of the sleeve, the stiffener pattern around an equipment hatch must be modeled explicitly. The technique of “smearing” local stiffening details is limited application to analyses of global behavior and cannot be used to obtain accurate predictions of leakage from ovalization of pressure seating equipment hatches.

Cherry and Smith [18] and Petti and Spencer [97] provided additional consideration for modeling of steel containments subjected to corrosion damage. Their recommendations on failure criteria should be applied judiciously, however, since the purpose of the analyses were to demonstrate how analyses could be used to estimate the effects of damage and were not benchmarked against actual test data.

#### *A.4.1.2 Special Considerations for Concrete Containments*

The composite nature of reinforced concrete structures requires considerations beyond those for steel containments when developing the model geometry. In addition to representing the visible dimensions of the structure, the model must also be capable of accurately reflecting the embedded features of structure, primarily the pattern of reinforcing. Prestressed (or posttensioned) reinforcing adds further complexities if accurate modeling of variations in loading and anchorage details are considered to be important. Since all operating US plant with concrete containments include a steel liner, the anchorage and stiffening details of the liner are also important. These geometric considerations are closely coupled with selection of element type and constitutive material models. For example, finite element codes offer the capability of modeling the reinforcing as 'smeared' with the concrete, embedded in the concrete element or modeled discretely as separate elements. Fortunately, the experimental evidence suggests that many of these details do not have a significant effect on the limit states of the containment. Unfortunately, because of the large variety of details used in construction of even geometrically similar containments, it is not always obvious which of these details can safely be ignored.

Because the details associated with the component materials can be quite complex, most analysts are required to choose which details they will include, simplify or ignore, depending on the postulated modes of response and or failure. Predicting loss of containment function in concrete containments generally requires that leakage be predicted, or at least not overlooked as the pressure-temperature demand increases.. The experiments suggest that generalized liner yielding is a necessary condition for liner tearing to occur if there are no construction or material defects. Once generalized yielding occurs, the initiation of tearing in the liner is dependent on the strain concentrations associated with local details. Recognizing when liner tearing occurs, however, may be problematic because the criteria for liner material failure are dependent, in part on the element size.

The experiments also suggest that cracking of the concrete may be a precondition for liner tearing and especially large, i.e. wide, cracks may initiate tearing in the liner by concentrating the strain. At high pressures, cracking-induced liner-anchorage-concrete interaction is similar in both reinforced and prestressed containment structures even though it is initiated earlier in reinforced structures. As the concrete cracks, the liner begins to deform plastically, generally earlier in reinforced containments than in prestressed containments. A comparison of event sequences in reinforced concrete versus prestressed concrete containments was illustrated in Figures 88 and 89. While the experiments are not, conclusive on this matter, they suggest that some attention be paid to these mechanisms.

It should be noted that, again based on the experiments, the leak rate does not appear to depend on whether the concrete is uncracked or cracked. Apparently, even relatively intact concrete contains enough shrinkage cracks or other leak paths that the flow of gas is not significantly impeded. This appears to be true whether the concrete is posttensioned or not. The conclusion from this discussion is that simulation of discrete cracks is probably not important for steel lined concrete containments. The significance of generalized cracking for containment analysis is primarily the loss of stiffness, which affects the global strains which lead to tearing of the liner or rupture.

This is not true for unlined concrete containments used outside the US, notably in France. For these containments, the prediction of concrete cracking and the character of these cracks are essential for simulating containment performance. This may also become important for future US nuclear power plants if unlined concrete containments or 'confinement' structures are proposed.

Liner tearing, under quasi-static pressurization, will probably manifest itself as leakage, if there is residual structural strength in rebar and tendons. If significant tearing and leakage of the liner does not occur, as the pressure and global strains increase, perhaps rapidly, the probability of catastrophic rupture becomes more significant.

#### *A.4.1.3 Element Types for Concrete Containments*

- a. Concrete is typically modeled with continuum elements. In 2D planar or axisymmetry, 8-node (quadratic edge) continuum elements, but reasonable accuracy can also be obtained with a finer mesh using 4-node (linear edge) continuum elements. In 3D, 20-node (quadratic edge) or 8-node 'brick' elements are recommended.
- b. In concrete elements which crack at the finite element integration points, it is best to select elements with reduced integration, as long as appropriate care is taken as to mesh-size and to control of numerical issues such as 'hour-glass.' (These issues are beyond the scope of this guidelines appendix, but are usually well covered by the theory manuals of finite element programs.) The reason for this is improved convergence characteristics once cracking begin to develop.
- c. An axisymmetric liner should be modeled with two-node or three-node shell elements (whatever is compatible with the adjoining concrete elements), and beam elements can be used for representing liner angle anchors or stiffeners. In most models except for those studying very localized effects of liner/concrete interaction, the liner is considered to be fully bonded to the concrete. In 3D models, the liner should be modeled with 3D shell elements. (It should be noted that for the original designs, the liner was generally ignored in analysis.)
- d. smeared rebar sub-elements should be used to model reinforcement. Such elements assume strain compatibility between rebar and concrete.
- e. Smeared rebar sub-elements can be used to model tendons for global axisymmetric analysis of a P/C containment. (In an axisymmetric analysis, strain compatibility of hoop tendons is automatic, but with meridional tendons, the analyst has a choice of modeling tendons as ordinary rebar, or as separate truss elements external to the grid and attached to the grid with linkage elements. (Extensive study of axisymmetric analysis for the 1:4 PCCV did not show good 'return on invested labor' (in terms of improved accuracy) for modeling vertical tendons with explicit elements that could slide relative to the concrete. A different conclusion was reached, however, for 3D local models targeting circumferential variations related to hoop tendon behavior; such analytical goals require special treatment of prestressing tendons with separate elements tied to the concrete, but also allowed to slip and have different hoop strain than the neighboring concrete.)

#### *A.4.1.4 Mesh Size*

Properly discretizing the model depends on the analyst's ability to anticipate the type of behavior (i.e., membrane action, bending, shear, etc.) that will occur in any given location. In this respect, a background in plate and shell behavior is needed, as well as an understanding of the differences in element formulations. For example, bending occurs at discontinuities such as intersections between penetrations and pipes and the containment shell. It occurs where there are changes in the shell geometry and thickness. The elastic bending response of a shell typically has the form of an exponentially decaying sinusoid. The maximum size of the elements in areas characterized by bending can be estimated if the characteristic wavelength of the elastic response, which

depends on the radius and thickness of a shell, and the element shape functions are known. For instance, to represent the bending response of a shell with a characteristic wavelength, at least four or five linear elements are needed per wavelength.

The analyst must exercise judgment in constructing the model and discretizing the mesh. The element choices must be assessed by verifying that the solutions do not violate fundamental mechanics (for example, force equilibrium), and perhaps even with sensitivity studies with element size and element 'order' as the sensitivity parameters. The best advice to an analyst with little experience in modeling containments, is to conduct a modeling exercise using one of the Sandia test models most similar to the structure of interest, and validate decisions on element types and sizes by comparison of results to the published test data. Then once validated, the analyst can proceed to the real structure and make similar meshing decisions with confidence.

In addition to these general guidelines, the following specific guidelines apply to containment analysis.

- a. Grid refinement at the wall-base juncture is mandatory to capture the large shear and moment gradients that occur at the base of the wall. At a region of high bending moment, it is important to calculate the strain in the various rebar layers correctly by explicit modeling of the discrete layers, rather than smearing properties for the entire wall section.
- b. In most cases, relatively coarse, idealized modeling of basemats is adequate. More detailed modeling of the basemat has been found to be important only in some circumstances, namely, if there were any possibility of potential failures at the wall-base juncture. Basemat discretization is generally not important in predicting the response of the barrel and the dome. Accuracy is required in predicting basemat liftoff that can occur at high pressures and control the global behavior, as in the case of the Sizewell-B 1:10-scale model. Local basemat details, such as sumps, cutouts, and keyholes, are generally ignored in global analyses, particularly because they have not been included in the test models, and this appears to be reasonable, even for evaluating a full scale prototype.
- c. For axisymmetric analyses, a regularly spaced grid is recommended over to the symmetry line to adequately calculate the bending moment in the basemat, which is a maximum at the axis of symmetry. This bending moment causes the possibility of yielding the basemat bottom bars that, in the cases of the 1:10-scale containment and the 1:6-scale containment, led to basemat liftoff (more so in the 1:10-scale containment). But in most actual reinforced or prestressed containments, leakage is likely to occur before yielding of the basemat bottom bars in bending.

#### A.4.2 Boundary Conditions

For global axisymmetric analysis, the boundary conditions are straightforward - constraint of displacement  $u_r$  at the symmetry axis ( $R=0$ ), and constraint of  $u_z$  along the underside of the basemat (i.e., if foundation springs are modeled,  $u_z=0$  on the ground side of the springs). For 3D global analysis, the boundary conditions are similarly intuitive, with vertical displacement constraint under the basemat, and horizontal displacement constraint applied at the center of the basemat.

For sector models representing a vertical slice of the structure, the boundary conditions are similar to axisymmetric analysis, but with the caveat that care must be taken to assign



displacement constraint along the “slice edges” which are truly perpendicular to the slice plane, i.e., free radial expansion must be allowed.

For all other forms of sub-models, the derivation and application of boundary conditions can be very complex, and in past work has often required the development of boundary condition input processors/subroutines. The 3D local models of the 1:6 Scale RCCV, 1:4 Scale PCCV, and mixed scale SCV, were all “driven” by combinations of pressure applied to the liner or steel shell, and boundary condition “displacement histories” applied at the nodes along the boundaries of the model. These displacement histories are nodally unique displacements in three coordinates, which change with pressure, and they are derived or extracted from another analysis that provides global behavior simulation. The challenges to analysts for these models include:

- a. Ensuring that boundaries are cut far enough away from the local area of interest in the analysis that the behavior at the boundary is not influenced by the behavior of the local component
- b. Ensuring that the 3D local simulation of the containment wall is compatible with the global one – if not, a local stress/strain concentration can occur near the boundary when the displacement boundary conditions are applied.
- c. Ensuring (for example with a 3D R- $\theta$  slice model) that rigid body displacements are adequately constrained, without over-constraining the sub-model.

For more details on how these challenges were addressed in past analytical studies, the reader is directed to the analysis reports for the 1:6 Scale RCCV, 1:4 Scale PCCV, and mixed scale SCV.

#### A.4.3 Material Properties

The materials of construction of the containment structure are usually provided in the engineering design drawings or construction specifications. Depending on the stage of design, construction or operation, the analyst may only have access to preliminary material specifications, properties of sample materials, properties of specimens of the actual materials taken during construction or, possibly properties of materials which may have been degraded during the operating life of the plant. The analyst must decide which set of properties to use in the analysis. In the case where not actual material data exists, the analyst’s options are limited, but even here, information from previous construction experience, e.g. results of tests on similar materials for previous projects, may be used to modify the nominal properties of the specified materials. When test data is available, it is usually desirable to use this information, however, the analyst should be familiar with the scope of material testing and whether it is statistically significant.

When performing probabilistic assessments, the range in material properties from actual or representative test data can be used, with some judgment, to estimate the range of uncertainty, either directly or by defining the parameter variation when multiple analyses are performed, e.g. Monte Carlo or Latin-Hypercube Sampling.

##### A.4.3.1 *Special Considerations for Steel Containments*

- a. The basic material properties, yield strength, ultimate strength, and maximum elongation, should be determined from standard uniaxial tensile tests on the actual materials of construction, if possible. Again, an adequate number of specimens should be tested in order to have a statistically representative sample. Also, for plate material, specimens should be taken both parallel and perpendicular to the rolling direction. While properties

may vary as a function of heat (i.e., production run) and thickness, variations of properties within a particular heat are probably negligible.

- b. The experiments have shown, however, that direct application of uniaxial tests of small gage length specimens tends to over predict these properties. This may be due to the fact that these materials are typically subjected to stresses and strains in the fabrication process (cold rolling, weld-induced stresses) which are typically not considered in the analysis. It has also, appears, although this is not conclusive, that there may be a size effect that tends to decrease the apparent properties of full-scale structures. Regardless of the reason, it appears prudent to apply a reduction factor on the order of 10 to 20% to both the yield and tensile strength.
- c. While certain failure mechanisms may require additional material tests to model correctly, e.g. fracture toughness, fatigue strength, the basic properties discussed above are generally adequate for most containment analyses. When measuring these properties, it is desirable to obtain the full engineering stress-strain relationship, rather than just the basic values, to characterize the post-yield material response. Depending on the finite element code, the stress-strain relationship can be input directly or approximated. For non-linear analysis, the engineering stress-strain is usually converted to true stress-true strain.
- d. Since steel containments are constructed by welding, the behavior of the welds is important. The experiments have shown that most, if not all pressure-induced failures in steel containment structures (excluding penetration leakage) occur at or near the welds, usually in the heat-affected zone (HAZ) of the parent material. This may be due to local changes in the properties of the parent material, weld induced stresses or both. While this is not normally done for actual containments, it is helpful to test welded specimens, preferably at the same thickness as the materials used in the construction. If this is not possible, posttest inspection of the steel models suggests that estimates of changes in material properties can be obtained from surface hardness tests.
- e. Since severe accidents impose both thermal and pressure loads on steel containments, it is desirable to know the dependence of the yield strength, post-yield response (i.e. hardening), tensile strength and maximum elongation on temperature. Again, these properties are not normally measured during construction, however, reasonable estimates can be made based on published studies. Since all of the Sandia experiments were conducted at ambient temperature, the data from these tests do not provide any insights regarding response of steel containments at elevated temperatures. For many severe accident scenarios, the estimated temperatures are not high enough or of long enough duration, to have a significant effect on the material properties. In these cases, the primary effect of temperature loading is stresses induced due to constraint of thermal expansion.

#### *A.4.3.2 Special Considerations for Concrete Containments*

- a. Again, due to the composite nature of reinforced concrete, the material issues are considerably more complex, and subject of variation, than for steel containments.
- b. First the concrete itself provides special challenges since it is a brittle material which responds differently in tension and compression. Material testing for concrete construction is primarily for quality control purposes and not to define properties for analysis. While methods have been developed for direct or indirect measurement of

tensile properties, most material models are based on a fundamental parameter, the unconfined compressive strength,  $f_c'$ . The other necessary material parameters are typically derived from  $f_c'$  based on large amounts of empirical data. It is far more difficult to obtain uniaxial tensile properties than it is for compression. For containment capacity analyses, however, the tensile and shear properties of concrete both are usually much more important than the compressive properties. Shear strength is usually addressed as diagonal tension in concrete models using solid elements, however, care should be exercised in evaluating shear behavior in models using shell elements.

While the concrete containment models tested by Sandia utilized more exhaustive testing, including measurement of tensile and compressive stress-strain behavior, it appears that defining tensile strength, elastic modulus, etc. based on  $f_c'$  is generally adequate, although again it appears to overestimate these properties. If more extensive testing is conducted, it is important that a statistically significant number of specimens are tested.

In the absence of detailed tensile stress-strain data, the following values are recommended:

$4\sqrt{f_c'}$  ( $f_c'$  in psi) as the tensile stress at first cracking, and

0.0001 for tensile strain at first cracking

Though there are some observable differences in Young's Modulus in compression versus tension, it has been found adequate to use Young's Modulus in compression for both compression and tension

The post-cracking stress-strain curve is known as 'tension-stiffening,' and this is discussed further in Section A.4.3, Constitutive Modeling.

Poisson's Ratio is typically not measured and a conventional value of 0.2 can be assumed.

- c. Considerations for the material properties of the liner and embedments are similar to those discussed for steel containments. Since the liner does not typically contribute significantly to the overall pressure capacity of concrete containments and is relatively thin compared to steel containment walls, the reduction factor does not apply.
- d. Tensile properties of reinforcing bars and prestressing tendons or strands, if measured, should include the full stress-strain curve obtained for full size specimens of each bar type and size used in construction.

For normal reinforcing, larger bars typically exhibit lower strength properties and elongation than small bars even though the material is nominally identical. Tensile properties obtained from machined specimens of rebar typically over predict the tensile strength and should be used with caution or a reduction factor.

Tensile properties of prestressed reinforcing determined for quality control usually test the individual wires or strands rather than full tendons. The experiments suggest that the tensile properties of the tendon system, including anchor hardware are weaker and less stiff than would be expected from the strand test data. Since it is not always feasible to test the tendon systems to failure, a reduction factor (5 to 10%) should be applied on stiffness and strength of the individual wire or strand data. On stiffness, this reduction is

associated with “strand wrap angle” effects. On strength, this reduction would be associated with failures in the anchorage systems. It should be noted, however, that it is possible, but not 100% certain, for tendon systems to achieve their full strength as implied from a strand test.

#### A.4.4 Constitutive Modeling

After selecting or defining a set of material properties, the next choice is the selection of an appropriate constitutive model. For linear-elastic analysis, this choice is straight forward, but for non-linear, quasi-static or dynamic analysis, this is more difficult and requires experienced judgment. This is further complicated by the fact that constitutive models are often dependent on the code and solution strategy used. It is not possible to specify a particular constitutive model that is applicable in all cases, but the considerations given below may help guide the analysis of containment structures.

##### *A.4.4.1 Special Considerations for Steel Containments*

Pertinent details for modeling steel materials are discussed in Chapter 3, "Steel Containment Analysis" of the report. These factors must also be included in reinforced and prestressed concrete containment analyses for modeling the liner. In particular, the strain hardening of liner steels in the yield plateau requires careful verification of the strains in the nonlinear response range. In general, with the caveats previously noted, standard J-2 plasticity models have been shown reliable for containment steel material response prediction. There generally is no need for special characterization of cyclic response for severe accident loading analysis, so this simplifies the selection of “hardening” options, e.g., choosing isotropic versus kinematic hardening, and obviates the need for including the Bauschinger Effect.

##### *A.4.4.2 Special Considerations for Concrete Containments*

- a. Concrete constitutive models should include tensile cracking (normally treated as occurring in the principal stress directions at the integration points). Alternatively, the concrete can be treated as a no-tension material in analyses aimed at predicting global response.
- b. There is a wide range of opinion within the industry as to the proper simulation of the concrete post-cracking stress-strain curve. From the many years of analysis during the Sandia containment research program it has been concluded that while it is the most theoretically robust to implement an experimentally-verified tension stiffening curve, it is not absolutely necessary to achieve reasonable failure predictions for containments. What is more important is to caution against using overly “strong” tension-stiffening curves, which is often tempting to analysts, because their use can significantly improve convergence characteristics. For failure prediction, it is better (and conservative!) to assign little or no tension stiffening to post-cracked concrete than to assign too much.
- c. Some method for simulating post-cracking shear retention should also be included. Shear retention is particularly important at the wall base junction, and numerical solutions in this region are found to be sensitive to the shear retention algorithm used. Description of these methods, and a reasonable assessment of the current “state of the practice” in concrete modeling are available in the report on the Round-Robin Pretest Analyses of the 1:4 Scale PCCV Model [74].

- d. While most of the concrete elements in a computational grid will probably experience no compressive stress at high pressures, a few elements at the outer wall base and along the top of the basemat will experience compression, sometimes large enough to exceed the concrete compressive strength,  $f_c'$ . Thus, it is important to properly model concrete crushing. An elastic/perfectly plastic stress-strain curve has shown reasonable results in most cases, but inclusion of strain-softening is preferred for completeness. (Although, the associated plasticity algorithm is more complex.) As complex behavior is to be expected at the wall base, it is important that the concrete compressive yield algorithm properly treat the effective stress and strain calculation. Compressive yield is more likely to be reached by the combination of vertical compressive stress and shear stress rather than any one component stress reaching  $f_c'$ . This condition is essential for predicting potential wall-base shear failure.
- e. Geometric Nonlinearities. Though not a constitutive modeling issue, it is still a nonlinearity. Contrary to the recommendations for steel containment analysis in which geometric nonlinearity formulation is required to predict failure, it has been found that second order and large rotation terms need not be included in the strain-displacement relations for concrete containment analyses. The stiffness matrix need not be updated to reflect the changes in geometry or thinning of the wall, as it is in steel shells. This recommendation carries with it some practical advantages, especially for modeling such complexities as prestressing tendons. Restricting the solution to small-displacement theory provides some options as to approximate formulations for friction and other effects.

The constitutive modeling aspects of simulating temperature property degradation were described in Chapter 3. Most finite element programs handle the mechanical analysis of thermal expansion well, and it is generally adequate to assign a linear thermal expansion coefficient. But the analyses of coupled pressure and temperature accident scenarios become exceedingly more complex when temperatures reach high enough to cause significant material property degradation. These thresholds are approximately 150°C (300°F) for concrete and 427°C (800°F) for steels; these are the temperatures at which material strengths degrade by about 10%. And degradation curves become much steeper beyond these temperatures.

#### A.4.5 Boundary Conditions

For global axisymmetric analysis, the boundary conditions are straightforward - constraint of displacement  $u_r$  at the symmetry axis ( $R=0$ ), and constraint of  $u_z$  along the underside of the basemat (i.e., if foundation springs are modeled,  $u_z=0$  on the ground side of the springs). For 3D global analysis, the boundary conditions are similarly intuitive, with vertical displacement constraint under the basemat, and horizontal displacement constraint applied at the center of the basemat.

For sector models representing a vertical slice of the structure, the boundary conditions are similar to axisymmetric analysis, but with the caveat that care must be taken to assign displacement constraint along the “slice edges” which are truly perpendicular to the slice plane, i.e., free radial expansion must be allowed.

For all other forms of sub-models, the derivation and application of boundary conditions can be very complex, and in past work has often required the development of boundary condition input processors/subroutines. The 3D local models of the 1:6-Scale RCCV, 1:4-Scale PCCV, and mixed scale SCV, were all “driven” by combinations of pressure applied to the liner or steel shell, and boundary condition “displacement histories” applied at the nodes along the boundaries of the

model. These displacement histories are unique displacements at each node in three coordinates, which change with pressure, and they are derived or extracted from another analysis that provides global behavior simulation. The challenges to analysts for these models include:

- d. Ensuring that boundaries are cut far enough away from the local area of interest in the analysis that the behavior at the boundary is not influenced by the behavior of the local component
- e. Ensuring that the 3D local simulation of the containment wall is compatible with the global one – if not, a local stress/strain concentration can occur near the boundary when the displacement boundary conditions are applied.
- f. Ensuring (for example with a 3D R- $\theta$  slice model) that rigid body displacements are adequately constrained, without over-constraining the sub-model.

For more details on how these challenges were addressed in past analytical studies, the reader is directed to the analysis reports for the 1:6-Scale RCCV, 1:4-Scale PCCV, and mixed scale SCV.

#### A.4.6 Loading

Consideration of loadings parallels the above discussion on boundary conditions, but has some unique challenges, particularly for prestressed concrete containments.

For global and local models, loading application should follow basic principles; dead loads are applied using body forces (therefore proper assignment of mass densities to elements should be made), and pressure loads are applied perpendicular to the surface of the liner or steel shell. For the containment scale models that were tested hydrostatically, it was appropriate to add linearly varying hydrostatic force to the dead loading.

For prestressed concrete containments, an essential part of the pre-loading of the structure is the application of prestress, and in the past research program, this has been addressed and studied with varying levels of detail. The following discussion addresses most aspects of prestress loading that should be considered.

Prestressing losses should be estimated to accurately represent the actual stresses that will exist in the containment. In general, the philosophy used should be

- a. calculate best estimate “in service” values based on the nominal design values and modified for creep or any other in situ conditions;
- b. apply tendon stresses according to best estimate values, and allow the model to equilibrate to final tendon stresses that are reasonably close to these best estimate values, including anchor slip.

In axisymmetric analysis, there is no opportunity to simulate the progression of friction along the tendon path in the hoop tendons, but this phenomenon can be included in the meridional tendons. Standard prestressing losses, from Reference [16], along with a brief explanation of the basis for their consideration are listed below:

- (1) Elastic Shortening – occurs simply due to equilibrium-seeking displacement within the finite element analysis.
- (2) Steel Relaxation – normally considered by the containment designers in calculating the “nominal in-service” values.

- (3) Shrinkage of Concrete – normally considered in combination with creep, and also, normally considered by designers in calculating “in-service” values.
- (4) Creep of Concrete – studied in detail for the PCCV, but for design, should probably be addressed using standard design formulae. The combination of creep and shrinkage comprises a significant prestress loss over time, often reaching 5%-10% of overall prestressing.
- (5) Anchorage Slip – can be considered explicitly in local model analysis; but not directly relevant for axisymmetric analysis. For conventionally anchored tendons, anchor slip in the range of 4-6mm is typical. The amount of actual stress loss resulting from this is tied to the angular friction assumption.
- (6) Angular Friction (and wobble friction) - Considered explicitly in local analysis of hoop tendons, and in global axisymmetric analysis of meridional tendons in dome. Also considered in calculating the average hoop tendon stress to be assigned in global axisymmetric analysis. (Also see below.)
- (7) Others: Temperature - Not considered, but it should be noted that for a thermal analysis, if tendons become significantly heated, significant loss of prestress can occur simply due to  $\alpha\Delta T$  expansion and the associated stress relaxation.

With post-tensioning, the amount and distribution of elastic shortening depends on the order of post-tensioning. In general, it should be assumed that the tendons are jacked in a sequence appropriate to reacting the total desired lock-off force. In ABAQUS, an option called "PRESTRESS HOLD" allows an initial post-tensioning equilibrium step that holds the tendon stresses at a preset value while the structure iterates to equilibrium and thus maintains a constant stress regardless of elastic shortening. However, in some past versions of the program, various program errors were encountered using this option, so in general an iterative procedure is recommended for arriving at the appropriate tendon stresses after the prestressing step. This can generally be achieved within two or three attempts, by applying larger than target prestress, reaching equilibrium in the containment, noting the final prestress, then adjusting and applying the prestress load step again.

Angular Friction, Wobble friction and friction in straight portions of meridional tendons in the barrel below the springline can generally be neglected. From standard prestressed concrete texts, the angular friction should be included in the curved tendon portions with the formula:

$$T_2 = T_1 e^{-(\mu\alpha)}$$

where  $\alpha$  is the angle between  $T_1$  and  $T_2$ , and  $\mu$  is the coefficient of static angular friction.  $T_1$  is the tendon force next to a jack before friction losses, and  $T_2$  is the tendon force at some angle  $\alpha$  away from  $T_1$ . In the 1:4 Scale PCCV, the angular friction coefficient was observed (by ancillary testing) to be 0.21, but for a full-scale prototype, a coefficient of 0.15 is probably more appropriate.

Example

Meridional Tendons:

$$\alpha = 90^\circ = 1.57 \text{ Radians, } \mu = 0.21 \text{ from specifications}$$

$$T_1 = T_2 e^{-1.57 \times 0.21} = T_2 (1.0817)$$

$$T_2 = 92.4\% T_1$$

this is the percentage loss from the springline up to the dome apex.

## A.5 Solution Strategy

Solution strategy for containment analysis of severe accident conditions and quasi-static loadings has consisted mostly of implicit-based, incremental loading, with equilibrium iteration. A few of the Round Robin analysis submittals for the three large scale model tests have utilized explicit-based calculations (using some form of numerical damping to suppress dynamic response to quasi-static loading), but the norm has been implicit. The equilibrium iteration schemes vary, but for ABAQUS, a standard “Full-Newton” method is typically employed. The stiffness is reformed at each new load increment, but not at each successive equilibrium iteration. Equilibrium iterations modify the residual force vector, one iteration to the next. The choice of increment step size is sometimes left to an automatic “time stepping” algorithm (based on convergence), and sometimes pre-set by the user. This is discussed in more detail below.

It is also typical to apply initial loads (like dead loads and prestress) first, reach equilibrium, and then apply the accident loads. For combined pressure and temperature loads this creates a unique set of challenges as described in more detail below.

### A.5.1 Special Considerations for Steel Containments

Steel containment analysis tends to have far less difficulties for convergence than concrete containment analysis, but in the pressure range near failure, steel containments have their own unique challenge. Since it is possible for steel containments (as demonstrated by scale model tests) to be loaded to the point of actual thinning (‘necking’) of the shell, the primary stress carrying element of the structure, normal force-incremented solutions (and the structure itself) can become very unstable. A special loading algorithm (found in ABAQUS, and possibly in other programs) which has worked well in the past is the RIKS method, which computes and applies deformation-based selections of load increments. When successfully applied, this has allowed solutions to reach maximum pressure and continue to track somewhat past peak pressure (while wall-thinning is occurring) with reasonable accuracy. The method is, however, an advanced user option, should be used with caution, and tested prior to use.

### A.5.2 Special Considerations for Concrete Containments

Experience (and calculations) shows that substantial hoop cracking can occur in a reinforced concrete containment between 70% and 90% of the design pressure, depending on the percentage of steel. Therefore, a reinforced containment, unlike a prestressed containment, will experience extensive cracking before the design pressure is reached. So unlike steel containments, very significant nonlinearities and difficult convergence issues tend to crop up relatively early in concrete containment analysis. Over the years, and for the analyses in support of the Sandia large scale model testing, good structure simulation success was achieved using ANACAP-U (developed by Rashid, et al, at ANATECH) concrete material modeling in conjunction with ABAQUS, and using a convergence algorithm/philosophy known in ABAQUS nomenclature as “DIRECT=NOSTOP.” With this approach, the user can select load incrementation ‘directly’, and the solution can proceed under less stringent convergence criteria than would be normally be used. Long a subject of debate amongst concrete analysis researchers, a well-known difficulty of smeared-cracking analysis (where multi-directional cracks can form at the element integration points) is the fundamental lack of convergence of internal element forces relative to the element’s possible cracking states. With experience, test validation, and judgment, it has been found that a



lack of internal element force convergence is not necessarily a good measure of the quality of solution, and in fact, the philosophy of ignoring internal element force convergence (but still enforcing global external force convergence and displacement convergence) has led to many good pretest predictions of containment large scale tests for many years. But it should also be noted that other programs, concrete models, and solution/convergence philosophies have also been used with reasonable success. The key remains to test and validate a program and a modeling/solution-strategy approach before attempting an in-depth containment analysis.

A few comments comparing reinforced and prestressed concrete containment solution strategies are also in order. When a reinforced containment cracks, the main reinforcement is stressed only to approximately 30% of its yield, whereas tendon reinforcement in a prestressed containment is at 80% or 90% of yield when the concrete cracks. This, combined with the fact that conventional rebar has greater ductility than prestressing tendons, gives reinforced containments an after-cracking pressure capability range that is significantly larger than in prestressed containments. This implies that leakage before catastrophic rupture may be more likely to occur in a reinforced containment than in a prestressed containment. It also makes solution incrementation more critical and difficult early in the pressure history for RCCVs versus later in the pressure history for PCCVs. On the other hand, once tendon yield is reached in PCCVs, structure response can grow very quickly with small increments of additional pressure, so at this stage PCCV solution convergence can become even more challenging.

### A.5.3 Thermal Analysis

The subject of temperature remains largely an untested issue with regard to global containment behavior. This is due to the experimental difficulties involved with modeling elevated temperatures. Conclusions about global behavior must be taken primarily from analytical studies. In early work in the 1980s, and then in post-test work for the 1:4 Scale PCCV, typical prestressed and reinforced geometries have been investigated by analysis for combined pressure and global temperature up to 400°F (204°C), plus the addition of a local temperature spike simulating a local hydrogen burn. The results of that work showed that temperatures in the ranges predicted to occur (by NUREG-1150, for example, 350° to 400°F (177° to 204°C)) have only a small effect on the ultimate pressure capacity of both reinforced and prestressed containment structures because the cracked concrete carries no tension regardless of temperature. Also, temperatures in this range have only a minor effect on typical rebar (or steel containment shell) properties.

But if temperatures were developed in the range of 700° to 800°F (370° to 427°C) and existed long enough to heat up the embedded rebar or tendons, ultimate pressure capacities could be dramatically reduced because of degradation of the modulus and yield strength of the steel elements.

As performed for the 1:4 Scale PCCV for an International Standard Problem (ISP-48) exercise, the thermal-mechanical analysis of a containment can be approached in two steps: 1) add temperature to the mechanical solution without consideration of material property degradation due to temperature, and 2) perform analysis including temperature and material property degradation. Analysis results were presented in ISP-48 for these cases individually to gain better understanding of the behavior differences and the causes of failure, when temperature is introduced. The primary tool for the ISP Exercise was axisymmetric modeling (and ABAQUS). The steps are as follows.

### Step '1'

Perform a Heat Transfer analysis. (In some programs like ABAQUS, this means all elements relevant for thermal analysis need to be changed to diffusive heat transfer element types which only have temperature degrees of freedom.) Thermal boundary conditions are imposed at the outer surface of the cylinder and dome wall consisting of “free convection with air. The heat transfer coefficient,  $h$ , varies with temperature according to the following relationship:

$$h = 0.00382(\Delta T)^{1/3} \text{ lb}_f/\text{in-s-}^\circ\text{F} \text{ (T in } ^\circ\text{F) for a full scale containment analysis [79],}$$

The boundary condition on the basemat foundation consists of heat conduction with soil with a sink temperature ( $T_f^\circ$ ). An example of a heat transfer coefficient developed for the horizontal surface of the foundation in contact with soil is:

$$h = 5.76 \bullet 10^{-5} \text{ lb}_f/\text{in-s-}^\circ\text{F for a full scale containment [79]}$$

For a proposed accident temperature scenario, a steady state heat transfer analysis step would precede a dynamic heat transfer analysis with the time history temperature input. The steady state heat transfer step is used to bring the model up to an ambient/operating temperature of 25°C. Figure A-2 shows the location of the prescribed boundary conditions for the axisymmetric model of the PCCV.

Step “1” provides a heat transfer solution, either steady state, or transient versus time, and thus provides unique temperatures (either single-valued or versus time) at all the nodes in the model.

Literature reviews were conducted to develop reasonable concrete thermal properties, and for degradation of concrete and steel material properties, and these were provided in Chapter 3.

### Step '2'

Conduct the semi-coupled heat transfer and pressure mechanical solution analysis. Here the solution is advanced step by step by incrementally applying all the nodal point temperatures (which cause  $\alpha\Delta T$  deformations) and applying the pressure loads. The material property degradation can either be tied directly to the constitutive modeling of the materials, or as a more approximate approach, introduced manually to zones of elements particularly influenced by temperature. Such an approach is called semi-coupled because the mechanical solution is influenced by the temperature, but not vice-versa.

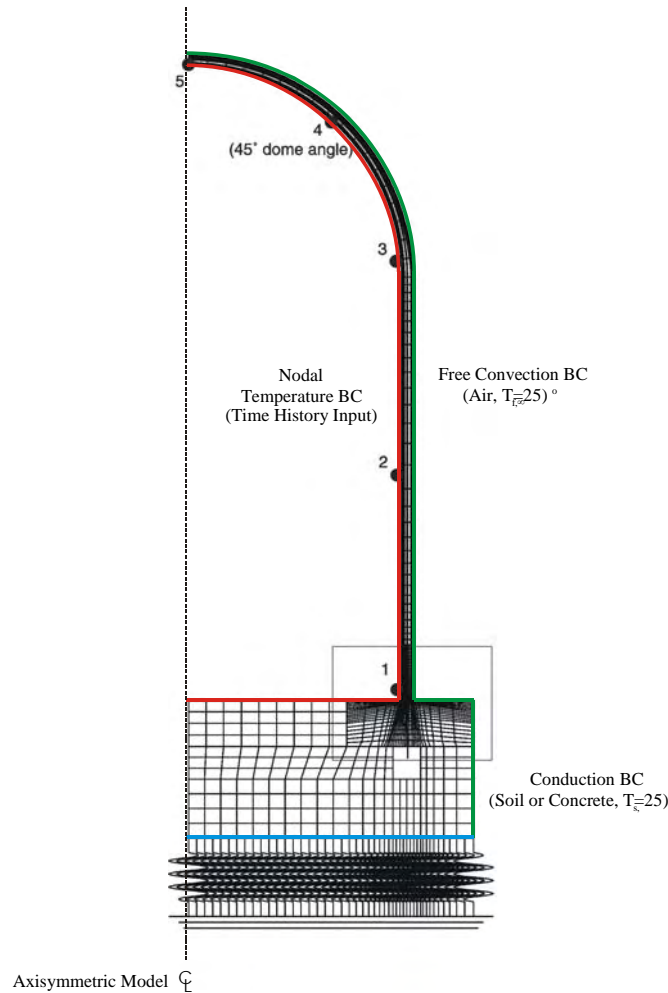


**Figure A-2 Typical Axisymmetric Model and Temperature Boundary Conditions**

## A.6 Interpretation and Evaluation of Results

### A.6.1 Basic Model Checks

Conducting basic quality and “sanity” checks are essential to completing a containment analytical study. And although many such checks are part of the ‘skills of the trade’ learned through experience, for containment global analysis, at a minimum, the analyst should conduct basic hand calculation of approximate event milestones (in terms of pressure) for the radial expansion of the containment cylinder. The calculations are not overly complex, and a detailed example of such a calculations (conducted for the 1:4 Scale PCCV) is provided in Section A.6.3, “Example Verification Analysis”.

### A.6.2 Failure Criteria and Interpreting Analytic Solution

The importance of defining failure criteria to the implementation of finite element results cannot be overstated. Is it a performance-based criteria that requires prediction of actual release of containment contents, or is it a criteria which predicts the onset of a material failure. Until very recently, nearly all containment analysis in the Sandia research program has invoked the latter. And the criteria that is widely used is the multiaxial stress ductility limit for steel plate material

(either the shell of a steel containment or the liner of a concrete containment) defined by Manjoine [xx]. This criteria, which uses the 'Davis Triaxiality Factor,' is provided in Chapter 3. Some performance-based criteria concepts are introduced at the end of the report.

But even with the ductility-based criteria (which predicts failure when steel strains are in the range of 15%-25%), engineering judgment is needed to interpret finite element analysis results. It is only with the very finest of meshes and detailed modeling approaches that such high strains can be reliably predicted, and even with very fine meshes, some measure of mesh-size sensitivity will always be present near structural discontinuities. This means that for most analysis, judgment will be required to extrapolate from global model predicted strains of 1%-2% to high strains likely to exist near structural discontinuities. And though a comprehensive database of strain concentration factors is still lacking, there is substantial evidence (found in test and analysis reports cited herein) to support such engineering judgment and failure prediction based on global analysis.

Investigation and validation of methods for evaluating other potential failure modes is still needed. Shear failure is particularly difficult to evaluate; there is no generally recognized method of determining shear capacity of a reinforced concrete section under simultaneous application of tensile load and bending moment. Failure of large rebars where they are bent around penetrations, as occurred in an EPRI test [47], are also of some concern. The effects of cold working on the available ductility to these bars should be studied further. Rates of pressurization and effects of temperature must be considered in more detail. At high rates of pressurization, there is a possibility that sequential failure modes could occur; that is, for very high rates of pressurization, liner tearing may not arrest the pressure buildup within the containment, and another failure mode could occur at slightly higher pressure. This is the basic reason for emphasizing the development and validation of analysis methods. A reliable evaluation of containment performance must be based on careful, detailed analysis of the specific containment geometry and loading of interest.

### A.6.3 Example Verification Analysis

#### 1:4-Scale Prestressed Concrete Containment Vessel Model

As with any nonlinear analysis of a complex structure, the first step is to identify and categorize structural components and to compute the approximate response behavior to use for guidance in establishing the load stepping strategy for nonlinear finite element analysis. A summary of the major milestones predicted by hand calculation was developed and is described in this subsection. The following definitions refer to the formulae in this subsection.

$\rho$  = reinforcement ratio

$\rho_{\text{hoop rebar}} = \rho_{\text{hr}} = \text{Area of hoop reinforcement/gross concrete area}$

$\rho_{\text{liner}} = \text{Area of liner/gross concrete area}$

$\rho_{\text{hoop tendons}} = \rho_{\text{ht}}$

$t_{\text{liner}} = \text{thickness of liner} = 0.16\text{cm}$

$t_{\text{eq}} = \text{equivalent concrete thickness or transformed section thickness (concrete section area with steel portion transformed by ratio of Young's Moduli)}$

$t'_{\text{eq}} = t_{\text{eq}} \text{ including rebar and tendons}$

$t_c$  = thickness of concrete wall = 32.5cm

$\sigma_o(\text{concr})$  = compressive concrete stress after prestressing

$R$  = Inside radius of cylinder = 538cm

$E_{\text{rebar}}, E_c, E_{\text{liner}}$  = Young's Moduli of rebar, concrete, and liner, respectively

$\epsilon_{\text{cr}}$  = Concrete cracking strain =  $80 \times 10^{-6}$

$\epsilon_{\text{ry}}$  = rebar yield strain

$\sigma_{\text{bar,ult}}$  = rebar ultimate strength

$\sigma_{\text{tendon,ult}}$  = tendon ultimate strength

(stress at 4.77% strain was used in this analysis as an upper bound; the PCCV test suggests ultimate tendon strains of 1 to 2% might be more realistic.)

### Pressure at Which Cylinder Stress Overcomes Prestress, $P_o$

Since there are three 16mm hoop bars and five 13mm bars every 45cm (measured vertically)

$$\rho_{\text{hoop rebar}} = \frac{3 \times 2.01\text{cm}^2 + 5 \times 1.33\text{cm}^2}{32.5\text{cm} \times 45\text{cm}} = 0.00865$$

$$\rho_{\text{liner}} = \frac{t_{\text{liner}}}{32.5\text{cm}} = \frac{0.16}{32.5} = 0.00492$$

$$t_{\text{eq}} = \left(1 + \frac{E_{\text{rebar}}}{E_c} \rho_{\text{hr}} + \frac{E_{\text{liner}}}{E_c} \rho_{\text{liner}}\right) t_c$$
$$= \left(1 + \frac{200}{33} (0.00865) + \frac{200(0.00492)}{33}\right) t_c$$

$$t_{\text{eq}} = 35.2\text{cm}$$

There are four hoop tendons of area  $3.39\text{cm}^2$  in every 45cm wall segment.

$$\rho_{\text{hoop tendons}} = \frac{4 \times 3.39\text{cm}^2}{32.5 \times 45} = 0.00927$$

$$\rho_{\text{total}} = 0.00865 + 0.00492 + 0.00927 = 0.0228$$

In compression under tendon action,

$$\sigma_o(\text{concr}) = -\rho_{\text{tendon}} \sigma_{\text{itendon}} = -0.00927 \times 953 \text{ MPa}$$

(Avg. prestress in hoop tendons including assumed losses)

$$\sigma_o = -8.83 \text{ MPa}$$

pressure to overcome prestress,  $P_o$  is

$$P_o = \frac{-\sigma_o t_{eq}}{R} = \frac{-8.83(35.3)}{538} = 0.580 \text{ MPa}$$

### Cylinder Hoop Cracking Pressure, $P_{hc}$

Total equivalent t including tendons =  $t'_{eq}$

$$t'_{eq} = \left(1 + \frac{E_{steel}}{E_c} \rho_{total}\right) t_c =$$

$$\left(1 + \frac{200}{33}(0.0228)\right) 32.5 = 37.0 \text{ cm}$$

$$P_{hc} = \frac{t'_{eq} E_c \epsilon_{cr}}{R} + P_o = \frac{37.0 \times (33,000) \times 80 \times 10^{-6}}{538} + 0.580$$

$$P_{hc} = 0.762 \text{ MPa}$$

### Pressure at Rebar Yield, $P_{ry}$

Assuming the tendons have not yielded, the hoop stiffness after cracking is approximately that of elastic rebar, liner and tendons acting alone. Therefore,

$$\epsilon_{ry} = \frac{(P_{ry} - P_o)R}{(\rho_{total}) t_c E_s} = \frac{\sigma_y}{E_s} = \frac{455}{200,000} = 0.00228$$

Solving,

$$P_{ry} = \frac{0.00228(0.0228)32.5(200,000)}{538} + 0.580$$

$$P_{ry} = 1.21 \text{ MPa}$$

### Ultimate Barrel Failure Based on Ultimate Strengths of Steel Components, $P_{ult}$

$$P_{ult} = \frac{\sigma_{bar_{ult}} \rho_{hr} t_c}{R} + \frac{\sigma_{tendon_{ult}} \rho_{ht} t_c}{R} + \frac{\sigma_{liner_{ult}} \rho_{liner} t_c}{R}$$

$$P_{ult} = 32.5[658(0.00865) + 1876(0.00927)$$

$$+ 498(0.00492)] / 538$$

$$= 1.54 \text{ MPa} = 4.0 \text{ Pd}$$